Understanding the relationship between antibacterial activity and iron-restriction mechanisms in egg-white

Louis Alex Julien

DOCTORAT ECOLOGIE BRETAGNE GEOSCIENCES LOIRE AGRONOMIE ALIMENTATION

University of Reading

l'institut Agro agriculture • alimentation • environnement

AGRO CAMPUS OUEST

THESE DE DOCTORAT DE

INSTITUT AGRO

ECOLE DOCTORALE N° 600
Ecole doctorale Ecologie, Géosciences, Agronomie et Alimentation
Spécialité : *Microbiologie, virologie et parasitologie*

UNIVERSITY OF READING

Par

Louis Alex Julien

Understanding the relationship between antibacterial activity and iron-restriction mechanisms in egg-white

Thèse présentée et soutenue à Rennes, le 29 septembre 2020
Unité de recherche : STLO, INRAE, Institut Agro, 35042, Rennes, France
Thèse N° : B-339_2020-17

Rapporteurs avant soutenance :

Jennifer Cavet	Lecturer, School of Biological Sciences, University of Manchester, Manchester, UK
Paul Menut	Professeur, IPA, INRAE, AgroParisTech, Massy, France

Composition du Jury :

Examinateurs :	Anne Gougeon	Professeure, Université de Rennes I, INSERM, NUMECAN/CIMIAD, Rennes, France
	Christina Nielsen-LeRoux	Directrice de Recherche, Micalis Institute, INRAE, AgroParisTech, Jouy en Josas, France
Dir. de thèse :	Sophie Jan	Maître de conférences (HDR), STLO, INRAE, Institut Agro, Rennes, France
	Simon Andrews	Professeur, School of Biological Sciences, University of Reading, Reading, UK

Understanding the relationship between antibacterial activity and iron-restriction mechanisms in egg-white

A thesis submitted to

INSTITUT AGRO *'École nationale supérieure des sciences agronomiques, agroalimentaires, horticoles et du paysage'*

Spécialité : *Microbiologie, virologie et parasitologie*

Ecole doctorale Ecologie, Géosciences, Agronomie et Alimentation (EGAAL)

&

THE UNIVERSITY OF READING *'The Faculty of Life Sciences'* in partial fulfilment of the requirements for the Degree of Doctor of Philosophy

by

Louis Alex Julien

(*BSc. Bioscience with Biomedical Sciences, MSc. Microbiology*)

September 2020

Acknowledgements

I wish to thank the members of my dissertation committee: Jennifer Cavet, Paul Menut, Anne Gougeon, Christina Nielsen-LeRoux for generously offering their time, support, and good will throughout the preparation and review of this document. I would also like to acknowledge my supervisors: Prof Simon Andrews and Dr Sophie Jan, my co-supervisors: Dr Florence Baron, Prof Françoise Nau, Dr Kimon-Andreas Karatzas, and Dr Sylvie Bonnassie, for their guidance, and their valuable advice. I am grateful to Clémence Fau who has significantly contributed to this project during her master's internship.

I wish to thank my colleagues, Aida Allawati, Alice Harrison, Antoine Culot, Baptiste Gauducheau, Elham Rakhshi, Fabienne Gonnet, Fanny Canon, Florian Blanchet, Floriane Gaucher, Jordan Kirby, Julien Bauland, Kang Sen Ooi, Maellis Belna, Marie-Françoise Cochet, Manon Granger Delacroix, Manon Hiolle, Michel Gautier, Noël Grosset, Quentin Bruey, Stefano Nebbia, and Zara Rafaque, who had to answer my unending questions and cope with me in the laboratory/office. Likewise, I would like to thank the technical team of the University of Reading and Institut Agro who provided me with the material required for my project. At last, I would like to thank my family, my friends, and my partner for loving me and supporting me through this PhD journey.

Original authorship

I confirm that this is my own work and the use of all material from other sources has been properly and fully acknowledged.

Louis Alex Julien 

Conflict of interest

This work is supported by the Regional Council of French Britany (Allocation de Recherche Doctorale, ARED) and by the Strategic Fund of the University of Reading. The author has no affiliations with or involvement in any organisation or entity with any financial interest, or non-financial interest in the subject matter or materials discussed in this report.

Publications

1/ A large part of the introduction presented in Chapter 1 was published in the following paper: Julien LA, Baron F, Bonnassie S, Nau F, Guérin C, Jan S & Andrews SC (2019) The anti-bacterial iron-restriction defence mechanisms of egg white; the potential role of three lipocalins in resistance against *Salmonella*. *BioMetals*. **32**: 453–467

Biometals (2019) 32:453–467
https://doi.org/10.1007/s10534-019-00180-w

Check for updates

The anti-bacterial iron-restriction defence mechanisms of egg white; the potential role of three lipocalin-like proteins in resistance against *Salmonella*

Louis Alex Julien · Florence Baron · Sylvie Bonnassie · Françoise Nau · Catherine Guérin · Sophie Jan · Simon Colin Andrews

2/ A large part of the work presented in Chapter 3, 4 & 5 was published in the following paper: Julien LA, Fau C, Baron F, Bonnassie S, Guérin-Dubiard C, Nau F, Gautier M, Karatzas KA, Jan S & Andrews SC (2020) The three lipocalins of egg-white: only Ex-FABP inhibits siderophore-dependent iron sequestration by *Salmonella* Enteritidis. *Front. Microbiol.* **11**: 1–13

frontiers in Microbiology

ORIGINAL RESEARCH
published: 15 May 2020
doi: 10.3389/fmicb.2020.00913

Check for updates

The Three Lipocalins of Egg-White: Only Ex-FABP Inhibits Siderophore-Dependent Iron Sequestration by *Salmonella* Enteritidis

*Louis Alex Julien[1,2], Clémence Fau[3], Florence Baron[2], Sylvie Bonnassie[2,4], Catherine Guérin-Dubiard[2], Françoise Nau[2], Michel Gautier[2], Kimon Andreas Karatzas[5], Sophie Jan[2] and Simon Colin Andrews[1]**

Poster presentations and prizes

1/ Julien LA, Karatzas KA & Andrews SC (21st of March 2018) Understanding the relationship between antibacterial activity and iron-restriction mechanisms within egg-white. Prize for best poster presentation in biomedical sciences / engineering at the annual University of Reading PhD symposium. Reading, UK

2/ Julien LA (26th of June 2018) Poster presentation / project proposal outlined to the Vice Chancellor of the University of Reading. Reading, UK

3/ Julien LA, Baron F, Bonnassie S, Jan S & Andrews SC (23rd of June 2019) The anti-bacterial iron-restriction defence mechanism of egg white: the potential role of lipocalins in resistance against *Salmonella*. Poster presentation at the American Society for Microbiolgy (ASM) Microbe. San Francisco, USA

Oral communications

1/ Julien LA, Cochet MF, Bonnassie S, Nau F, Jan S & Baron F (24th of September 2018) Iron-acquisition genes and siderophores production are induced by *Salmonella* Enteritidis in egg white at temperatures around the natural body temperature of hens. Twenty minutes oral presentation at the International Symposium *Salmonella* and Salmonellosis (I3S). Saint Malo, France

2/ Julien LA (23rd of January 2019) Egg white *vs Salmonella*! The antibacterial properties of egg white. Thirty minutes oral presentation as main speaker of the CINNergies Talk & Drinks (lay audience). Reading, UK

3/ Julien LA (1st of April 2019) My thesis in 240 s. Ecole Internationale de Recherche-Agreenium (EIR-A). Dijon, France

4/ Julien LA, Baron F, Bonnassie S, Nau F, Guérin-Dubiard C, Andrews SC & Jan S (5th of July 2019) Are egg white lipocalins involved in iron acquisition by *Salmonella* Enteritidis? Fifteen minutes oral presentation at the The Scientific Days of ED EGAAL (Ecole doctorale Ecologie, Géosciences, Agronomie & Alimentation). Rennes, France.

5/ Julien LA, Baron F, Bonnassie S, Nau F, Karatzas KA, Andrews SC & Jan S (June 2020) Understanding the relationship between antibacterial activity and iron-restriction mechanisms in egg-white. Ten minutes oral presentation at the University of Reading Web-PhD symposium.

6/ Julien LA, Baron F, Bonnassie S, Nau F, Karatzas KA, Andrews SC & Jan S (July 2020) The role of the three lipocalins of egg-white in inhibition of *Salmonella* Enteritidis under iron restriction. Five minutes flash presentation at the 12th Interational Biometals Web-Symposium.

Student supervision

Clémence Fau (MSc) - internship student - 3 months

"Characterisation of three egg-white lipocalins: α1-ovoglycoprotein, Cal-γ and Ex-FABP"

Mina Schneider (MSc) - internship student - 6 months

"Induction of hexonate / hexuronate-utilization genes of *Salmonella enterica* upon exposure to lysozyme"

Camilla Rossi (BSc) - project student - 11 weeks

"Hydrogen production of *Escherichia coli* with focus on the novel hydrogenase-4 and its interaction with endopeptidase HycI"

Clément Réguème (BSc) - internship student - 2 months

"Complementation of *Salmonella enterica* mutants deficient in iron-acquisition systems"

Hansween Kaur (A level) - Nuffield Research Placement student – 4 weeks

"Investigation of *Campylobacter jejuni* ferrous-iron transporter encoded by the *ftr-p19* genes"

Demonstration

At the University of Reading (United Kingdom)

- Foundation biology (16 h); task: improving student's practical skills including microscope, experimental work, and qualitative testing.

- Introductory microbiology (30 h); task: teaching how to put into practice a range of elementary skills and techniques used in the study of micro-organisms.

- Infectious diseases (77 h); task: teaching bacterial and virological techniques applied to clinical samples, including organism isolation, amplification, quantitation, and identification.

- The bacterial cell (12 h); task: teaching how to perform membrane preparations, transposon mutagenesis, and biofilm and evolution experiments.

At Institut Agro (France)

- UE Démarche Scientifique (10 h eq. TD); task: introducing students to scientific approaches, from writing a bibliographic report to implementation of an experimental protocol and poster presentation.

Volunteering

Member of the organising committee of the 2018 University of Reading PhD Symposium.

International labels

In addition to this joint PhD, applications were filled to obtain the "European Doctorate" and "EIR-A" labels.

TABLE OF CONTENTS

LIST OF ABBREVIATIONS

α1-AGP	α1-acid-glycoprotein
α1-M	α1-microglobulin
α1-ovoglyco	α1-ovoglycoprotein
apoD	Apolipoprotein D
APEC	Avian Pathogenic *Escherichia coli*
Amp	Ampicillin
Amp^R	Ampicillin Resistant
Amp^S	Ampicillin Sensitive
APS	Ammonium Persulphate
BB	Binding Buffer
BBP	Bilin Binding Protein
BC50	Median Binding Concentration
β-lg	β-lactoglobulin
BLI	BioLayer Interferometry
B-PER	Bacterial Protein Extraction Reagent
BSA	Bovine Serum Albumin
CAS	Chrome Azurol S
Cat cassette	cassette that carries the chloramphenicol acetyltransferase gene
Cam	Chloramphenicol
Cam^R	Chloramphenicol Resistant
Cam^S	Chloramphenicol Sensitive
CFU	Colony-Forming Units
CV	Column Volume
DGE	Di-Glucosylated Enterobactin
DHBA	2,3-Dihydroxybenzoic Acid
DIP	2,2-Dipyridyl
DTPA	Diethylenetriaminepentaacetic Acid
EB	Elution Buffer
EDTA	Ethylenediaminetetraacetic acid

EEA	European Economic Area
EFSA	European Food Safety Authority
Ent	Enterobactin
ESI-MS	Electrospray Ionization-Mass Spectrometry
EU	European Union
EW	Egg White
EWF	Egg White Filtrate
GW	CLC Genomics Workbench
HDTMA	Hexadecyltrimethylammonium Bromide
HRP	Horseradish Peroxidase
IPTG	Isopropyl β-D-1-thiogalactopyranoside
ITC	Isothermal Titration Calorimetry
k_a	Association rate constant (s^{-1})
Kan	Kanamycin
Kan^R	Kanamycin resistant
k_{dis}	Dissociation rate constant ($M^{-1}s^{-1}$)
K_D	Equilibrium dissociation constant (M)
LB	Lysogeny Broth
LCN2	Human lipocalin-2
LPA	Lysophosphatidic Acid
LPS	Lipopolysaccharides
MALDI-ISD	Matrix Assisted Laser Desorption/Ionization - In Source Decay
M9	M9 salts
MGE	Mono-Glucosylated Enterobactin
MIC	Minimum Inhibitory Concentration
MUP	Major Urinary Proteins
MW	Molecular Weight
OVAX	Ovalbumin-related protein X
OVAY	Ovalbumin-related protein Y
PBS	Phosphate-Buffered Saline
PCR	Polymerase Chain Reaction
PTGDS	Prostaglandin-D Synthase (β-lg),

PelB	Pectate lyase B
pI	Isoelectric point
pmf	Proton Motive Force
Psp	Phage Shock Protein
PT	Phage Type
RBP	Retinol Binding Protein
SCR	Structurally Conserved Region
SOC	Super Optimal broth with Catabolite repression
SPI2-T3SS	*Salmonella* Pathogenicity Island 2 encoded 'Type III Secretion System'
TBE	Tris/Borate/EDTA
TBS	Tris-buffer saline
TEMED	Tetramethylethylenediamine
TCS	Two Component System
Tm	Melting Temperature
TQF	Tryptophan Quenching Fluorescence
Ts	Temperature sensitive
UPEC	Uro-Pathogenic *Escherichia coli*
UV	Ultraviolet
WB	Western Blot
WT	Wild type
2-DE	2D-Polyacrylamide Gel Electrophoresis

Introduction

Supervision

This thesis resulted from a joint PhD program between the United Kingdom and France. It was supported by the Strategic Fund of the University of Reading (UK) and the Regional Council of Britanny (allocations de recherche doctorale, ARED; France). The first phase of the project was performed at the University of Reading (School of Biological Sciences - from the 24th September 2017 to the 31st March 2019; 18 month). Subsequent work took place at Institut Agro (UMR1253, Sciences et Technologie du Lait et de l'Œuf - from the 1st April 2019 up to the 30th September 2020; 18 month). Prof Simon C. Andrews is leading a research group internationally reknowned for its publications on the role of iron in bacterial infections. Members of the STLO are involved in diverse projects linked to antibacterial properties of egg white. Their 20 years of experience make them experts in this field. Both teams are focussing on a major food pathogen: *Salmonella enterica* serovar Enteriditidis (*S.* Enteritidis). Because of areas of common interest and complementary expertise, they launched a collaboration and worked in tandem to develop a PhD project. The originality of the subject lies in a twofold approach, making it possible to explore, on one hand, the antimicrobial properties of egg white, and on the other hand, the responses of *Salmonella* Enteritidis when exposed to this harsh environment. This international collaboration allowed to reinforce the relationships between two leading institutions.

Socio-economic context

Major outbreaks of *Salmonella enterica* foodborne infection have focused the attention of the scientific community and governmental institutions on this pathogen (Vignaud *et al*., 2017; Jackson *et al*., 2013; Braden, 2006). Annually *S. enterica* causes 93.8 million human cases of gastroenteritis and bacteraemia worldwide which subsequently results in 155,000 deaths (Majowicz *et al.*, 2010). Out of the 2,500 serovars identified so far, *S.* Enteritidis serovar is the most frequently detected *Salmonella* in foodborne outbreaks in the European Union (EU) (Figure 1). Salmonellosis occurs mainly through consumption of contaminated food and drink, including water, milk, poultry meat and eggs; although, among outbreaks reported, egg and egg products were identified as the most common vehicles of infection (European Food Safety Authority, EFSA, 2014).

Risks are particularly high when raw or partially cooked eggs are ingested, such as in chocolate mousse, ice-cream and other chilled egg-based food products.

From 2010 to 2013, the number of confirmed human salmonellosis cases in the EU decreased by ~15% but increased again after 2014 (EFSA Panel on Biological Hazards, 2019; ECDC and EFSA, 2017) with more than 750 strongly-evidenced food-borne *Salmonella* outbreaks reported between 2014 and 2016. This is not only a serious public health issue but the concerns arising from *S.* Enteritidis contamination can also lead to significant socio-economic cost (e.g in England; Santos *et al.*, 2011), bringing further attention on this pathogen.

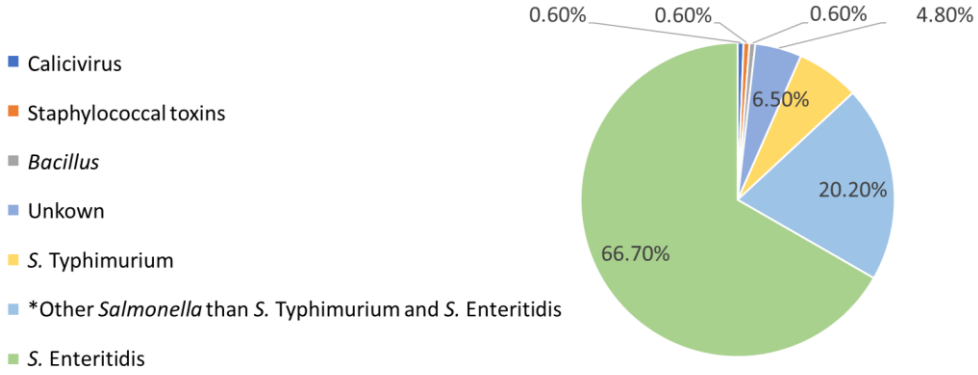

Figure 1. Distribution of strong-evidence outbreaks caused by eggs and egg products, by causative agent, in the EU, in 2012. Data from 168 outbreaks are included: France (33), Germany (3), the Netherlands (1), Poland (51), Slovakia (3), Spain (74) and the United Kingdom (3) (EFSA Panel on Biological Hazards, 2014).

Scientific context

Understanding how pathogens survive within egg white (EW), and how EW resists bacterial infection, are of clear importance to microbiologists, as well as to the agricultural and food industries, and are of great interest to the general public and government (Baron *et al.*, 2016). Recent global expression studies showed that one of the major responses of *S.* Enteritidis to EW exposure is the induction of genes encoding iron uptake functions along with the repression of genes involved in iron storage and utilisation (Baron *et al.*, 2017; Huang *et al.*, 2019). These results are consistent with current understanding of EW bacterial resistance mechanisms, since EW is known to provide a highly iron-restricted environment due to the presence of ovotransferrin (oTf, an-iron binding protein; Sauveur, 1988). Previous work (Lock & Board, 1992; Baron *et al.*, 1997; Garibaldi, 1970) has shown that EW bacteriostatic activity is entirely reversed by addition of iron. This

suggests that the major EW factor limiting bacterial growth is oTf-imposed iron restriction. Salmonellae are unusual in their capacity to infect eggs and survive in EW (Clavijo *et al.,* 2006; Vylder *et al.,* 2013; Gantois *et al.,* 2008), and must therefore resist the powerful anti-bacterial activities of EW. An important mechanism used by bacteria to circumvent iron restriction involves the synthesis of siderophores that bind exogenous ferric iron with high affinity and specificity, and enable acquisition of iron from host sources (Andrews *et al*., 2003). *S.* Enteritidis can synthesise two types of siderophores, enterobactin and its di-glucosylated derivative, salmochelin. Glucosylation of enterobactin is considered to be a strategy employed by pathogens to prevent siderophore sequestration and removal from circulation by the human lipocalin-2 (LCN2). Thus, salmochelin could offer a clear advantage over enterobactin during infection. Recent work suggests that Ex-FABP, identified as EW lipocalin, can inhibit bacterial growth *via* its siderophore-binding capacity in a similar fashion to that of LCN2 (Correnti *et al.,* 2011). However, it remains unclear whether Ex-FABP performs such a function in EW or during bird infection. Two other lipocalins were also identified in EW (Cal-γ and α1-ovoglycoprotein), but there is currently no evidence to indicate that they sequester siderophores and inhibit bacterial growth.

Methods and technical approach

The aim was to determine whether EW lipocalins inhibit bacterial growth through their siderophore-binding activity and whether *S.* Enteritidis can avoid this effect through deployment of salmochelin. This would allow the identification of a new antibacterial mechanism associated with EW immunity and provide further understanding of how bacteria such as *S.* Enteritidis are able to successfully infect EW. This was explored by, firstly, overexpressing and purifying α1-ovoglycoprotein, Cal-γ and Ex-FABP. Secondly, antibodies raised against EW lipocalins were used to estimate their EW concentrations by Western-blotting (WB); this was followed by the study of the siderophore-binding activity of the EW lipocalins using tryptophan-quenching fluorescence, biolayer interferometry and isothermal titration calorimetry. Thirdly, mutants knocked-out for enterobactin synthesis, salmochelin synthesis/export, or salmochelin import/utilisation were used to determine whether exposure to lipocalin proteins limits *S.* Enteritidis growth in standard growth media (M9 minimal medium or LB rich medium supplemented with 2,2-dipyridyl; DIP) and several EW-based media.

Chapter 1. Bibliographic study

1.1 *Salmonella* Enteritidis in eggs, a matter of public health

1.1.1 European regulation relative to *Salmonella* monitoring prevention and control

In the early 20th century, *Salmonella enterica* serovar Gallinarum and Pullorum, were predominant in European and American poultry flocks (Bullis, 1977). Epidemiology and population biology suggest that *S.* Gallinarum competitively excluded *S.* Enteritidis from poultry flocks. Hence, eradication of *S.* Gallinarum from commercial poultry flocks by the 1970s resulted in the emergence of *S.* Enteritidis, which became a major concern for the food safety by the 1980s (Rabsch *et al.*, 2000). Poultry infected with *S.* Pullorum and *S.* Gallinarum experience increased mortality, drastic weight loss and sharply decreased egg production (Shivaprasad, 2000). In contrast, *Salmonella* Typhimurium or *S.* Enteritidis can persist in the digestive tract of birds for months with no or mild clinical signs, with the exception of very young chicks where high mortality rates are recorded (Barrow *et al.*, 1987; Kinde *et al.*, 2000). Hence, it can be challenging for farmers to determine if the poultry flock might pose a public health threat. Furthermore, it is often difficult to detect the presence of *S.* Enteritidis in contaminated eggs as there are no obvious change to either appearance or odour for infections below 10^9 CFU/mL. Above this level there is increasing turbidity in the albumen and eventually the yolk membrane will break down (Humphrey, 1994).

Currently, *S.* Enteritidis and *S.* Typhimurium remain the major serovars found in poultry in the EU (EFSA Panel on Biological Hazards, 2019), highlighting the importance of measures that can reduce the risk of contamination. Hence, European regulations were implemented to monitor *S.* Enteritidis and *S.* Typhimurium and prevent these serovars from infecting flocks. Since 1992, it is required that member states of the EU draw up plans for monitoring *Salmonella* in poultry and to establish rules specifying the measures to be taken to avoid the introduction of *Salmonella* onto farms (Council Directive 92/117/EEC). Six years later, this council directive was transcribed into French law "*Arrêté du 26 octobre 1998 relatif à la lutte contre les infections à* Salmonella *Enteritidis ou* Salmonella *Typhimurium dans les troupeaux de l'espèce* Gallus gallus *en filière ponte d'oeufs de consummation*" (NOR AGRG9802175A). This decree aimed to establish:

- systematic screening for *S.* Enteritidis and *S.* Typhimurium infections in breeding hens (whose primary purpose is the production of hatching eggs) of the *Gallus gallus* species;

- routine screening for *S.* Enteritidis infections in egg-laying poultry (whose primary purpose is to lay eggs for consumption) of the *Gallus gallus* species;
- the slaughter of flocks infected with *S.* Enteritidis and *S.* Typhimurium, or the remediation of the products derived therefrom.

To take into account technical and scientific progress, in 2002 the EFSA was established. Subsequently, the Council Directive 92/117/EEC was repealed and replaced by the directive 2003/99/EC. This regulation establish that member states must set up *Salmonella* National Control Programmes (NCP) aimed at reducing the prevalence of *Salmonella* serovars considered relevant for public health. According to the 2019 report (EFSA Panel on Biological Hazards, 2019), member states should consider the following five serovars as main targets in NCPs: *S.* Enteritidis, *S.* Typhimurium, *Salmonella* Infantis, *Salmonella* Kentucky, either *Salmonella* Heidelberg or *Salmonella* Thompson.

Control measures to limit *Salmonella* in the avian gastrointestinal tract, such as use of probiotics or prebiotics, or dietary change, have been studied (Dunkley *et al.*, 2009 for a review). Live and inactivated oral vaccination are also strategies available (Clifton-Hadley *et al.*, 2002; Methner, 2018). It is important to note that these control methods are also regulated. Since 2006, the Commission Regulation 2006/1177/EC obliges the use of vaccination programmes against *S.* Enteritidis in the European member states if its prevalence exceeds 10% in poultry flocks. Moreover, the same regulation states that antimicrobials should not be used as part of NCPs, other than in exceptional circumstances, to avoid spreading antibiotic resistance.

1.1.2 *Salmonella* Enteritidis in the nomenclature of the *Salmonella* genus

Salmonellae are facultative-anaerobic bacteria belonging to the Enterobacteriaceae family. *Salmonella* spp. are Gram-negative, rod-shaped, non-spore forming bacteria. They can colonise different organs and hosts by switching from respiration to fermentation for energy generation (D'Aoust & Maurer, 2007). They are intestinal parasites and intracellular pathogens in many mammalian hosts, and are also found in birds, reptiles, amphibians and plants (McQuiston *et al.*, 2008).

Salmonellae can grow between 5 to 45 °C (with an optimum growth at 37 °C) and are oxidase negative and catalase positive. The catalysis of D-glucose and other carbohydrates results in the production of acid and gas. Salmonellae can be identified by biochemical tests through growth on citrate, production of hydrogen sulphide and decarboxylation of lysine and ornithine. Bismuth sulphite agar is often used as a selective medium and confirms the ability to use ferrous sulphate to generate hydrogen sulphide (D'Aoust & Maurer 2007).

According to the judicial commission of the International Committee on Systematics of Prokaryotes (ICSP), Salmonellae are divided into two species: *Salmonella enterica* and *Salmonella bongori* (Trüper, 2005). The former is further divided into six subspecies (Figure 1.1) (Tindall *et al.,* 2005). In addition, the salmonellae subspecies are further subdivided in serotypes based on two surface structures: the somatic (O) antigen and the flagellar (H) antigen (McQuiston *et al.,* 2008). During latex agglutination serotyping, *S.* Enteritidis reacts with O antigens 1, 9, and 12; phase 1 H antigens g and m; and not to any phase 2 H antigens (Grimont & Weill, 2007). Within the *S.* Enteritidis serovar, Ward *et al.* (1987) differentiated 27 phage types (PT). Among them, PT4, PT8, and PT13a cause most outbreaks reported worldwide (Pan *et al.,* 2009). In this study, experiments were conducted with the strain PT4-P125109 from Matthew McCusker, Center for Food Safety and Food Borne Zoonomics, Veterinary Sciences Centre, University College Dublin, Ireland (NCTC13349, isolated from a food poisoning outbreak in the UK).

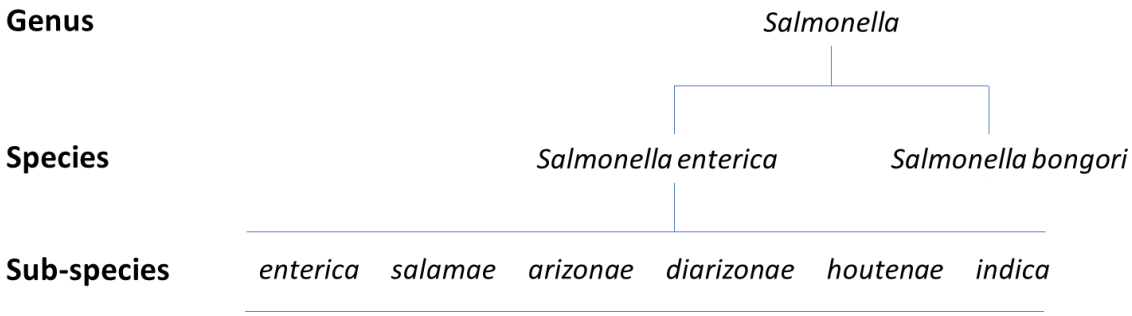

Figure 1.1. Diagram of *Salmonella* species and sub-species (Trüper, 2005 and Tindall *et al.,* 2005).

1.1.2 The two routes of egg contamination

Salmonellae are normal hosts of poultry. Hence, asymptomatic carriers can transmit *S.* Enteritidis in table eggs and poultry meat to humans. Two possible routes of egg contamination have been described, either horizontal or vertical transmission. The former refers to penetration through the eggshell whilst the latter results from the infection of reproductive organs with *S.* Enteritidis (Gantois *et al.*, 2009 for a review).

The level of hygiene under which hens are housed plays a major role in *S.* Enteritidis outbreaks since pores or cracks might lead to penetration of bacteria present on the egg surface through the shell and the eggshell membranes. Eggs can also be infected when formed in the reproductive organs. Indeed, Salmonellae can be taken up orally by the hen and enter the intestinal tract. Colonisation of intestinal epithelial cells then leads to the recruitment of macrophages which, once infected, migrate to internal organs, including reproductive organs (systemic infection). Contamination of egg components has been reported at all stages of egg formation, from ovaries to the vagina via the oviduct (Figure 1.2). EW is formed in the magnum and is therefore likely to be infected in this organ (Keller *et al.*, 1995).

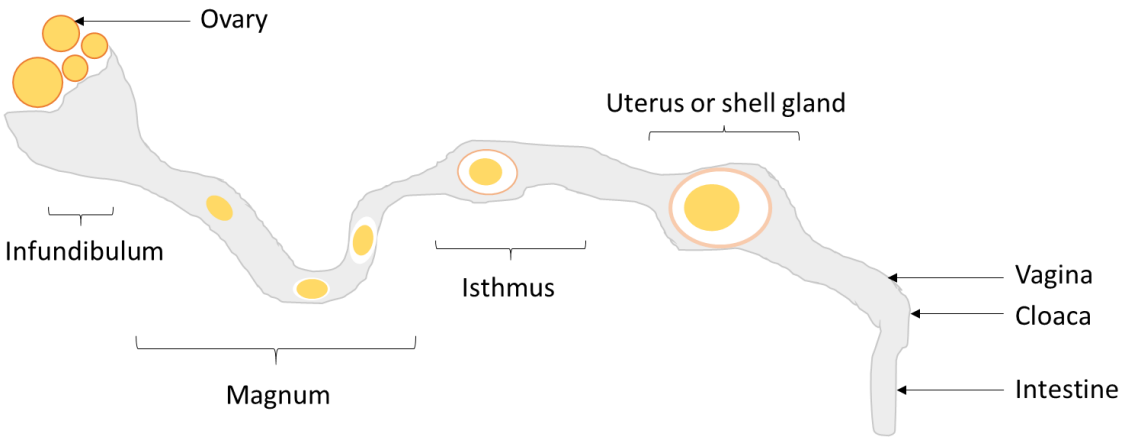

Figure 1.2. Egg formation in the hen reproductive organs. From the ovary, the formation of the yolk takes place in the infundibulum. Then, the egg white and shell membrane are formed in the magnum and isthmus, respectively. The egg undergoes a final transformation in the uterus, where the crystalline shell is formed before oviposition through the cloaca (adapted from Gantois *et al.*, 2009).

1.1.3 *Salmonella* Enteritidis colonisation and survival in egg white

Oral infections with three different *S.* Enteritidis and *S.* Typhimurium strains revealed that both serotypes are able to colonise reproductive tissues and the forming egg, but only *S.* Enteritidis was found after oviposition (Keller *et al.,* 1997). Subsequent studies have also shown that *S*E appears to be very well suited to infection of, and survival within, eggs (Clavijo *et al.,* 2006; Vylder *et al.,* 2013; Gantois *et al.,* 2008). This suggests that this serotype harbours intrinsic or induced factors related to resistance in eggs. Despite *S.* Enteritidis being isolated from both the yolk and the albumen, the latter is most frequently contaminated (for a review, see Gantois *et al.,* 2009). The albumen is also the first medium encountered by *S.* Enteritidis after penetration through the eggshell and eggshell membranes. Therefore, it is necessary to have a better understanding of *S.* Enteritidis colonisation and survival in EW. It is important to note that following the contamination, survival strategies of *S.* Enteritidis in EW might vary depending on temperature and infection load (Baron *et al.,* 2016 for review). Survival and growth at 30, 37 and 42 °C are of importance. Indeed, *S.* Enteritidis survival or growth can be observed from 30 to 37 °C in EW, depending on the inoculum (Alabdeh *et al.,* 2011; Bradshaw *et al.,* 1990; Clavijo *et al.,* 2006; Růzicková, 1994; Kang *et al.,* 2006). Further, 42 °C (which matches the chicken body temperature) and higher temperatures are associated with a bactericidal activity of EW on *S.* Enteritidis (Alabdeh *et al.,* 2011; Guan *et al.,* 2006; Kang *et al.,* 2006). Beyond temperature, *S.* Enteritidis must adapt to the matrix, pH and ionic environment of EW upon infection.

1.2 The powerful antibacterial defence mechanisms of egg white

1.2.1 Physico-chemical factors

Eggs are made up of shell and eggshell membranes (9-12%), EW (60%) and yolk (30-32%) (Zaheer, 2015). The shell is surrounded by a cuticle and separated from the EW by two membranes (Figure 1.3). Altogether, they are barriers to *S.* Enteritidis penetration into the EW, wereas the vitellin membrane protects the yolk.

Hen EW composition, as well as protein and mineral abundance, can be found in Tables 1.1, 1.2 and 1.3, respectively. EW is noted for its strong antimicrobial activity which indicates that *S.* Enteritidis has powerful EW-resistance mechanisms. Indeed, the various antimicrobial activities exhibited by EW can be considered to present a unique set of challenges for bacterial invaders. These include physico-chemical factors, in particular high pH (inhibiting growth; Sharp & Whitaker, 1927) and high viscosity (limiting motility; Schneider & Doetsch, 1974; Yadav & Vadehra, 1977); in addition, high osmolarity (potentially causing osmotic stress) has been suggested (Clavijo *et al.*, 2006). The pH of EW shifts from ~7.6 (upon oviposition) to 9.3 (a few days later) as a result of CO_2 release (Sharp & Powell, 1931). The viscosity of EW (with a shear rate of 400 s^{-1}: 5 $mPa.s^{-1}$ at 20 °C; Lang & Rha, 1982) is mainly caused by the presence of ovomucin, a glycoprotein contributing to 3.5% w/w of the total protein.

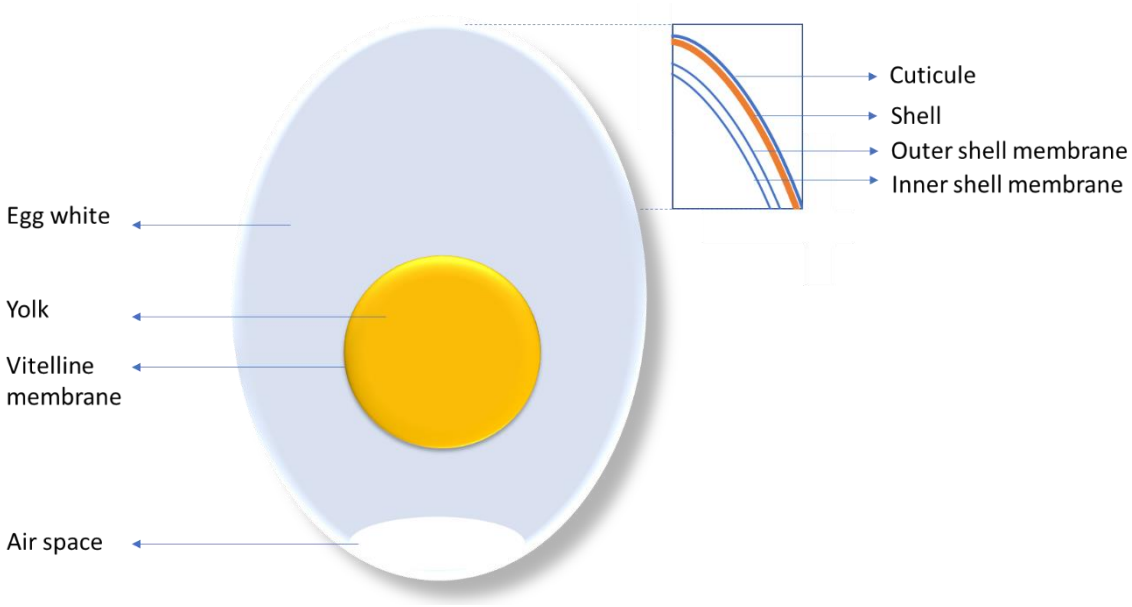

Figure 1.3. Physical structure of hen egg. The shell is surrounded by a cuticle and separated from the albumen by two membranes (the outer membrane adheres to the shell and the inner membrane to the EW). The yolk is in the centre and is separated from the white by the vitelline membrane (adapted from Gantois *et al.*, 2009).

Table 1.1. Chemical composition of hen egg white (Sauveur 1988; Nys & Sauveur 2004).

Nutriments	*g/100 g of egg white*
Water	87.5
Proteins	10.6
Carbohydrates	0.8
Ashes	0.5
Minerals	0.5
Lipids	0.1
Vitamins	0.0007

Table 1.2. Protein abundance in hen egg white (Sauveur 1988; Kovacs-Nolan *et al.*, 2005).

Proteins	*g/100 g of egg white*
Ovalbumin	5.4
Ovotransferrin	1.2 - 1.3
Ovomucoid	1.1
Ovomucin	0.15 to 0.35
Lysozyme	0.34 to 0.35
Globulin	0.4 to 0.8
Ovoinhibitor	0.15
Ovoglycoprotein	0.05 to 0.01
Ovoflavoprotein	0.08 to 0.01
Ovostatin	0.05
Cystatin	0.005
Avidin	0.005

Table 1.3. Minerals in hen egg white (Sauveur 1988; Nys & Sauveur 2004; ANSES, 2017).

Minerals	*mg/100 g of egg white*
Sulfur	163 to 195
Sodium	155 to 186
Chlorine	155 to 186
Potassium	150 to 167
Phosphore	15 to 22
Magnesium	9 to 12
Calcium	6 to 12
Iron	0.02 to 0.14
Zinc	0.01 to 0.12
Copper	0.02
Manganese	0.01
Iode	0.001

In addition to these physico-chemical factors, EW possesses an array of proteins (~10% w/w) that provide further defence against pathogens (Baron *et al.*, 2016 for a review), notably:

- ovotransferrin (oTf), involved in iron deprivation (Garibaldi, 1970) and bacterial membrane damage (Aguilera *et al.*, 2003);
- lysozyme (Derde *et al.*, 2013) and defensins (Hervé-Grépinet *et al.*, 2010; Gong *et al.*, 2010), that would be expected to disrupt bacterial membrane integrity;
- ovalbumin X, a heparin-binding protein exhibiting antimicrobial activity (Réhault-Godbert *et al.*, 2013);
- ovostatin (Nagase *et al.*, 1983) and cystatin (Wesierska *et al.*, 2005), presumed to inhibit exogenous proteases; and
- avidin (Banks *et al.*, 1986), a biotin sequestration protein.

1.2.2 Iron deprivation and bacterial membrane damage by ovotransferrin

1.2.2.1 Effect of ovotransferrin on iron availability

Biologically, iron can be found in both ferrous (Fe^{2+}) and ferric (Fe^{3+}) forms (Table 1.4). In EW, iron would be expected to be largely in the ferric state due the elevated pH and aerobic conditions inside the egg (egg-shell and -membranes are permeable to oxygen; Lomholt, 1976; Tullett & Board, 1976). It is generally accepted that the major factor limiting bacterial growth in EW is iron restriction. This results from the presence of oTf, a powerful iron-binding protein (Garibaldi, 1970; Lock & Board, 1992; Baron *et al.*, 1997). The iron restriction of EW was first discovered by Schade & Carolin (1944) who found that exposure to EW inhibits the growth of *Shigella dysenteriae*. Among 31 growth factors added to EW, only iron overcame the observed EW-imposed growth inhibition. Two years later, Alderton *et al.* (1946) identified the EW factor responsible as 'conalbumin', which is now known to be a member of the transferrin family and is more commonly referred as oTf.

Since these early studies, subsequent work has confirmed the role of oTf as an EW iron-restriction agent preventing growth of a range of microbial species, including *Salmonella* (Schade & Caroline, 1944; Valenti *et al.*, 1983, 1985; Ibrahim, 1997; Baron *et al.*, 1997, 2000). Indeed, iron-acquisition mutants of *S.* Enteritidis display decreased survival and/or growth in EW (Kang *et al.*, 2006). Such studies confirm the antibacterial

role of iron restriction in EW. Recent global transcriptomic studies (Baron *et al.*, 2017; Huang *et al.*, 2019) revealed a major iron-starvation response of *S.* Enteritidis upon exposure to EW which was caused by relief of Fur (the global transcriptional regulator of iron-dependent gene expression; Bjarnason *et al.*, 2003; Rabsch *et al.*, 2003; Balbontín *et al.*, 2016) mediated repression. Fur is a homodimer composed of 17 kDa subunits that binds one ferrous ion (Fe^{2+}) per subunit. Fur represses transcription of genes involved in iron acquisition upon interaction with its co-repressor, Fe^{2+}, and causes de-repression of these genes in the absence of Fe^{2+} (Coy & Neilands, 1991; Bags & Neilands, 1987). Additionally, a recent quantitative proteomic analysis (isobaric tags for relative and absolute quantitation; iTRAQ) showed that iron-acquisition-system-related proteins are induced by EW (Qin *et al.*, 2019). Altogether, these findings confirm that *S*E suffers from iron limitation in EW.

The low iron availability in EW exerts a strong bacteriostatic influence (Bullen *et al.*, 1978; Baron *et al.*, 1997) because iron is essential for growth of nearly all organisms, including bacteria (Andrews *et al.*, 2003). In many ways, the antibacterial iron-restriction strategy of EW is comparable to the iron-dependent 'nutritional immunity' defence mechanisms observed in mammals, where serum transferrin maintains concentrations of extracellular free iron at levels (10^{-18} M) well below those that support bacterial growth (Bullen *et al.*, 2005).

Table 1.4. Comparison of the properties of ferrous and ferric iron (Andrews *et al.*, 2013)

	Ferrous (Fe^{2+})	*Ferric (Fe^{3+})*
State	Reduced form	Oxidised form
Acquired form	Acquired in its free form	Acquired in a complex form by siderophores
Solubility at pH 7	Relatively soluble (0.1 M)	Poor solubility (10^{-18} M)
Colour	Colourless	Rusty brown
Other main features	Fenton reaction: reacts with peroxide (H_2O_2) to form hydroxyl radicals (•OH)	Most abundant environmentally

OTf is believed to be the critical iron-restriction component in EW. Like other members of the transferrin family, its structure consists of two 'lobes', each with a strong affinity for a single Fe^{3+} ion (apparent binding constant of around 10^{32} M^{-1}, with of 1.5 ×

10^{18} M^{-1} and 1.5×10^{14} M^{-1} for the C- and N-terminal lobes, respectively, at pH 7.5; Guha-Thakurta *et al.,* 2003; Chart & Rowe, 1993; Schneider *et al.,* 1984). The iron-restriction-based bacteriostatic activity of oTf is enhanced by bicarbonate (which is likely related to the apparent dependence of metal binding on the presence of a suitable anion; Valenti *et al.,* 1983) and high pH (Valenti *et al.,* 1981; Lin *et al.,* 1994). EW contains levels of iron estimated to be between ~0.02 to ~0.14 mg per 100 g (equivalent to ~3 to ~25 µM; USDA 2010; Nys & Sauveur, 2004; ANSES, 2017). This is consistent with the observed induction of Fur-repressed iron-transport genes upon exposure of *S.* Enteritidis to EW; such genes are de-repressed in iron-restricted environments (below 5 to 10 µM external iron concentration; Andrews *et al.,* 2003) (Baron *et al.,* 2017; Huang *et al.,* 2019).

EW iron content would normally be sufficient for bacterial growth. However, oTf is present in such high abundance in EW (170 µM; 13% of total protein content, second most abundant EW protein after ovalbumin; Sauveur, 1988) that oTf iron-binding capacity exceeds iron availability by 17-fold. Hence, it can be assumed that virtually all iron in EW is bound to oTf (Julien *et al.,* 2019). However, some bacteria are more susceptible to growth inhibition by oTf than others. Indeed, *in vitro* studies showed that the most sensitive species are *Pseudomonas* and *Escherichia coli*, and the most resistant are *Staphylococcus aureus, Proteus* and *Klebsiella* (Valenti *et al.,* 1983). Unsurprisingly, the effects of oTf can be relieved by iron-mobilising agents (e.g. citrate) (Valenti *et al.,* 1983).

1.2.2.2 Effect of ovotransferrin on the bacterial membrane

OTf also appears to possess additional antibacterial activities since its effects are diminished when separated from direct contact with bacteria through location in a dialysis bag or immobilisation on beads (Valenti *et al.* 1985). Indeed, through chelation of membrane-associated cations, transferrins can cause LPS release and alter outer-membrane permeability. LPS are negatively charged and are stabilised by cations such as calcium, magnesium and iron. Therefore, transferrins might be able to disrupt the integrity of the outer membrane (Ellison *et al.,* 1998). This contact-dependent activity is likely related to the presence of a Cys-rich antibacterial-peptide-like motif located on the surface of the oTf molecule which confers the ability to kill Gram-negative bacteria (Ibrahim *et al.,* 1998; 2000). It has also been shown that transferrins can alter both the

outer and inner membrane of *E. coli*, which results in permeation of ions. As a result, the proton motive force (pmf) can be significantly reduced by transferrin/oTf treatment (Aguilera *et al.*, 2003). Thus, the bacteriostatic effect of oTf could be due, in part at least, to its capacity to cause the passive flow of H^+ across the inner membrane dissipating the major driving force for ATP synthesis, motility and secondary transport. Further support for a direct impact of oTf on the pmf of the bacterial membrane was obtained when oTf was shown to cause depolarisation the cytoplasmic membrane of *Bacillus cereus* and mediate cell death, clearly suggesting a bactericidal effect of this protein (Baron *et al.*, 2014).

Recent findings also suggest that the *S.* Enteritidis membrane might be subject to attack in EW. Baron *et al.* (2017) showed that after 45 min exposure to 10% EW at 45 °C, functions related to bacterial envelope stress, including the phage-shock-protein (Psp) response, were induced. The Psp response is thought to maintain the pmf under extracytoplasmic stress conditions that impair the bacterial inner membrane of cells (Jovanovic *et al.*, 2010). It was suggested that oTf is at least one of two factors (with high pH) in EW that can cause dissipation of the pmf and induce the observed Psp response (Aguilera *et al.*, 2003; Darwin, 2005). Global expression data from Baron *et al.* (2017) also indicated that both the EnvZ-OmpR and CpxAR modulons (responding to bacterial envelope stress response; Raivio, 2014) were activated upon exposure of *S.* Enteritidis to 10% EW, further suggesting damage to the bacterial membrane.

1.2.3 Impairment of cell wall integrity by lysozyme and defensins

A better-known protein leading to bacterial cell wall damage is lysozyme. This bacteriolytic protein of 14 kDa accounts for 3.5% of albumen (Kovacs-Nolan *et al.*, 2005 for a review). Lysozyme acts by hydrolysis of the β-linkage between N-acetylmuramic acid and N-acetylglucosamine of bacterial cell walls. The enzymatic activity of EW lysozyme was shown to be optimum at pH 9.2 (Davies *et al.*, 1969), suggesting that it could contribute to EW defence against infection after ovoposition.

However, lysozyme is largely ineffective against Gram-negative bacteria since the presence of an outer membrane prevents lysozyme from reaching the peptidoglycan. Considering the arsenal of antimicrobial defence in EW, it is possible to argue that the outer membrane might lose its integrity in EW; especially in the presence of the potent

membrane disruptor effect of oTf, as described above. However, bacteria might be able to evade the lytic activity of lysozyme by producing inhibitors. Callewaert *et al.* (2008) identified a new family of lysozyme inhibitors (PliC) that contribute to lysozyme tolerance in *S.* Enteritidis.

Derde *et al.* (2013) highlighted that EW lysozyme might also have a non-enzymatic activity. Despite the presence of an outer membrane, *E. coli* suffered membrane disruption by lysozyme through permeabilisation. Additionally, changes in the inner membrane pmf support the hypothesis of membrane disruption in presence of native lysozyme. Nevertheless, lysozyme mechanisms of disruption against Gram-negative bacteria, such as *S.* Enteritidis, are still to be investigated.

Proteomic analysis of EW revealed the presence of two other proteins that could impair vital membrane functions: β-defensin-11 and gallin (Mann, 2007). Whereas the gallin antibacterial spectrum is restricted to *E. coli* (Hervé-Grépinet *et al.,* 2014), β-defensin-11 antibacterial activity toward *S.* Enteritidis has been proven by Hervé-Grépinet *et al.* (2010) who observed a minimum inhibitory concentration (MIC) of 0.40 and 0.05 µM for *S.* Enteritidis and for *E. coli*, respectively.

1.2.4 Other proteins potententially antibacterial

1.2.4.1 Ovalbumin X, a heparin-binding protein exhibiting antimicrobial activity

Ovalbumin accounts for more than 50% of the total protein content of EW. Yet, little is known about its function. As for hormone-binding globulins and angiotensinogen, ovalbumin belongs to the serpin family even though it does not exhibit any protease inhibitory functions (Huntington & Stein, 2001). This protein comprises 386 amino acid residues and a molecular mass of 45 kDa, and is involved in the allergenicity of EW (Claude *et al.,* 2016; Lin *et al.,* 2016). Ovalbumin changes to a more stable form called ‘S-ovalbumin’ under high pH and temperature, resulting in runny egg whites and loss of food value (Miyamoto *et al.,* 2015).

Two other ovalbumin homologues are found in EW: ovalbumin-related protein Y (OVAY), and ovalbumin-related protein X (OVAX). Unlike ovalbumin and OVAY, OVAX can bind heparin (Réhault-Godbert *et al.,* 2013), and might contribute to

antimicrobial activities against both Gram-negative and -positive bacteria (Da Silva *et al.*, 2015).

1.2.4.2 Potent inactivation of exogenous proteases by cystatin, ovomucoid and ovoinhibitor

Other antimicrobial molecules that have been identified in EW are protease inhibitors. Three of them have been reported in EW: ovomucoid, ovoinhibitor and cystatin. Ovomucoid accounts for 11% and ovoinhibitors for 3.5% of the albumen (Kovacs-Nolan *et al.*, 2005). Both ovomucoid and ovoinhibitor inhibit trypsin. In addition, ovoinhibitor prevents bacterial and fungicidal proteases, and contributes to the viscous nature of EW (Omana & Wu, 2009). As for cystatin, this molecule has been classified as a very strong inhibitor towards ficin, papain and cathepsins (Kopeć *et al.*, 2005).

1.2.4.3 Sequestration of vitamins by avidin and riboflavin-binding proteins

Along with the molecules described above, avidin is known to play a role in antimicrobial activity through combination with biotin or vitamin B8 (White *et al.*, 1976). Likewise, chelation of riboflavin (vitamin B2) by riboflavin-binding proteins (RBP) might contribute to sequestration of nutrients (Winter *et al.*, 1967). The study from Baron *et al.* (2017) showed a strong induction of *S.* Enteritidis genes involved in biotin biosynthesis (*bioABCDF* operon) upon exposure to 10% EW; reinforcing the assumption of avidin restriction in EW.

1.2.4.4 Ex-FABP: a lipocalin binding bacterial siderophores

Three lipocalin homologues have already been identified in *Gallus gallus* hen EW (Guérin-Dubiard *et al.*, 2006): Ex-FABP (quiescence specific protein, Ch21 protein), chondrogenesis-associated lipocalin (CAL-γ, prostaglandin H2 D-isomerase) and α1-ovoglycoprotein (or orosomucoid). It has been hypothesised by Correnti *et al.* (2011) that one of them (i.e Ex-FABP) might be responsible for sequestration of *S.* Enteritidis bacterial siderophores. The potent role of Ex-FABP will be further described in section 1.3.2.2.

1.3 Iron in the fight between *Salmonella* Enteritidis and egg white

1.3.1 Iron acquisition by *Salmonella*

1.3.1.1 The role of the two siderophores of *Salmonella* in iron uptake and pathogenicity

Among all the antibacterial defence mechanisms described above, iron restriction imposed by oTf is generally considered to be the most important. A key mechanism used by bacteria to circumvent this restriction involves the synthesis of siderophores that bind exogenous Fe^{3+} iron with high affinity and specificity, which enables acquisition of iron from host sources. Siderophores can be divided into three major families based on the chemical groups involved in iron binding: catecholates, hydroxamates and hydroxycarboxylates. In addition to these three families, many mixed-type siderophores (i.e having elements of two or more siderophore families) have been characterised (Holden & Bachman, 2015).

S. Enteritidis can synthesise two catecholate siderophores: enterobactin and salmochelin. Enterobactin was first identified in *E. coli* (O'Brien & Gibson, 1970) and *S.* Typhimurium (Pollack & Neilands, 1970). Although enterobactin synthesis was shown to be required for survival of *S.* Typhimurium in low-iron *in vitro* environments (Pollack *et al.,* 1970), its role in pathogenesis is limited for reasons that were, initially, unclear (Benjamin *et al.,* 1985; Rabsch *et al.,* 2003). Salmochelin (which is closely similar to enterobactin) was not identified until more than three decades after enterobactin when it was found to be a product of pathogenic enterobacteria, such as *Salmonella* (Hantke *et al.,* 2003). It was designated 'salmochelin' as it appeared at first to be a characteristic of *Salmonella* strains. However, salmochelins have now been reported in avian pathogenic *E. coli* (APEC), uropathogenic *E. coli* (UPEC) (Caza *et al.,* 2008; Gao *et al.,* 2012), *S.* Typhimurium (Crouch *et al.,* 2008) and *Klebsiella pneumoniae* (Bachman *et al.,* 2012), where they contribute to virulence.

1.3.1.2 Enterobactin – a powerful siderophore, but with limited effect *in vivo*

Enterobactin is a serine macrotrilactone that has a far higher affinity for iron than oTf (formation constants of 10^{52} and 10^{32} M^{-1}, respectively), which allows siderophore-producing bacteria to use oTf as a source of iron (Chart & Rowe, 1993). Although the metabolism of enterobactin is best studied in *E. coli*, *Salmonella* possesses a highly similar set of enterobactin-related genes which are assumed to play similar roles. The enterobactin precursor, 2,3-dihydroxybenzoate (DHB), is synthesized from chorismate by enzymes encoded by the *entC*, *entB* and *entA* genes (Figure 1.4). In a second step, an amide linkage of DHB to L-serine is catalyed; three molecules of DHB-serine are

combined, polymerized and cyclized to form enterobactin (Figure 1.5) by enzymes encoded by the *entE, entB, entD* and *entF* genes (Gehring *et al.,* 1998). EntS is required for enterobactin export through the cytosolic membrane (Furrer *et al.,* 2002) whereas TolC is involved in enterobactin efflux across the outer membrane (Bleuel *et al.,* 2005) (Figure 1.6). Once complexed with ferric iron, uptake of ferric-enterobactin into the periplasm is mediated by the iron-regulated outer-membrane proteins, FepA and CirA (and IroN in *Salmonella*) (Rabsch *et al.,* 1999, 2003); the energy-transducing TonB-ExbBD complex is also required for this step (Skare *et al.,* 1993; Figure 1.6). Ferric-enterobactin is then imported into the cytoplasm by the ATP-binding cassette transporter, FepBDGC (Langman *et al.,* 1972; Chenault & Earhart, 1992). Finally, the imported ferric-enterobactin complex is processed by the Fes esterase which cleaves the cyclic ring of the siderophore, lowering affinity for the bound iron which enables dissociation (O'Brien, 1971).

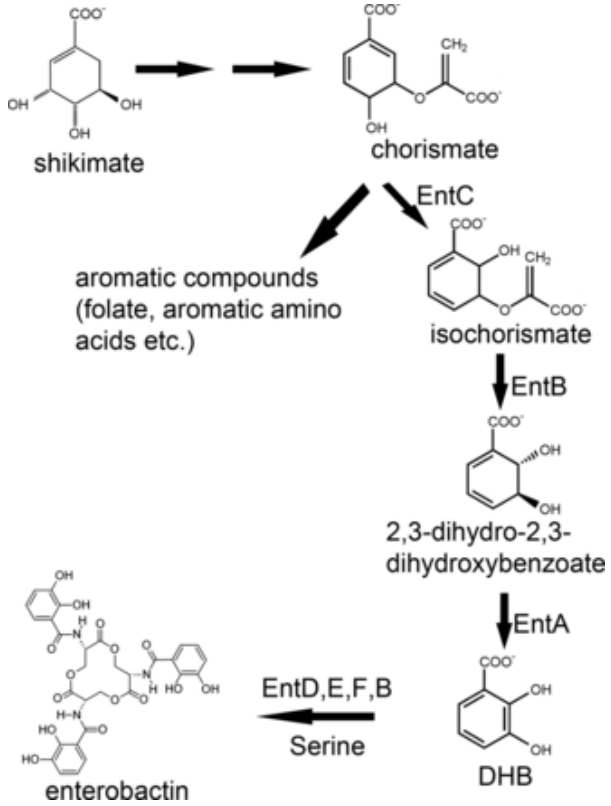

Figure 1.4. The function of six genes (*entA* to -*F*) encoding enzymes for enterobactin biosynthesis. Enterobactin is synthesized from chorismate, which is derived from the shikimic acid pathway. EntC, the isochorismate synthase, converts chorismate to isochorismate; EntB, the isochorismatase, converts isochorismate to 2,3-dihydro-2,3-dihydroxybenzoate; and EntA, the 2,3-dihydro-2,3-dihydroxybenzoate dehydrogenase, converts 2,3-dihydro-2,3-dihydroxybenzoate to DHB. EntDEF, together with the bifunctional enzyme EntB, converts DHB to enterobactin, which is the precursor of salmochelin (Ma & Payne, 2012).

Despite its high affinity for iron, enterobactin is not as effective as other siderophores *in vivo* (Konopka *et al.,* 1982; Montgomerie *et al.,* 1984), and this poor performance appears to be related to its rapid clearance from the serum (Konopka & Neilands, 1984). An unknown factor in serum was found to impede transfer of iron from transferrin to enterobactin, and from Fe-enterobactin to *E. coli* (Konopka & Neilands, 1984). However, serum has little impact on iron chelation by another siderophore synthesised by *E. coli*, aerobactin (Konopka & Neilands, 1984). Aerobactin was also shown to provide a significant selective advantage for *E. coli* growth *in vitro* (Williams & Carbonetti, 1986), and in a cutaneous infection model (Demir & Kaleli, 2004), even though its affinity for iron is weaker than that of enterobactin (formation constants of 10^{23} and 10^{52} M^{-1}, respectively; Neilands, 1981). Similar findings were found for *S. enterica*, as enterobactin is not a virulence factor for *S.* Typhimurium or *S.* Enteritidis in mouse and chicken infection models (Benjamin *et al.,* 1985; Rabsch *et al.,* 2003). Later, the serum factor responsible for limiting the action of enterobactin was identified as an acute-phase protein, called LCN2 (lipocalin 2 or neutrophil gelatinase-associated lipocalin) (Goetz *et al.,* 2002), that previously had an unclear specific purpose. LCN2 was subsequently found to be induced and secreted in response to activation of Toll-like innate immune receptors (Flo *et al.,* 2004), bind to enterobactin (Goetz *et al.,* 2002) and inhibit enterobactin activity partly through rapid clearance from the serum (Devireddy *et al.,* 2005), and thus shown to function as a 'siderocalin' (siderophore-binding lipocalin).

1.3.1.3 Salmochelin – a glucosylated siderophore, promoting *Salmonella* pathogenicity through LCN2 evasion

Salmochelin S4 is a diglucosyl-C enterobactin (DGEnt; Figure 1.5). The affinity of salmochelin for Fe^{3+} is not reported (Valdebenito *et al.,* 2006; Watts *et al.,* 2012), however, it is assumed that glucosylation does not significantly impact Fe^{3+} ligation or affinity (Luo *et al.,* 2006). The genetic locus responsible for the glucosylation of enterobactin in *Salmonella* is the *iro*-gene cluster (or '*iroA* locus') (Hantke *et al.,* 2003). This locus consists of two convergent transcription units, *iroBCDE* and *iroN* (Figure 1.7; Bäumler *et al.,* 1998). Salmochelin synthesis involves the di-glucosylation of enterobactin into S4 in a step catalysed by the glucosyltransferase, IroB (Bister *et al.,* 2004); the resulting salmochelin is then exported across the cytosolic membrane by IroC (Crouch *et al.,* 2008; Figure 1.6). Once complexed with ferric iron, ferric-salmochelin is

taken up across the outer membrane via IroN (Hantke *et al.*, 2003) and is subsequently linearized to the S2 form by the periplasmic IroE esterase (Lin *et al.*, 2005; Zhu *et al.*, 2005). The S2 form is then transported into the cytoplasm *via* FepBCDG (which also imports enterobactin) (Crouch *et al.*, 2008). The imported S2 salmochelin is further esterified by IroD into monomeric and/or dimeric forms, which is presumed to facilitate iron release (Lin *et al.*, 2005; Zhu *et al.*, 2005). The resulting degradation products, S1 and SX (mono-glucosylated dimer and monomer, respectively; Figure 1.5), are exported from the cytoplasm into the medium where they potentially contribute to iron acquisition (Lin *et al.*, 2005; Zhu *et al.*, 2005).

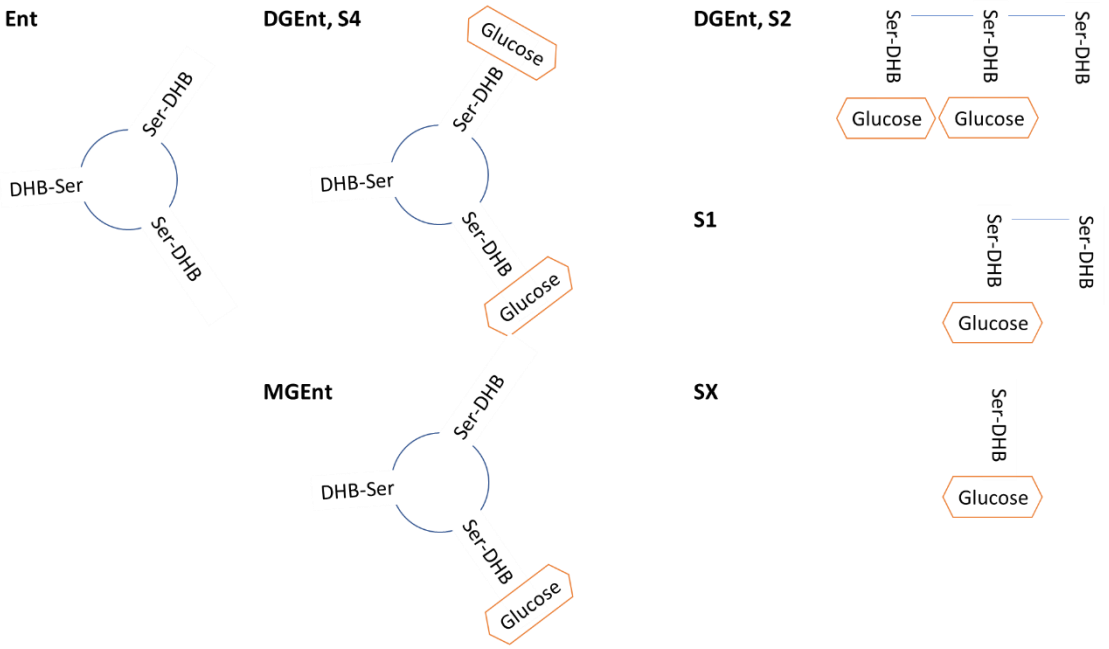

Figure 1.5. Schematic representation of Ent, S4 and its derivatives. Salmochelin S4 and S2 are both di-glucosylated forms of enterobactin (DGEnt) but the latter is linear. MGEnt is a 2,3-dihydroxybenzoyl serine macrotrilactone that is glucosylated only once. The salmochelin degradation products, S1 and SX are the mono-glucosylated dimer and monomer, respectively. Ser, serine; DHB, dihydroxybenzoate (Julien *et al.*, 2019).

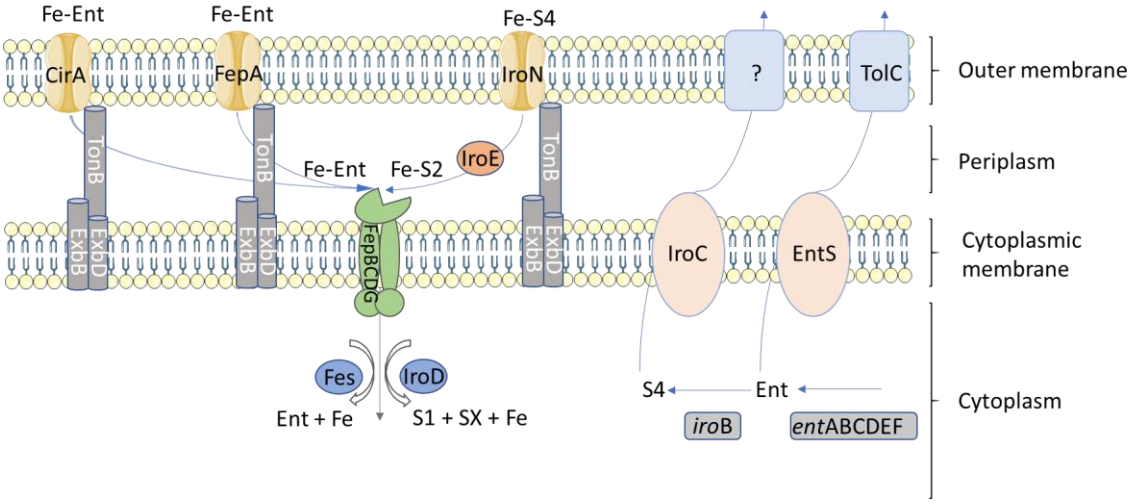

Figure 1.6. Summary of synthesis, export, import, utilisation of enterobactin and salmochelin. Enterobactin (synthesised by EntABCDEF) is mono- or di-glucosylated by IroB. The first is exported outside the cytoplasm through EntS and the latter through IroC. TolC is then involved in enterobactin efflux across the outer membrane. Once complexed with ferric iron, ferri-salmochelin is taken up across the outer membrane via IroN and is then linearized to the S2 form by the periplasm IroE esterase, whereas ferri-enterobactin is taken up via CirA, or FepA. The Fe-S2 and Fe-Ent are then transported into the cytoplasm via the FepBCDG ATP-binding cassette transporter; they are then esterified by the IroD and Fes esterase, respectively, which are presumed to facilitate iron release. The resulting salmochelin degradation products, S1 and SX are exported from the cytoplasm into the medium. It is important to note that the iro-gene cluster is coding for proteins that have better affinity for salmochelin but can also interact with enterobactin (Julien *et al.*, 2019).

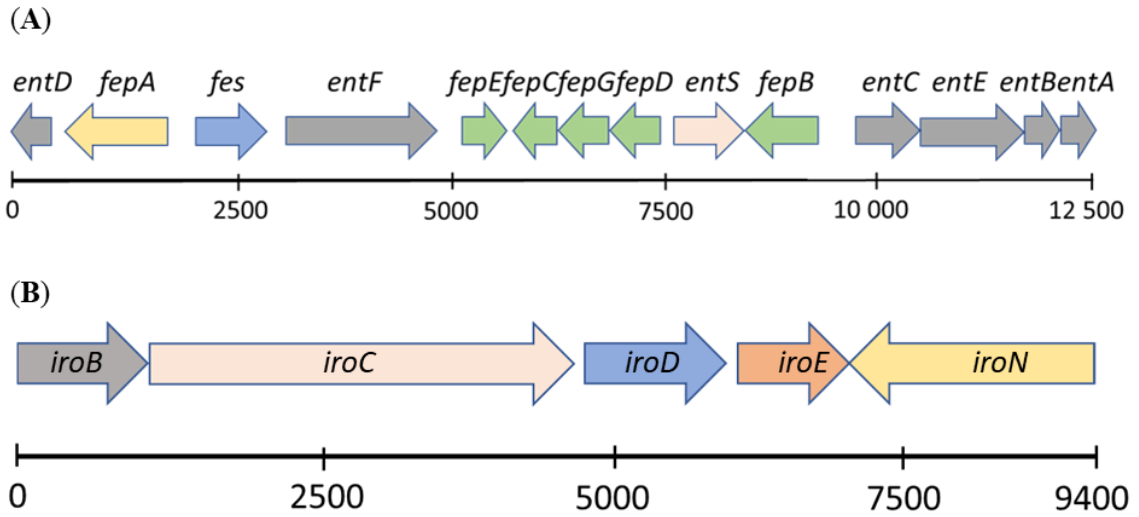

Figure 1.7. **A.** Genetic organisation of the enterobactin synthesis (*entABCDE*), export (*entS*), import (*fepABCDEG*) and utilisation loci (*fes*) (adapted from Crouch *et al.*, 2008) **B.** Operon of the iron-regulated, *iroBCDE* and *iroN* genes in *Salmonella*. The scale indicates the length of the operon in bp (Müller *et al.*, 2009).

Initially, the reason for the glucosylation of enterobactin (generating salmochelin) was unclear. Subsequently, it was discovered that although LCN2 has high affinity for enterobactin (equilibrium dissociation constant or K_D of 0.41 ± 0.11 nM) and its derivatives/precursors (DHB, K_D of 7.9 ± 1.8 nM), as well as other catecholate-type ferric siderophores (e.g. parabactin, cepabactin and carboxymycobactins; Goetz *et al.,* 2002; Holmes *et al.*, 2005), it does not effectively bind to salmochelin S4 (Fischbach *et al.,* 2006; Valdebenito *et al.,* 2006). Furthermore, the LCN2 receptor, 24p3, was shown to mediate the import of ferri-siderophore-bound LCN2 into mammalian cells, removing both the iron and enterobactin from circulation (Devireddy *et al.,* 2005). Thus, glucosylation of enterobactin is considered to be a strategy employed by pathogens to prevent siderophore sequestration and removal from circulation by LCN2.

LNC2 was originally identified as a component of neutrophil granules but is also expressed in epithelial cells in response to inflammatory signals (Kjeldsen *et al.,* 1993). Nielsen *et al.* (1996) revealed that LCN2 might bind lipophilic inflammatory mediators like platelet-activating factor, leukotriene B4 and lipopolysaccharides. This led to the initial suggestion that LCN2 acts as immune-modulatory factor through transport of lipophilic molecules to inflammation sites (Goetz *et al.,* 2000). As eluded to above, a clearer purpose for LCN2 became apparent when the protein was produced heterologously in *E. coli* and was isolated bound, surprisingly, to a red chromophore, which was subsequently identified as enterobactin (Goetz *et al.*, 2002).

This finding led to further studies demonstrating a role for LCN2 in host-pathogen interactions (Bachman *et al.*, 2012; Fischbach *et al.,* 2006; Flo *et al.,* 2004). These further studies showed that the *iro*-gene cluster confers resistance to the growth inhibitory effects of LCN2 *in vitro* and that mice rapidly succumb to infection by *E. coli* H9049 harbouring the *iro*-gene cluster, but not its *iro*-free counterpart (Fischbach *et al.,* 2006). Other studies showed that salmochelin contributes to virulence of both avian pathogenic and uropathogenic *E. coli* (APEC and UPEC) through its iron-binding activity (Gao *et al.,* 2012). Indeed, salmochelin-defective mutants of APEC E058 and UPEC U17 showed significantly decreased pathogenicity compared to the wild-type (WT) strains in a chicken infection model (Gao *et al.,* 2012). Likewise, the efficient glucosylation (IroB), transport (IroC and IroN) and processing (IroE and IroD) of salmochelins were shown to be required for APEC virulence (Caza *et al.,* 2008). The role of glucosylation in *S. enterica* pathogenicity was further illustrated by the observation that the *iro* locus confers a

competitive advantage to *S.* Typhimurium in colonizing the inflamed intestine of WT, but not of LCN2-deficient, mice (Raffatellu *et al.* 2009). It should be noted that it has been suggested that the glucosylation and linearisation of enterobactin enhances the activity of salmochelin through increasing its hydrophilic nature, which might be advantageous for iron scavenging in a membrane-rich microenvironment (Luo *et al.*, 2006).

1.3.2 Egg white 'lipocalins' – role in enhancing iron restriction through sequestration of bacterial siderophores?

1.3.2.1 Evidence for the presence of lipocalins in egg white

LCN2 belongs to the 'lipocalin superfamily' which includes a variety of proteins (e.g purpurin, retinol-binding protein, α-1-glycoprotein, apolipoprotein, probasin, α-1-microglobulin and prostaglandin D synthetase) involved in transport of hydrophobic ligands. Although the family members display low overall sequence identity (Greene *et al.*, 2003), lipocalins share a common three-dimensional structure characterised by an eight-stranded β-barrel with a small C-terminal helix that forms a calyx, at the bottom of which the hydrophobic ligand is bound (Figure 1.8; Gachon, 1994). Due to their diversity, lipocalins have various functions e.g. in immune response, pheromone transport, biological prostaglandin synthesis, retinoid binding and cancer cell interactions (Flower, 1996). Lipocalins can be divided into two major subfamilies (see the Pfam database; El-Gebali *et al.*, 2019). One subfamily (PF00061) consists of ~4000 Pfam entries that are mostly (88%) from Metazoan species, and includes LCN2, whereas the other subfamily (PF08212) consists of ~3000 entries, mostly from (67%) Bacteria. Lipocalins are predominantly (92%) single domain proteins and multiple homologues are found in vertebrates (e.g. there are 37 lipocalins identified in the human genome; Du *et al.*, 2015).

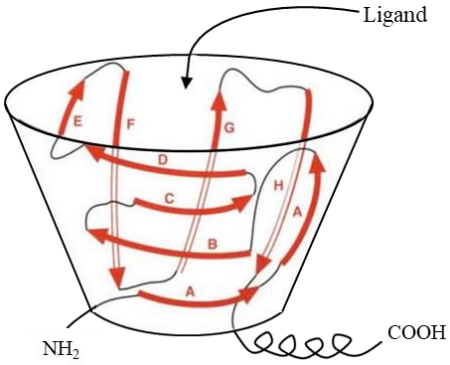

Figure 1.8. Schematic representation of the structure of lipocalins. The structure in calyx allows binding of a hydrophobic ligand (Gachon, 1994).

Since lipocalins are found throughout most of the living kingdom, it may not be surprising to find that they are present in EW. Extracellular fatty-acid-binding protein (Ex-FABP) was the first lipocalin identified in EW and was discovered by a proteomic analysis of hen EW using 2-dimensional gel electrophoresis (2-DE) followed by liquid chromatography-mass spectroscopy (LC-MS/MS) (Desert *et al.*, 2001). Further work by Guérin-Dubiard *et al.* (2006) using 2-DE, LC-MS/MS and MALDI-TOF identified a total of 16 proteins in hen EW, including Ex-FABP as well as two other lipocalins, chondrogenesis-associated lipocalin (Cal-γ or prostaglandin D synthase) and α1-ovoglycoprotein (Figure 1.9). The presence of the three lipocalins in EW was later confirmed by further proteomic analyses involving 1-DE with LC–MS/MS, 2-DE combined with protein-enrichment (peptide ligand libraries) technology, and a dual-pressure linear-ion-trap Orbitrap instrument (LTQ Orbitrap Velos) (Mann, 2007; D'Ambrosio *et al.*, 2008; Mann & Mann, 2011).

The level of α1-ovoglycoprotein in EW was previously estimated as ~1 g/L (Ketterer, 1965). Although the concentrations of the two other lipocalins have not been reported, in the Guérin-Dubiard *et al.* (2006) study the intensities of the Cal-γ and Ex-FABP 2-DE spots were weak suggesting a very low concentration (Figure 1.9). In other work (Mann, 2007; Mann & Mann 2011), the exponentially-modified-protein abundance index (emPAI) was used to provide an estimate of the absolute abundance of each EW protein, which indicated that Cal-γ and Ex-FABP belong to the 'minor proteins' set (such as avidin, cystatin, apolipoprotein D, HEP21, Defensin-11) rather than the 'major proteins' set (such as ovalbumin (Figure 1.9), ovotransferrin, lysozyme, ovomucoid and ovoinhibitor). In summary, although several studies have shown that three lipocalins are

present in EW, the exact concentrations of Cal-γ and Ex-FABP remains unclear. Their biological significance in EW also remains to be established.

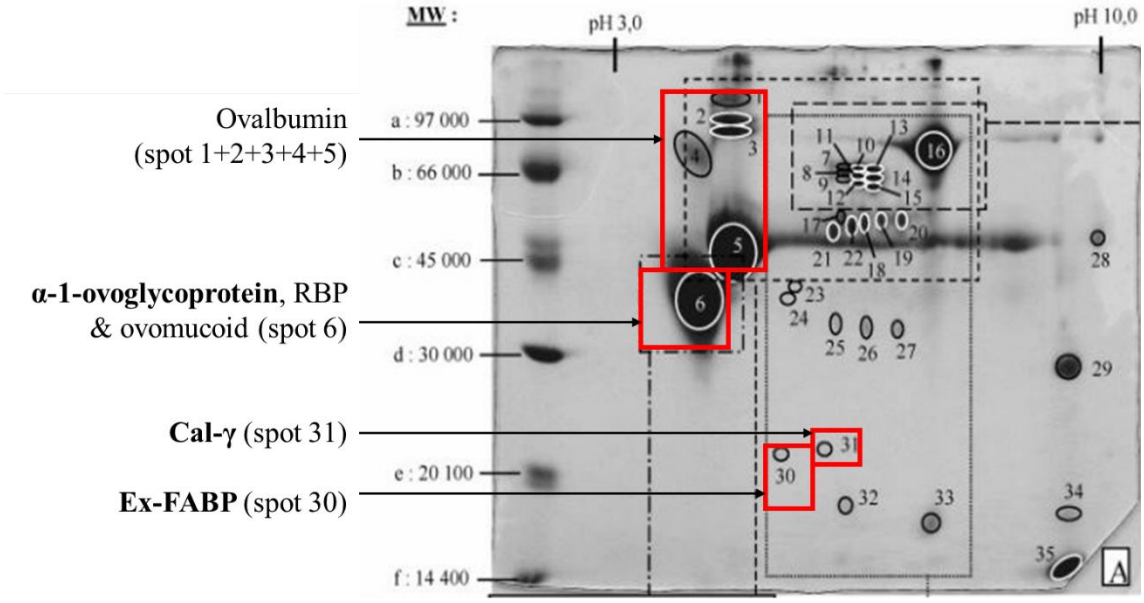

Figure 1.9. Two-dimensional electrophoresis of hen EW proteins. An amount of 1000 µg of total protein was loaded on the gel (Guérin-Dubiard *et al.*, 2006). In bold are indicated the three EW lipocalins. Ovalbumin is indicated as a reference as it is the most abundant protein of EW (54 g/L; Table 1.2).

1.3.2.2 Sequestration of bacterial siderophores by the lipocalin Ex-FABP

Ex-FABP was first discovered as a fatty-acid-binding protein with a role in hen-embryo development. Cancedda *et al.* (1988) were the first to report and identify Ex-FABP (Ch21) as a protein expressed and secreted by *in vitro* differentiating hen chondrocytes at a late stage of development. Ex-FABP was later shown to be a 21 kDa protein in cartilage (Cancedda *et al.*, 1988), muscle tissue (Gentili *et al.*, 1998) and granulocytes (Dozin *et al.*, 1992) of chicken embryos. This protein was classified as a member of the superfamily of lipocalins and thus was considered to have a likely role in the transport of small hydrophobic molecules (Cancedda *et al.*, 1990). The protein was renamed (from Ch21) 'extracellular fatty acid-binding protein' because of its ability to selectively bind and transport fatty acids (i.e. oleic, linoleic, and arachidonic acids) in extracellular fluids and serum (Cancedda *et al.*, 1996). It was shown to be expressed during muscle-fibre formation (Gentili *et al.*, 1998) and later shown to be involved in endochondral-bone formation (Cermelli *et al.*, 2000, Gentili *et al.*, 2005). Transfection of proliferating chondrocytes and myoblasts with an expression vector expressing antisense Ex-FABP cDNA led to a decreased cell viability. Therefore, Ex-FABP seems to play a

part in cell differentiation and cell survival (Di Marco *et al.*, 2003; Gentili *et al.*, 2005). It was more recently shown that Ex-FABP binds the C16 and C18 isoforms of lysophosphatidic acid (LPA, 1- or 2-acyl-*sn*-glycerol-3-phosphate) (Correnti *et al.*, 2011). LPAs are phospholipids mediating differentiation, inflammation, immune function, oxidative stress, cell migration, smooth muscle contraction, apoptosis and development (Zhao & Natarajan, 2014). It is likely that the functions of Ex-FABP reported above depend on its role in sensing or transporting phospholipids (Sia *et al.*, 2013).

More recent reports indicate that Ex-FABP functions in pathogen defence through an ability to bind siderophores, in a manner analogous to that of LCN2 (Correnti *et al.*, 2011; Garénaux *et al.*, 2013). This suggests that Ex-FABP may have two distinct purposes, one in fatty acid/LPA binding and another as a siderophore-binding factor. Work of Correnti *et al.* (2011) shows that Ex-FABP sequesters ferric-enterobactin, as well as its mono-glucosylated (Fe-MGEnt) form, with an equilibrium dissociation constant (K_D) of 0.22 and 0.07 nM, respectively, but not its di-glucosylated form (Fe-DGEnt; K_D > 600 nM; Table 1.5). Furthermore, Ex-FABP at 4 µM caused growth inhibition of both *E. coli* and *Bacillus subtilis* under iron-limited *in vitro* conditions. Growth was restored by supplementing the cultures with stoichiometric amounts of $FeCl_3$ (Correnti *et al.*, 2011). Thus, Ex-FABP might act to reduce bacterial growth in EW by enhancing iron restriction. Ex-FABP did not inhibit *Pseudomonas aeruginosa* growth under iron limitation, which correlates with the observation that Ex-FABP does not bind the corresponding siderophores. Indeed, both enterobactin and bacillibactin produced by *E. coli* and *B. subtilis* (respectively) were found to be sequestrated by Ex-FABP (K_D of 0.5 and 30 nM, respectively; Table 1.5), while pyochelin and pyoverdine produced by *P. aeruginosa* were not (Correnti *et al.*, 2011). These findings are also in accordance with those from Garénaux *et al.* (2013) showing that *E. coli* K-12 is subject to a 10^5-fold growth reduction when exposed to 2.5 µM Ex-FABP or LCN2. However, when transformed with a plasmid harbouring the *iroBCDEN* cluster, no growth defect was observed with 2.5 µM Ex-FABP or LCN2. Exposure of six poultry APEC isolates to 2.5 µM Ex-FABP or LCN2 inhibited the growth of strains producing enterobactin as sole siderophore, but not those producing additional siderophores (salmochelin, aerobactin and/or yersiniabactin) (Garénaux *et al.*, 2013). Therefore, it can be concluded that Ex-FABP is an avian siderocalin-type lipocalin with a function similar to that of LCN2.

Table 1.5. Apo and ferric siderophore binding affinities with Ex-FABP. The detection threshold for this assay corresponds to a $K_D \leq 600$ nM (Correnti *et al.*, 2011).

Siderophore	***K_D (nM)***	***Siderophore type***	***Specie***
Apo-Ent	0.5 ± 0.15	catechol	*Escherichia coli* *Salmonella enterica*
Fe-Ent	0.22 ± 0.06	catechol	*Escherichia coli* *Salmonella enterica*
Fe-Parabactin	42 ± 8	catechol/hydroxyphenyl-oxazoline	*Paracoccus denitrificans*
Apo-Bacillibactin	30 ± 2	catechol	*Bacillus* sp.
Fe-Bacillibactin	14 ± 2.0	catechol	*Bacillus* sp.
Apo-MGE	1.1 ± 0.15	catechol derivative	*Salmonella enterica*
Fe-MGE	0.07 ± 0.02	catechol derivative	*Salmonella enterica*
Fe-DGE	> 600	catechol derivative	*Salmonella enterica*
Fe-(Pyochelin)$_2$	> 600	hydroxyphenyl-thiazoline	*Pseudomonas aeruginosa*
Fe-Pyoverdine	> 600	catechol derivative	*Pseudomonas aeruginosa*
Fe-Rhizoferrin	> 600	citrate	Fungus
Fe-DesferrioxamineB	> 600	hydroxamate	*Streptomyces pilosus*
Fe-(Alcaligin)$_3$	> 600	hydroxamate	*Bordetella pertussis*
Fe-Petrobactin	> 600	citrate/catechol	*Bacillus anthracis* *Bacillus cereus*
Fe-Aerobactin	> 600	citrate/hydroxamate	*Escherichia coli*
Fe-ExochelinMS	> 600	hydroxamate	*Mycobacteriasmegmatis*
Fe-Coprogen	> 600	hydroxamate	*Neurospora crassa*

The pleiotropic function (i.e. siderophore and LPA binding) of Ex-FABP might be explained by the large binding site of the molecule (Sia *et al.*, 2013). Ex-FABP has a three-dimensional fold common to that of lipocalin family proteins but has an extra α-helix (residues 22–30) and a short helical element (residues 139–141). This results in an extended calyx that encompasses upper and lower cavities (Figure 1.10A). The upper cavity comprises a siderophore-binding site with three catechol-binding pockets involving basic residues (K82, R101 and R112) key to ligand binding (Correnti *et al.*, 2011). K82 forms hydrogen bonds with the 3-OH of the catechol groups, while R101 and R112 provide significant electrostatic contributions to ligand-binding. The lower cavity

acts as a hydrophobic binding site that can bind C16 and C18 LPA (Figure 1.10B). Modelling of the complex shows that the side-chains Y50, K82, R112 and Y114 of Ex-FABP make hydrogen bonds with LPA (Correnti *et al.*, 2011).

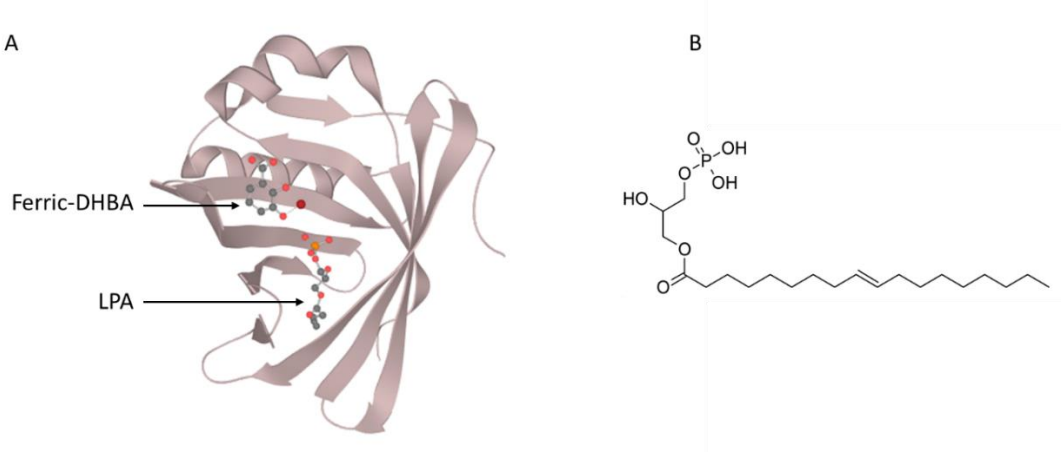

Figure 1.10. A. X-ray diffraction (1.8Å resolution) of Ex-FABP; two ligands are represented, ferric-DHB on the upper cavity and LPA on the lower cavity. Structure extracted from Protein Data Bank in Europe (PMID: 22153502; Correnti *et al.*, 2011). B. Structure of a C18 LPA (Julien *et al.*, 2019).

1.3.2.3 Alpha1-ovoglycoprotein and Cal-γ – their potential functions in EW

In EW, α1-ovoglycoprotein has an average molecular weight of 30 kDa, an isoelectric point of 4.37–4.51 and a sugar content of about 25% (Matsunaga *et al.*, 2004). While little is known about its function, this ovoglycoprotein is often used for its chiral properties to separate drug enantiomers (Sadakane *et al.*, 2002; Haginaka & Takehira, 1997). However, its biochemical, functional and biological properties in EW remain unknown.

Cal-γ is a lipocalin-like prostaglandin synthase (PTGDS). In EW, two isoforms, of 22 kDa, can be separated by 2-DE thanks to their different isoelectric points (pI of 5.6 and 6.0) (Guérin-Dubiard *et al.*, 2006). Pagano *et al.* (2003) have shown that Cal-γ expression correlates with endochondral bone formation and the inflammatory response. As for Ex-FABP, Cal-γ mRNA is increasingly synthesized during chondrocyte differentiation both *in vivo* and *in vitro*. Although Ex-FABP and Cal-γ may both play a part in bone formation and the inflammatory response, any possible role for Cal-γ in siderophore sequestration remains to be explored.

1.4 Approaches set in the PhD proposal

The antibacterial iron-restriction activity of EW, as mediated by oTf, is well established and it is now apparent that the EW lipocalin, Ex-FABP, can inhibit bacterial growth *via* an enhanced iron-restriction effect that is mediated by its siderophore-binding capacity (i.e. Fe-enterobactin sequestration). However, the siderophore-sequestering activity of Ex-FABP has neither been studied in EW, nor with appropriate *S.* Enteritidis or hen infection models. Furthermore, the concentration that this protein is found in EW remains unknown. As of yet, it is unclear whether the other lipocalins of EW (Cal-γ and α1-ovoglycoprotein) might also sequester siderophores. Although many EW proteins have been shown to be components of the arsenal of defence factors within EW, the contribution (if any) of the three lipocalins as new EW defence factors remains an open question. As matters stand, it is unclear whether the capacity of salmochelin to assist *S.* Enteritidis virulence in mammalian models can be extended to include support of *S.* Enteritidis survival or growth in EW (Figure 1.11). Thus, there remains much scope for further understanding of the role of lipocalin proteins in the defence of EW against bacteria and more research is required to understand all the components involved.

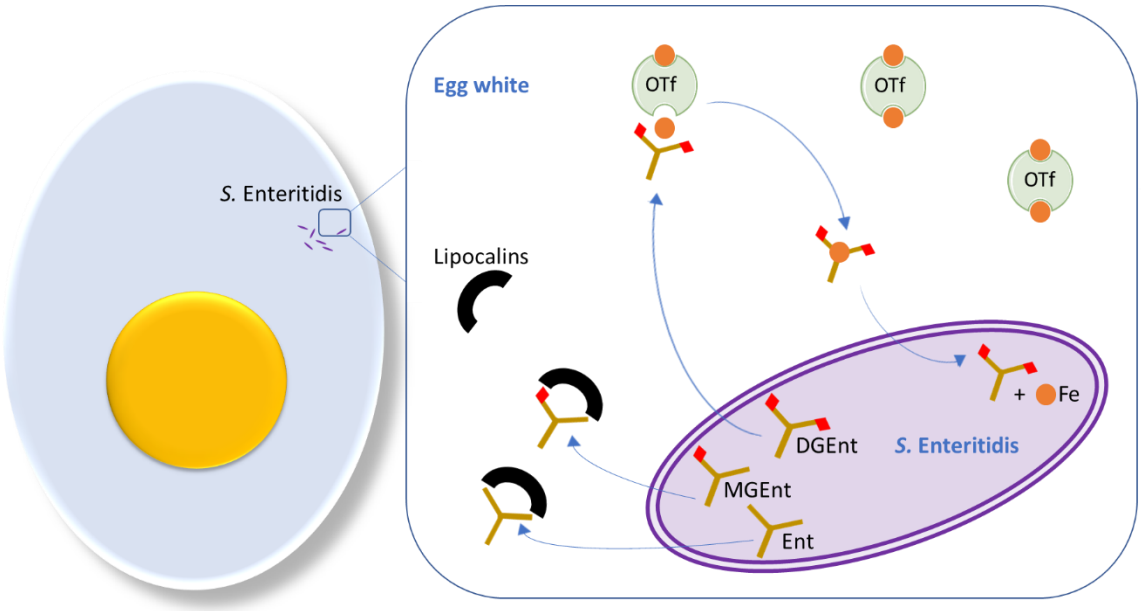

Figure 1.11. Potential interactions between *S.* Enteritidis siderophores and EW lipocalins. In the EW, enterobactin (Ent) and MGEnt might be sequestrated by lipocalin (represented by black semi-circles), while DGEnt would remain free to chelate iron from ovotransferrin (oTf indicated as green) and thus provide iron (drawn as orange circles) to *S.* Enteritidis (glucosylation are shown as red diamonds). After import into the cytoplasm, at last, iron is released into the cytoplasm (Julien *et al.*, 2019).

The aim of this PhD project is to determine whether EW lipocalins inhibit bacterial growth through their siderophore-binding activity and whether *S.* Enteritidis can avoid this effect through deployment of salmochelin. Part of this aim involves the followings:

- *Isolation of recombinant EW-lipocalins* (Chapter 3). Genes encoding the three EW lipocalins (Ex-FABP, Cal-γ and α1-ovoglycoprotein) and human lipocalin-2 (LCN2) will be codon-optimised (for *E. coli*) and overexpressed in *E. coli* to give C-terminal hexa-His-tagged recombinant proteins. The EW proteins will be expressed with an N-terminal PelB signal sequence (PelBss) to enable their secretion into, and purification from, the periplasm. Purification will then be achieved using Ni^{2+}-affinity and ion-exchange chromatography.

- *Quantification of EW lipocalins and determination of their siderophore-binding activity* (Chapter 4). Antibodies against lipocalins will be raised to quantify the amount of proteins naturally found in EW. Then, analysis of the lipocalin binding activity with 2,3-dihydroxybenzoic acid (2,3-DHBA) and derivatives will be measured through tryptophan quenching fluorescence, biolayer-interferometry and isothermal titration calorimetry. The human lipocalin-2 will be used as a control since it is well known to exert a growth-inhibitory effect by sequestering ferric-enterobactin (Goetz *et al.*, 2002).

- *Determination of the role of EW lipocalins in inhibiting siderophore-dependent iron sequestration by* Salmonella *Enteritidis* (Chapter 5). The production of mutants knocked-out for enterobactin synthesis (*entB*) as well as for salmochelin synthesis/export (*iroBC*) and import (*iroDEN*) will be generated. The mutants will be used to determine whether exposure to lipocalins limits *S.* Enteritidis growth and whether salmochelin secretion overcomes any observed inhibition by lipocalins and might thus contribute to *S.* Enteritidis survival or growth in standard growth media and EW.

Chapter 2. Materials and methods

2.1 Reagents and chemicals

2.1.1 Growth media

2.1.1.1 Standard growth media

Lysogeny broth (LB, 5 g/L yeast extract, 10 g/L tryptone and 5 g/L NaCl) was used as the growth medium for *E. coli*. Tryptone soy broth (TSB, Merck, Darmstadt, Germany) or LB were used for the growth of *Salmonella*. When siderophore production was not desirable, LB (~4 µM Fe) was enriched with 10 µM ferric citrate. On the other hand, to trigger production of siderophores, minimal medium (1X M9 salts, 1 mM $MgSO_4.7H_2O$, 0.2% gucose, 5 µg/mL thiamine, 0.1 mM $CaCl_2$, 0.3% casamino acids in acid washed glassware: soaked in 5% HCL for 20 min) was used for growth. Sterile super optimal broth (SOC) with catabolite repression (2% tryptone, 0.5% yeast extract, 10 mM NaCl, 10 mM $MgCl_2$ and 10 mM $MgSO_4$) was used for electroporation. It is important to note that in the above recipes, casamino acids, thiamine and $MgCl_2$ were filter sterilised (0.22 µm Millipore filters). When solid medium was required, agar (15 g/L) was added to the recipes above before sterilisation (for 21 min at 120 °C).

2.1.1.2 Egg white media

Eggs between one week to ten days old from conventional hen housing systems were purchased. Eggs were washed with 100% ethanol and blazed for 2 s before use. Then, egg white (EW) and egg white filtrate (EWF) were prepared as described below.

EW was aseptically separated from the egg yolk and homogenised using a sterilised Ultra Turrax Disperseur DI 25 (Yellow^{line}, IKA, Staufen, Germany) for 1 min at 9500 rpm. Between each EW sample, the Ultra Turrax spindle was washed with 2% detergent (RBS, Merck) for 30 s, then sterile dH_2O for 30 s, 70% ethanol for 30 s and finally sterile dH_2O for 30 s.

EWF was prepared by ultrafiltration using a pilot unit (TIA, Bollène, France) equipped with an Osmonics membrane (5.57 m^2, 10 kDa cut-off; PW 2520F, Lenntech BV, Delft, Netherlands) according to Baron *et al.* (1997). EWF was sterilised by filtration (Nalgene® filter unit, pore size < 0.2 µm, Osi, Elancourt, France), and then stored at 4 °C until use. EWF has the same pH and ionic strength as EW but does not contain EW macromolecules above 10,000 Da. ICP-OES analysis of EWF (conducted in another project) showed that iron content is under the method detection threshold (< 0.02 µM).

Both EW and EWF pH (9.3 ± 0.1) and sterility were routinely assessed. Steriliy was confirmed by inoculating motlen tryptone soy agar (TSA, Merck) with 1 mL of medium in a Petri dish. Lack of colony formation after overnight incubation at 37 °C confirmed sterility.

2.1.2 Antibiotics

Ampicillin (Amp) sodium salt and kanamycin (Kan) stocks (100 mg/mL) were dissolved in Milli-Q water and stored at -20 °C. Chloramphenicol (Cam) stock (50 mg/mL) was dissolved in 95% ethanol and stored at -20 °C. Selective plates contained either 100 µg/mL Amp, 25 µg/mL Kan or 25 µg/mL Cam in LB broth with 15 g/L of agar.

2.1.3 Bacterial strains

Bacterial strains (Table 2.1) were stored at -80 °C in 20% (v/v) glycerol.

Salmonella enterica subsp. *enterica* serovar Enteritidis (*S.* Enteritidis) PT4-P125109 was provided by Matthew McCusker (Center for Food Safety and Food Borne Zoonomics, Veterinary Sciences Centre, University College Dublin, Ireland; NCTC13349). This strain was isolated from a food poisoning outbreak in the UK (genome accession number: AM933172). From this strain, three mutants deficient in siderophore production and/or utilisation were engineered (Δ*iroDEN*, Δ*iroBC*, Δ*entB*)

Cells for cloning. The host *E. coli* Top10 (Invitrogen, Madison, USA) was used to clone plasmids with high yield and quality. The latter was chosen for its reliability, growth and transformation efficiency due to the *endA* mutation in the non-specific endonuclease I and the *recA* mutation in the gene responsible for general recombination of DNA.

Cells for protein overproduction. λDE3-hosts (carrying a chromosomal copy of T7 RNA polymerase) were used for overexpression of lipocalin-genes cloned into pET21a. BL21(λDE3) cells, convenient for high-level protein production, were used at first (Studier *et al.,* 1990). C41-(λDE3) and Lobstr-BL21(λDE3) were then used in an attempt to enhance the solubility of the α1-ovoglycoprotein (Miroux & Walker, 1996; Andersen *et al.,* 2013). Finally, to ensure that lipocalins were not co-purified with bacterial siderophores, an *E. coli* strain deficient in siderophore synthesis (JW0587; GE Healthcare, Chicago, USA) was converted to λDE3-lysogen status.

Table 2.1. Bacterial strains used and their genetic features

Strain name	*Features*	*Source*
BL21(λDE3)	F$^-$ *ompT hsdSB* (rB$^-$ mB$^-$) *gal dcm* (λDE3)	Studier *et al.*, 1990
C41(λDE3)	F$^-$ *ompT hsdSB* (rB$^-$ mB$^-$) *gal dcm* (λDE3)	Miroux & Walker, 1996
E. coli Top10	F$^-$ *mcrA* Δ(*mrr-hsdRMS-mcrBC*) Φ80*lacZ*ΔM15 Δ*lacX74 recA1 araD139* Δ(*ara leu*)7697 *galU galK rpsL* (Str^R) *endA1 nupG*	Invitrogen
JW0587	*E. coli* K-12, strain BW25113 (Δ*entB*)::*kan*	GE Healthcare
JW0587(λDE3) (SCA2264)	*E. coli* K-12, strain BW25113 (Δ*entB*)::*kan* (λDE3)	This study
LOBSTR-BL21(λDE3)	F$^-$ *ompT hsdSB* (rB$^-$ mB$^-$) *gal dcm* (λDE3)	Andersen *et al.*, 2013
PT4-P125109	Wild type *Salmonella enterica* serovar Enteritidis PT4-P125109	McCusker Dublin, Ireland
PT4-P125109 ΔentB (SCA2263)	*Salmonella enterica* serovar Enteritidis PT4-P125109 Δ*entB*	This study
PT4-P125109 ΔentB::cat (SCA2260)	*Salmonella enterica* serovar Enteritidis PT4-P125109 Δ*entB*::*cat*	This study
PT4-P125109 ΔiroDEN (SCA2269)	*Salmonella enterica* serovar Enteritidis PT4-P125109 Δ*iroDEN*	This study
PT4-P125109 ΔiroDEN::cat (SCA2266)	*Salmonella enterica* serovar Enteritidis PT4-P125109 Δ*iroDEN*::*cat*	This study
PT4-P125109 ΔiroBC (SCA2273)	*Salmonella enterica* serovar Enteritidis PT4-P125109 Δ*iroBC*	This study
PT4-P125109 ΔiroBC::cat (SCA2270)	*Salmonella enterica* serovar Enteritidis PT4-P125109 Δ*iroBC*::*cat*	This study

2.1.4 Plasmids

Plasmids used during this study are summarised in Table 2.2.

Plasmids carrying lipocalin-genes. Plasmids pMK (kanamycin resistant) containing the *LCN2, Ex-FABP, α1-ovoglycoprotein* or *Cal-γ* insert were synthesized by GeneArt (Invitrogen). Plasmid pET21a was used for overexpression (Novagen, Madison, USA). This high copy number plasmid served as a vector for overexpression in λDE3-hosts.

Plasmids used for λRed homologous recombination. pKD3 is a template plasmid for amplification of the FRT-flanked Cat cassette. pKD46 is a temperature sensitive (Ts) plasmid (30 °C) that enhances homologous recombination thus increasing the efficiency of the chromosomal gene deletion process. This lambda red expressing vector encodes *exo, beta* and *gam* which are induced when *araC* repression is relieved with the addition of L-arabinose (Datsenko & Wanner, 2000). pCP20 is also a Ts plasmid (30 °C) that encodes FLP recombinase and allows Cat^R cassette removal (Cherepanov & Wackernagel, 1995).

Table 2.2. Plasmids used and their features

Plasmid	*Size (bp)*	*Features*	*Resistance*	*Source*
pMK-lcn2	2930	Encodes *lnc2*	Kan	GeneArt
pMK-Ex-FABP	2860	Encodes *Ex-Fabp*	Kan	GeneArt
pMK-Cal-γ	2881	Encodes *Cal-γ*	Kan	GeneArt
pMK-α1-ovoglyco	2935	Encodes *α1-ovoglyco-protein*	Kan	GeneArt
pET21a	5443	Requires T7 RNA polymerase and under LacUV5 control	Amp	Novagen
pET-lcn2	5904	pET21a vector used for LCN2 overproduction	Amp	This study
pET-Ex-FABP	5907	pET21a vector used for Ex-FABP overproduction	Amp	This study
pET-Cal-γ	5928	pET21a vector used for CAL-γ overproduction	Amp	This study

pET-α1-ovoglyco	5982	pET21a vector used for α1-ovoglycoprotein overproduction	Amp	This study
pKD3	2804	λ *red* template vector	Cam, Amp	Datsenko & Wanner, 2000
pKD46	6329	Ts (30 °C), λ red expressing vector encoding *exo*, *beta* and *gam* and under *araC* control	Amp	Datsenko & Wanner, 2000
pCP20	9332	Ts (30 °C) vector encoding FLP recombinase	Cam, Amp	H. Mori, Japan

2.1.5 Oligonucleotides used for polymerase chain reaction (PCR)

PCR primers used in an attempt to generate pET21a clones *via* the Gibson method (Thomas *et al.*, 2015) are summarised in Table 2.3. PCR primers used to generate *Salmonella* deletion mutants and for post-deletion confirmation are summarised in Tables 2.4 and 2.5, respectively. The nucleotide sequences amplified can be found in Appendices 1, 2 and 3.

Table 2.3. PCR primers used in an attempt to generate pET21a clones *via* the Gibson method (bold and underlined sequences are identical to the target gene inserted in the cloning vector).

Primers	*Sequence from 5' to 3' end*	*Restriction Enzyme*	*Length (nucleotides)*	*Tm (°C)*	*Amplicon (bp)*
Lcn2_for	**AAGAAGGAGATATA**CATATGCAGGACTCCACCTCAGAC	*Nde*I	38	59.1	599
Lcn2_rev	**GGTGGTGGTGGTG**CTCGAGTTAGCCGTCGATACACTGGTCGATTG	*Xho*I	45	60.8	

Table 2.4. PCR primers used to generate *Salmonella* deletion mutants (bold colour sequences are homologous sequences to the Cat^R cassette).

Primer	*Sequence from 5'-3' end*	*Length (nucleotides)*	*Tm (°C)*	*Amplicon (bp)*
iroBC-del_for	ACTTGTTCGATTTATGACGTGGAGAGA GAGGATTTCTCATGCGTATTCTG**TGTG TAGGCTGGAGCTGCTTC**	71	64.5	1115
iroBC-del_rev	AACAGCCGCTTGCGGGCTTTCTTTTGC GTAAATCGTGGCGATAAAAACTA**CAT ATGAATATCCTCCTTAGT**	71	65	
iroDEN-del_for	TTGAGGGCAACAGCGCTACTTTAGAC ATTATTTAGGGAATGGGTATGAAA**TG TGTAGGCTGGAGCTGCTTC**	71	64.5	1115
iroDEN-del_rev	AGTACTAACCGAAATATAAATGAGAT GGAATACAAAGAATGAGACTGAGC**CA TATGAATATCCTCCTTAGT**	71	65	
entB-del_for	CGTTCACCGCTCTGAAGGAGAAAGAG AGATGGCAATCCCG**TGTGTAGGCTGG AGCTGCTTC**	61	64.5	1095
entB-del_rev	ACCCATACCGTTTTGTCTGAAAAATCA ATACAGGCCATTA**CATATGAATATCC TCCTTAGT**	61	65	

Table 2.5. PCR primers used to generate post-deletion confirmation (underlined amplicons correspond to the expected size prior to gene knockout and bold amplicons correspond to the expected size after gene knockout).

Primer	*Sequence 5'-3'*	*Length (nucleotides)*	*Tm (°C)*	*Amplicons (bp)*
iroBC_for	ATGATATTGGTAATTATTAT	20	64.5	5157 / **1209**
iroBC_rev	CGTTAGTACTAATAGCTAAAGCGGC	25	62.4	
iroDEN_for	CGTAACCTGGCAAGGATGT	19	63	4993 / **1159**
iroDEN_rev	GCCACGATTTACGCAAAA	18	62.7	
entB_for	GCCGGTTGGTAAAGTCG	17	62.2	1002 / **1177**
entB_rev	GCGTAACCGATCCCTTTC	18	62.5	

2.2 *In vitro* DNA procedures

General procedures were as previously described (Sambrook & Russell, 2001).

2.2.1 Plasmid purification

Plasmids were purified using the GeneJet plasmid miniprep kit (Thermo Scientific, Waltham, USA) according to the manufacturer's guidelines. The purified products were eluted in 30 µL of MilliQ water and stored at -20 °C.

2.2.2 Agarose gel electrophoresis

DNA fragments were analysed by electrophoresis using 0.7% agarose gels containing a final concentration of 1X GelRed™ nucleic acid gel stain. Samples (2-4 µL) were mixed with 2 µL loading dye (6X ADD; Thermo Scientific) and 6 µL MilliQ water prior to loading onto the gel. The gel was then electrophoresed in 0.5X TBE buffer (0.4 M Tris, 0.4 M boric acid, 1 mM ethylenediaminetetraacetic acid (EDTA) pH 8) at 60 V for 70 min with a 1 kb ladder as a size marker (Thermo Scientific). To reveal DNA fragments, the gel was placed under ultraviolet (UV) light using a G:BOX (Syngene, Bangalore, India). Images taken were further analysed with GeneSys image capture software (Syngene).

2.2.3 Restriction digestion

A range of 60 to 100 ng of plasmid DNA was digested with 0.5 µL (10 units) fast digestion enzyme (NEB, Ipswich, USA), and 1X fast digest buffer in a final volume of 20 µL. The mix was incubated for 7 min at 37 °C for an optimal digestion. Enzymes were then inactivated by 10 min exposure at 70 °C and left on ice. The digestion product was analysed by agarose electrophoresis (2.2.2).

2.2.4 Clean-up of restriction digestion reactions

The GeneJET^{TM} gel extraction kit (Thermo Scientific) was used according to the manufacturer's guidelines. The purified products were eluted in 30 µL of MilliQ water and stored at -20 °C.

2.2.5 Polymerase Chain Reaction (PCR)

A Thermo Scientific Phusion Hot Start II DNA Polymerase kit was used for DNA amplification. For every reaction, 10 ng of DNA template were mixed with 1X Fusion HF buffer, 0.5 µM of forward and reverse primers, 200 µM of each dNTP, 3% DMSO, 0.02 U/µL Phusion Hot Start II DNA Polymerase in a final volume of 20 µL. Cycling instructions used were as follows: initial denaturation for 3 min at 98 °C, followed by 34

cycles (30 s denaturation at 98 °C, 30 s annealing at average Tm of primers minus 3 °C , 1 min extension at 72 °C), and then a final extension for 5 min at 72 °C.

2.2.6 Clean-up of PCR products

The GeneJET^{TM} PCR purification kit (Thermo Scientific) was used according to the manufacturer's guidelines. The purified PCR products were eluted in 30 µL of MilliQ water and stored at -20 °C.

2.2.7 Fast DNA ligation kit

The Rapid DNA ligation kit (Thermo Scientific) was used for ligation. Linearised vector and insert were mixed together in 1:3 respective molar ratios. Then, 2 µL of this mix (with ~100 ng DNA) were added to 4 µL 5X ligation buffer, 1 µL T4 DNA ligase 5 U/µL and exonuclease free water (up to 20 µL). The mixture was vortexed before incubation at 22 °C for 5 min. The reaction mixture was kept at 4 °C until use for transformation of *E. coli* Top10.

2.2.8 Genomic DNA purification

Genomic DNA was purified using the Thermo Scientific GeneJet genomic DNA purification kit according to the manufacturer's guidelines. The purified products were eluted in 200 µL of MilliQ water and stored at -20 °C.

2.2.9 Plasmid sequencing

To confirm successful cloning into pET21a, plasmid samples were sent to Eurofins (Köln, Germany) for Sanger sequencing. Both primers (forward T7 and reverse T7 term) from Eurofins were used to sequence the fragment inserted in the multi-cloning site of pET21a.

2.3 Bacterial transformation

Procedures were adapted from Sambrook & Russell (2001). To obtain cells at the mid-log phase of growth, an overnight culture was diluted in 100 mL fresh LB to an OD_{600} of 0.05 and incubated until it reached an OD_{600} of 0.3-0.6.

2.3.1 Heat shock transformation for *E. coli*

Preparation of competent cells. For every reaction, 1 mL of culture in mid-log phase was pelleted (60 s, 4500 x g, 22 °C), resuspended in 500 µL of sterile ice-cold 50 mM $CaCl_2$ and left on ice for 10 min. Samples were then centrifuged for another 60 s (4500 x g, 22 °C), resuspended in 300 µL of sterile ice-cold 50 mM $CaCl_2$, and stored at -80° C.

Transformation. Competent cells were thawed and 2 µL of plasmid DNA, ligation reaction or PCR product were added (except in the negative control) and the reaction was left on ice for a further 30 min. After a heat shock at 42 °C for 2 min, 1 mL of fresh LB was added and the samples were incubated at 37 °C for 1 h. Selection of cells successfully transformed was achieved by plating 50 µL of cells under selective conditions.

2.3.2 Electroporation for *Salmonella*

Preparation of competent cells. A 100 mL volume of culture in mid-log phase was split into two 50 mL Falcon tubes. Cells were harvested by centrifugation (15 min, 4500 x g, 4 °C), and combined into one Falcon tube using residual supernatant. The pellet was washed twice with 5 mL ice-cold, sterile 10% glycerol (15 min, 4500 x g, 4 °C) and resuspended in 200 µL ice-cold, sterile GYT (10% glycerol, 0.125% yeast extract, 0.25% tryptone). Forty microliters aliquots were made in pre-chilled Eppendorf tubes.

Transformation. Electroporation was performed using a Gene Pulser (Bio-Rad, Hercules, USA) and a pre-chilled 1 mm cuvette (1 h in ice). Two microliters of plasmid of interest or PCR fragments were mixed with the 40 µL competent cells previously prepared. The cuvette was wiped dry and placed into the electroporation holder for 5 ms (25 µF, 200 Ohms, 1.8 kV for 1mm gap cuvettes). Following this, 1 mL of pre-warmed sterile SOC medium was added to the cuvette. Cells were transferred into a fresh Eppendorf and incubated for 2 h at 30 °C. Selection of cells successfully transformed was achieved by plating 100 µL of cells under selective conditions.

2.4 Protein procedures

2.4.1 Quantification, concentration, and storage

The Bradford protein assay (Bio-Rad) was used to estimate lipocalin concentration. A stock solution of 2 mg/mL bovine serum albumin (BSA, Bio-Rad) was diluted to generate a serial dilution of 2, 1, 0.5, 0.25, 0.125 mg/mL BSA. Five microliters of each dilution and samples were then combined with 250 µL Bio-Rad dye. The absorbance at 595 nm was then determined in order to plot a calibration curve. The concentration of unknown samples was estimated from the line fit equation of the curve. Every result was confirmed using a Nanodrop spectrophotometer (Thermo Scientific). Results from the Nanodrop (absorbance at 280 nm) were corrected using the theoretical absorption coefficient of each protein (1.20 for LCN2 and Ex-FAPB, 1.36 for Cal-γ, 0.48 for α1-ovoglycoprotein).

As required, lipocalins were concentrated using Vivaspin20 concentrators (Sartorius, Göttingen, Germany) of 10,000 MWCO at 5000 x g for 10 to 20 min (depending on the volume applied). Aliquoted proteins were then stored in 50 mM sodium phosphate buffer (pH 7.4) at -80 °C.

2.4.2 Dialysis

Protein samples were dialysed at different stages. Dialysis tubing used was composed of a cellulose membrane of 12 kDa cut-off (Sigma-Aldrich) and was boiled in 25 mM EDTA prior to use, washed in Milli-Q water and then kept refrigerated (4 °C) in 30% ethanol until use. A suitable length of tubing was then cut, rinced in Milli-Q water, sealed at one end with a clip and then the tubing was loaded with the sample. Once done, any remaining air was squeezed out and the other side of the tubing was sealed. The tubing was then placed in 500-1000 mL of the appropriate buffer (i.e. binding buffer prior to ion exchange chromatography or 1X phosphate buffer saline: PBS; 137 mM NaCl, 2.7 mM KCl, 10 mM Na_2HPO_4, 2 mM KH_2PO_4, pH 7.4) and stirred gently at 4 °C. The equilibrium in the two liquid spaces being reached after 6 h, the dialysing solution was changed every 6 h until the required dilution was achieved (~3 times; McPhie, 1971).

2.4.3 Separation by SDS-PAGE electrophoresis

Procedures were adapted from Sambrook & Russell (2001) and a BioRad Mini-Protean III system was employed.

2.4.3.1 Polyacrylamide gel preparation

Five millilitres of resolving gel (0.375 M Tris-Cl pH 8.8, 15% acrylamide, 0.1% SDS, 0.035% ammonium persulphate (APS), 0.1% tetramethylethylenediamine [TEMED]) were mixed and poured between two glass plates and left to set for 30 min. A thin layer of water-saturated isopropanol was temporarily added on top to give a smooth and flat separation line between the two layers. After removal of the isopropanol, 1 mL of stacking gel (0.125 mM Tris-Cl pH 6.8, 4.5% acrylamide, 0.1% SDS, 0.035% APS, 0.1% TEMED) was added on top of the resolving gel into which a comb was inserted to form the loading wells. After a 30 min setting period, the gel was wrapped in tissue soaked with running buffer and kept at 4 °C for a maximum of two days before use

2.4.3.2 Sample preparation

Samples were diluted 1:1 in digestion buffer (0.545 M Tris-Cl pH 6.8, 4.2% SDS, 0.2% bromophenol blue, 12% glycerol, 9% 2-mercaptoethanol). For bacterial cells, 100 µL of digestion buffer were added per 0.5 OD_{600} units of cells. To denature proteins, samples diluted in digestion buffer were then boiled for 10 min at 100 °C. Following 10 min centrifugation (4500 x g, 22 °C), 10 µL of supernatant were loaded into each well polyacrylamide gel along with 5 µL of 200 kb PageRuler Unstained Protein Ladder (Thermo Scientific) as a size marker in a separate well.

2.4.3.3 Electrophoresis

Once loaded, the gel that was electrophoresed for 45 min at 30 mA in running buffer (3.05% Tris, 14.4% glycine, 1% SDS, pH 8.3). The gel was then stained with Coomassie blue (0.2% Coomassie blue, 30% v/v methanol, 10% v/v acid acetic) for 1 h on a shaking platform. Following this, the gel was destained overnight in 30% v/v methanol, 10% v/v acetic acid solution. Visible protein bands were recorded using a Syngene G: BOX and further analysed with GeneSys image capture software.

2.4.4 Identification from a complex mixture by Western-blotting

2.4.4.1 Raising polyclonal antibodies in rabbit

Polyclonal antibodies were raised in two white New Zealand rabbits by DC Biosciences (see Table 4.1 for rabbit number details). Two to 2.5 mg of EW lipocalins were sent for immunisations and dot blot analysis (DC Biosciences, Dundee, UK). A 90-day protocol using Freud's adjuvant as a stimulating agent was scheduled as follows:

Week 0:	Collection of pre-immune sera
Week 2:	First immunisation of antigen
Week 4:	Second immunisation of antigen
Week 6:	Collection of second bleed and testing
Week 7:	Third immunisation of antigen
Week 9:	Collection of third bleed and testing
Week 10:	Fourth immunisation of antigen
Week 12:	Terminate animals

The final immune sera were tested for antigen-specific anibody titre by dot blot.

2.4.4.2 Electrotransfer using BioRad semi-dry blotting

Samples were fractionated by SDS-PAGE and transferred onto a 0.45 μm pore-size nitrocellulose membrane (Thermo Scientific). For SDS-PAGE, the protocol described in section 2.4.3 was followed except that the ladder was changed for a PageRuler™ Prestained Protein Ladder, 10 to 180 kDa from Thermo Scientific. Following SDS-PAGE, the gel was sliced off at the bottom right-hand corner as an orientation mark. The upper part of the gel was cut-off, leaving behind the resolving gel. The gel was then washed with transfer buffer (25 mM Tris, 192 mM glycine, 20% methanol v/v, pH 8.3) and sandwiched in filters, sponges and a nitrocellulose membrane pre-soaked with transfer buffer. The semi dry Trans-Blot® Turbo™ Transfer System (BioRad) was used to transfer the samples to the nitrocellulose membrane for 40 min at a constant voltage (25 V) and ampage of up to 1 A. After electrophoresis, the sandwich was disassembled to separate the gel from the nitrocellulose membrane. The membrane was washed with Tris-buffer saline (TBS; 20 mM Tris-HCI, 500 mM NaCl, pH 7.5) and further used for immunodetection.

2.4.4.3 Immunodetection with horseradish peroxidase (HRP) conjugated antibodies

Immunodetection was achieved using primary antibodies raised in rabbit and goat anti-rabbit IgG HRP-conjugated secondary antibody. The nitrocellulose membrane was blocked with 5% milk powder in TBS either for 1 h at room temperature or overnight at 4 °C. Afterwards, the membrane was washed twice in TBS-NP40 (TBS with 0.5% Nonidet P-40) for 10 min at room temperature. The membrane was then incubated with 10 mL of primary antibodies (sera diluted 1:500 or 1:1000 in TBS-NP40 with 5% milk powder) for 1 h at room temperature or overnight at 4 °C, and washed again, three times with TBS-NP40 for 10 min at room temperature. Ten milliliters of secondary antibodies (goat anti-rabbit IgG [Sigma A-6154] diluted 1:5000 in TBS-NP40 with 5% milk powder) were then added onto the membrane, which was further incubated at room temperature for 1 h. Prior to signal development, the membrane was washed twice in TBS-NP40 (for 10 min) at room temperature. Westar C 2.0 chemiluminescent substrate (Cyanagen, Bologna, Italy) was for signal development; 1 mL Peroxidase solution and 1 mL Luminol-Enhancer solution were added onto the membrane. After 30 s of incubation at room temperature, the membrane was sealed in plastic film and a picture was taken using Syngene G:BOX. The chemiluminescent pictures of Western blots (WB) were analysed with ImageJ software in order to determine the signal intensity of every sample.

2.4.5 Mass determination by Electrospray Ionization - Mass Spectrometry (ESI-MS)

Isolated lipocalin proteins were dialysed against ultrapure water prior to analysis by MicroTOF-Q mass spectrometry (column Ace C8 50x2.1, mass spectrometer Thermo Scientific LTQ Orbitrap XL with an ESI source *via* a Thermo Scientific Accela HPLC). Chromatrographical peaks had their spectra extracted, averaged and deconvolution to uncharged neutral mass using Xtract within the Xcalibur software (the BioCentre, University of Reading).

2.5 Production of the human lipocalin and its homologues found in egg white

2.5.1 Cloning of lipocalin genes for overproduction in *E. coli*

Nucleotide sequences for the human LCN2 and chicken Ex-FABP, α1-ovoglycoprotein and Cal-γ genes were obtained from the NCBI GeneBank database using the ID numbers 3934, 396393, 395220, and 374110, respectively. The sequences were codon optimised for expression in *E. coli* (GeneArt optimisation portal; https://www.thermofisher.com/fr/fr/home/life-science/cloning/gene-synthesis.html) and

then synthesised by GeneArt with flanking restriction sites to assist subsequent cloning from the pMK carrier plasmid together with an N-terminal signal sequence (except for LCN2, which does not have an N-terminal signal sequence) to allow secretion of the encoded hexa-His tagged proteins into the periplasm (Appendix 4). The lipocalin-coding regions were released from the pMK plasmid using *Nde*I and *Xho*I, and then ligated into the corresponding sites of plasmid pET21a using the Rapid DNA Ligation kit (section 2.2.7). The resulting constructs were confirmed by restriction digestion and nucleotide sequencing (section 2.2.9).

2.5.2 Protein overproduction

Overnight cultures of λDE3-hosts (bacterial strains, Table 2.1) were diluted 1:100 in 50 mL (for small scale overexpression) or 500 mL (for large scale overexpression) of fresh LB-Amp and grown in a shaking incubator at 37 °C to an OD_{600} of 0.5. At this point, isopropyl β-D-1-thiogalactopyranoside (IPTG) was added to get a final concentration of 0.5 mM. This enabled release of transcription repression from the Lac repressor and promotion of genomic T7 RNA polymerase required for expression of the desired protein.

2.5.2.1 Small scale overproduction for optimisation

Following ITPG induction, growth was monitored by measuring the OD_{600} for 5 h. To assess protein overproduction, each hour a volume of culture (calculated as described below) was sampled and diluted into fresh LB in order to obtain a 1 mL sample of culture with an OD_{600} of 0.5. Diluted cultures were then centrifuged at 4500 x g and 22 °C for 5 min and stored at -20 °C. Lipocalin overproduction over time was then measured following protein separation by SDS-PAGE (section 2.4.3). Solubility analysis was carried-out using a bacterial protein extraction reagent (B-PER, Thermo Scientific), according to the manufacturer guidelines.

$$\text{Volume of culture sampled (in mL)} = \frac{(1\ \text{mL} * 0.5\ \text{OD600nm})}{\text{measured OD600nm}}$$

2.5.2.2 Large scale overproduction for purification

Following ITPG induction, cultures were incubated for 4 h (the optimum time as determined in the small-scale overexpression study) at 37 °C. Cultures were then centrifuged at 4500 x g for 30 min (4 °C), washed in 1X PBS buffer and centrifuged again

at 4500 x g for 30 min (4 °C). Pellets were weighted and stored at -80 °C before protein periplasmic extraction and purification.

2.5.3 Periplasmic extraction using osmotic shock

Following large-scale overproduction, harvested cells (~5 g in total) were resuspended in 1 mL of osmotic shock solution (20% sucrose, 30 mM Tris pH 8.0, 10 mM EDTA; Nossal & Heppel, 1966) per 50 mg of cells. After 10 min at room temperature, the supernatant was harvested at 4500 x g for 30 min (4 °C).

2.5.4 Protein purification

Chromatography were performed using the Biologic™ LP workstation from BioRad. A flow rate of 1 mL/min was used throughout. All buffers and solutions used were degassed and filtered using a nitrocellulose filter membrane (0.45 µm; Durapore, Merck) and a vacuum pumping system.

2.5.4.1 First step purification using nickel affinity chromatography

The supernatant (carrying proteins released from the periplasm) was dialysed thoroughly against binding buffer 1 (0.3 M NaCl, 50 mM Na_3HPO_4, 15 mM imidazole, pH 8.0) at 4 °C. The C-terminally hexa-His-tagged lipocalin proteins were isolated from the retentate by Ni^{2+}-affinity chromatography using a 5 mL Mini Nuvia™ IMAC Ni-charged cartridge (BioRad). Buffer 1 was used for equilibration and washing, and a linear gradient of 0.5 M imidazole in the same buffer was used for elution (according to manufacturer's instructions).

2.5.4.2 Second step purification using ion-exchange chromatography

Eluted Ex-FABP and α-1-ovoglycoprotein were further purified using a 5 mL HiScreen Capto Diethylaminoethyl column (DEAE-sepharose, GE Healthcare) equilibrated in binding buffer 2 (20 mM Tris-HCl, pH 8) with elution achieved with a linear gradient of 1 M NaCl in the same buffer. LCN2 and Cal-γ were further purified using a 5 mL HiScreen Capto Multimodel Cation exchanger ImpRes column (MMC, GE Healthcare) equilibrated with binding buffer 3 (50 mM sodium acetate, pH 6); elution was achieved with a linear gradient of 1 M NaCl in the same buffer or in Tris-HCl at pH 8. The purity of the resulting proteins was determined by SDS-PAGE (section 2.4.3) and identities were confirmed by ESI-MS (section 2.4.5).

2.6 Measure of biomolecular interactions between lipocalins and siderophores

2.6.1 Tryptophan quenching fluorescence

Tryptophan quenching fluorescence (TQF) is a binding assay used to monitor protein conformation changes in presence of a ligand. The procedure used in this study was adapted from Chen *et al.* (2016). A set of Fe^{3+} standards was prepared from a stock of 10 mM ferric citrate in dH_2O with the following concentrations: 640, 320, 160, 80, 40, 20, 10, 5, and 2.5 µM. Likewise, a serial dilution of DHBA was prepared: 1920, 960, 480, 240, 120, 60, 30, 15, 7.5 and 3.75 µM from a stock of DBHA (0.1 M HEPES, 1 mM DHBA, pH 8). Equal volumes of the Fe^{3+} and DHBA solutions were mixed and incubated at room temperature for 10 min to allow the formation of a $Fe(DHBA)_3$ complex. The mix was then diluted 5-fold in Assay Buffer (50 mM HEPES, 150 mM NaCl, 10 mM $CaCl_2$, pH 7.5). In a black-walled, clear-bottom 96-well microplate, 50 µL of the diluted $Fe(DHBA)_3$ complex was mixed with 50 µL of 5 µM lipocalins (Ex-FABP, Cal-γ, α1-ovoglycoprotein or LCN2) diluted from a -80 °C stock with Assay Buffer. The excitation wavelengths was 280 nm whereas the emission was 340 nm (for Cal-γ) or 320 nm (for LCN2, α1-ovoglycoprotein and Ex-FABP). The endpoint mode was achieved at room temperature using a Flexstation III (Molecular Devices, San Jose, USA).

2.6.2 Bio-layer Interferometry

Bio-layer interferometry (BLI) allows monitoring of the binding between a protein immobilised on a biosensor tip surface and a ligand in solution. Prior to running the experiment, Ex-FABP was biotinylated to allow loading onto avidin supports (Dip and Read™ Streptavidin Biosensors; FortéBio). BLI was then achieved using the Octet-K2 (FortéBio, Fremont, USA) according to the manufacturer guidelines. Sensors were programmed to be incubated at 30 °C in wells containing 200 µL of:

- 1X PBS for the baseline - 240 s
- Biotinylated protein (i.e 400, 200, 100, or 0 nM Ex-FABP diluted in 1X PBS) for the loading - 900 s
- 1X PBS for a second baseline - 240 s
- Ligand (100 nM $Fe[DHBA]_3$ in 1X PBS) to obtain an association rate constant (k_a) - 300 s
- 1X PBS to obtain a dissociation rate constant (k_{dis}) - 300 s

A graph similar to Figure 2.1 was then plotted from the Octet-K2 software (BioForté); k_a and k_{dis} were given by the software model. The following equation was used to calculate the dissociation constant: $K_D = \frac{1}{(\frac{ka}{kdis})}$

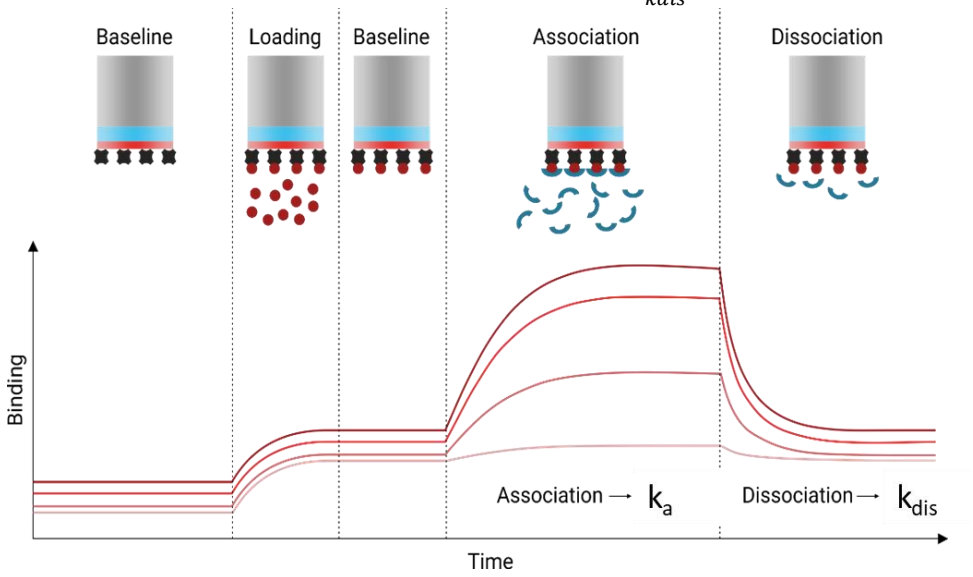

Figure 2.1: Schematic of a sensorgram obtained after BLI (https://2bind.com/bli/).

2.6.3 Isothermal Titration Calorimetry

Isothermal titration calorimetry (ITC) enables determination of biomolecular interactions through measuring heat transfer during binding. The procedure used in this study was adapted from Li *et al.* (2015). Experiments were carried out with a GE Healthcare Microcal VP-ITC microcalorimeter according to the manufacturer's guidelines. The device consists of a motorised injection syringe in which the ligand is loaded and the two adiabatic cells are set at 30 °C or 20 °C. The left cell is filled with the reference (TBS [20 mM Tris, 500 mM NaCl, pH 7.4] with 1.3% DMSO or EWF [section 2.1.1, pH 9.2] with 1.3% DMSO), whereas the right cell is filled with the macromolecule dissolved in the same buffer (5 µM lipocalin). Twenty-nine injections of ligand (10 µL each) were successively applied with either 50 µM enterobactin (Sigma-Aldrich, St. Louis, USA) or 50 µM salmochelin (EMC siderophore, Tübingen, Germany) dissolved in TBS (with 1.3% DMSO, pH 7.4) or EWF (with 1.3% DMSO, pH 9.2). Samples were degassed and pre-equilibrated at the desired temperature using a GE Healthcare MicroCal ThermoVac degassing station before loading into the syringe, sample cell and reference cell. From the binding isotherm obtained, an equilibrium dissociation constant (K_D) was derived using the software model Origin®.

2.7 Genetic engineering techniques

2.7.1 Gene inactivation procedure: λRed disruption system

The *entB* (enterobactin biosynthesis), *iroBC* (salmochelin uptake and synthesis) and *iroDEN* (salmochelin uptake and utilisation) genes of *S.* Enteritidis were inactivated using the λRed gene disruption system encoded by plasmid pKD46 (Datsenko & Wanner, 2000). The *S.* Enteritidis genes of interest were replaced by the Cat (chloramphenicol acetyltransferase gene) cassette from pKD3, which was subsequently removed using FLP recombinase encoded by the temperature-sensitive plasmid, pCP20 (Cherepanov & Wackernagel, 1995).

Gene knockout. PCR primers were designed (Table 2.4, section 2.1.5) to anneal to 20 nucleotides of the flanking regions of the Cat cassette in the pKD3 template and to include approximatively 50 nucleotides of the flanking regions of the target genes (Figure 2.2). A gradient temperature from 61.1 to 65.4 °C was set in order to optimise the PCR (section 2.2.5). After optimisation, PCR products were obtained using the following program: 1 cycle of 3 min at 98 °C for initial denaturation; 34 cycles of 30 s at 98 °C, 30 s at 63 °C, 1 min at 72 °C; 1 cycle of 5 min (final extension) at 72 °C. Following isolation of the PCR amplification products, pKD46 was electroporated into *S.* Enteritidis. An overnight culture (5 mL LB-Amp at 30 °C) of *S.* Enteritidis-pKD46 transformant was diluted 1:100 in 25 mL fresh LB-Amp-10 mM arabinose and incubated at 30 °C until an OD_{600} of 0.6-0.7 was achieved. Cells were then electroporated (section 2.3.2) with 1000 ng of pure PCR product (Cat fragment). finally, Cam^R transformants were incubated at 44 °C to cure the thermo-sensitive pKD46.

Knockout confirmation and removal of the Cat cassette. Following genomic DNA isolation, deletion of the target gene was confirmed by PCR amplification of the chromosomal target locus (primers used at this step can be found in Table 2.5, section 2.1.5). *S.* Enteritidis Cam^R deletion mutants thus identified were transformed with pCP20 at 30 °C and the resulting transformants were grown overnight at 45 °C to induce FLP recombinase expression and cure transformants of pCP20. The overnight culture was then diluted 1:100 and plated on LB agar. After 1.5 days of incubation at 30 °C, six colonies were picked for each mutant, resuspended in 0.85% NaCl and plated on LB, and replicate plated on LB with Amp, and LB with Cam for screening. The plates were then incubated overnight at 37 °C. Successful genomic recombination and plasmid loss candidates were

both Amp and Cam sensitive (Amp^S, Cam^S). Mutant candidates were confirmed by whole-genome sequencing (Illumina; MicrobesNG, Birmingham, UK).

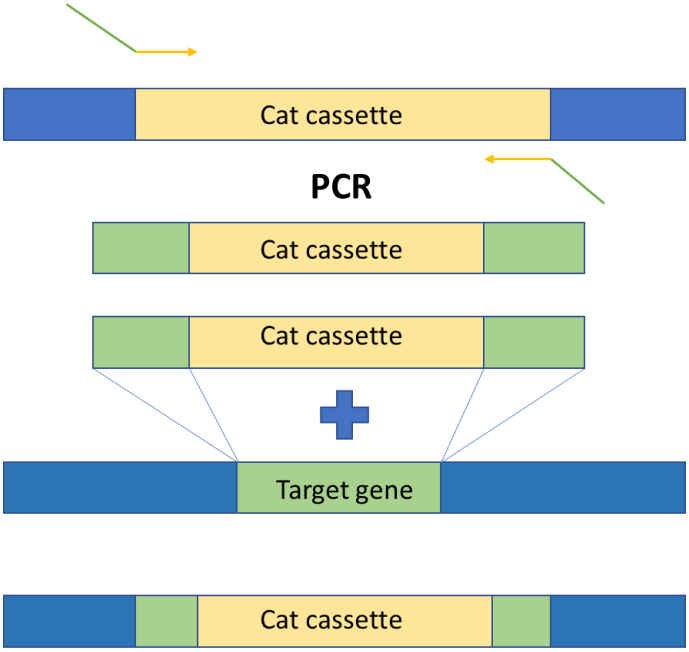

Figure 2.2. Schematic diagram of the lambda red recombineering system used to inactivate genes with the insertion of a Cat cassette (adapted from https://blog.addgene.org/).

2.7.2 λDE3 lysogenisation

E. coli K-12 BW25113 Δ*entB*::*kan* (JW0587) was converted to λDE3-lysogen status using a Lysogenization kit (Merck) and the resulting strain then acted as host for overexpression of the lipocalin genes from pET21a. This enterobactin-deficient host strain was used to avoid association of overexpressed lipocalins with host-specified enterobactin. The λDE3-lysogen employed has the gene coding T7 RNA polymerase under *lacUV5* control. Once λDE3 is incorporated in the host strain, upon induction with 0.5 mM IPTG, the *lacUV5* promoter is de-repressed allowing overexpression of T7 RNA polymerase and thus expression of the T7-promoted target gene from the pET expression plasmid.

2.7.2.1 Generation of λDE3-lysogens.

Lysogens were prepared by co-infection of the host strain, *E. coli* K-12 JW0587, with three different phages:

- the λDE3 phage, which must integrate its DNA (by site-specific integration) into the recipient cell to give the desired recombinant;
- the helper phage, which provides the *int* function that λDE3 lacks and needs for its recombination at the *att* locus of *E. coli* genome. This phage cannot form lysogen by itself; and
- the selection phage, which cannot kill resistant *E. coli* K-12 JW0587 λDE3 lysogens but can kill sensitive non-lysogenic cells. *E. coli* K-12 JW0587 cells able to form colonies on LB in the presence of the selection phage would be expected to be λDE3 lysogens.

The coinfection was realised with 10^8 plaque forming units (pfu) of each phage mixed with 5 µL of host strain (*E. coli* K-12 JW0587) grown to an OD_{600} of 0.5 in LB supplemented with 0.2% maltose and 10 mM $MgSO_4$. The resulting host/phage mixture was incubated for 20 min at 37 °C and then poured onto LB agar to be further incubated at 37 °C overnight.

2.7.2.2 Verification of λDE3 lysogens.

Surviving colonies were grown overnight in LB supplemented with 0.2% maltose, and 10 mM $MgSO_4$. The T7 tester phage was diluted to $1x10^3$ pfu/mL in 1X phage dilution buffer (20 mM, Tris-HCl pH 7.4, 100 mM NaCl, 10 mM $MgSO_4$). Then, 100 µL of host cells (OD_{600} of 0.5) were mixed with 100 µL of diluted tester phage (in duplicate) and incubated 10 min at room temperature. Three milliliters of molten top agarose (1 g tryptone, 0.5 g NaCl, 0.6 g agarose) were added to each tube containing host and phage. One duplicate was poured onto an LB agar plate, while the other duplicate was poured onto an LB agar plate supplemented with 0.4 mM IPTG to evaluate induction of T7 RNA polymerase. Plates were incubated at room temperature overnight. In the presence of ITPG, large plaques should be observed due to high induction of T7 RNA polymerase.

2.8 Siderophore detection assay

CAS (chrome azurol S) plates were made according to Louden *et al.* (2011). A Dark Blue solution was first prepared: 10 mL of 1 mM $FeCl_3H_2O$ were dissolved in 10 mM HCl and mixed with 40 mL of 2 mM CAS, then 50 mL of 5 mM hexadecyltrimethylammonium bromide (HDTMA), were added while gently stirring (to avoid any precipitation of the CAS dye). At last, the medium was prepared by mixing 100 mL of 10X minimal medium with 100 mL Dark Blue solution and 800 mL base culture medium (0.1 M HEPES, 15 g agar, pH 6.8). The final mixture was poured into Petri dishes. CAS plates were streaked with strains to test for siderophore production. After 12 h of incubation at 37 °C, strains producing siderophores turned the medium to a yellow-golden colour while CAS plates streaked with non-producing siderophore strains remained green.

2.9 Measurement of *Salmonella* Enteritidis growth dynamics

2.9.1 Optical Density monitoring (λ 600 nm)

For growth comparison in M9 medium, overnight cultures of *S.* Enteritidis and its mutant strains were grown in LB at 37 °C with agitation (250 rpm). Cells were then washed in iron-free M9 medium and diluted into M9 medium (provided with lipocalins with or without 10 µM ferric citrate) to give an OD_{600} of 0.05 (8 µL overnight in 192 µL medium). To prepare the growth medium, 2.5 mL of M9 (with or without 10 µM ferric citrate) were supplemented with lipocalin protein stored in 1X PBS (i.e Ex-FABP, CAL-γ or α1-ovoglycoprotein, or LCN2 [positive control]) in order to reach a final concentration of 5 µM. Then 192 µL of medium was dispensed into each well and inoculated with 8 µL of previously washed overnight culture. For the negative control, 96 µL of PBS were added to 96 µL of M9 medium and inoculated with 8 µL of previously washed overnight culture. Growth was then tested in 100-deepwell Honeycomb plates incubated in a Bioscreen C (Lab Systems, Hull, UK) apparatus (at 37 °C with constant shaking at 200 rpm) for 20 h. For growth comparison in LB medium, conditions were as above except that overnight cultures were grown in TSB and diluted into LB (with/without 200 µM 2,2-dipyridyl; DIP) without washing. Growth was monitored using 96-well microplates incubated in a Spectrophotometer SpectraMax 340 PC (Molecular devices) at 37 °C with 60 s shaking at 200 rpm every 15 min (for 20 h).

2.9.2 Bacterial cell enumeration

Before use, *S.* Enteritidis were propagated twice overnight at 37 °C in TSB without shaking. When intracellular iron depletion was desired, the second overnight culture was achieved in EWF or LB with 200 µM DIP instead of TSB. After propagation, bacterial suspensions were centrifugated at 5600 x g at 15 °C for 7 min, and cells were washed three times with tryptone salt (8.5 g NaCl, 1 g tryptone). Inoculation was made in 96-well plates, whole eggs, or dialysis models.

In 96 well plates. Plates (deep: 2 mL), were filled with 800 µL EW or EWF (section 2.1.1) supplemented or not with 5 µM Ex-FABP and inoculated with *S.* Enteritidis washed cells to obtain an initial load of 3, 6, 6.5 $\log_{10}$ CFU/mL. Plates were then incubated at 30, 37 or 42 °C in a water bath (up to 32 days) before sampling and enumeration.

In whole eggs. Eggs were washed as described in section 2.1.1. EW was inoculated with washed bacterial suspensions *via* a sterile needle injection through the shell (3 mm deep; without puncturing the yolk) to obtain an initial load of 6.5 $\log_{10}$ CFU/mL. For calculations, the EW volume in an egg was estimated to be 30 mL. The punctured egg was then sealed with melted parafin and incubated at 30 °C. Subsequently (i.e after 24 h, 48 h or 5 days incubation), the eggshell was broken and the EW was aseptically separated from the egg yolk (in 50 mL Falcon tubes). EW was then homogenised (section 2.1.1) before sampling and enumeration.

In a dyalisis bag model. Eggs were washed as described in section 2.1.1. EW was aseptically separated from the egg yolk. EW was transferred into a sterile 125 mL vessel whereas the egg yolk was transferred into a dialysis membrane (12-14 kDa; 4.8 cm diameter; boiled in dH_2O for 10 min). The dialysis bag was folded in two and sealed with a sterile toothpick placed upward. From the 125 mL vessel, 2 mL of EW were sampled to check sterility and pH (section 2.1.1). EW was then inoculated with washed bacterial suspensions to obtain an initial load of 6.5 $\log_{10}$ CFU/mL. Once inoculated, EW was then homogenised (section 2.1.1). The egg yolk (confined in the sealed dialysed bag) was then immersed in the inoculated homogeneised EW (Figure 2.3). The vessel was hermetically closed and incubated at 30 °C (up to 120 h) before sampling and enumeration.

Samples of 100 µL of EW were used to monitor growth. Bacterial cell enumeration from 100 µL of EW were carried-out using a miniaturised plate-counting method, according to Baron *et al.* (2006) with a TSA overlay procedure. Following incubation at 37 °C for 20 to 24 h, the number of colony-forming unit (CFU) was recorded.

Figure 2.3. Picture of the dialysis bag egg model placed in a 125 mL sterile vessel. The homogeneised EW was inoculated with 10^7 CFU/mL washed cells. The sterile yolk was confined in a dialysis bag sealed with a toothpick (12-14 kDa; 4.8 cm diameter) and immerged in EW. The vessel was hermetically closed and incubated at 30 °C.

2.10 Statistical analysis

Means and standard deviations were calculated using Excel. The standard error is equal to the standard deviation divided by the square root of the sample size. For comparison of two means, t-test was achieved using Excel. For multiple comparison of means, one way-ANOVA followed by a Tukey Contrasts test was achieved using R software (version 3.5.3). This allowed identification of groups that were significantly different (identified as “a”, “b”, and “c”).

Chapter 3. Isolation of recombinant egg-white lipocalins

The work conducted by Correnti *et al.* (2011) shows that Ex-FABP, one of the three EW lipocalin identified so far, could play a crucial role in EW's defence against pathogens. Based on this assumption, an experimental plan requiring the isolation of the three EW-lipocalins was designed. Putative functions of lipocalins found in EW were then assigned based on phylogenetic analysis. Secondly, genes coding for the three EW lipocalins were codon optimised and cloned into pET21a for overproduction in *E. coli.* Finally, C-terminal hexa-His-tag proteins were purified by Ni^{2+} affinity and ion-exchange chromatography.

3.1 Bioinformatic analysis of lipocalin-2 homologues found in egg white

3.1.2 Multiple sequences alignment and conserved residues

LCN2 was chosen as a reference for sequence alignments since its structure and functions are well described. Seed alignments of LCN2 homologues were extracted from the Pfam database. Ex-FABP, Cal-γ and α1-ovoglycoprotein FASTA files were obtained from Uniprot and added to the seed alignment using CLC Genomics Workbench (GW) software (Qiagen, Hilden, Germany). To highlight the similarity between the sequences, the Clustal-W algorithm was used to perform multiple alignments (http://www.ebi.ac.uk/Tools/msa/clustalo/). The validity of alignments was then verified through the GW software. Then, the closest homologues to LCN2, Ex-FABP, Cal-γ and α1-ovoglycoprotein were used to build a tree with GW. Multiple alignments of sequences generated by GW (Figure 3.1) showed that there are residues that are conserved between all sequences: tryptophan, arginine and two cysteines (W51, C96, R160 and C195 on human LCN2 amino acid sequence).

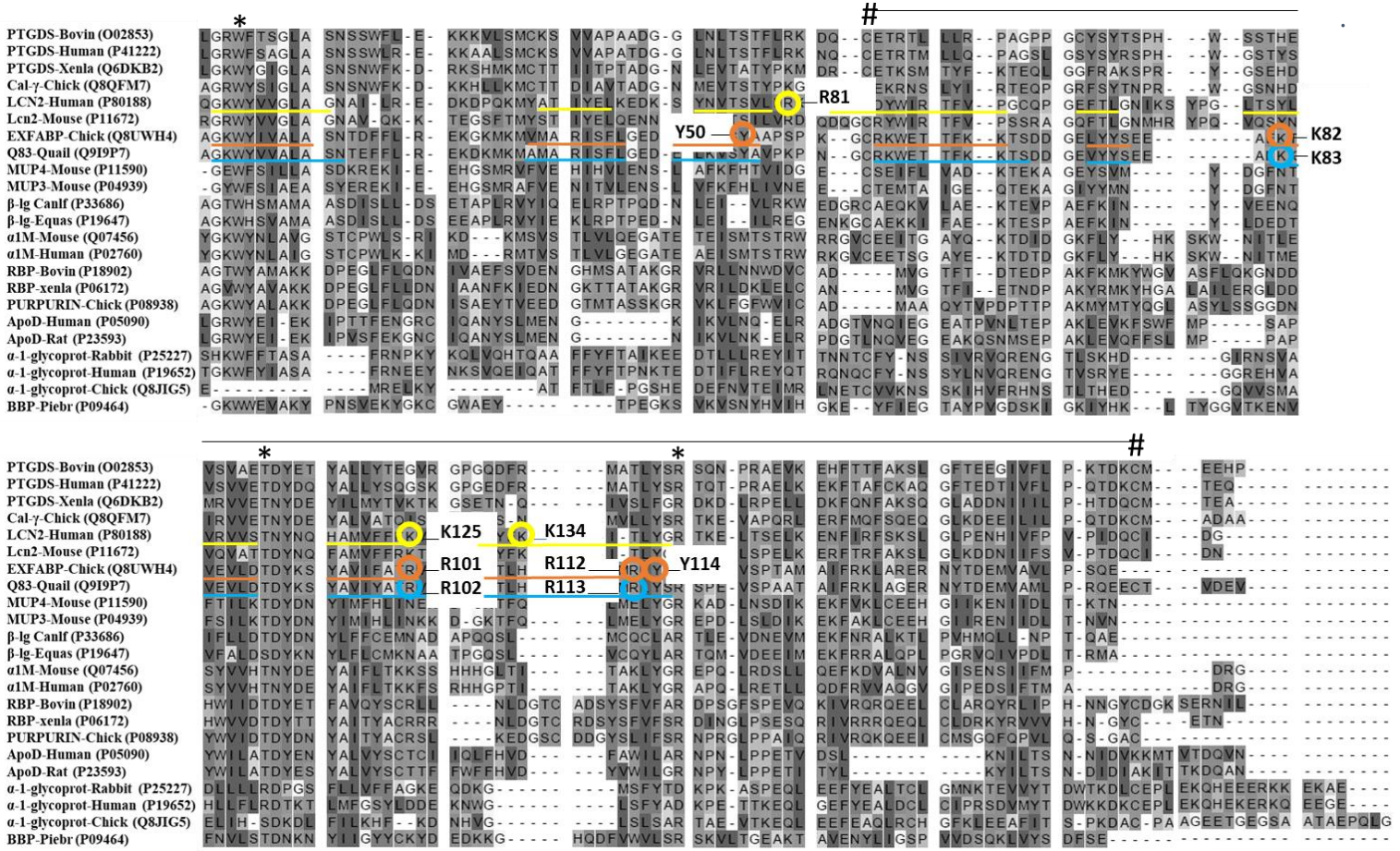

Figure 3.1. Multiple-sequence alignment (GW) of lipocalins found in EW with their closest homologues extracted from the Pfam database (El-Gebali *et al.*, 2019) and NCBI (2019). The Uniprot accession number of each protein is in brackets. Three motifs are shown (*) centred on the conserved tryptophan (W), threonine (T) and arginine (R) residues. These residues are known to be conserved in lipocalins and together with the 310-helix, close the smaller end of the barrel at the bottom of the calyx (Bao *et al.*, 2015). Two cysteine residues (C, #) playing a role in disulphide bridging are also conserved. Residues (putatively) involved in siderophore binding are circled in yellow for LCN2: R81, K125, and K134 (Goetz *et al.*, 2002) and in blue for Q83: K83, R102, and R113 (Coudevylle *et al.*, 2010). For Ex-FABP, residues involved in siderophore (K82, R101, and R112) and LPA (Y50, K82, R112, Y114) binding are circled in orange. The β-strands of the eight-stranded β-barrel of the LCN2, Q83 and Ex-FABP are underlined in yellow, orange and blue, respectively.

The arginine and tryptophan residues are located in two of the three structurally conserved regions (SCR1 and SCR3) that contribute to folding stability (Figure 3.2). The conserved arginine from strand H forms several hydrogen bonds with the N terminal 3_{10}-like helix and packs across a conserved tryptophan from the strand A (Flower *et al.*, 2000). The two cysteine residues are 91% conserved; they form a disulphide bond which links the C-terminus to the strand C (Flower, 1996). The presence of these conserved residues demonstrates a shared evolutionary relationship between the lipocalins found in EW. The level of conservation observed indicates that LCN2 from *Homo sapiens* is more closely related to Cal-γ (32% of identity), than to the other two lipocalins found in chicken EW (26% of identity for Ex-FABP and 21% for α1-ovoglycoprotein). This percentage of identity is relatively low, although the pair-wise sequence identity between many homologues is below 30% (Greene *et al.*, 2003). From this alignment, it is also possible to differentiate a core set of lipocalins from α1-ovoglycoprotein, which displays a match in just two (SCR1 and SCR3) of the three structurally conserved regions highlighted on Figure 3.2. This suggests that α-1-glycoprotein could be considered as an outlier among the lipocalin family.

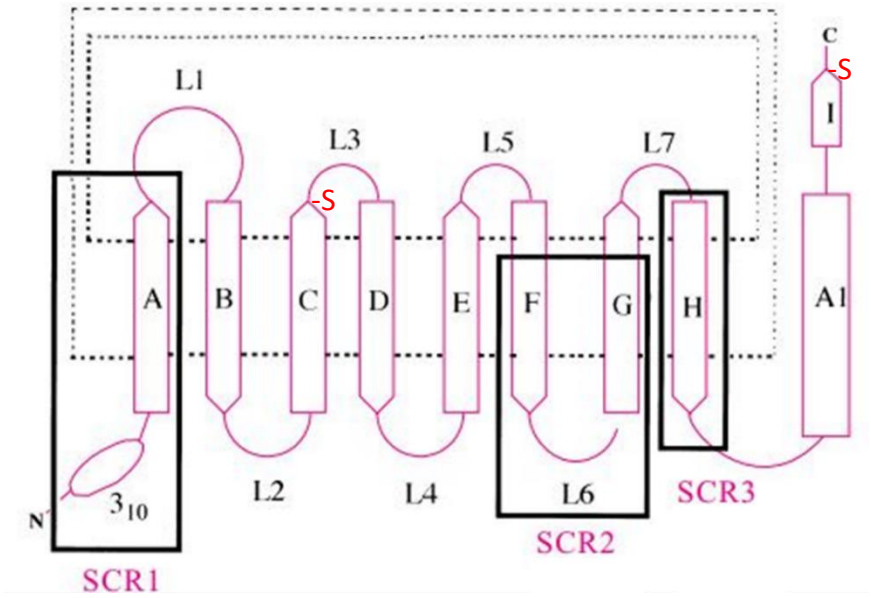

Figure 3.2. Characteristic features of the lipocalin fold. The eight β-strands of the antiparallel β-sheet are shown as arrows and labelled A–H. The N-terminal 3_{10}-like helix and C-terminal α-helix (labelled A1) are also marked. The hydrogen-bonded connection of two strands is indicated by a pair of dotted lines between them. The disulphide bond which links the C-terminus to the strand C is indicated by the letter S. Connecting loops are shown as solid lines and labelled L1–L7. Parts which form the three main structurally conserved regions (SCRs) of the fold, SCR1, SCR2 and SCR3, are marked as boxes (Flower, 1996).

3.1.2 Putative functions of lipocalins based on phylogenetic analysis

A phylogenetic analysis of the lipocalin homologues Ex-FABP, CAL-γ and α1-ovoglycoprotein was conducted to provide insight into their potential functions in EW. The alignment of lipocalins found in EW with their closest homologues extracted from the Pfam database (Figure 3.1) was used to build a phylogeny tree (Figure 3.3) with GW. This tree can be sub-divided into three lobes, as described by Flower *et al.* (2000): proteins in the green lobe include prostaglandin D synthase (PTGDS), neutrophil lipocalin and α-1-microglobulin (α-1M); the blue lobe includes bilin binding protein (BBP), retinol binding protein (RBP) and apolipoprotein D (apoD); the last lobe (orange) is formed of major urinary proteins (MUP) and β-lactoglobulins (β-lg), primarily found in rodents.

Cal-γ. The phylogenetic analysis (Figure 3.3) indicates that the closest homologue of Cal-γ is lipocalin-like prostaglandin synthase (PTGDS). In mammals, PTGDS is secreted into various body fluids. This protein catalyses the isomerization of prostaglandin H2 to prostaglandin D2 and was reported to bind a variety of lipophilic molecules such as biliverdin, bilirubin and retinoic acid. In man, this protein is likely to be involved in both maturation and maintenance of the central-nervous system and male reproductive system (Saito *et al.,* 2002; Urade & Hayaishi, 2000).

α1-ovoglycoprotein. This protein shares a closely-related common ancestor with other α-1-acid glycoproteins found in various animals (Figure 3.3). Despite its induction as an acute-phase protein, and its role in cellular inflammation and transport of drugs in man serum, its biological purpose is unclear (Huang & Ung, 2013). In man, this protein is found in the serum where it is heavily glycosylated and highly acidic due to the presence of sialic acid. Human α1-acid-glycoprotein (α1-AGP) is a highly glycosylated protein (approximatively 45%) of 43 kDa with a pI of 2.7 (Schmid, 1975). There are at least two genes encoding α1-AGP that have been identified; thus, it was suggested that the protein found in plasma is a mixture of the products of these two distinct genes (Dente *et al.,* 1985). The normal plasma concentration in man is between 0.7-1.0 g/L. However, as an acute-phase protein, its concentration can reach 3 g/L under inflammatory conditions (Kremer *et al.,* 1988). It is known to bind lipopolysaccharide and can stimulate the activation of inflammatory cell lines (Boutten *et al.,* 1992). Interestingly, α1-AGP has a protective effect in a mouse meningococcal shock model, suggesting a potential antibacterial role (Moore *et al.,* 1997).

Ex-FABP. According to Figure 3.3, the Q83 lipocalin from quail is a close homologue of Ex-FABP: (88% identity; NCBI 2019). Q83 was originally identified based on its overexpression in quail embryo fibroblasts transformed with the v-myc oncogene. Q83 sequesters enterobactin with a mode of binding equivalent to that of LCN2 (Coudevylle *et al.*, 2010). This resembles Ex-FABP's function, as described above, in siderophore inhibition, and is consistent with its presence in EW. Surprisingly, there is no close homologue of Ex-FABP in human, nor of LCN2 in chicken: the closest human homologue of Ex-FABP is lipocalin 15 and the closest chicken homologue of LCN2 is Cal-γ (28 and 30% amino-acid sequence identity, respectively; NCBI 2019). Yet, despite their limited sequence identities (26%; NCBI 2019), hen Ex-FABP and human LCN2 have similar ligand-binding affinities (Correnti *et al.*, 2011). This suggests that the siderophore-binding activities of these two proteins have evolved independently, in related proteins, in order to fulfil similar functional requirements in innate immunity.

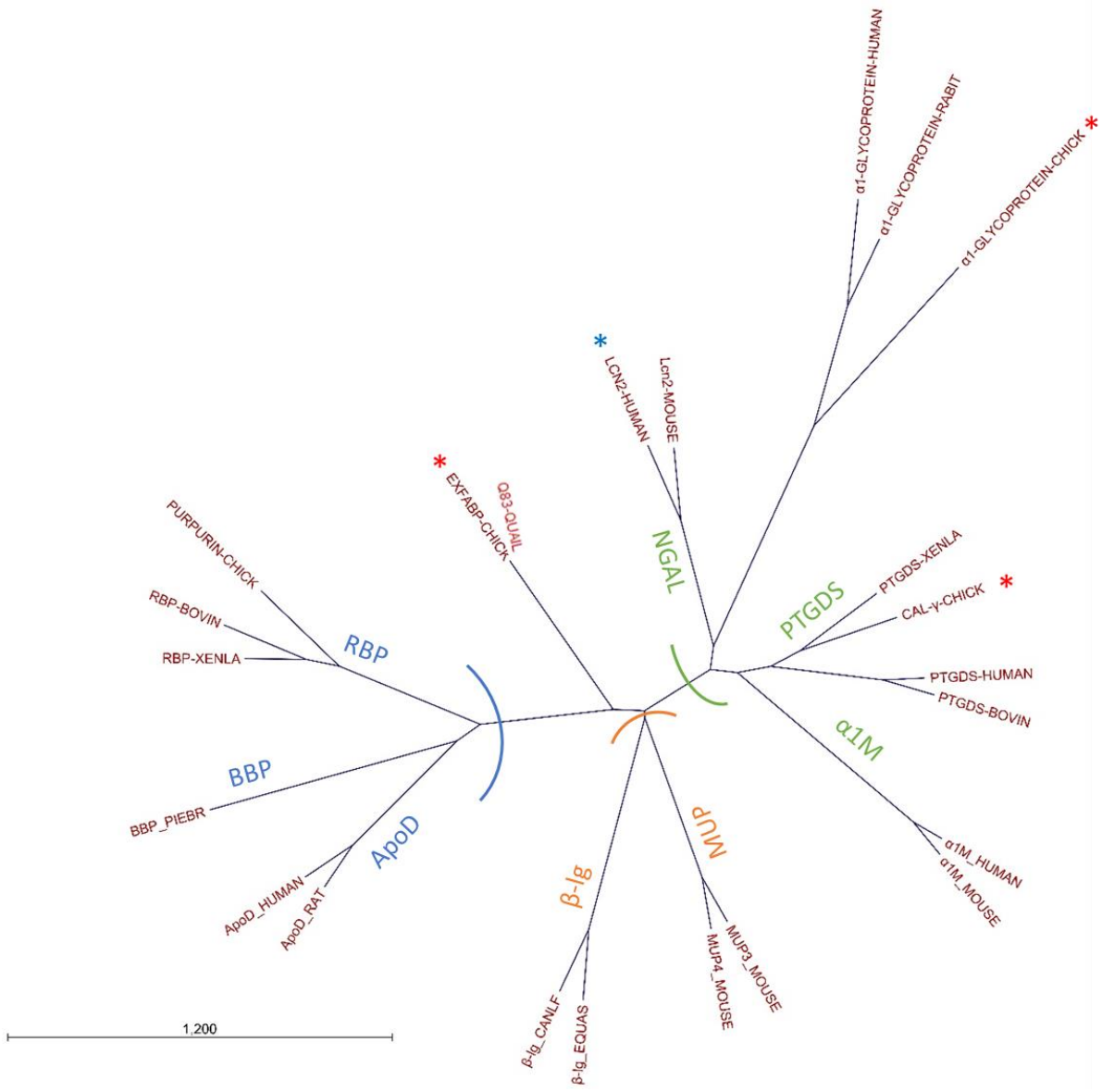

Figure 3.3. Neighbour-joining tree of the lipocalins found in EW and their closest homologues. The alignment of lipocalins extracted from the Pfam family PF00061 and NCBI (2019) was used to build the phylogeny tree with CLC GW (protein distance was estimated from the Jukes-Cantor model). Three lobes are identified with coloured half-circles (green for NGAL, PTGDS and α-1M; orange for β-lg and MUP; blue for RBP, BBP and ApoD). Red stars are showing the lipocalin homologues found in EW that will be studied in this project. The blue star is indicating the human lipocalin-2.

3.2 Overproduction of the lipocalin-2 and egg white lipocalins

LCN2, CAL-γ and α1-ovoglycoprotein were targeted for overexpression, purification and functional analysis. The LCN2 gene from humans, and the Ex-FABP, α1-ovoglycoprotein and Cal-γ genes from chicken were codon optimised to assist their overexpression in *E. coli*. This yielded plasmid pMK-*lcn2* (encoding the codon-optimised human *LCN2* gene to give LCN2 with a C-terminal His tag but no N-terminal signal sequence) and plasmids pMK-*Ex-FABP*, pMK-*α-1glyco* and pMK-*Cal-γ* (encoding codon-optimised *Ex-FABP, α1-ovoglyco* and *Cal-γ* genes specifying a C-terminal His tag and a PelB signal sequence instead of the natural N-terminal signal sequence).

3.2.2 Cloning of lipocalin genes for overproduction in *E. coli*

3.2.2.1 pET-*lcn2* construct

A first attempt to clone *LCN2* into pET21a was made using Gibson method (Thomas *et al.,* 2015). However, PCR primers (section 2.1.5; Table 2.3) did not provide an amplicon of the *LCN2* gene, despite multiple attempts. It was therefore decided to use a fast DNA ligation kit protocol for subcloning into pET21a. Plasmids pET21a and pMK-*lcn2* were double digested with the enzymes *Xho*I and *Nde*I. Following this, the linearised pET21a and the 0.543 kb *LCN2* fragment were extracted using a GeneJET^{TM} gel extraction kit (section 2.2.4). The isolated linearised vector and insert were mixed together in a 3:1 molar ratio in a fast DNA ligation reaction (section 2.2.7). The ligation reaction was then used to transform *E. coli* Top10. The two Amp^{R} transformants obtained were subject to plasmid extraction followed by DNA digestion to determine whether the *LCN2* fragment was present.

According to agarose gel electrophoresis (Figure 3.4), transformant I contained pET21a without insert, while transformant II contained a recombinant pET21a with the *LCN2* insert. Therefore, the ligation appeared successful for transformant II; this plasmid was designated pET-*lcn2*. Both forward and reverse primers used for DNA sequencing (section 2.2.9) confirmed the correct insertion of the *LCN2* fragment at the multicloning site (Figure 3.5).

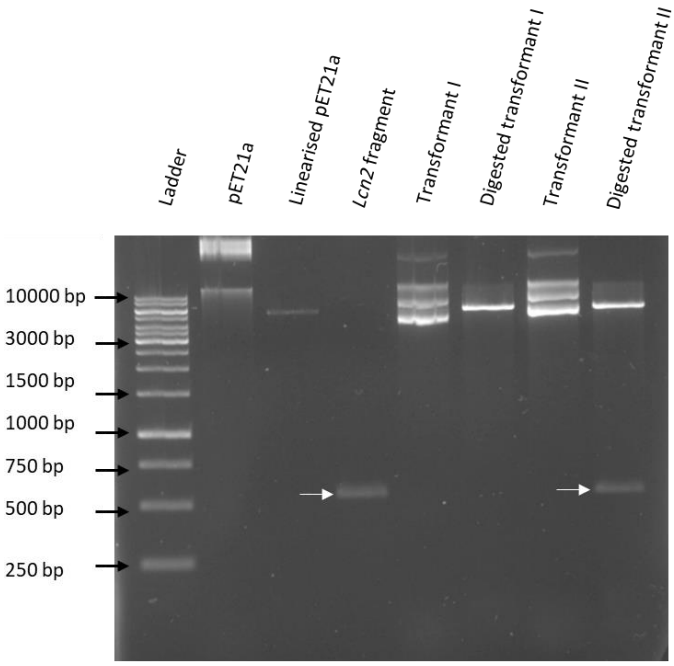

Figure 3.4. DNA electrophoretic analysis of potential pET-*lcn2* isolates. Digested (*Xho*I and *Nde*I) and non-digested DNA were analysed. DNA fragments were subject to electrophoresis in a 0.7% agarose gel in 0.5X TBE (section 2.2.2). pET21a and its linearised form, as well as the 0.543 kb LCN2 fragment, were used as controls. White arrows indicate the LCN2 fragments.

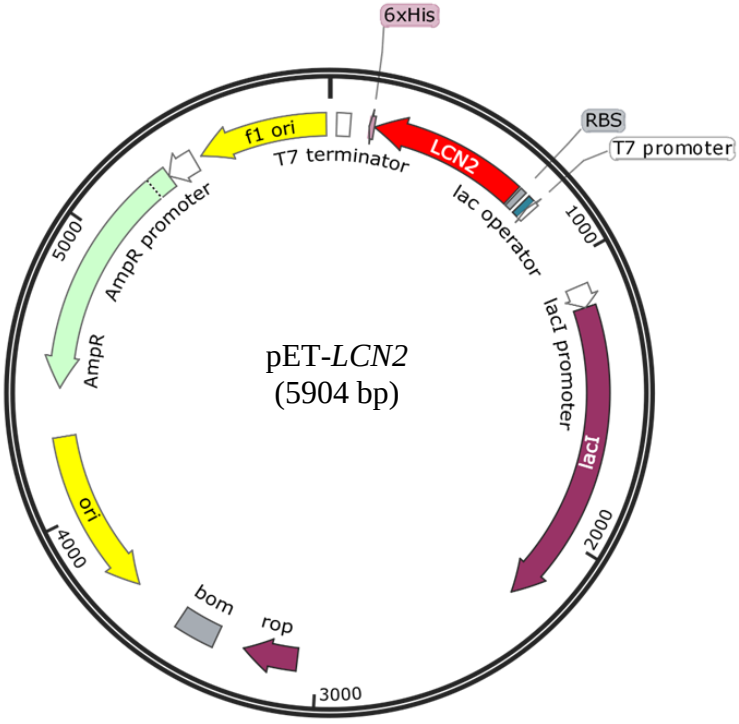

Figure 3.5. Map of pET-*lcn2* vector (transformant II) constructed from sequencing. Both forward and reverse primers used for DNA sequencing (section 2.2.9) confirmed the proper insertion of inserts at the multicloning site of pET21a in frame with its hexa-His-tag. RBS stands for Ribosome Binding site. The bom region (functional for conjugation) and rop sequence (encoding for the protein rop that egulates plasmid DNA replication) are also shown.

3.2.2.2 pET-*Ex-FABP*, pET-*α1-ovoglyco* and pET-*Cal-γ* constructs

To construct pET-*Ex-FABP*, pET-*α1-ovoglyco* and pET-*Cal-γ* expression vector, the fast DNA ligation kit was used as described above (section 2.2.7). The Amp^R transformants obtained were subject to plasmid extraction followed by DNA digestion to determine whether the inserts were present. According to the agarose gel electrophoresis (Figure 3.6), all transformants tested contained a recombinant pET21a. Ex-FABP, α1-ovoglyco and Cal-γ encoding inserts have a respective size of 0.480, 0.555 and 0.501 kb, which is in accordance with sizes calculated using migration of the DNA ladder, respectively 0.490, 0.550 and 0.500 kb. Both forward and reverse primers used for DNA sequencing (section 2.2.9) confirmed the correct insertion of the fragments at the multicloning sites (Figure 3.7).

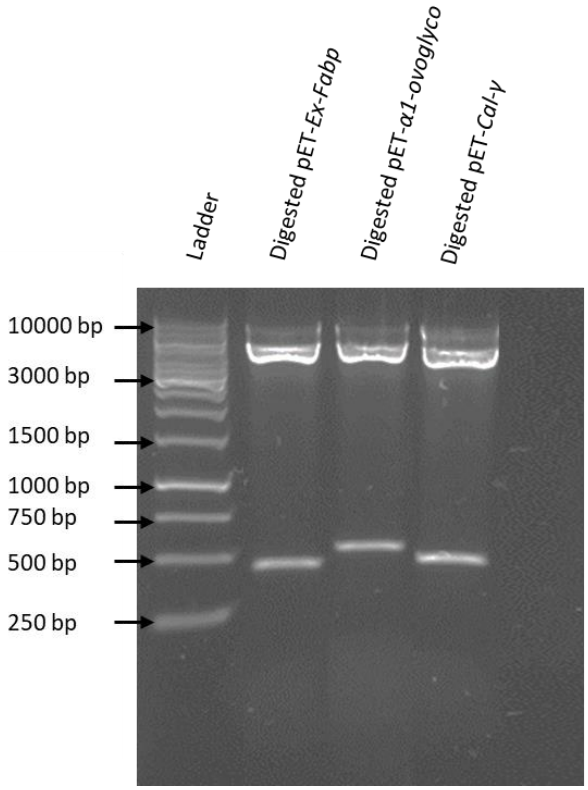

Figure 3.6. DNA electrophoretic analysis of pET-*Ex-FABP*, pET-*α1-ovoglyco* and pET-*Cal-γ* constructs digested with *Xho*I and *Nde*I. DNA fragments were subject to electrophoresis in a 0.7% agarose gel in 0.5X TBE (section 2.2.2). Size of Ex-FABP, α1-ovoglyco and Cal-γ encoding inserts was calculated using migration of the DNA ladder: 0.490, 0.550 and 0.500 kb, respectively.

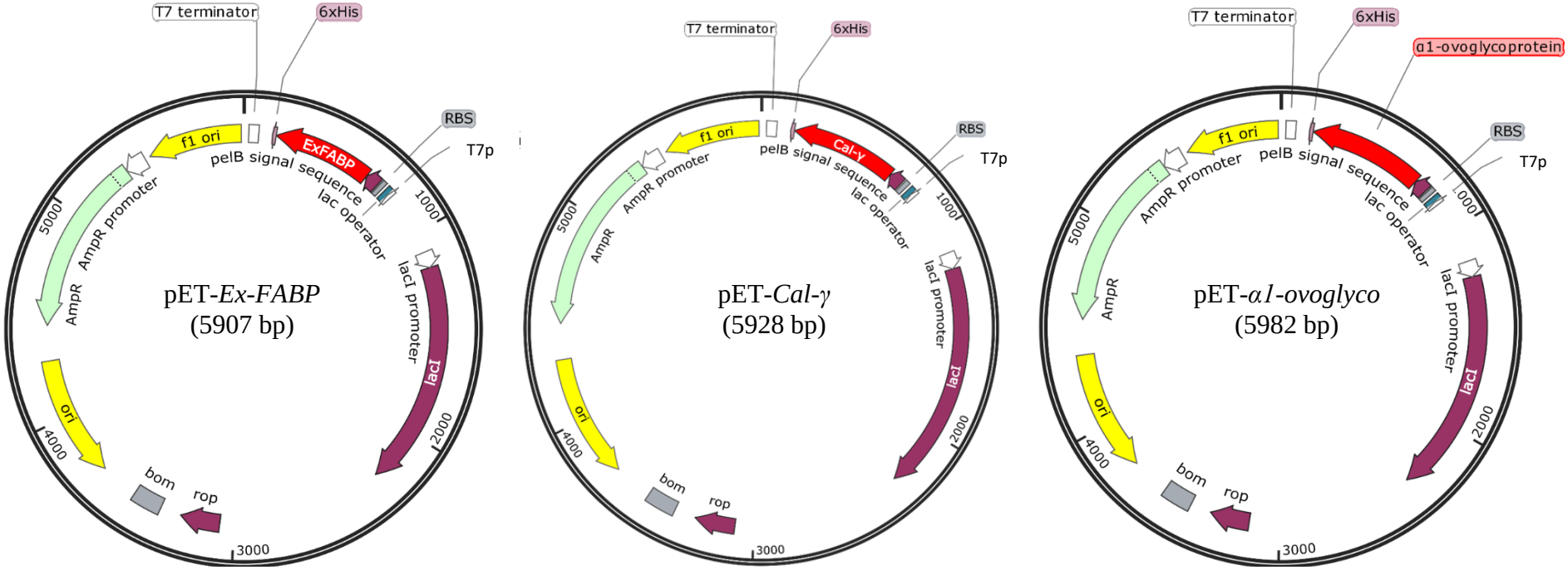

Figure 3.7. Map of pET-*Ex-FABP*, pET-*α1-ovoglyco* and pET-*Cal-γ* constructed from sequencing. Both forward and reverse primers used for DNA sequencing (section 2.2.9) confirmed the proper insertion of inserts at the multicloning site of pET21a in frame with its hexa-His-tag. T7p stands for T7 promoter and RBS for Ribosome Binding site. The *bom* region (functional for conjugal transfer) and *rop* sequence (encoding for the protein Rop that regulates plasmid copy number) are also shown.

3.2.3 Protein overproduction

Small scale (50 ml LB medium) overexpression was used to determine the optimum time for protein overproduction into BL21(λDE3) after induction with IPTG (section 2.5.2). SDS-PAGE analysis showed a major overexpression product at 19.80 kDa (Figure 3.8A), similar to the size expected for LCN2 (21.74 kDa calculated from http://www.peptide synthetics.co.uk). Densitometry showed that maximum LCN2 production occurred at 4 h post induction, accounting for 55% of the total cellular protein (Appendix 5). Solubility analysis using bacterial protein extraction reagent (B-PER, Thermo Scientific) suggested that 52% of the overproduced LCN2 is in the supernatant and 48% is in the pellet (Figure 3.8B). Such results imply that a high proportion of the protein is of sufficient solubility to enable purification by Ni^{2+}-chromatography without need for denaturation/renaturation. However, for the LCN2 homologues found in EW, a PelB secretion signal was included at the N-terminus of the overproduced proteins to enable export to the periplasm (as recommended by Correnti *et al.*, 2011 for Ex-FABP). This should assist subsequent purification and ensure that the proteins are in an extracytoplasmic location where conditions are non-reducing (similar to the final extracellular destination of these proteins in their original host).

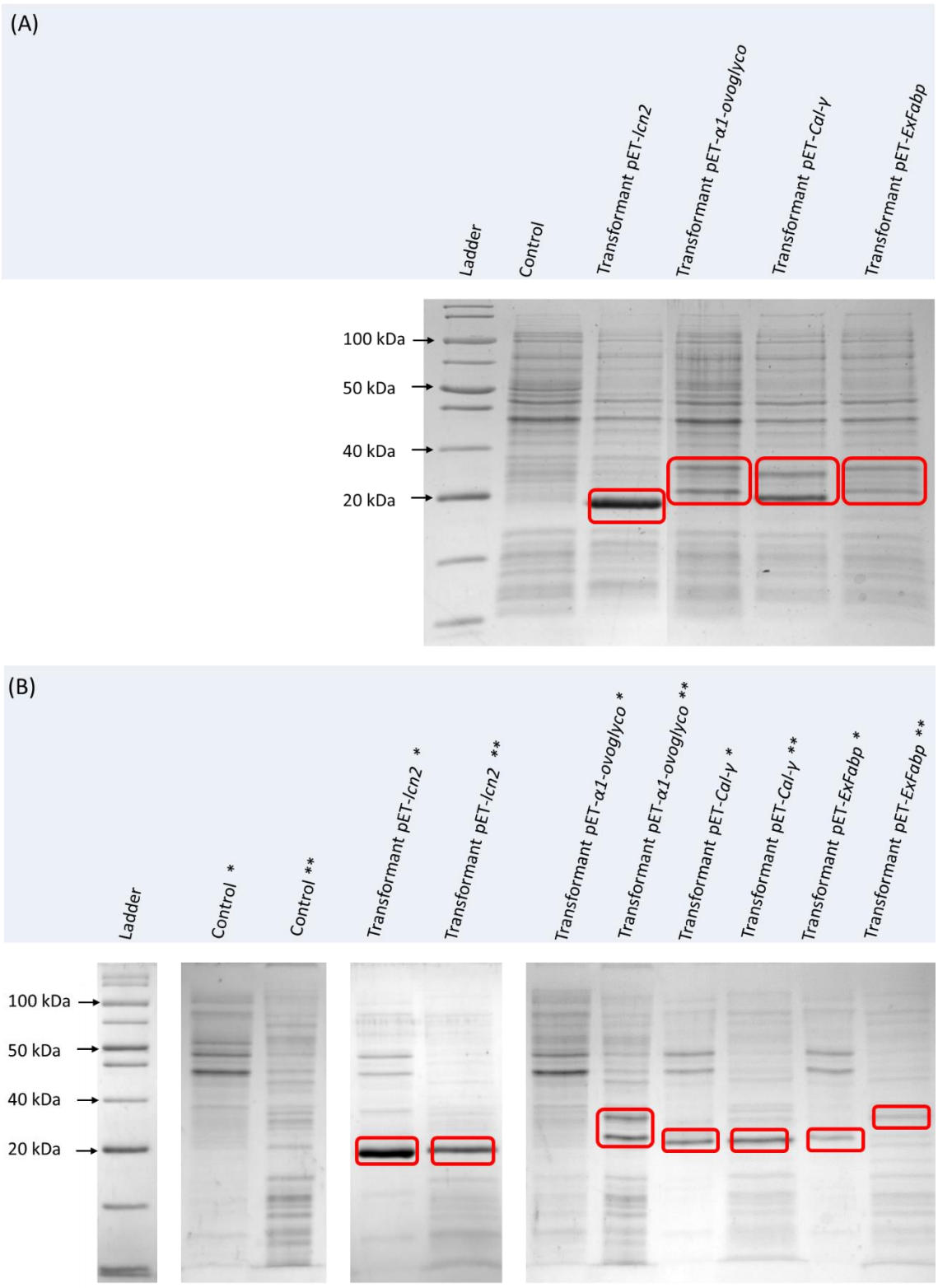

Figure 3.8. **A.** SDS-PAGE analysis of BL21(λDE3) cells transformed with pET-*Icn2* and pET21a (control). Cells were withdrawn 4 h after IPTG induction and proteins were subject to electrophoresis in a 15% polyacrylamide gel (section 2.4.3). **B.** Proteins found in the supernatant* and in the pellet** after B-PER digestion.

Regarding pET-*Ex-FABP*, pET-*α1-ovoglyco* and pET-*Cal-γ* constructs, small-scale overexpression showed two distinct overexpression products for every transformant (Figure 3.8A). The migration during SDS-PAGE highlighted a difference of ~3 kDa between these two products. This suggests that proteins are found in two different forms: either attached to the PelB-leader sequence or cleaved from this same sequence. This hypothesis is supported by the mass calculation of the 22 amino acids PelB sequence estimated to be of 2.23 kDa (http://www.peptidesynthetics.co.uk). The overexpressed lower molecular weight products (21.10, 22.47 and 20.52 kDa) closely matched the expected size of the mature forms of Ex-FABP, α1-ovoglycoprotein and Cal-γ, respectively. Indeed, the mature forms (cleaved from their N-terminal signal sequences) were calculated have predicted masses of 19.13, 21.39 and 19.89 kDa, respectively (http://www.peptidesynthetics.co.uk). Densitometry showed that maximum protein production occurred at 4 h post induction, accounting for 17, 20 and 38% of the total cellular protein, respectively (Appendix 5). Solubility analysis using B-PER extraction suggested that overproduced α1-ovoglycoprotein is mostly insoluble, whereas 47% of Cal-γ and 45% of Ex-FABP appear in the supernatant (Figure 3.8B). To enhance solubility of α1-ovoglycoprotein, growth conditions were modified as follows: temperature was lowered to 30 °C and IPTG concentration was decreased to 0.1 mM. Since modification of those parameters was ineffective to enhance solubility, plasmid pET-*α1-ovoglyco* was transformed into different host strains (C41/λDE3 and Lobstr-BL21/λDE3) that can enhance soluble expression of difficult recombinant proteins (Sørensen & Mortensen, 2005). Unfortunately, use of these strains did not enhance solubility (data not shown). It was therefore decided to progress with large-scale overproduction for all proteins to determine if sufficient yield could be achieved (as described in section 2.5.2) despite the poor solubility of α1-ovoglycoprotein.

3.3 Purification and characterisation of the overproduced lipocalins

3.3.1 First step purification of Hexa-his tagged proteins using nickel affinity column

3.3.1.1 LCN2 purification

Following large-scale overexpression, osmotic shock was conducted in an attempt to release the protein from the cell (section 2.5.3). Protein samples were then dialysed in binding buffer before purification using nickel chromatography (section 2.5.4). During the elution process, the UV absorbance was closely monitored for any elution peak corresponding to a potential protein emerging from the column (Figure 3.9A). Every fraction was analysed by SDS-PAGE to determine protein content (Figure 3.9B).

The SDS-PAGE analysis using Syngene software showed that the peak seen in the 280 nm elution profile (Figure 3.9A) corresponds to a major purification product at 19.82 kDa mainly distributed in fractions 8 to 10 (Figure 3.9B). Syngene was used to quantify the purity of the purified product obtained. Software analysis estimated the purification product as 97, 98 and 99% of the density in fractions 8, 9 and 10, respectively. These fractions were combined (9 mL) and dialysed in 50 mM sodium phosphate buffer (pH 8) before concentration using Vivaspin20 concentrators to a final volume of 2 mL. From Bradford assay, the final sample was estimated to contain 6.82 mg/mL of protein which is equivalent to a 357 µM stock solution. A fraction of this sample was then dialysed in 20 mM ammonium acetate in ultrapure water (pH 7.4) and analysed by Electro Spray Ionisation – Mass Spectrometry (ESI-MS). However, repeated failure to fly in the ESI-MS or loss during dialysis resulted in lack of any utilisable spectrum.

(A)

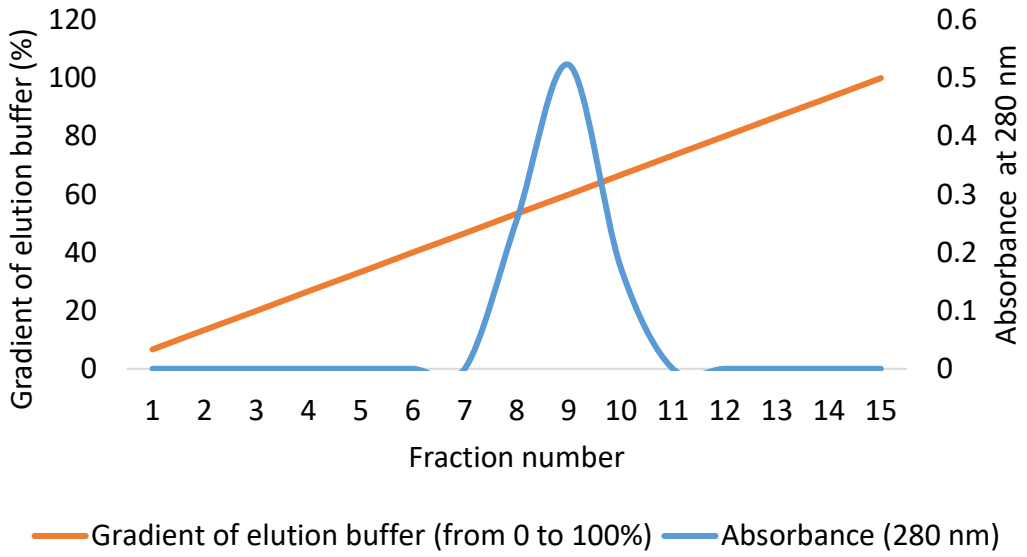

(B)

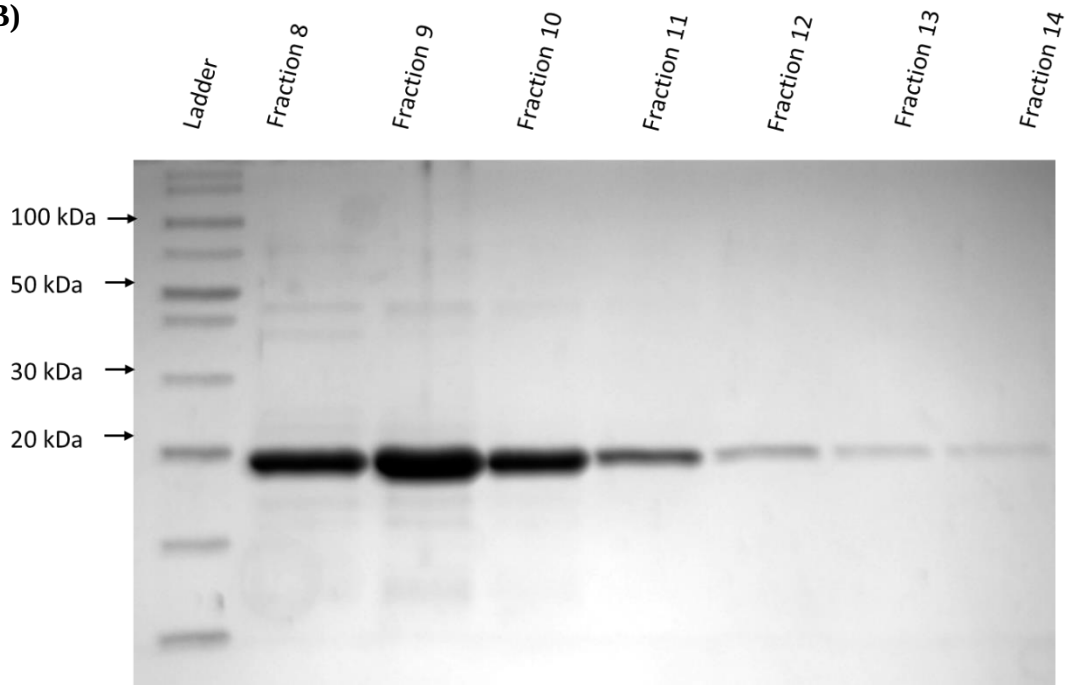

Figure 3.9. **A.** Elution profile of LCN2 from nickel affinity chromatography. A linear gradient of elution buffer (from 0 to 100%) was applied to the column until a final concentration of 500 mM imidazole was reached. **B.** The SDS-PAGE analysis shows that the peak seen in the elution profile corresponded to a major purification product at 19.82 kDa mainly distributed in fractions 8 to 10.

3.3.1.2 Ex-FABP purification

Since Ex-FABP was also shown to be partly soluble during small-scale overexpression, osmotic shock was used for extraction of periplasmic content before purification. The purification process was conducted as for LCN2.

The SDS-PAGE analysis resulting from nickel chromatography showed that the peak observed in the elution profile (Figure 3.10A) corresponds to two products at 19.63 and at 22.30 kDa in fractions 7 to 10 (Figure 3.10B). The presence of the two major protein bands was unexpected since only one product was found to be soluble during small-scale overproduction. Such differences could be explained by the different treatments applied to release the protein (i.e. B-PER reagent versus osmotic shock). This suggests that the protein was purified in at least two different forms: either attached to the PelB leader sequence (upper band, PelB-Ex-FABP) or cleaved from this same sequence (lower band, mature form). Analysis with Syngene estimated that the two products combined corresponded to 98, 99 and 97% of the density associated with fractions 8, 9 and 10, respectively. These fractions were combined, dialysed and concentrated, as above. From Bradford assay, the final sample was estimated to contain 1.2 mg/mL of protein which is equivalent to 62 µM stock solution, in a volume of 2 mL. A fraction of this sample was then dialyzed in 20 mM ammonium acetate in ultrapure water (pH 7.4) and analysed by ESI-MS (section 2.4.5). The true mass obtained was of 19.13 kDa, which is in accordance with the mass calculated online (http://www.peptidesynthetics.co.uk) (19.13 kDa) corresponding to the mature form of the protein (Figure 3.12A, Table 3.1).

It is also important to note that the LPA-Ex-FABP complex was discovered after recombinant Ex-FABP purification (Correnti *et al.,* 2011). In this study, we did not identify the presence of LPA through ESI-MS. This could be due to either the extra transesterification step performed by Correnti *et al.* (2011) or due to the presence of the hexa-His tag (that has not been cleaved off in this study).

(A)

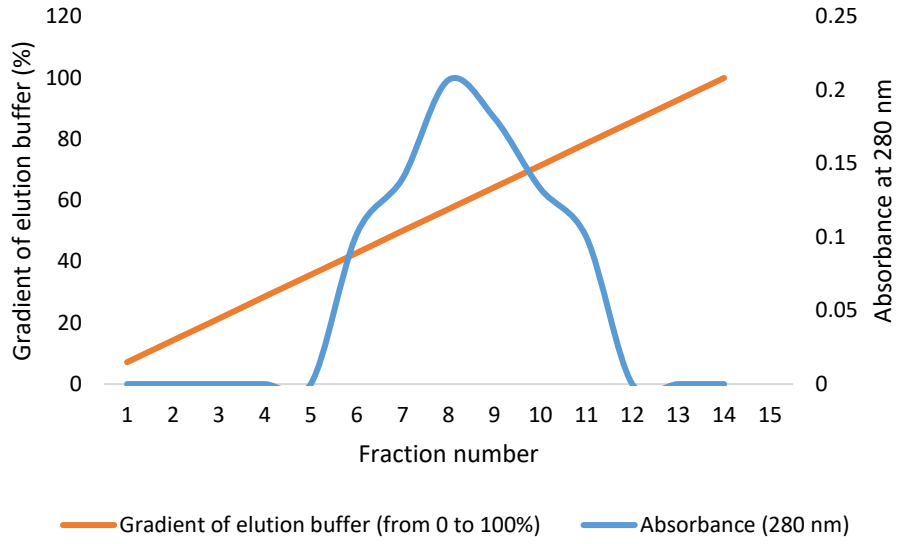

(B)

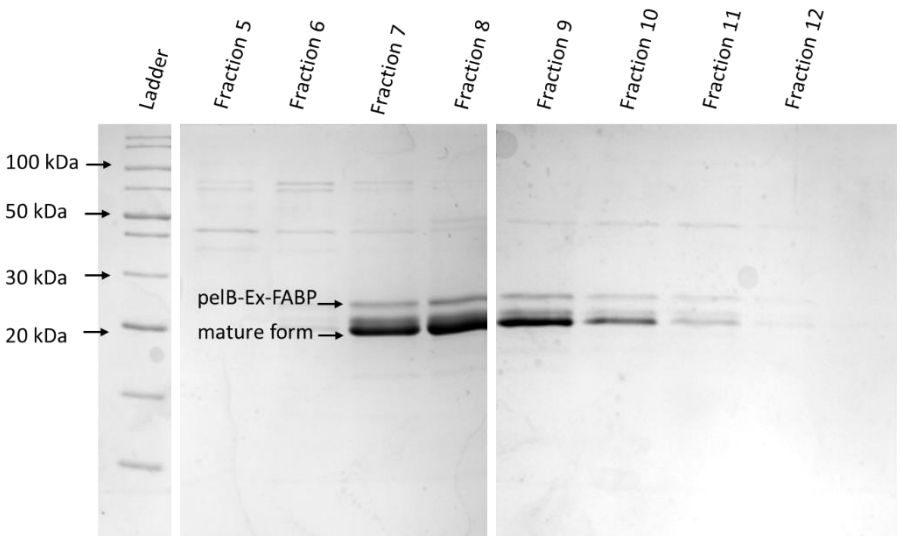

Figure 3.10. **A.** Elution profile of Ex-FABP from nickel affinity chromatography. A linear gradient of elution buffer (from 0 to 100%) was applied to the column until a final concentration of 500 mM imidazole was reached. **B.** The SDS-PAGE analysis shows that the peak seen in the elution profile corresponded to a major purification product at 20.15 kDa in fractions 7 to 11.

3.3.3.3 Cal-γ purification

Cal-γ was purified following the same protocol as described above (elution profile not shown). Three products (Figure 3.11) resulted from the purification (20.52, 21.40 and 23.8 kDa). This suggests again that proteins were purified in more than one form: e.g. either attached to the PelB leader sequence (upper band, PelB-Cal-γ) or cleaved from this same sequence (lower band, mature form), although the presence of a third product (middle band) remains unexplained. Combined, these bands represent 95% of staining density of the final sample. Using ESI-MS analysis, only two out of the three purification products observed on SDS-PAGE were detected (Figure 3.12B). ESI-MS indicated a mass that is 763 Da greater than that predicted for both the major mature and minor immature (PelB-Cal-γ) forms.

Furthermore, it was observed that the fraction collected after the purification step had a reddish-brown colour in the visible spectrum (Figure 3.11). This colour is characteristic of phenolate bound to iron and has been assigned to the interaction of the phenolate groups with the Fe^{3+} ion (Gaber *et al.*, 1974). The absorbance spectrum of the fractions collected was plotted, which highlighted a shoulder at ~412 nm (data not shown). This was in accordance with the visual observation of the reddish-brown colour (Figure 3.11). From these results, it appears that Cal-γ might tightly bind a coloured ligand of 763 Da.

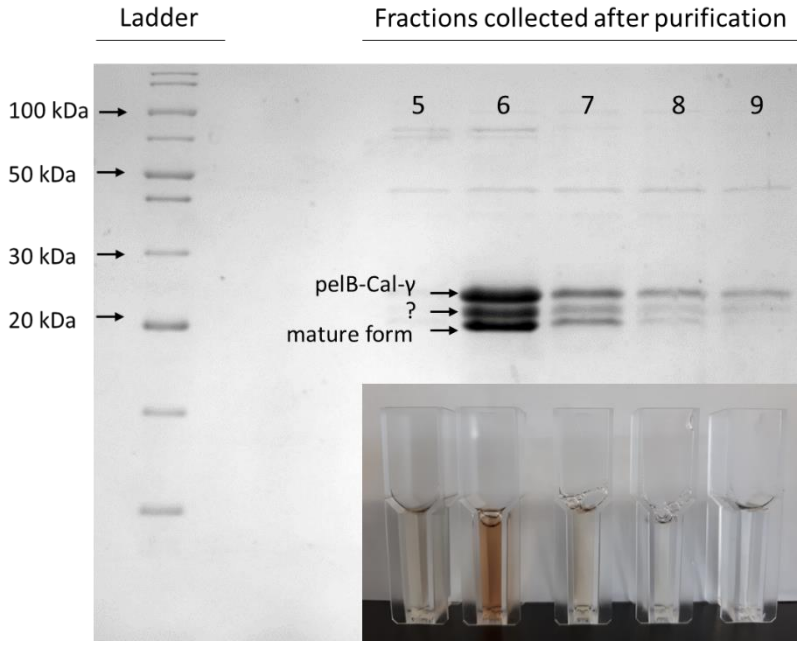

Figure 3.11. Fractions 5 to 9 resulting from Cal-γ purification using Ni^{2+} column. The SDS-PAGE analysis shows that the elution of three major purification products at 20.52, 21.40 and 23.8 kDa in fractions 5 to 9 was correlated with the appearance of a strong reddish-brown colour.

3.3.3.4 α1-ovoglycoprotein purification

After small-scale overexpression of α1-ovoglycoprotein, B-PER extraction suggested that this protein was mostly insoluble. This implied that this protein might require a denaturant before purification by Ni^{2+}-chromatography. To confirm these findings, osmotic shock was conducted on 100 mg of pelleted cells after large scale-overexpression. According to Syngene analysis, ~25% of α1-ovoglycoprotein was found in the periplasmic fraction (data not shown). Hence, the soluble α1-ovoglycoprotein fraction resulting from B-PER extraction might have had a density too weak to be identified on SDS-PAGE during small scale overexpression.

Accordingly, it was decided to purify this protein without any preliminary denaturation step, following the same protocol as described above. Two purification products resulted from the purification (19.50 and 21.82 kDa; Figure 3.13). Combined, they represent 70% of staining density of the final sample. Results from ESI-MS analysis allowed determination of the true mass of the two purification products: 21,377.0 Da, which is in accordance with the anticipoated mass (http://www.peptidesynthetics.co.uk) of 21,381.9 Da corresponding to the mature form of the protein (Figure 3.12, Table 3.1); another purification product of lower abundance was found at 23,586.7 Da, corresponding to the protein attached to the PelB sequence. This is in accordance with the two purification products observed on SDS-PAGE (Figure 3.13).

Table 3.1. Comparison of the purification products detected through ESI-MS and the theoretical mass of the lipocalins.

	Mass determined through ESI (Da)	*Theoretical mass (Da)*	*Difference between the theory and the observed Mass (Da)*
Mature Ex-FABP	19127.4	19130.6	3.2
Mature Cal-γ	20654.8	19892.2	762.7
PelB-Cal-γ	22866.1	22103.0	763.1
Mature α1-ovoglyco	21377.5	21381.9	4.4
PelB-α1-ovoglyco	23586.7	23592.7	5.9

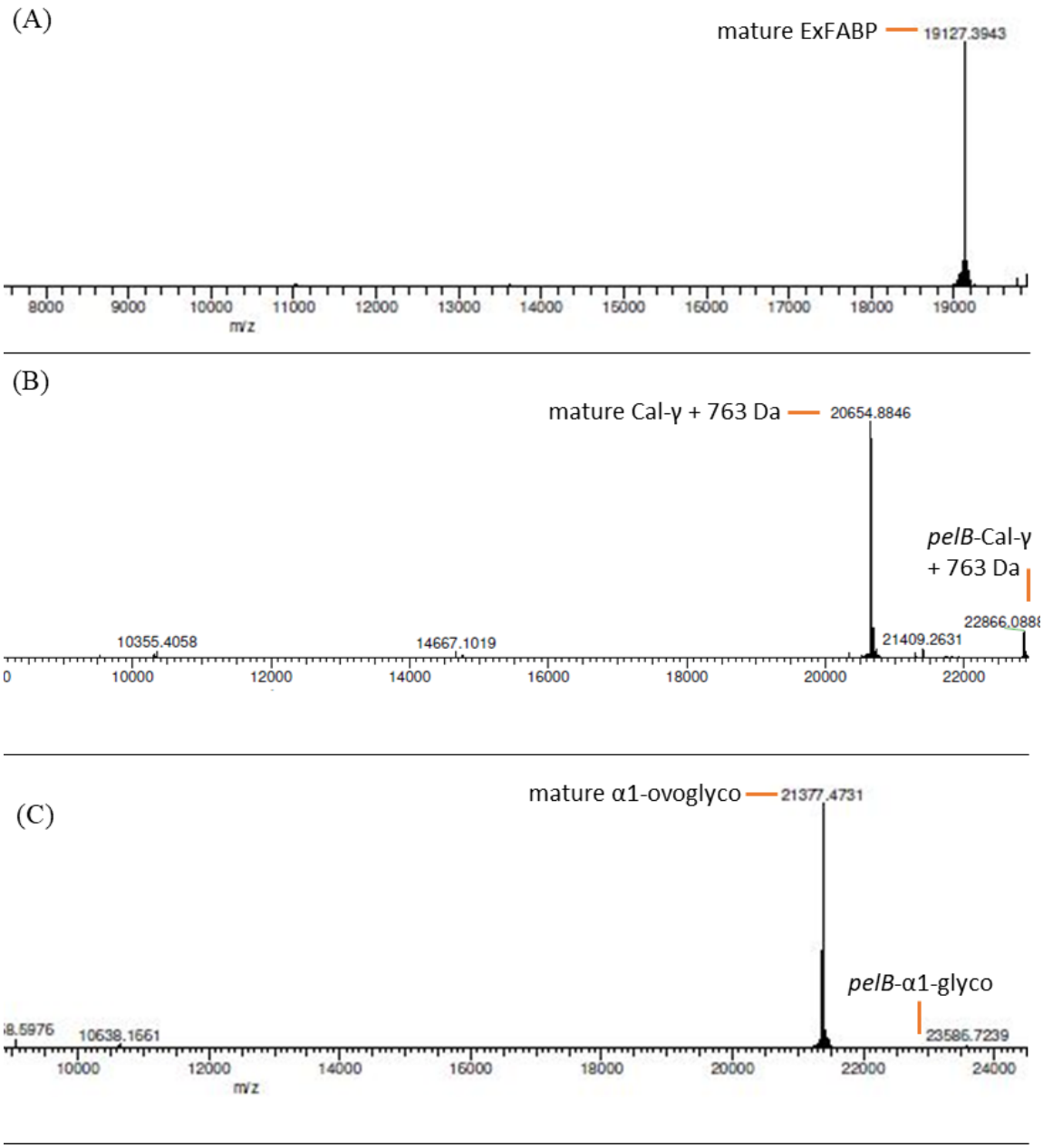

Figure 3.12. Mass of the purification products detected by ESI-MS i.e after the first step purification of Ex-FABP (A) Cal-γ (B) α1-ovoglycoprotein (C). The X axis represents the mass divided by charge: m/z.

3.3.2 Second step purification using ion exchange chromatography

Every protein purified was then further purified by ion exchange chromatography. Ex-FABP and α1-ovoglycoprotein have a pI of 6.65 and 5.86, respectively (as estimated from their amino acid sequence on http://protcalc.source forge.net). Therefore, an anion exchange column (DEAE-sepharose) set at pH 8.5 was use to allow binding and purification (section 2.5.4). Regarding LCN2 and Cal-γ, their pI is estimated to be 8.73 and 7.21, respectively. Thus, a second purification step involving a cation-exchange column (MMC column) set at pH 6 was followed (section 2.5.4). It is important to note that for LCN2, the elution gradient of EB from 0 to 1 M NaCl was not sufficient to elute the protein (tightly binding to the column) and that an extra step of elution was required using a linear gradient consisting of Buffer A (50 mM sodium acetate, pH 6) and Buffer B (1 M NaCl, Tris-HCl, pH 8).

As described in Figure 3.13 and Table 3.2, the percentage of purity increased significantly after this second step purification. Since more than 90% purity was achieved in each case, 2 mg aliquotes of pure protein were submitted to DC Bioscience (section 2.4.4) to raise antibodies. These antibodies were used for measurement of the natural concentration of lipocalins in EW.

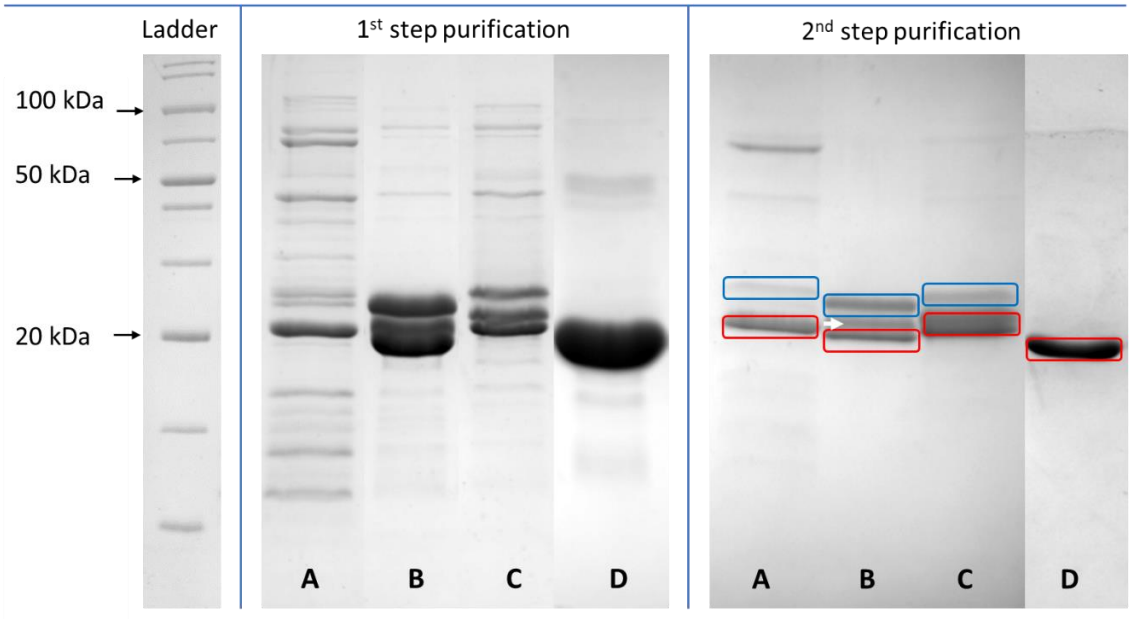

Figure 3.13. Fractions resulting from chromatography after first step purification (Ni^{2+} column) and second step purification (MMC and DEAE-sepharose columns). α1-ovoglycoprotein (A) Cal-γ (B) Ex-FABP (C) LCN2 (D). Blue boxes highlight the PelB-lipocalins and red boxes their mature forms. The white arrows indicate the third unknown purification products observed for Cal-γ.

Table 3.2. Comparison between the percentage purity of the lipocalins obtained before and after ion-exchange chromatography.

	% of raw volume - 1st step purification	*% of raw volume - 2nd step purification*
(A) α1-ovoglyco	70	90
(B) Cal-γ	97	99
(C) Ex-FABP	95	98
(D) LCN2	97	99

Following this second purification step, a sample of purified Cal-γ was subjected to ESI-MS. The purified product at 20.65 kDa was confirmed as being the major compound of the sample (data not shown). This suggests that dialysis against sodium acetate at pH 6 (before cation exchange chromatography) did not cause dissociation of any 763 Da ligand potentially associated with the protein.

3.3.3 Production of an JW0587(λDE3) strain for protein overproduction

To ensure that the mass addition (763 Da) seen for Cal-γ is not an enterobactin ligand, it was decided to generate an *E. coli* strain deficient in siderophore synthesis for lipocalin overproduction (as described by Garénaux *et al.*, 2013 and Correnti *et al.*, 2011). To achieve this, *E. coli* K-12 BW25113 Δ*entB*::*kan* (JW0587) was converted to λDE3-lysogen status using a Lysogenization kit. This enabled an *E. coli* JW0587 strain (defient in enterobactin synthesis) to express T7 RNA polymerase and therefore to be compatible with pET21 plasmid expression.

Following the lysogenisation protocol (section 2.7.2), more than 200 CFU/plate were recovered following treatment with the selection phage. To confirm the integration of λDE3 in prophage form into the genome of the host cell, overnight cultures of five colonies randomly picked were grown with 10^4 pfu/mL T7 tester phage on LB agar plates and LB agar plates supplemented with IPTG (section 2.7.2). T7 tester phage is completely defective unless T7 RNA polymerase is provided by the host cell. Therefore, the presence of plaques observed in Figure 3.12 confirms that lysogenisation was successful (results are shown for only one lysogeny candidate). It can be observed in Figure 3.14 that plaques observed on LB agar were smaller than on LB agar supplemented with IPTG. This suggests that basal level expression of T7 RNA polymerase is low. Lysogen with the

lowest basal expression levels was chosen as host for overexpression of the lipocalin genes from pET21a to avoid association of overexpressed lipocalins with host-specified enterobactin.

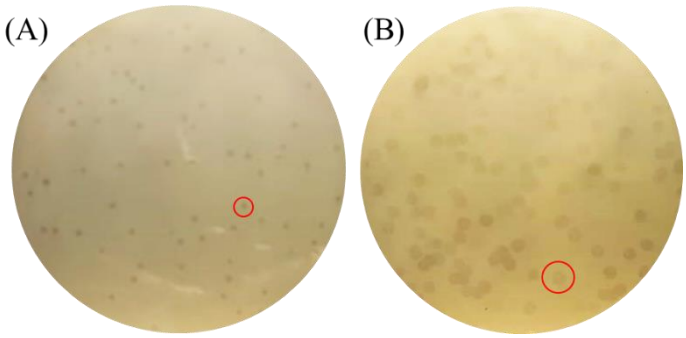

Figure 3.14. λDE3 lysogen candidates evaluated by their ability to support the growth of the T7 tester phage. Red circles highlight plaques: 1 mm on LB agar (A) and 3 mm on LB agar supplemented with IPTG (B).

Using JW0587(λDE3), as produced above for overexpression, purification of every protein was repeated as described in 3.3.1 and 3.3.2. After purification, Cal-γ still had a reddish-brown colour. Furthermore, the absorbance spectrum of the sample highlights a shoulder at ~412 nm, again (Figure 3.15). Purification products were sent for ESI-MS analysis. The purified product at 20.65 kDa was still the major compound found in the Cal-γ sample. This suggest that the extra mass associated with Cal-γ is not related to Ent.

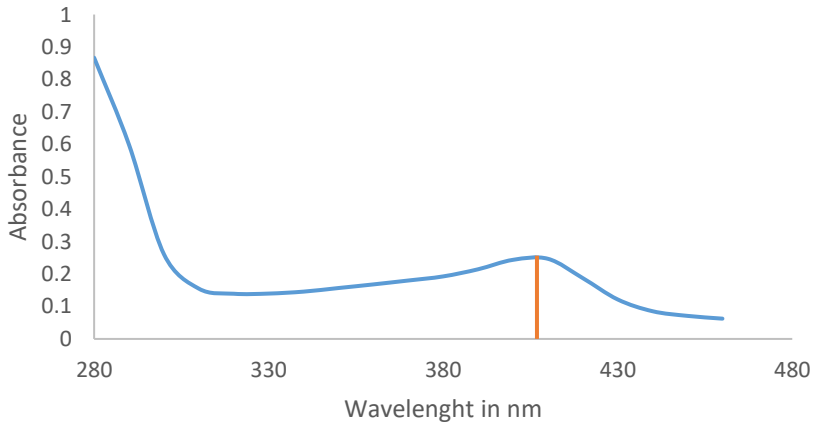

Figure 3.15. Absorbance spectrum (from 280 nm to 450 nm) of Cal-γ fractions collected after overexpression in JW0587(λDE3) and Ni^{2+} purification (pH 8). This spectrum highlights a shoulder at ~412 nm.

In an attempt to separate Cal-γ from any potential ligand that might account for the additional 763 Da of mass, low pH was used (0.1 M HCl) to denature the protein followed by application to a desalting column (GE Healthcare HiTrap^{TM} desalting; exclusion limit of 5000 Da) also in 0.1 M HCl. The eluted sample was analysed by ESI-MS. However, a difference of 763 Da was still observed (data not shown). Further studies were conducted by the University of York (Metabolomics and Proteomics Bioscience Technology facility centre). MALDI-ISD showed that the N- and C-terminal amino acid sequences (residues 1 to 36 and 161 to173) of the mature form were as expected. ESI-MS analysis carried out under native and denaturing (50% acetonitrile, 1% formic acid) conditions showed that the additional mass (763 Da) was likely a covalent association. Furthermore, the analysis conducted by the University of York also showed that haem ($C_{34}H_{32}FeN_4O_4$) was present in the purification sample. Yet, haem alone (616 Da), cannot explain the mass addition of 763 Da seen under native and denaturing conditions. Since Ex-FABP can bind two ligands in it calyx (Fe-enterobactin and LPA; Correnti *et al.*, 2011), it could be hypothesised that Cal-γ might (i) bind haem and another ligand that would explain the remaining 103 Da, or (ii) bind a 763 kDa ligand or (iii) several unknown ligand(s).

Although the 763 Da mass addition does not seem to be linked with the production of enterobactin, as a precaution, it was decided all further overexpression and purifications should utilise JW0587(λDE3) as host. Proteins were sent again for ESI-MS, which confirmed successful purification.

3.4 Conclusion and future work

Recombinant EW lipocalins (α1-ovoglycoprotein, Cal-γ and Ex-FABP) as well as the human lipocalin-2 were successfully overproduced and purified. However, a 763 Da mass addition was observed for Cal-γ. To determine if any extra amino acids are found in the protein sequence, peptide mass fingerprinting could be considered. Using trypsin digestion, Cal-γ would be cleaved into smaller peptides and mapped after MALDI-TOF or ESI-TOF. Since haem was also identified in the Cal-γ purification sample, a JW0587(λDE3) strain knocked out for haem synthesis (encoded by hemBCDEFGH) could be used. Since *E. coli* haem synthesis is not essential in rich medium, use of a strain carrying a *hemD* deletion could be attempted as described by Wang *et al.* (2015). If the red-brownish colour of Cal-γ observed was not observed after overexpression and isolation from this new Δ*hem*D strain, this would suggest that Cal-γ binds haem. Subsequently, structural binding assays could be carried-out on this protein to test its affinity for haem. The isolated lipocalins achieved in this chapter enable their subsequent characterisation. In the next chapter, quantification of EW lipocalins and determination of their siderophore-binding activity will be addressed.

Chapter 4. Quantification of egg-white lipocalins and determination of their siderophore-binding activity

How and in what quantities lipocalins are incorporated into EW remain unknown. Antibodies raised against EW lipocalins were used to determine their concentration in EW. Once the presence and levels of the lipocalins was confirmed in EW, lipocalins siderophore-binding activity was explored using tryptophan quenching fluorescence (TQF), biolayer interferometry (BLI) and isothermal titration calorimetry (ITC). The human lipocalin-2 (LCN2) was used as a positive control since its siderophore-binding activity is well characterised (i.e. sequestration of 2,3-DHBA and related siderophores; Goetz *et al.,* 2002)

4.1 Egg white contains micro-Molar levels of all three lipocalins

To quantify the amounts of lipocalins naturally found in EW, antibodies were raised in two rabbits for each protein (except Ex-FABP; section 2.4.4.1). The volume of sera received for each rabbit can be found in Table 4.1. For each rabbit, the selectivity of the sera was confirmed by testing antibodies in the presence of the vector control (i.e. JW0587/λDE3 cell extract; negative control) and the three EW lipocalins. Sera were also tested for immunological sensitivity through exposure to serial dilutions of the previously purified lipocalins. Once selectivity and sensitivity were tested, the antisera were used for identification and quantification of lipocalins in EW.

Table 4.1. Volume of sera received after a 90-day immunisation protocol using Freud's adjuvant as a stimulating agent. Ab stands for antibodies.

Ab vs α1-ovoglycoprotein	*Rabbit 21*		*Rabbit 49*	
Final bleed	~ 80 mL	Pre-sera: 1mL	~ 80 mL	Pre-sera: 1 mL
3rd immunisation	5 mL		5 mL	
2nd immunisation	5 mL	Pre-sera: 1 mL	5 mL	Pre-sera: 1 mL

Ab vs Ex-FABP	*Rabbit 22*	
Final bleed	~ 80 mL	Pre-sera: 1 mL
3rd immunisation	5 mL	
2nd immunisation	5 mL	Pre-sera: 1 mL

Ab vs Cal-gamma	*Rabbit 23*		*Rabbit 48*	
Final bleed	~ 100 mL	Pre-sera: 1 mL	~ 100 mL	Pre-sera: 1 mL
3rd immunisation	5 mL		5 mL	
2nd immunisation	5 mL	Pre-sera: 1 mL	5 mL	Pre-sera: 1 mL

4.1.1 Selectivity testing of the antibodies

Selectivity of antibodies raised in rabbit was assessed by Western blot analysis (WB) of 10 µL of 1 µM α1-ovoglycoprotein, Cal-γ or Ex-FABP, and JW0587(λDE3) cell extracts (OD_{600} = 0.05) using primary antibodies raised against α1-ovoglycoprotein, Cal-γ or Ex-FABP for immunodetection. Although there appeared to be a slight cross reaction between the Cal-γ and Ex-FABP anti-sera (Figure 4.1A), anti-sera from rabbit 23 (immunised against Cal-γ), rabbit 22 (immunised against Ex-FABP) and rabbit 49 (immunised against α1-ovoglycoprotein) were shown to be the most specific and therefore selected to carry out further experimentation (Figure 4.1).

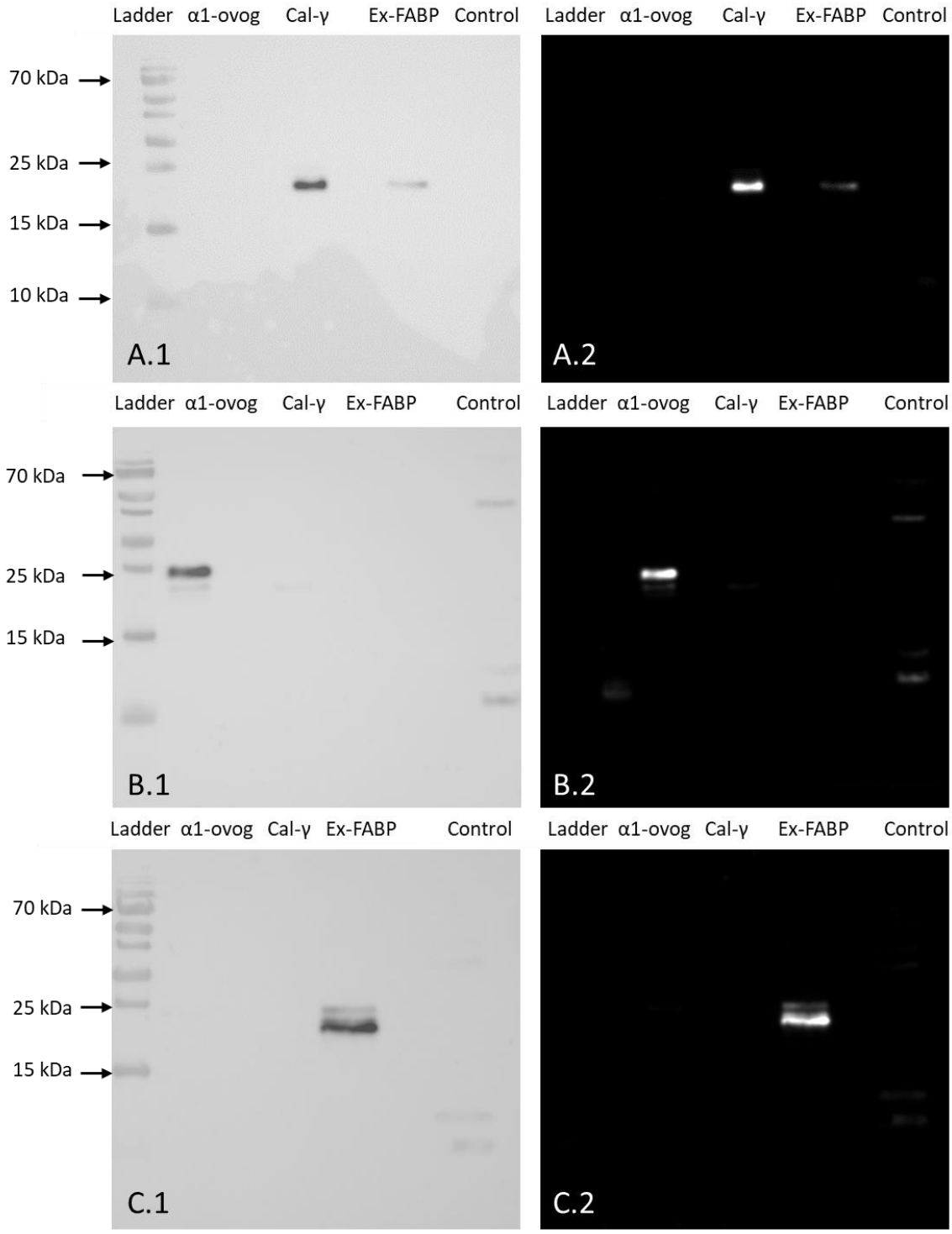

Figure 4.1. Selectivity testing of the polyclonal antibodies raised against A. Cal-γ (sera from rabbit 23 diluted 1:1000), B. α1-ovoglycoprotein (sera from rabbit 21 diluted 1:500), C. Ex-FABP (sera from rabbit 22 diluted 1:500). 1. Picture combining the visible marker and the chemiluminescent imaging. 2. Chemiluminescent WB. For every protein, 10 µL of 20 µg/mL stock (= 200 ng) were loaded into each well. For the negative control, 10 µL of JW0587(λDE3) cell extract (OD = 0.05) was loaded, since it is the vector used for protein over-production.

4.1.2 Egg-white protein content fractionation on SDS-PAGE

EW proteins were fractionated using 15% acrylamide SDS-PAGE. Because of the viscosity and high concentration of ovalbumin in EW, dilutions in dH_2O were made to obtain 2, 5 and 20% EW (Figure 4.2). Four major proteins were identified on this gel: 1, oTf (75 kDa); 2, ovalbumin (50 kDa); 3, ovomucoid (40 kDa); and 4, lysozyme (15 kDa). Their relative density was in accordance with data from the literature (Sauveur, 1988): 54% ovalbumin, 13% oTf, 13% ovomucoid and 3.5% lysozyme. The best migration pattern on the gel was obtained with a 2% dilution.

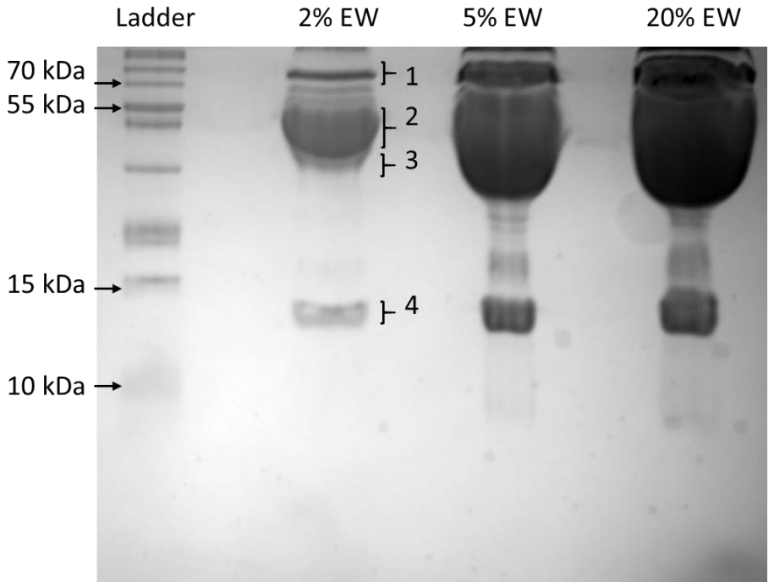

Figure 4.2. EW protein content fractionated using SDS-PAGE. Three of the major proteins found in EW can be identified; 1. Ovotransferrin (75 kDa); 2. Ovalbumin (50 kDa); 3. Ovomucoid (40 kDa). 4. Lysozyme (15 kDa)

4.1.3 Quantification of lipocalins found in egg white

The levels of each lipocalin in EW were then determined by WB (section 2.4.4) using corresponding lipocalin standards (6.25; 12.5; 50; 100 mg/L) along with EW dilutions (1:10 or 1:100 in dH_2O). The chemiluminescent WB images (Figure 4.3) were used to plot standard curves for every protein (Figure 4.4). The equations of the calibration curves were then used to calculate the amount of protein naturally found in EW (Figure 4.5). The lipocalin quantification was repeated three times with eggs of three different egg brands (free range eggs, the Cooperative; free range eggs, Clarence Court; and free-range eggs, Happy Egg). All eggs were certified Class A and produced in the UK. From the three concentration values gathered, an average and standard error were calculated.

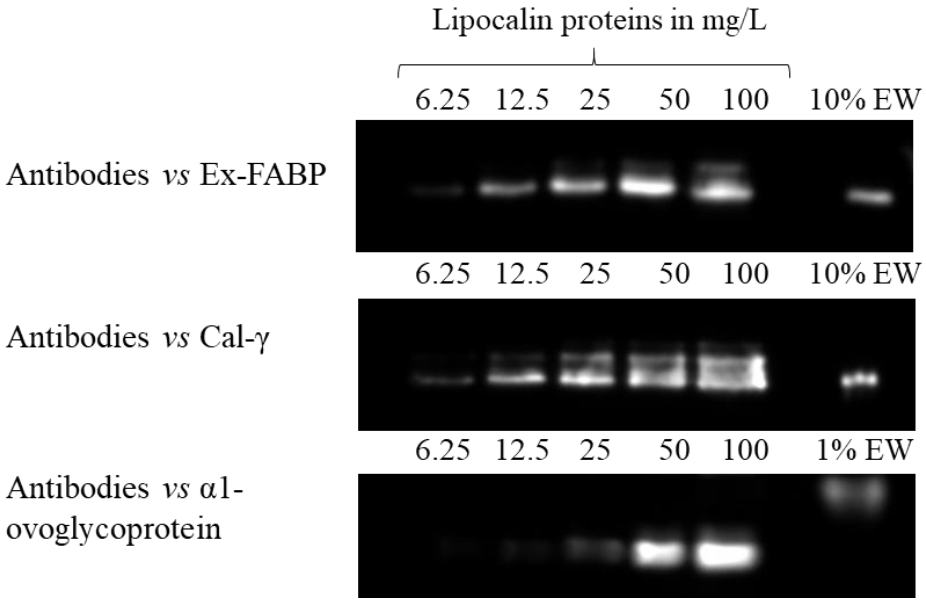

Figure 4.3. WB analysis of a range of EW lipocalin levels (as indicated) as well as a sample of EW (diluted 1:10 or 1:100 in dH2O) (Julien *et al.*, 2020). The calibration curves of purified EW lipocalins used to calculate the amounts found naturally in EW are provided in Figure 4.4.

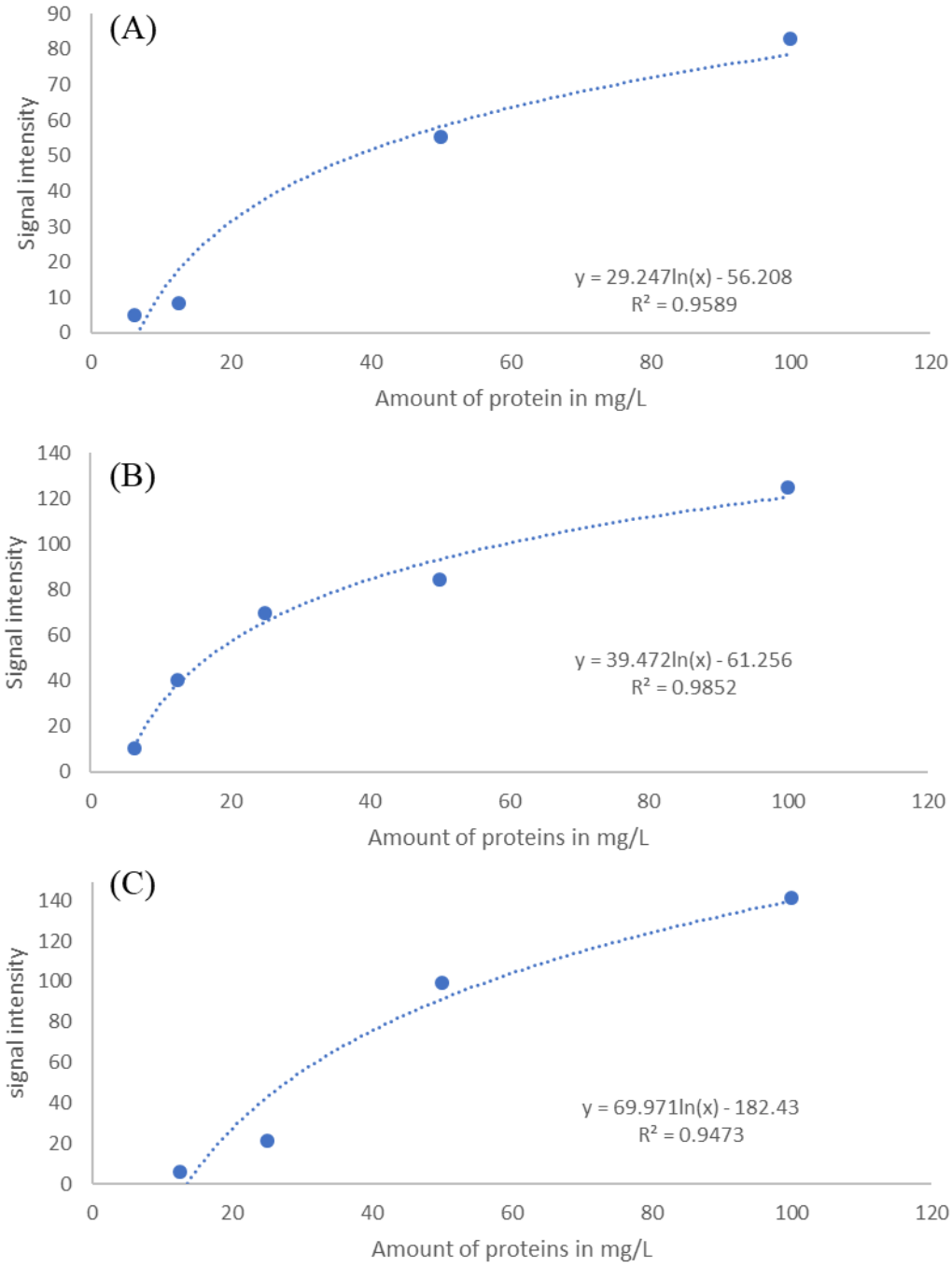

Figure 4.4. Calibration curves plotted from signal intensity of bands obtained following WB analysis (see Figure 4.3). Calibration curves for Ex-FABP (A), Cal-γ (B) and α-1-ovoglycoprotein (C). The calibration was repeated for each quantification replication.

$$\boldsymbol{A}: \boldsymbol{x} = \boldsymbol{e}^{\frac{\boldsymbol{y} + \mathbf{56.208}}{\mathbf{27.314}}} * \mathbf{10} = \mathbf{79}\ \boldsymbol{mg\ of\ Ex\_FABP\ protein/L\ of\ EW}$$

$$\boldsymbol{B}: \boldsymbol{x} = \boldsymbol{e}^{\frac{\boldsymbol{y} + \mathbf{61.256}}{\mathbf{39.472}}} * \mathbf{10} = \mathbf{95}\ \boldsymbol{mg\ of\ Cal\_\gamma\ protein/L\ of\ EW}$$

$$\boldsymbol{C}: \boldsymbol{x} = \boldsymbol{e}^{\frac{\boldsymbol{y} + \mathbf{182.43}}{\mathbf{69.971}}} * \mathbf{100} = \mathbf{2976}\ \boldsymbol{mg\ of\ \alpha\_1\_ovoglycoprotein/L\ of\ EW}$$

Figure 4.5. Amount of lipocalins found in EW according to WB analysis. Concentration were determined from the line-fit equations of corresponding calibration curves. Only the results regarding Cooperative eggs are shown.

WB analysis showed that all three lipocalins are present in EW at detectable levels, with mobilities matching those of the purified proteins for Ex-FABP and Cal-γ (Figure 4.3). However, α1-ovoglycoprotein in EW showed a higher apparent mass (37.4 kDa) than that of the recombinant protein (22.7 kDa). This discrepancy is presumed to arise from the N-type glycosylation of α1-ovoglycoprotein within EW (30.3% total glycosylation; Ketterer, 1965); glycosylation causes a reduced mobility during SDS-PAGE (Guérin-Dubiard *et al.* 2006). This hypothesis is supported by the mass of 30 kDa obtained for α1-ovoglycoprotein by MALDI-TOF mass spectroscopy (Haginaka *et al.*,1995).

The semi-quantitative WB indicated EW concentrations of 5, 0.1, and 0.1 g/L (Table 4.2) for α1-ovoglycoprotein, Cal-γ and Ex-FABP, respectively (equivalent to 232.9, 5.6, and 5.1 µM, respectively). They are therefore the 4th, 11th and 12th most abundant proteins in EW by mass (see Kovacs-Nolan *et al.*, 2005 for a review). The levels observed were relatively consistent between egg producers which suggests that the abundances reported here are likely to be generally reflective of those found in chicken eggs. Although the 2-DE and MS analyses of previous workers (Guérin-Dubiard *et al.* 2006) indicated that Ex-FABP and Cal-γ are considerably less abundant in EW than α1-ovoglycoprotein, no concentration values had been assigned to Ex-FABP and Cal-γ in EW, until the results reported herein.

Table 4.2. Concentration of lipocalin-like proteins found in EW (three trademarks coming from different providers in the UK) according to WB analysis. To convert the concentration from g/L to molarity, the theoretical MW of the mature proteins was used: 19.1, 19.9 and 21.4 kDa for Ex-FABP, Cal-γ and α1-ovoglycoprotein, respectively.

	Ex-FABP		*Cal-γ*		*α1-ovoglycoprotein*	
	g/L	µM	g/L	µM	g/L	µM
Cooperative	0.079	4.1	0.095	4.8	2.976	139.1
Clarence Court	0.115	6.0	0.123	6.2	6.497	303.6
Happy egg	0.098	5.1	0.113	5.7	5.480	256.1
Average	**0.097**	**5.1**	**0.110**	**5.6**	**4.984**	**232.9**
SD	**± 0.018**	**± 1.0**	**± 0.014**	**± 0.7**	**± 1.812**	**± 84.7**

The level of α1-ovoglycoprotein in EW was previously estimated as ~1 g/L (Ketterer, 1965), whereas here a considerably higher concentration of 5 g/L is reported. This difference may reflect the use of alcohol precipitation before quantification in the previous report (Ketterer, 1965), which could lead to incomplete protein recovery. Since in the work reported here quantification was achieved directly on EW, it seems reasonable to suggest that the estimation obtained is closer to the true value but might still represent an underestimate as the glycosylation of the native EW protein might reduce its immunoreactivity against the antibodies raised to the non-glycosylated form. Given the previous classification of EW proteins based on abundance (Kovacs-Nolan *et al.*, 2005), α1-ovoglycoprotein belongs to the high concentration group of 'major EW protein' set along with ovalbumin (54 g/L), ovotransferrin (12 g/L), ovomucoid (11 g/L), globulin (4 g/L), ovomucin (3.5 g/L), lysozyme (3.4 g/L) and ovoinhibitor (1.5 g/L). However, Ex-FABP and Cal-γ would belong to the 'minor EW protein' set, which include ovoflavoprotein (0.8 g/L), ovostatin (0.5 g/L), cystatin (0.05 g/L), and avidin (0.05 g/L).

4.2 Ex-FABP binds enterobactin with high affinity and strong preference for the ferrated form

In this section, the ability of the three EW lipocalins to specifically bind $Fe(DHBA)_3$, apo- and ferric-Ent, as well as apo- and ferric-Sal was compared with that of LCN2, using three different techniques: TQF, BLI, and ITC. TQF was the first method used as it had already been used to measure intercations between lipocalins and siderophores (Correnti *et al.*, 2011; Goetz *et al.*, 2002). BLI was then used as part of a trial offered by FortéBio. Finally, ITC was carried-out with enterobactin and salmochelin.

4.2.1 Tryptophan quenching fluorescence

Tryptophan quenching fluorescence (TQF) is a binding assay used to monitor protein conformational changes (section 2.6.1). Previous studies showed that this assay can be used to measure LCN2 affinity for 2,3-DHBA due to the presence of a single tryptophan residue in the LCN2 iron-binding pocket. Indeed, Devireddy *et al.* (2010) and Goetz *et al.* (2002) both showed that the addition of 2,3-DHBA quenched its intrinsic fluorescence (K_D of 7.9 nM and 8 nM, respectively). In our study, to optimise the TQF, the fluorescence spectrum of every protein was plotted. Figure 4.6 shows that the optimum emission wavelength was 320 nm for LCN2, α1-ovoglycoprotein and Ex-FABP, whereas for Cal-γ, the optimum emission wavelength was 340 nm.

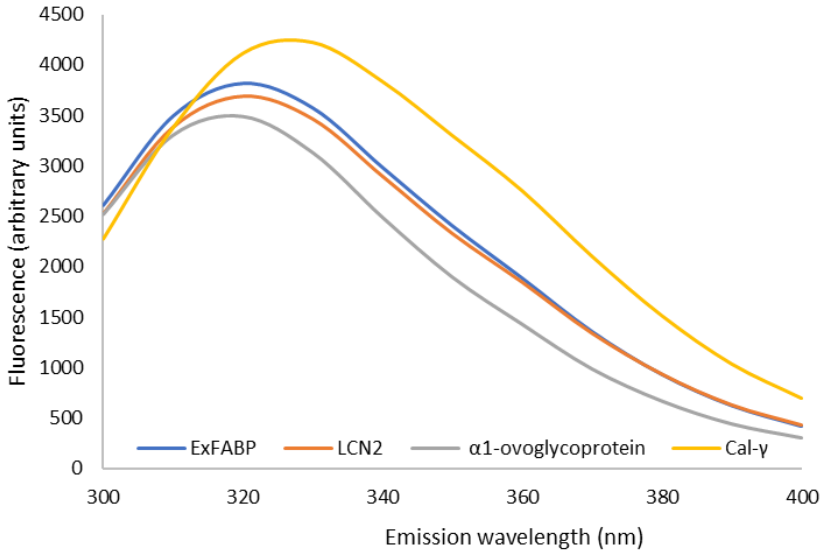

Figure 4.6. Intrinsic fluorescence of Ex-FABP (in blue), LCN2 (in orange), α1-ovoglycoprotein (in grey), Cal-γ (in yellow), depending on the emission wavelength. Excitation was at 280 nm; proteins were dissolved at 5 µM in 1X PBS buffer.

According to the preliminary experiment above, TQF was achieved with excitation wavelengths at 280 nm and emission wavelengths at 340 nm (for Cal-γ) and 320 nm (for LCN2, α1-ovoglycoprotein, and Ex-FABP). Figure 4.7 shows that there is a quenching effect when human lipocalin (LCN2) is exposed to $Fe(DHBA)_3$ concentrations ranging from 0.065 to 32 µM. Results were expressed in BC50: the concentration of $Fe(DHBA)_3$ required for 50% binding to recombinant human lipocalin-2. LCN2 was able to bind $Fe(DHBA)_3$ with a BC50 of 1.5 µM. This is in accordance with Chen *et al.* (2016) who calculated a BC50 value of 1.54 µM by exposing LCN2 (2 µM) to $Fe(DHBA)_3$ (concentration ranging from 0 to 40 µM). Regarding Ex-FABP, evidence that it can bind $Fe(DHBA)_3$ had never been shown. However, it is known that Ex-FABP can bind enterobactin, as well as its mono-glucosylated form and that this can be observed *via* fluorescence quenching (K_D of 0.22 and 0.07 nM, respectively; Correnti *et al.*, 2011). According to the results presented here, the affinity of Ex-FABP for $Fe(DHBA)_3$ would be 2-fold lower than for LCN2 (BC50 of 3 µM and 1.5 µM, respectively). No quenching effect were noted for Cal-γ and α1-ovoglycoprotein, indicating that neither bind $Fe(DHBA)_3$.

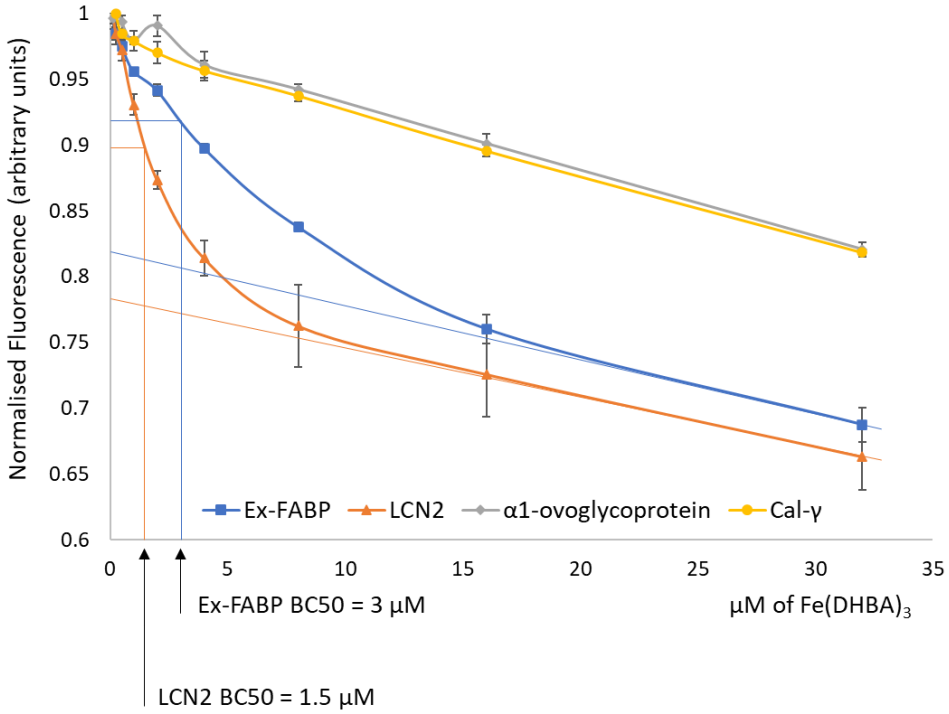

Figure 4.7. Fluorescence emission of lipocalins according to concentration of ligand $Fe(DHBA)_3$. Fifty milliliters of 5 µM proteins were mixed with an equal volume of standard curve ranging from 0 to 32 µM of $Fe(DHBA)_3$ in black-walled, clear-bottom 96-well microplates. BC50 was calculated as the concentration of $Fe(DHBA)_3$ required to bind 50% of the ligand. Error bars are the standard error calculated from three biological replicates with two technical replicates.

4.2.2 Bio-Layer Interferometry

Since TQF has shown possible interactions between Ex-FABP and $Fe(DHBA)_3$, BLI was used to confirmation these interactions (section 2.6.2). BLI is a label-free technology for measuring biomolecular interactions. It is an optical analytical technique that analyses the interference pattern of white light reflected from two surfaces: a layer of immobilised protein on the biosensor tip, and an internal reference layer. Any change in the number of molecules bound to the biosensor tip causes a shift in the interference pattern that can be measured in real-time. The sensorgrams showing binding kinetics between Ex-FABP and $Fe(DHBA)_3$ are presented in Figure 4.8. The equilibrium dissociation constant (K_D) between Ex-FABP and $Fe(DHBA)_3$ was then calculated using the association rate constant (k_a) and dissociation rate constant (k_{dis}) given by the software models (formula in section 2.6.2; summary Table 4.3).

The average K_D extracted from this dataset was 71.8 ± 20.8 nM (with average k_a of $1.06 \pm 0.36 \times 10^5$ $M^{-1}s^{-1}$ and an average k_{dis} of $6.21 \pm 0.54 \times 10^{-3}$ s^{-1}). It is important to note that this value corresponds to a lower affinity than the one described by Correnti *et al.* (2011) (i.e K_D of 0.07 ± 0.02 nM for Fe[Ent]). However, Correnti *et al.* (2011) used enterobactin not $Fe(DHBA)_3$ and obtained their affinity constant value using TQF and rather than BLI. Further experiments with ITC using enterobactin and salmochelin S4 were then used to give additional information on the strength of the binding towards *S.* Enteritidis siderophores.

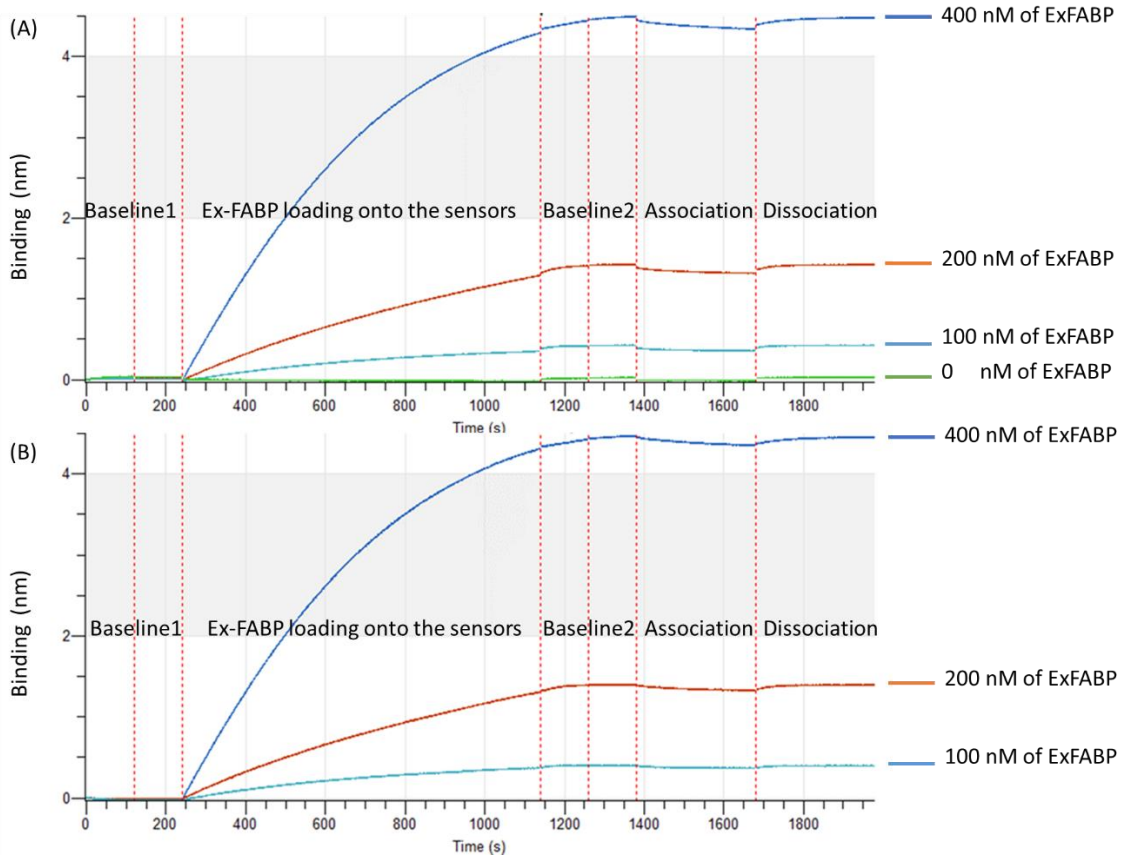

Figure 4.8. Sensorgram showing binding kinetics between Ex-FABP and $Fe(DHBA)_3$. After an initial baseline step in 1X PBS (240 s), streptavidin biosensors are dipped into solution containing 400, 200, 100, or 0 nM of biotinylated Ex-FABP (900 s). A second baseline in 1X PBS (240 s) step is performed followed by association with 100 nM $Fe(DHBA)_3$ (300 s) and dissociation in 1X PBS (300 s). **A.** Raw data graph. **B.** Processed data graph (zero baseline subtracted to the data set).

Table 4.3. Equilibrium dissociation constant (K_D), association rate constant (k_a) and dissociation rate constant (k_{dis}) between Ex-FABP and $Fe(DHBA)_3$.

$Fe(DHBA)_3$ concentration (nM)	*Ex-FABP concentration (nM)*	*K_D (nM)*	*k_a ($M^{-1}s^{-1}$)*	*k_{dis} (s^{-1})*
100	400	110 ± 0.32	4.68×10^4	5.16×10^3
100	200	67.4 ± 0.23	1.03×10^5	6.94×10^3
100	100	38.2 ± 0.16	1.71×10^5	6.53×10^3

4.2.3 Isothermal titration calorimetry (ITC)

4.2.3.1 Protein and ligands dissolved in TBS pH 7.4

Although TQF and BLI successfully showed that Ex-FABP can bind the precursor of enterobactin, $Fe(DHBA)_3$, it remained important to test the ability of the three EW lipocalins to specifically bind enterobactin (Ent) and salmochelin (diglucosylated form, DGE) in comparison with LCN2. The method employed was ITC. This method utilises a motorised injection syringe, in which the ligand is loaded, and two adiabatic cells (i.e. a sample cell filled with a lipocalin and a reference cell filled with buffer only) set at 30 or 20 °C. When the ligand is injected in the sample cell, the ITC measures the difference of heat required to maintain both cells at a constant temperature. Hence, if lipocalins can bind *S*E siderophores, the ITC should measure the heat consumed or released when the ligand is injected into the sample cell. The area of each peak is then integrated and plotted versus the molar ratio of ligand to protein. The resulting isotherm can be fitted to a binding model from which the affinity (K_D) is derived. When binding was observed, control blank titrations were performed by injecting ligand into buffer to assess if consumed or released heat could be due to ligand dilution (Appendix 6).

LCN2 affinity for apo-siderophores. Apo-Ent addition to the sample cell containing LCN2 caused a downward peak in the binding isotherm (Figure 4.9A). This indicates that the sample cell became warmer than the reference cell due to an exothermic reaction. The molar ratio between the ligand and protein was gradually increased through a series of ligand injections. Indeed, apo-Ent (50 µM) was added ten time in excess compared to LCN2 (5 µM), bringing the reaction towards saturation. From this binding isotherm, an equilibrium dissociation constant (K_D) of 58 ± 12 nM (at pH 7.4; Figure 4.9; Table 4.4) was derived. This K_D is 16-fold higher than the value previously reported using TQF (3.57 nM; Abergel *et al.,* 2006). No binding was observed with apo-DGE (Figure 4.9A), which matches previous findings showing that LCN2 does not bind Fe^{3+}-DGE (Fischbach *et al.,* 2006).

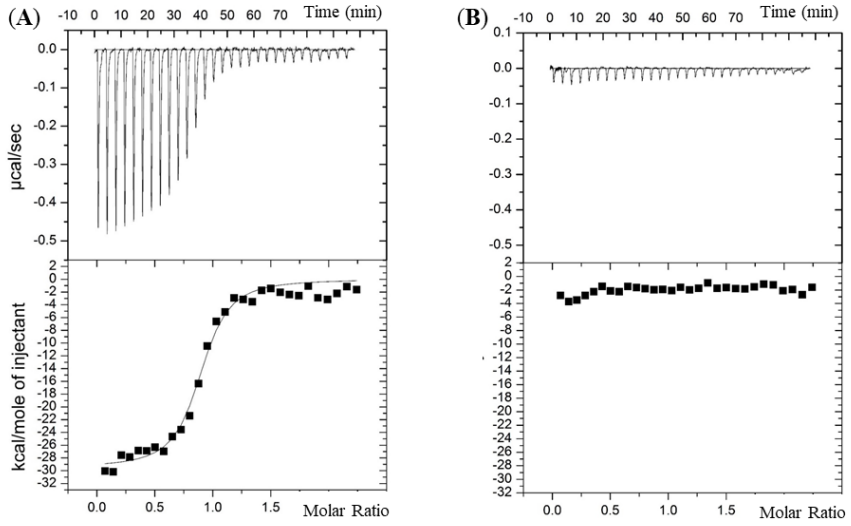

Figure 4.9. Measurement of LCN2 affinity for (A) apo-Ent (B) apo-DGE. Isothermal Titration Calorimetry was achieved with 29 injections (10 µL) of 50 µM ligand (apo-Ent or apo-DGE) in an adiabatic well containing 5 µM of LCN2. Experiments were achieved in TBS (20 mM Tris, 500 mM NaCl, 1.3% DMSO, pH 7.4) at 30 °C. LCN2 has a K_D of 58 ± 12 nM in those conditions.

Ex-FABP affinity for apo-siderophores. Ex-FABP also bound apo-Ent at high-affinity, giving an exothermic reaction with a dissociation constant (K_D) of 86 ± 5 nM at pH 7.4 (Table 4.4; Figure 4.10) and likewise failed to interact with apo-DGE, as observed previously (Correnti *et al.*, 2011). It should be noted that the Ex-FABP binding affinity for apo-Ent found here is 172-fold weaker than that determined previously (0.5 ± 0.15 nM) using TQF under similar (TSB buffer, pH 7.4) conditions (Correnti *et al.*, 2011). This discrepancy could result from the difference in the techniques used (ITC *vs* TQF), differences in reaction conditions (e.g. Ex-FABP and DMSO concentrations) or differences in protein preparation. For both LCN2 and Ex-FABP, the apo-Ent molar-binding stoichiometry was close to 1:1 at 0.872 and 0.617, respectively (Table 4.4), which again is consistent with previous reports (Correnti *et al.*, 2011; Goetz *et al.*, 2002).

Cal-γ and α1-ovoglycoprotein affinity for apo-siderophores. ITC indicated that neither Cal-γ nor α1-ovoglycoprotein bind either apo-Ent or apo-DGE (Table 4.4; Figure 4.10) which suggests that these lipocalins do not act as 'siderocalins'. This was in accordance with the TQF results showing no quenching effect when $Fe(DHBA)_3$ was added to 2 µM of Cal-γ or α1-ovoglycoprotein. However, it remains possible that these EW lipocalins could have affinity for siderophores not considered here.

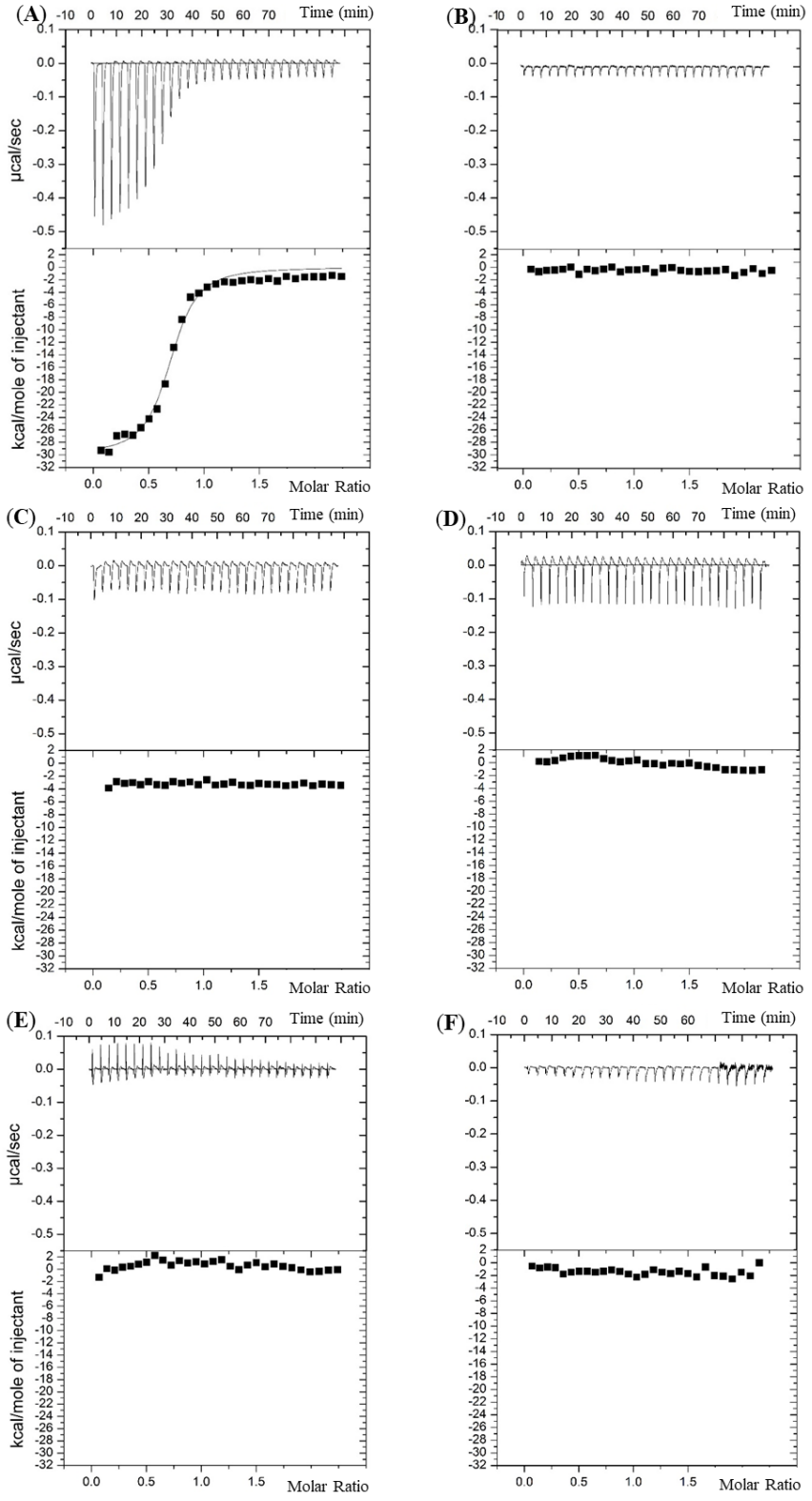

Figure 4.10. Interactions between lipocalins and *S.* Enteritidis siderophores. Isothermal Titration Calorimetry was achieved by doing 29 injections (10 µL) of 50 µM ligands (apo-Ent or apo-DGE) in an adiabatic well containing 5 µM lipocalins. Proteins and ligands were both dissolved in TBS (20 mM Tris, 500 mM NaCl, 1.3% DMSO, pH 7.4) and experiments were achieved at 30 °C. No interactions could be measured between Ex-FABP and apo-DGE (B), whereas a K_D of 86 ± 5 nM was measured between Ex-FABP and apo-Ent (A). No interaction could be measured between Cal-γ and apo-Ent (C), Cal-γ and apo-DGE (D), α1-ovoglycoprotein and apo-Ent (E) and α1-ovoglycoprotein and apo-DGE (F) (Julien *et al.*, 2020).

LCN2 and Ex-FABP affinity for Fe^{3+}-siderophores. Since a previous TQF study indicated that Ex-FABP binds Fe^{3+}-Ent with a higher (2.3-fold) affinity than apo-Ent (Correnti *et al.,* 2011), and similar findings have been made with LCN2 (8.7-fold; Abergel *et al.,* 2006), the interaction between Fe^{3+}-Ent and Ex-FABP was tested here by ITC. The results show a 16-fold higher affinity (K_D 5.3 ± 3.8 nM) for Fe^{3+}-Ent than for apo-Ent (Table 4.4; Appendix 7) which indicates a more considerable preference for the ferric- over the apo-form than was previously suggested (Correnti *et al.,* 2011). The ITC data also indicates that LCN2 possesses a 4.9-fold higher affinity (K_D 11.8 ± 8.8 nM) constant for Fe^{3+}-Ent than for apo-Ent (Table 4.4; Appendix 7); a similar higher affinity (8.7 fold) was reported by Abergel *et al*. (2006) and Bao *et al.* (2010) who showed that Fe^{3+} dramatically enhances the affinity of LCN2 for catechols (by at least 95-fold). It should be noted that the ITC-determined binding affinities of LCN2 for Fe^{3+}-Ent reported here (11.8 nM) and previously (240 nM; Li *et al.,* 2015) are both considerably weaker than those determined by TFQ (0.41 and 0.43 nM; Goetz *et al.,* 2002; Fischbach *et al.,* 2006) indicating that differences in published affinity values for LCN2 (and Ex-FABP) are to a large degree related to the methods employed.

Table 4.4. Lipocalins-binding affinities towards apo- and ferric-ligands obtained using Isothermal Titration Calorimetry (in TBS pH 7.4 at 30 °C) in this study and compared values from the literature. K_D is the equilibrium dissociation constant, n the binding stoichiometry, ΔS the entropy, and ΔH the enthalpy. DGE stands for di-glucosylated enterobactin. *Under the detection threshold (Julien *et al.*, 2020).

Protein	*Ligands*	*Reference*	*K_D nM*	*n*	*ΔS cal/ mol, K*	*ΔH cal/mol*
LCN2	*Apo -enterobactin*	This study	58.4 ± 12.5	0.872	-58.9	-2.78 x 10^4
		Abergel *et al.*, 2006	3.57			
	Fe^{3+}-enterobactin	This study	11.8 ± 8.8	0.863	-50.2	-2.62 x 10^4
		Goetz *et al.*, 2002	0.41			
		Fischbach *et al.*, 2006	0.43			
		Li *et al.*, 2015	240			
	Apo -salmochelin (DGE)	This study	*			
		Fischbach *et al.*, 2006	*			
Ex-FABP	*Apo -enterobactin*	This study	86.2 ± 14.6	0.617	-60.9	-2.83 x 10^4
		Correnti *et al.*, 2011	0.5 ± 0.15			
	Fe^{3+}-enterobactin	This study	5.3 ± 3.8	0.672	-26.1	-1.94 x 10^4
		Correnti *et al.*, 2011	0.22 ± 0.06			
	Apo -salmochelin (DGE)	This study	*			
		Correnti *et al.*, 2011	*			
Cal-γ	*Apo -enterobactin*	This study	*			
	Apo -salmochelin (DGE)	This study	*			
α1-ovoglyco -protein	*Apo -enterobactin*	This study	*			
	Apo -salmochelin (DGE)	This study	*			

4.2.3.2 Protein and ligands dissolved in EW filtrate (pH 9.2)

Since TBS buffer is not representative of the pH of EW, ITC experimentations were carried out to measure Ex-FABP affinity towards apo- and ferric-Ent in EW filtrate (this medium that does not contain macromolecules above 10,000 Da; section 2.1.1). Ex-FABP had K_D values of 925 nM ± 287 nM and 22.0 ± 13.1 nM for apo-Ent and Fe-Ent, respectively, in this medium (Figure 4.11; Table 4.5). Thus, the affinity of Ex-FABP for apo-Ent and Fe-Ent is 11- 4.2-fold higher in TBS than in EWF, suggesting that Ex-FABP affinity towards Ent is lower in EWF, and that it displays a greater preference for Fe-Ent (42- cf. 16-fold) in EWF than in TBS. This reduced affinity in EWF could be explained by the higher pH since Ex-FABP interaction with Ent is anticipated to involve three conserved, positively charged residues (R101, R112, K82; Figure 3.1). The relative charges of these residues will be reduced at the higher pH associated with EWF which could explain the observed 11- or 4.2- fold reduction in affinity.

The experiment was also conducted in the same medium using apo-DGE as a ligand. Again, no interaction between Ex-FABP and apo-DGE could be measured (data not shown).

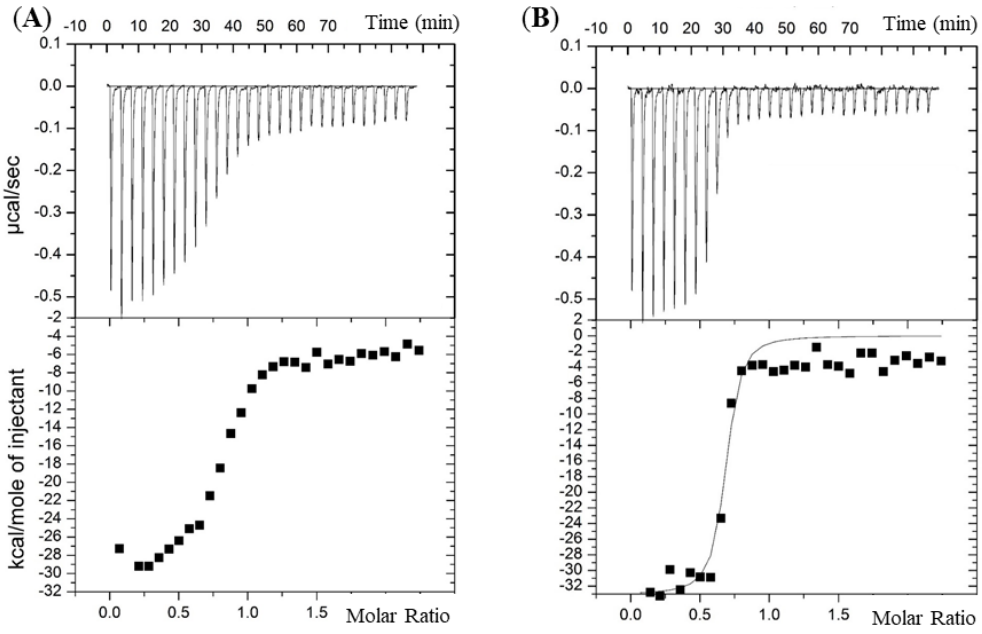

Figure 4.11. Measurement of Ex-FABP affinity for (A) apo-Ent and (B) ferric-Ent in EWF, 1.3% DMSO, pH 9.2 (30 °C). Isothermal Titration Calorimetry was achieved with 29 injections (10 µL) of 50 µM ligand (apo- or ferric- Ent) in an adiabatic well containing 5 µM of Ex-FABP. Ex-FABP has a K_D of 925.0 ± 286.8 nM for apo-Ent and has a K_D of 22.0 ± 13.1 nM for ferric-Ent in those conditions.

Table 4.5. Ex-FABP-binding affinities towards apo- and ferric-ligands obtained using Isothermal Titration Calorimetry (in EWF pH 9.3 at 30 °C). K_D is the equilibrium dissociation constant, n the binding stoichiometry, ΔS the entropy, and ΔH the enthalpy. *Under the detection treshold.

Protein	*Ligands*	K_D *nM*	*n*	*ΔS* *cal/ mol, K*	*ΔH* *cal/mol*
Ex-FABP	*apo-Ent*	925.0 ± 286.8	0.928	-99.0	-3.84 x 10^4
Ex-FABP	*Fe^{3+}-Ent*	22.0 ± 13.1	0.657	-74.1	-3.31 x 10^4
Ex-FABP	*apo-Sal*	*			

4.3 Conclusion and future work

Semi-quantitative WB indicated EW concentrations of 5, 0.1, and 0.1 g L^{-1} for α1-ovoglycoprotein, Cal-γ and Ex-FABP, respectively (equivalent to 232.9, 5.6 and 5.1 µM, respectively). TQF and ITC showed that neither Cal-γ nor α1-ovoglycoprotein bind $Fe(DHBA)_3$, enterobactin or salmochelin (DGE). However, it is important to note that α1-ovoglycoprotein is glycosylated in EW and such post-translational modifications were not achieved during overproduction in *E. coli*. This lack of glycosylation might have influenced the observed bioactivity of the recombinant protein. Likewise, evidence (ESI-MS) indicates that purified Cal-γ may bind an unidentified ligand that could interfere with the observed bioactivity. ITC confirmed the preference (16 fold) of Ex-FABP for the ferrated form (K_D of 5.3 nM) of enterobactin over the iron free form (K_D of 86.2 nM) at neutral pH, and its lack of affinity for salmochelin (DGE), as was previously observed by Correnti *et al.* (2011). It is important to note, however, that Ex-FAPB affinity for enterobactin appears to be decreased in EW, which might be due to the alkaline pH.

In this chapter, it was highlighted that differences in affinity values for LCN2 (and Ex-FABP) are to a large degree related to the methods employed. As future work, it would be worthwhile to compare the affinity values for LCN2 and Ex-FABP obtained with ITC (this study; Li *et al.*, 2005) and TQF (Correnti *et al*., 2011; Abergel *et al.*, 2006; Goetz *et al.*, 2002; Fischbach *et al.*, 2006) to a third method used in this study: BLI. Pros and cons for all three methods are summarised on Table 4.6.

Table 4.6. Pros and cons for methods used in this study to measure biomolecular interactions.

	Pros	***Cons***
TQF	Only a fluorimeter is required No need for reporter labels	Relatively high sample consumption Need for tryptophan residues to observe intrinsic fluorescence
BLI	Low sample consumption No need for reporter labels	Immobilisation of ligand to surface of tip required
ITC	Good reproducibility Heat is a universal signal No need for reporter labels	Low throughput High sample consumption

Following the successful quantification of EW lipocalins and determination of their siderophore-binding activity as described in this chapter, in the next chapter *S.* Enteritidis was exposed to lipocalins in order to study the impact of siderophores sequestration on growth.

Chapter 5. Determination of the role of egg-white lipocalins in inhibiting siderophore-dependent iron sequestration by *Salmonella* Enteritidis

Mutants deficient in iron-acquisition systems were generated and tested for: (i) siderophore production under low iron conditions; (ii) growth under low iron conditions with/without lipocalin proteins; and (iii) growth in EW medium. The aim was to determine whether exposure to lipocalins limits *S.* Enteritidis growth and whether salmochelin secretion overcomes any observed inhibition due to the enterobactin-binding ability of EW lipocalins which might thus contribute to *S.* Enteritidis survival or growth in EW.

5.1 Library construction of mutants deficient in iron acquisition systems

Mutants deficient in iron acquisition were generated using the λRed disruption system. Several genes were targeted giving rise to three *S.* Enteritidis mutants:

- Δ*entB*: EntB, the isochorismatase, converts isochorismate to 2,3-dihydro-2,3-dihydroxybenzoate (an enterobactin precursor). Hence the Δ*EntB* mutant should neither produce enterobactin nor its derivative (i.e salmochelin).
- Δ*iroBC*: IroB is a glucosyltransferase involved in the glucosylation of enterobactin into salmochelin and IroC is involved in its export across the cytosolic membrane. The Δ*iroBC* mutant therefore neither synthesise nor export salmochelin.
- Δ*iroDEN*: IroN takes up ferric-salmochelin across the outer membrane (OM), where it is subsequently linearized by the periplasm IroE esterase. The linearised form is then transported into the cytoplasm *via* FepBCDG where it is further esterified by IroD into monomeric and/or dimeric forms, which is presumed to facilitate iron release. Thus, the Δ*iroDEN* mutant should produce salmochelin but should not be able to utilise it directly due to absence of the IroN OM receptor and IroD/IroE esterases.

Note: Despite alterations to the salmochelin pathway, both Δ*iroBC* and Δ*iroDEN* should be able to produce and utilise enterobactin.

5.1.1 Production of putative mutants using the λRed disruption system

The λRed disruption system (based on homologous recombination) was used to inactivate genes *entB*, *iroBC* and *iroDEN* as described in section 2.7.1. Firstly, the Cat cassette of plasmid pKD3 was PCR amplified using bi-partite primers (Table 2.4, section 2.1.5). Electrophoretic analysis of PCR fragments obtained showed successful amplification of the Cat cassette (1100 bp, Figure (5.1).

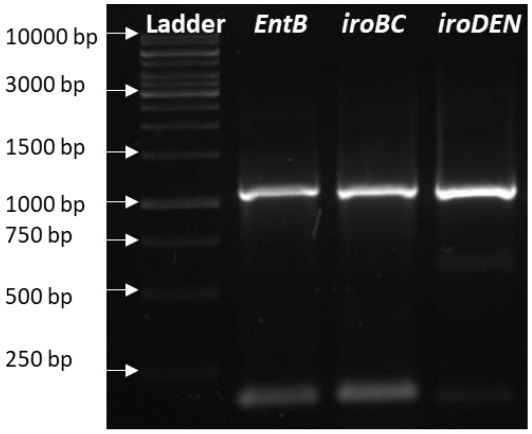

Figure 5.1. Electrophoretic analysis of DNA fragments resulting from PCR of pKD3 (Primers, Table 2.4, section 2.1.5). DNA fragments were subject to electrophoresis in a 0.7% agarose gel in 0.5X TBE (section 2.2.2). PCR products run approximatively 1100 bp, which match the expected size of the amplified Cat cassette flanked with sequences matching the targeted insert site (*entB*, *iroBC* and *iroDEN*, from the left to the right).

Secondly, heat shock transformation (section 2.3.1) was used in an attempt to introduce pKD46 into *S.* Enteritidis. After unsuccessful trials, electroporation was used as an alternative method. Once electroporation had been successfully achieved (section 2.3.2), Amp^R transformants were selected for plasmid purification. DNA fragments were then subject to electrophoresis to identify successful pKD46 transformant candidates (Figure 5.2).

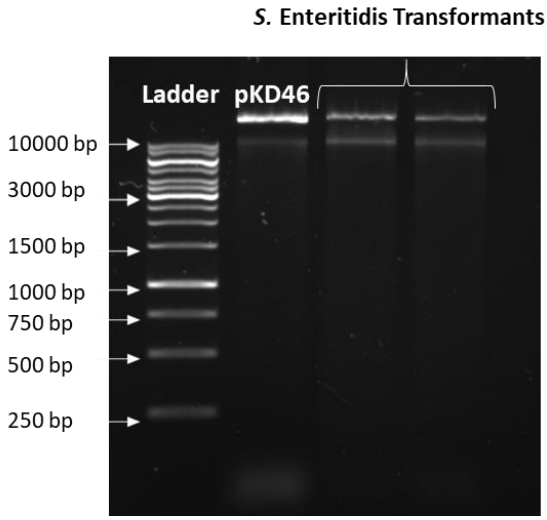

Figure 5.2. Electrophoretic analysis of plasmids extracted from two *S.* Enteritidis-pKD46 transformant candidates. DNA fragments were subject to electrophoresis in a 0.7% agarose gel in 0.5X TBE (section 2.2.2). pKD46 DNA was used as a control.

Thirdly, purified PCR fragments (that carry the Cat cassette flanked by regions matching the target loci) were electroporated into the *S.* Enteritidis-pKD46 transformant (section 2.3.2). Among the Cam^R transformants obtained (Table 5.1), three were stored at -80 °C for each mutant.

Table 5.1. Number of Cam^R transformants obtained after electroporation of PCR fragments in *S.* Enteritidis.

Cam^R transformants	*Concentration*
ΔiroDEN::*cat*	10 CFU/plate
ΔiroBC::*cat*	20 CFU/plate
ΔentB::*cat*	20 CFU/plate

5.1.2 Knockout confirmation by PCR

Following genomic DNA isolation of Cam^R transformants, knockout status was confirmed by PCR using primers (Table 2.5, section 2.1.5) hybridising upstream and downstream of the sequences used for recombination. As shown in Figure 5.3, fragments of 1200 bp (matching the size of the Cat cassette and the flanking region) were PCR amplified using post-deletion confirmation primers. This suggests that the Cat cassette had been inserted at the right location in the genome, replacing the targeted genes in each case (also PCR amplification for the WT; Figure 5.3).

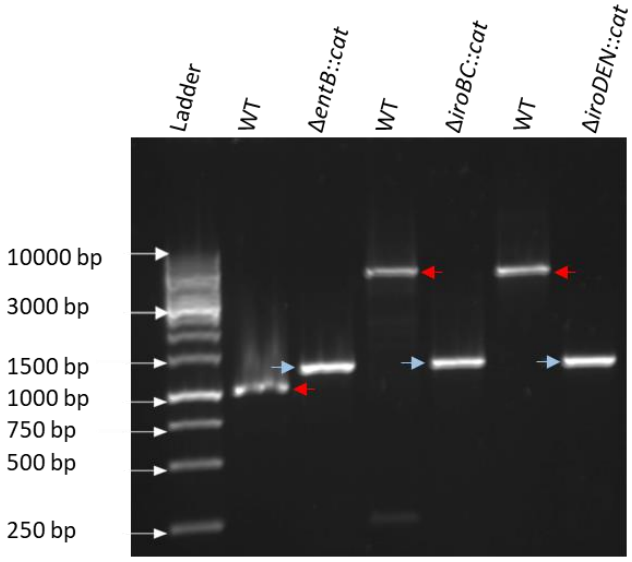

Figure 5.3. Electrophoretic analysis of DNA fragments resulting from PCR of genomic DNA isolated from mutant candidates or WT (primers, Table 2.5, section 2.1.5). PCR products were subjected to electrophoresis in a 0.7% agarose, 0.5X TBE gel (section 2.2.2). Red arrows show products matching the size of *entB*, *iroBC* and *iroDEN* loci in the WT (~1000, ~5200, and ~5000 bp, respectively); blue arrows show products matching the size of Cat cassette inserted in the genome to replace the genes at these loci (~1200 bp).

5.1.3 Characterisation of putative mutants deficient in siderophore production

In order to further characterise the mutants produced, siderophore production under low iron conditions was studied. Mutants identified above were screened on CAS plates (section 2.8) to confirm the defective phenotype (defect in siderophore production and/or export). The Δ*entB*::*cat* colonies grown on CAS plates did not produce any siderophore, suggesting successful knockout (Figure 5.4A). For both Δ*iroBC*::*cat* and Δ*iroDEN*::*cat*, colonies turned the CAS plates yellow as expected, since only salmochelin production or utilisation was expected to be impaired and enterobactin should remain unaffected. The experiment was repeated by inoculating with 50 µL of overnight culture (grown in M9 medium diluted to an OD of 0.5) on to a CAS plate punctured with 30 mm wells. More siderophore production was detected for the Δ*iroDEN*::*cat* mutant compared to the WT: 14 mm *vs* 17 mm yellow halos (3 technical replicates; Figure 5.4B). This could be explained by the fact that the Δ*iroDEN*::*cat* mutant is able to produce both enterobactin and salmochelin but cannot import salmochelin due to lack of IroN. It is thus likely to be more iron restricted than the WT, hence generating a higher level of exported siderophores in response, as detected in the CAS plate assay.

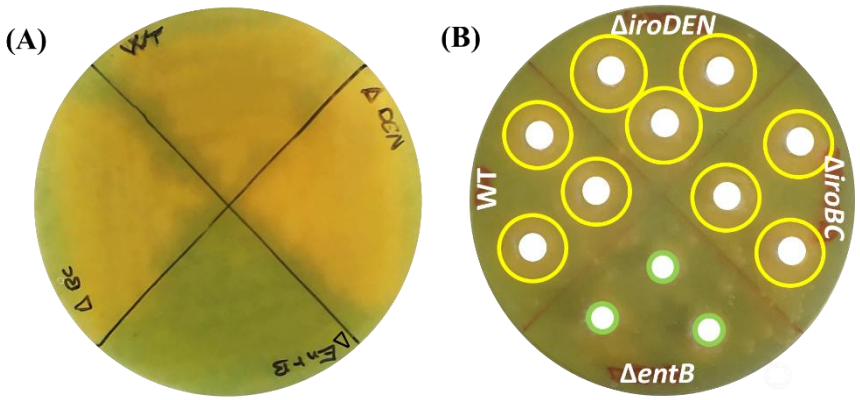

Figure 5.4. A. Candidates transformants screened on CAS plates to detect successful insertion of the Cat cassette. B Relative quantification of siderophore produced. After 12 h of incubation at 37 °C, strains producing siderophores turned the media to a yellow-golden colour while CAS plates streaked with non-producing siderophore strains remained green.

5.1.4 Removal of the Cat cassette and whole-genome sequencing

Stocks of pCP20 plasmid DNA were made by transforming *E. coli* Top10 (heat shock method, section 2.3.1), followed by plasmid isolation (growth was at 30 ˚C). pCP20 was then electroporated into *S.* Enteritidis Δ*entB*::*cat*, Δ*iroDEN*::*cat*, and Δ*iroBC*::*cat* (section 2.3.2). Electophoretic analysis of plasmids extracted from Amp^R transformants showed successful transformation (Figure 5.5).

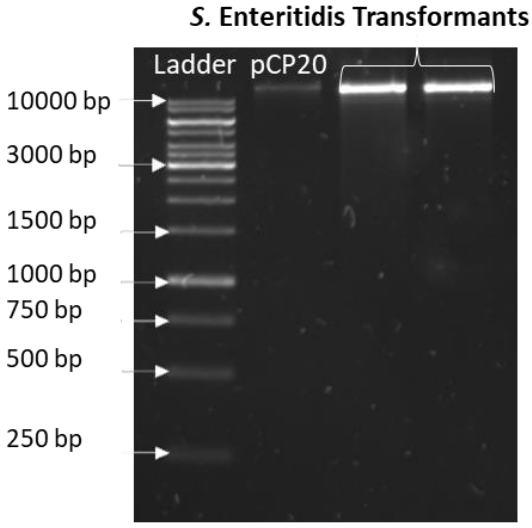

Figure 5.5. Electrophoretic analysis of plasmids extracted from two *S*E-pCP20 transformant candidates. DNA fragments were subject to electrophoresis in a 0.7% agarose gel in 0.5X TBE (section 2.2.2). pCP20 DNA was used as a control.

Subsequently, for each transformant, induction of FLP recombinase expression and selection for the loss of pCP20 was achieved at 45 °C (section 2.7.1). Cat cassette removal and pCP20 loss candidates were screened (section 2.7.1) to identify strains both Amp^S and Cam^S. For each mutant (Δ*iroDEN*, Δ*iroBC*, and Δ*entB*), three such candidates were selected and stored at -80 °C.

Removal of the Cat cassette and generation of clean deletions was confirmed (for one candidate per mutant) by PCR (Appendix 8) and whole-genome sequencing. Corresponding genome sequences were deposited at the ENA database under the following project accession number: PRJEB36543. A variant analysis was conducted to verify if any other mutations were inserted in the genome. Although the large deletion for *iroBC, iroDEN* and *entB* are clear (Figure 5.6 & 5.7), there are a few variations between the four genome sequences. The variations appear to be related to poor sequence coverage; it was therefore assumed that they are artefacts. With the identity of those three mutants confirmed, growth experiments were then conducted.

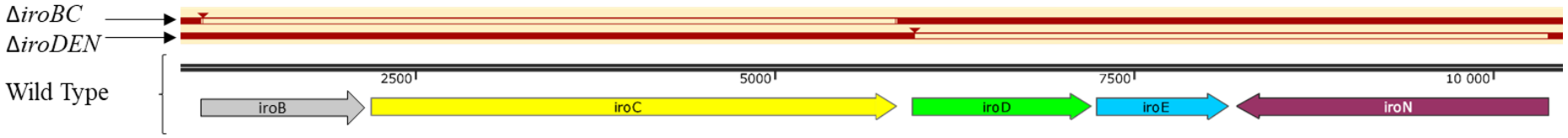

Figure 5.6. Genome alignment between the WT and the knockout strains showing the successful deletion of *iroD*, *iroE*, and *iroN* for the mutant Δ*iroDEN* as well as the deletion of *iroB*, and *iro*C for the mutant Δ*iroBC*. Red colour indicates matches and white colour indicates gaps with the reference genome (the WT for instance).

Figure 5.7. Genome alignment between the WT and the knockout strains showing the successful deletion of *entB* for the mutant Δ*entB*. Red colour indicates matches and white colour indicates gaps with the reference genome (the WT for instance).

5.2 Provision of Ex-FABP inhibits growth of a salmochelin-deficient *Salmonella* Enteritidis mutant in standard growth media

5.2.1 Effect of egg-white lipocalins on *Salmonella* Enteritidis growth in minimal medium (M9) with or without ferric citrate

To assess whether exposure to EW lipocalins negatively impacts *S.* Enteritidis growth through enterobactin (Ent) sequestration, growth of the siderophore-defective *S.* Enteritidis mutants and WT was monitored in the presence and absence of each of the EW lipocalins and LCN2. Lipocalins were added at Cal-γ and Ex-FABP concentrations found in EW (i.e 5 μM), under low- (minimal [M9] medium) and sufficient- (M9 supplemented with 10 μM ferric citrate) iron conditions (Figure 5.8). In the negative control (M9 with PBS; Figure 5.8I) all strains reached an OD of 0.48 under low-iron conditions, wereas they reached an OD of 0.62 under iron-sufficient conditions (Figure 5.8J). This ability of *S.* Enteritidis to grow under low- iron conditions confirms that this pathogen is well suited to survive in environments scarce in iron.

Of the lipocalins tested, only Ex-FABP and LCN2 had any impact on iron-deficient growth (Figure 5.8E, G), and none had any impact under iron sufficiency. The Δ*iroBC* mutant (producing enterobactin only) was particularly affected with a 2.5-fold growth reduction (at 6 h; Figure 5.9) under low-iron conditions with Ex-FABP or LCN2. This reduced growth is fully consistent with the enterobactin-sequestering activities of Ex-FABP and LCN2, and the dependence of the Δ*iroBC* mutant on Ent as the sole siderophore supporting its low-iron growth. The WT also displayed a reduced growth with Ex-FABP or LCN2 under low iron, but this was far more modest (at just 1.25-fold; at 6 h; Figure 5.9) than that seen for the Δ*iroBC* mutant. This mild reduction in iron-restricted growth is consistent with the co-dependence of the WT on enterobactin and salmochelin under iron deficiency conditions. Thus, production of salmochelin by the WT appears to largely overcome the impact of enterobactin sequestration by Ex-FABP or LCN2, as reported previously for other bacteria (Correnti *et al.*, 2011; Fischbach *et al.*, 2006).

In contrast to the Δ*iroBC* mutant, the siderophore-non-producing strain (the Δ*entB* mutant) exhibited better low-iron growth (1.2 fold at 6 h; Figure 5.9) than the WT in the presence of Ex-FABP or LCN2. The failure of Ex-FABP or LCN2 to inhibit the Δ*entB* mutant is consistent with the ability of this mutant to escape competition for iron by LCN2

or Ex-FABP due its lack of enterobactin production. Thus, the results indicate that production of enterobactin as sole siderophore is deleterious under low-iron conditions in the presence of Ex-FABP or LCN2. The Δ*iroDEN* mutant showed reduced growth with respect to the other three strains (~1.1 fold at 6 h. Figure 5.9) under low-iron conditions in the absence of any lipocalins, including Ex-FABP and LCN2. This indicates that the capacity to secrete salmonchelin, but not utilise it, results in deficient growth under iron restriction, which presumably arises due to sequestration of extracellular iron by secreted salmochelin.

Cal-γ and α1-ovoglycoprotein had no apparent effect on the growth of *S.* Enteritidis or its mutants under low- or sufficient-iron conditions (Figure 5.8). This is consistent with the ITC data which indicate that these lipocalins do not bind enterobactin or salmochelin. However, as mentioned in section 4.3, it is important to note that α1-ovoglycoprotein is glycosylated in EW and that such post-translational modifications were not achieved during overproduction in *E. coli*. This lack of glycosylation might have influenced the observed bioactivity of the recombinant protein. Furthermore, this protein was used at a working concentration lower (5 µM) than its concentration in EW (233 µM; due to limited availability). Regarding Cal-γ, ESI-MS results indicated that it may bind an unidentified ligand. The latter could also interfere with the observed bioactivity. Besides, it would be interesting to test the exposure of the strains to a mixture of lipocalins to detect any synergistic effect between them.

In M9 (200 rpm, 37 °C with shaking), Ex-FABP at 5 µM caused a major inhibition of iron-restricted growth for an *S.* Enteritidis strain relying on enterobactin as sole siderophore but had only a modest impact on the WT deploying salmochelin alongside enterobactin. Since the WB data indicated that Ex-FABP is present in EW at 5.1 µM, these results suggest that Ex-FABP concentrations in EW are sufficient to cause inhibition of iron-restricted growth for an *S.* Enteritidis strain, and potentially other bacterial species, relying on enterobactin as sole siderophore.

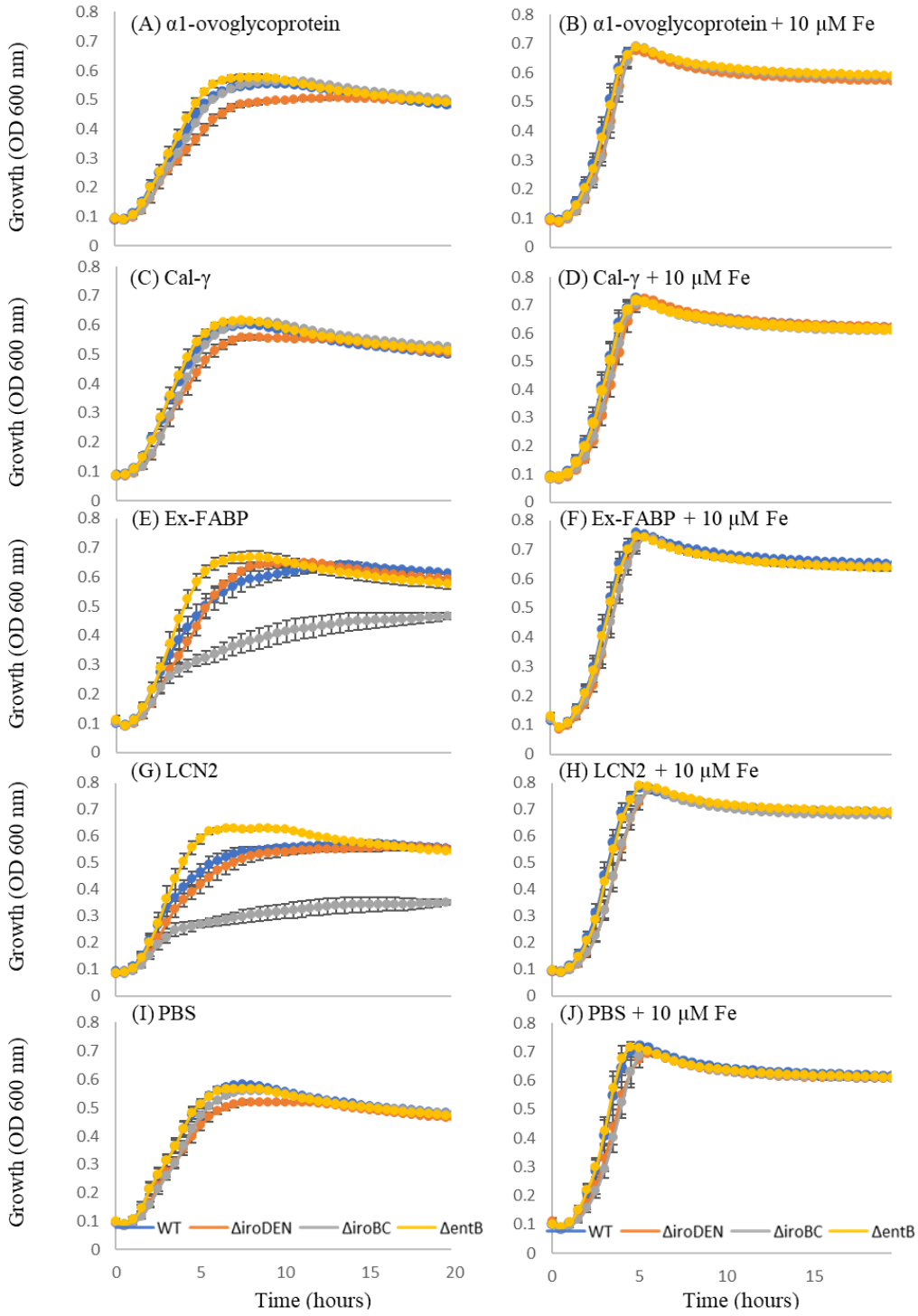

Figure 5.8. Effect of EW lipocalins on growth of *S*E and mutants defective in siderophore production and/or utilisation under iron restriction. Growth of the WT and the Δ*iroBC*, Δ*iroDEN* and Δ*entB* mutants was compared in M9 medium with (right) or without (left) 10 µM ferric citrate at 37 °C and 200 rpm, for 20 h. The medium included 5 µM of either α1-ovoglycoprotein (A, B), Cal-γ (C, D), Ex-FABP (E, F), LCN2 (G,H) or ~100 µL of PBS (I, J). Error bars indicate standard errors from three biological replicates with two technical replicates (Julien *et al.*, 2020).

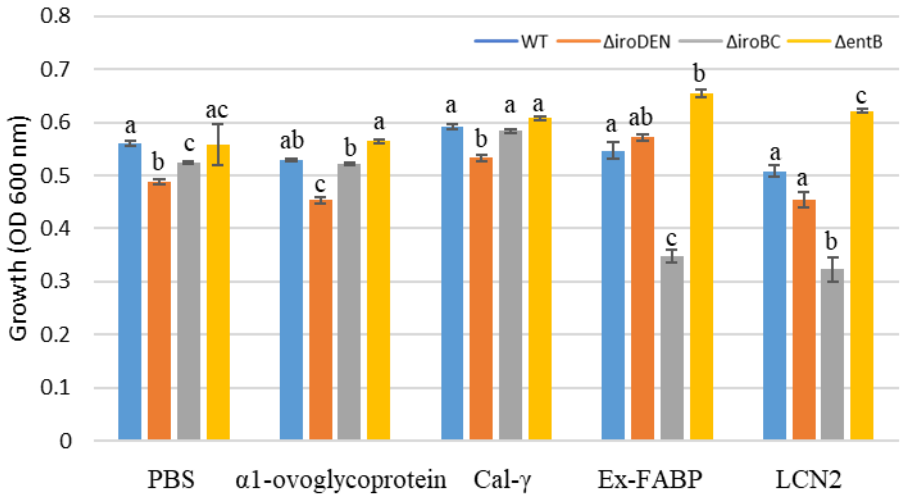

Figure 5.9. Effect of EW lipocalins on growth of *S.* Enteritidis and mutants defective in siderophore production and/or utilisation under iron restriction after 6 h incubation at 37 °C. These data are derived from those presented in Figure 5.8. Error bars indicate standard errors from three biological replicates with two technical replicates. For each growth medium, one way-ANOVA followed by a multiple comparison of means (Tukey Contrasts) was achieved using R software (version 3.5.3). This allowed to identify groups significantly different (identified as "a", "b", and "c", p-value $\leqslant 0.05$).

5.2.2 Effect of Ex-FABP on *Salmonella* Enteritidis growth in iron-rich medium (LB) with or without iron chelator (2,2-dipyridyl)

When iron was present at low level in the growth medium (only traces in M9), enterobactin synthesis did not seem to assist *S.* Enteritidis growth (section 5.2.1). To assess the role of Ex-FABP in inhibiting siderophore-dependent iron sequestration by *S.* Enteritidis, further experiments were performed in rich medium (LB) with an iron chelator (200 µM 2,2′-dipyridyl; DIP). Although no iron-restricted growth defect was observed for the Δ*entB* mutant in M9 medium, when growth tests were performed in LB with 200 µM DIP, a major reduction in growth (~4-fold), with respect to the WT, was observed (Figure 5.10). No growth defect was seen in the absence of DIP indicating that the phenotype obtained is related to iron restriction imposed by DIP chelation. This observation matches previous work (Liu *et al.*, 2015) and likely arises from the inability of the Δ*entB* mutant to effectively compete with DIP for iron due to its lack of enterobactin (and salmochelin) production. In contrast to the Δ*entB* mutant, the Δ*iroDEN* and Δ*iroBC* strains showed no growth defect in LB with DIP (Figure 5.10), presumably because they retain the ability to produce and utilise Ent, and can thus compete with DIP for iron.

The effect of Ex-FABP and LCN2 provision on *S.* Enteritidis growth were then assessed in the same medium. As expected, both Ex-FABP and LCN2 had little impact on the weak growth of the Δ*entB* mutant in LB with DIP (Figure 5.10). However, the Δ*iroDEN* and Δ*iroBC* mutants showed a significant growth defect (~1.5-2-fold reduction) compared to the WT in LB with DIP when 5 µM Ex-FABP or LCN2 were provided (Figure 5.10). This is consistent with the ability of Ex-FABP and LCN2 to sequester Ent, but not Sal. LCN2 caused a greater growth reduction than Ex-FABP (2-fold cf. 1.5-fold, respectively) for the Δ*iroDEN* and Δ*iroBC* mutants, and the growth of Δ*iroBC* mutant was slightly more reduced than that of the Δ*iroDEN* mutant (Figure 5.10).

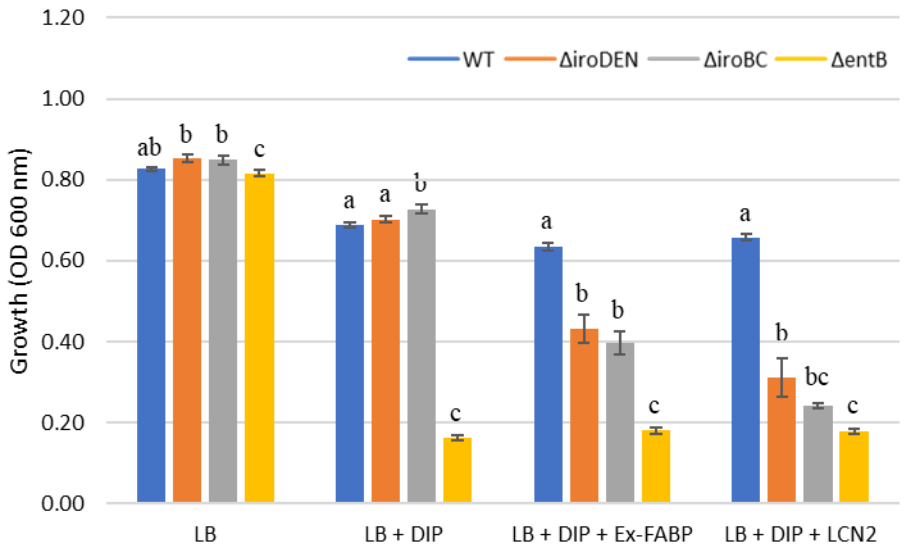

Figure 5.10. Effect of Ex-FABP on growth of *S.* Enteritidis and mutants defective in siderophore production and/or utilisation under iron restriction in rich medium (LB broth). Growth was at 37 °C with shaking (60 s every 15 min at 200 rpm). The OD values presented are those achieved at 20 h of growth. The chelator 2,2'-dipyridyl (DIP) was at 200 µM where indicated, and Ex-FABP or LCN2 were present at 5 µM (where indicated). The error bars are the standard errors calculated from three biological replicates with three technical replicates. For each growth medium, one way-ANOVA followed by a multiple comparison of means (Tukey Contrasts) was achieved using R software (version 3.5.3). This allowed identification of groups significantly different (identified as "a", "b", and "c"; p-value $\leqslant 0.05$) (Julien *et al.*, 2020).

The findings above are fully consistent with the Ent-sequestering roles of LCN2 and Ex-FABP, as shown here and previously (Goetz *et al.*, 2002; Fischbach *et al.*, 2006; Correnti *et al.*, 2011). The results above are also in accordance with previous work showing that mutations in *iroBC* (salmochelin production and export) and *iroN*

(salmochelin uptake) do not impair growth of *S.* Typhimurium in rich (LB) medium (Raffatellu *et al.*, 2009) but do significantly reduce growth in (low iron) tissue culture medium (DMEM) containing LCN2. The present study also shows that Ex-FABP is present at sufficient concentration in EW to cause inhibition of iron-restricted growth for an *S.* Enteritidis strain relying on enterobactin as sole siderophore, but not for *S.* Enteritidis deploying salmochelin alongside enterobactin. These results reflect previous findings showing that 2.5 and 10 µM Ex-FABP cause iron-restricted growth inhibition of Ent-producing *E. coli* (Correnti *et al.*, 2011; Garénaux *et al.*, 2013) and that complementation with *iroBCDEN* reverses inhibition by Ex-FABP (Garénaux *et al.*, 2013).

5.3 The ability to synthesise siderophore does not support *Salmonella* Enteritidis persistence in egg-white media

Among the proteins that have been shown to be components of the arsenal of defence factors within EW, the contribution, if any, of Ex-FABP as a new EW defence factor has remained an open question. Hence, *S.* Enteritidis and its mutants were grown in different EW media with and without Ex-FABP. Microbial concentrations were measured in terms of viable cells per mililiter (i.e. $\log_{10}$ CFU/mL, section 2.9.2). New conditions, better reflecting the *in vivo* environment found in eggs, were also used (i.e. incubation without shaking and at the hen's body temperature of 42 °C). Temperatures used in previous studies (30 °C; Baron *et al.*, 1997; 1999) and during *in vitro* experiments (37 °C, section 5.2) were also tested. Since it was shown that both inoculum and temperature impacts *S.* Enteritidis survival in EW (Alabdeh *et al.*, 2011), *S.* Enteritidis and its mutants were not only grown under various temperature regimes, but were also inoculated at various concentrations (3, 6, and 6.5 $\log_{10}$ CFU/mL). *S.* Enteritidis growth kinetics were measured in microplates (2 mL deep) or, when specified otherwise, in egg-models (section 2.9.2).

5.3.1 Behaviour of iron-acquisition mutants in egg white

In accordance with previous work (Alabdeh *et al.*, 2011), enumeration experiments (Figure 5.11 & 5.12) showed that both temperature (30, 37, and 42 °C) and innoculm size (3 and 6 $\log_{10}$ CFU/mL) impact *S.* Enteritidis behaviour in EW.

Low incubation temperature affects S. *Enteritidis survival in EW.* In TSB, *S.* Enteritidis reached 9 $\log_{10}$ CFU/mL after 24 h incubation at 30, 37 and 42 °C (Figure 5.11 & 5.12). In EW, depending on the temperature, a bacteriostatic effect (30 °C) or a bactericidal effect (37 and 42 °C) was observed. These results are in accordance with previous work showing that low incubation temperatures facilitate *S.* Enteritidis survival in EW. Indeed, it has previously been shown that *S.* Enteritidis can grow in EW at 20 to 30 °C (Gast & Holt, 2000; Kang *et al.,* 2006; Humphrey & Whitehead, 1993). At 37 °C, survival or growth vary depending on the inoculum size (Bradshaw *et al.,* 1990; Clavijo *et al.,* 2006; Růzicková, 1994; Kang *et al.,* 2006). Above 37 °C, a bactericidal effect of EW is observed for *S.* Enteritidis (Alabdeh *et al.,* 2011; Guan *et al.,* 2006; Kang *et al.,* 2006).

High concentrations of S. *Enteritidis facilitate survival in EW.* In TSB, *S.* Enteritidis reached 9 $\log_{10}$ CFU/mL after 24 h incubation when inoculated at 3 or 6 $\log_{10}$ CFU/mL (Figure 5.11 & 5.12). In EW, with both incocula at 3 and 6 $\log_{10}$ CFU/mL, a high bactericidal effect of EW was observed at 42 °C (CFU below the detection threshold after 24 h; Figure 5.11B, 5.12B), and a bacteriostatic effect of EW was observed at 30 °C (Figure 5.11F, 5.12F). At 37 °C, *S.* Enteritidis declined more rapidly with an inoculum of 3 $\log_{10}$ CFU/mL than with an inoculum of 6 $\log_{10}$ CFU/mL (24 and 120 h, respectively; Figure 5.11D, 5.12D). This is in accordance with previous studies showing that with an inoculum of ~3 $\log_{10}$ CFU/mL a bactericidal effect is observed at 37 °C (Bradshaw *et al.,* 1990; Clavijo *et al.,* 2006; Kang *et al.,* 2006). In addition, Kang *et al.* (2006) showed that in EW at 37 °C, *S.* Enteritidis could survive longer when inoculated at 5 $\log_{10}$ CFU/mL. Likewise, in the study presented here, increasing the inoculum to 6 $\log_{10}$ CFU/mL allowed *S.* Enteritidis to survive longer. This confirms that both incubation temperature and inoculum size influence survival of *S.* Enteritidis in EW (Kang *et al.,* 2006; Alabdeh *et al.,* 2011).

Whatever the inoculum and temperature tested, there was no difference in survival kinetics between the WT and mutant strains. This suggest that the ability to synthesise siderophores does not assist *S.* Enteritidis survival under the experimental conditions employed. Since it is likely that iron would be required for growth (rather than survival/persistence), it was decided to increase the incoculum above 6 $\log_{10}$ CFU/mL to promote bacterial growth.

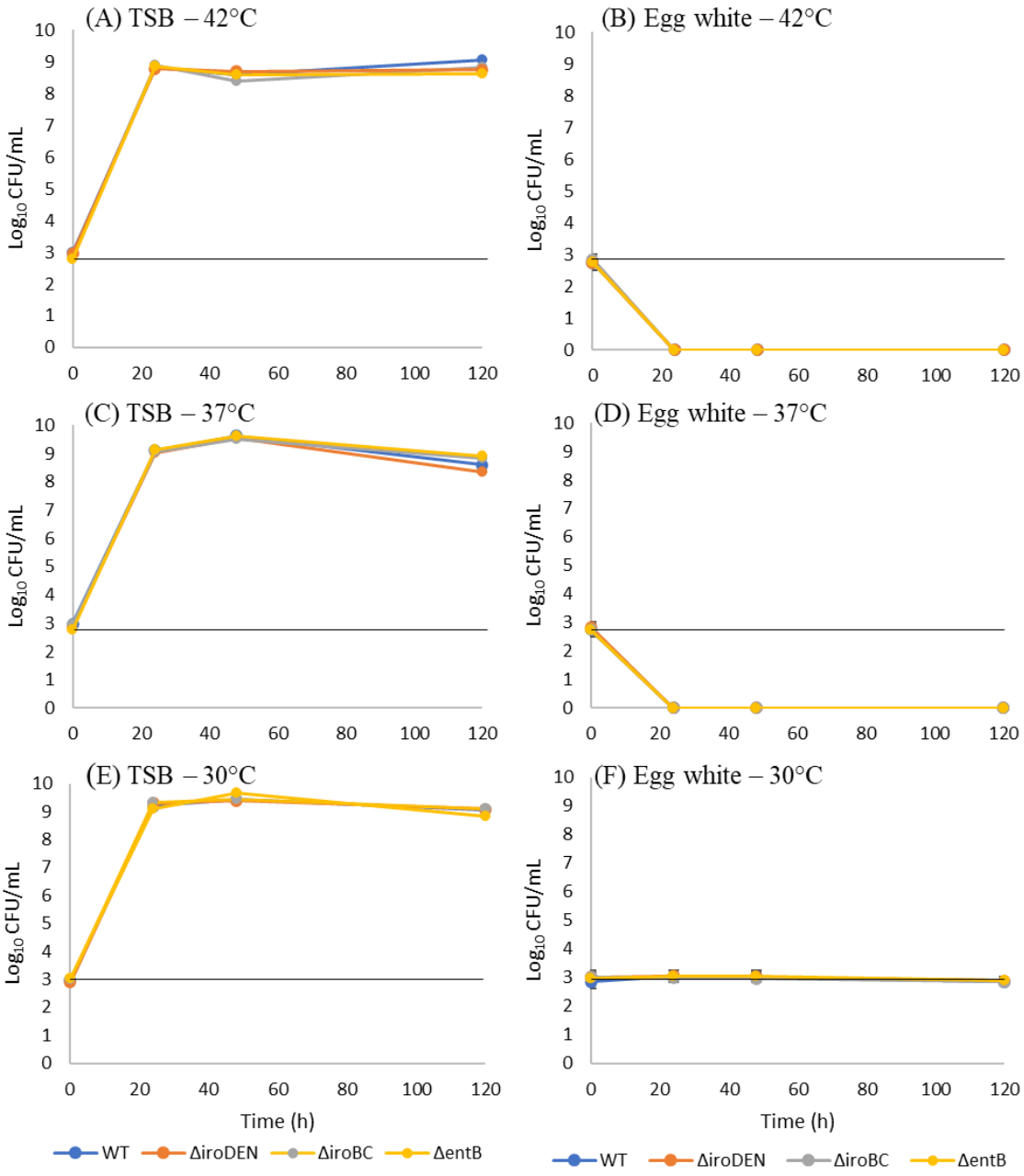

Figure 5.11. Influence of temperature on *S.* Enteritidis (and mutants deficient in siderophore production and/or utilisation) when inoculated at 3 $\log_{10}$ CFU/mL in TSB or EW. Cells were incubated at 42 °C (A, B), 37 °C (C, D) or 30 °C (E, F) for 5 d. The straight line represents the inoculum size. Error bars are the standard errors calculated from six technical replicates.

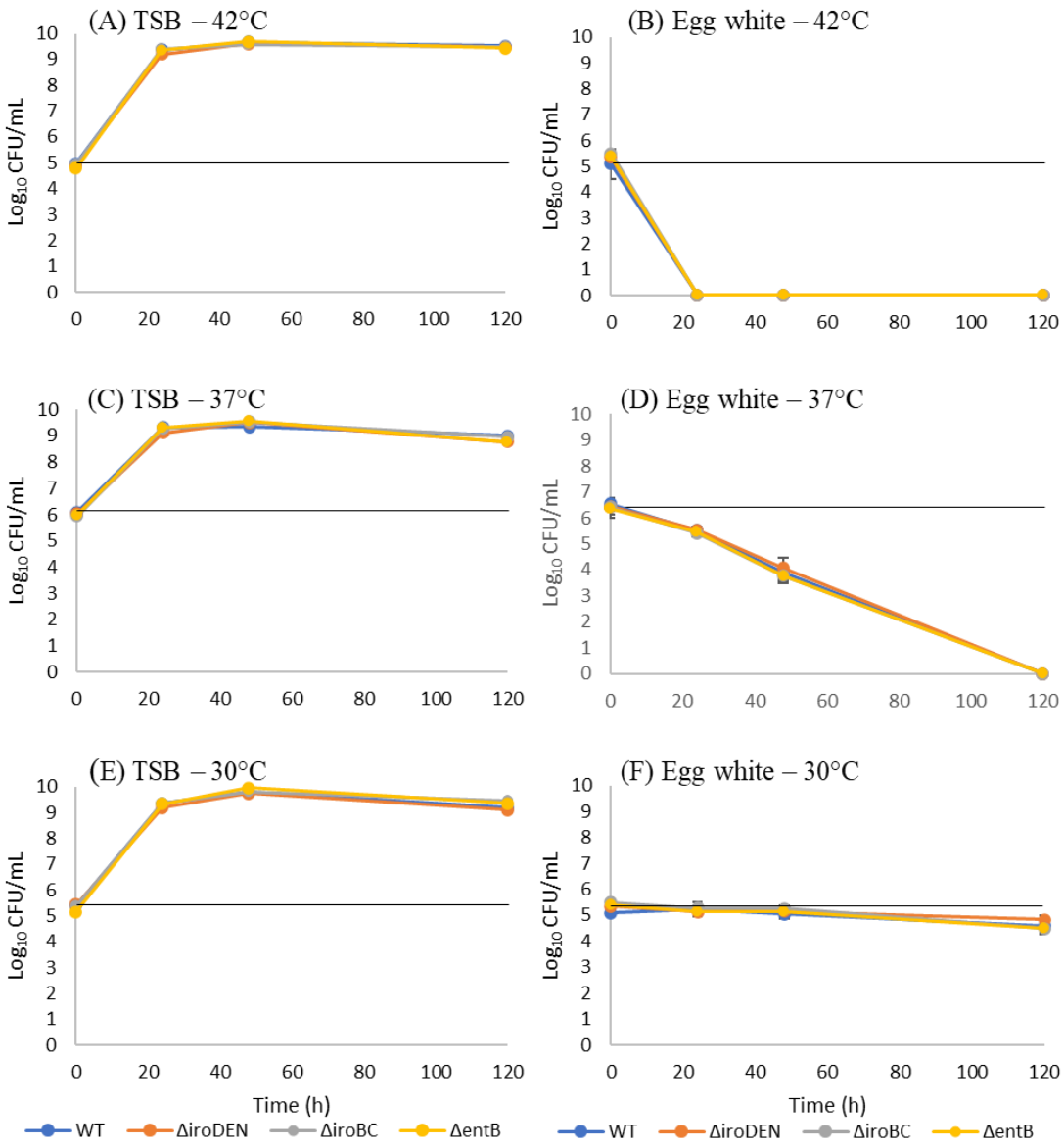

Figure 5.12. Influence of temperature on *S.* Enteritidis (and mutants deficient in siderophore production and/or utilisation) behaviour when inoculated at 6 $\log_{10}$ CFU/mL in TSB or EW. Cells were incubated at 42 °C (A, B), 37 °C (C, D), or 30 °C (E, F) for 5 day. The straight line represents the inoculum size. Error bars are the standard errors calculated from six technical replicates.

To highlight potential differences between the behaviour of *S.* Enteritidis and its mutants in EW, an experiment was performed with the aim of determining the conditions suitable for growth in EW. For this purpose, a higher inoculum (6.5 $\log_{10}$ CFU/mL), a low temperature (30 °C) and a shorter duration of incubation of 24 h were chosen (Figure 5.13). Under these conditions, one $\log_{10}$ growth per mL was achieved after 24 h. Thus, at high inoculation levels *S.* Enteritidis can overcome the bactericidal and bacteriostatic activities of EW.

No reliable significant difference in growth was observed between the WT and its mutants. A significant difference was observed between Δ*entB* and Δ*iroBC* (one-way ANOVA), however, this difference is below the error margin of plate-counting enumeration (0.5 $\log_{10}$ CFU/mL; AFSSA, 2008). This might suggest that siderophore synthesis does not assist bacterial modest growth in EW but it is more likely that the experiment was not sufficiently discerning to enable any relible difference to be identified. Since inoculum of 6.5 $\log_{10}$ CFU/mL and incubation at 30 °C provided good growth in EW, such experimental conditions were used to carry-out further experiments.

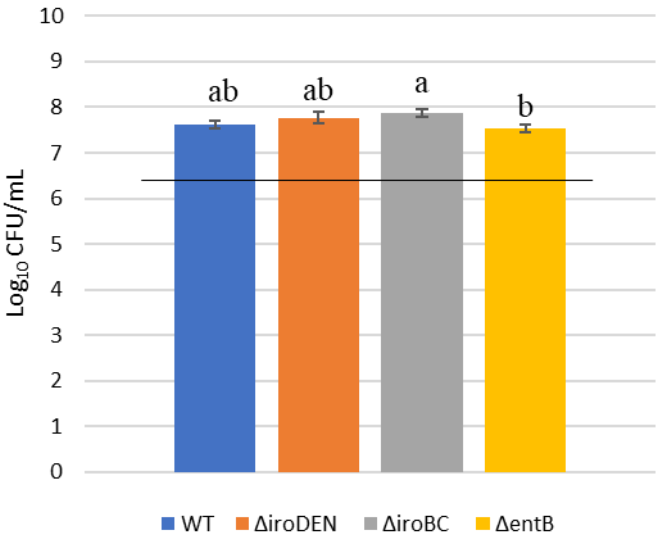

Figure 5.13. Growth of *S.* Enteritidis and mutants deficient in siderophore production and/or utilisation in EW (24 h incubation at 30 °C). The straight line represents the inoculum size. Error bars are the standard errors calculated from three technical replicates. For each inoculum, one way-ANOVA followed by a multiple comparison of means (Tukey Contrasts) was achieved using R software (version 3.5.3). This allowed to identify groups significantly different (identified as "a", "b", and "c", p-value $\leqslant 0.05$).

5.3.2 Does *Salmonella* Enteritidis rely on iron storage or siderophore synthesis for survival and growth in EW?

It is possible that *S.* Enteritidis utilises intracellular iron-reserves to assist *S.* Enteritidis weak growth in EW. Indeed, *S.* Enteritidis possesses three iron-storage proteins that can sequester Fe^{3+}: DNA-binding Dps (500 atoms); ferritin A (FtnA, 3000 atoms); and the haemoferritin, bacterioferritin (3000 atoms) (Andrews *et al.*, 2003). To assess whether *S.* Enteritidis utilise internal iron stores in EW, precultures were deprived of iron prior to incubation in EW by overnight growth in (i) EWF (< 0.02 µM iron) and (ii) LB with DIP (shown to limit growth of the Δ*entB* mutant (section 5.2.2).

Cells grown in EWF prior to inoculation in EW. Cells were initially propagated in TSB overnight (at 37 °C without shaking). This was followed by a second overnight culture in EWF (< 0.02 µM Fe) prior to inoculation at 6.5 $\log_{10}$ CFU/mL in EW. Despite this pre-treatment, the *S.* Enteritidis strains grew by ~1 $\log_{10}$ CFU/mL in EW at 30 °C by 24 h (Figure 5.14). Hence, growth observed is of the same order of magnitude as seen when cells were pregrown in TSB (Figure 5.13). After the intial ~24 h growth phase, *S.* Enteritidis levels did not increase overall for the remaining 31 days, but remained at a level above 6 $\log_{10}$ CFU/mL. There was no notable difference between strains indicating, once again, that siderophore production is not required to support modest growth followed by survival in EW under the conditions tested.

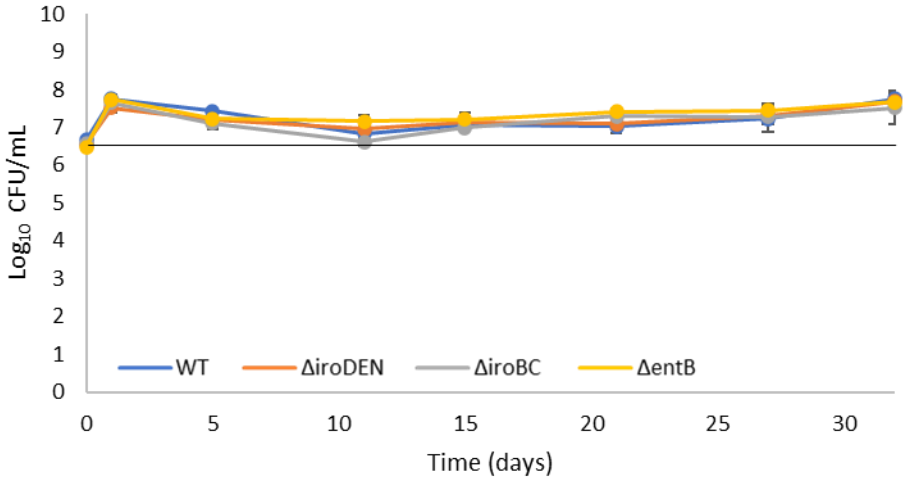

Figure 5.14. Growth of *S.* Enteritidis (and mutants deficient in siderophore production and/or utilisation) depleted in iron (by overnight growth in EWF) prior to inoculation in EW. Growth at 30 °C was monitored for 32 days. The straight line represents the inoculum: 6.5 $\log_{10}$ CFU/mL. Error bars are the standard errors calculated from three technical replicates.

Cells grown in LB supplemented with an iron chelator prior to inoculation in EW. Cells were first propagated in TSB overnight (at 37 °C without shaking), as above, but were then grown overnight in LB with 200 µM DIP (Liu *et al.*, 2015; Raffatellu *et al.*, 2009). The inability of the Δ*entB* mutant to produce siderophores was confirmed by the colour observed after centrifugation of the second overnight culture. A cream pellet was observed for the Δ*entB* mutant wereas a pink pellet (the colour of ferric-enterobactin/salmochelin) was observed for the strains able to synthesise at least one siderophore: WT, and Δ*iroBC* and Δ*iroDEN* mutants. The hypothesis being tested is that due to its inability to produce siderophores, the Δ*entB* mutant might need to withdraw iron from its storage protein(s) to support division in EW, which could subsequently result in a growth defect.

Following inoculation, growth (~1 $\log_{10}$ CFU/mL) was not observed until day 5 (Figure 5.15); this contrasts with the results obtained with EWF precultures where growth was maximal by day 1 (Figure 5.14). All four strains grew similarly reaching ~7.5 $\log_{10}$ CFU/mL at day 5. This suggests that neither iron stores nor siderophore synthesis have a major influence on *S.* Enteritidis modest growth and survival in EW.

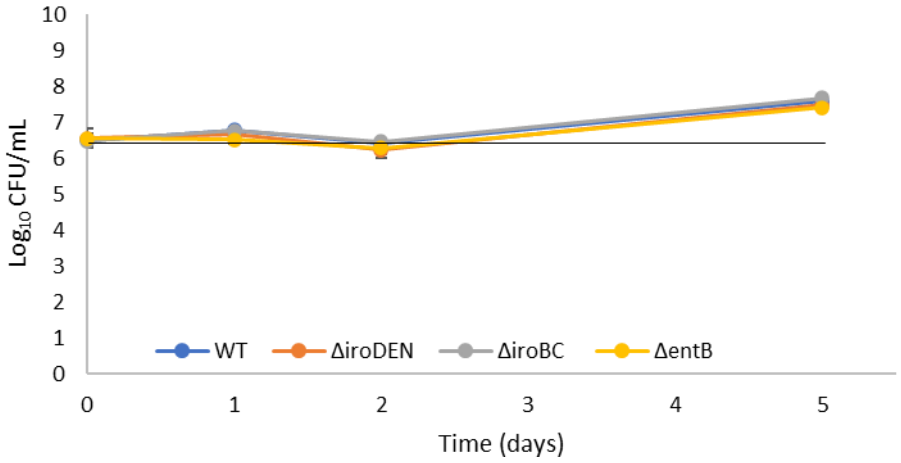

Figure 5.15. Growth of *S.* Enteritidis (and mutants deficient in siderophore production and/or utilisation) depleted in iron (through overnight growth in LB with DIP) prior to inoculation in EW. Growth at 30 °C was monitored for 5 days. The straight line represents the inoculum: 6.5 $\log_{10}$ CFU/mL. Error bars are the standard errors calculated from three technical replicates.

Such findings could be due to bias in the method. Indeed, previously (section 5.3.1 and 5.3.2) *S.* Enteritidis growth in EW was studied in microplates, where the yolk was excluded from experimental conditions - this is not fully representative of eggs. Also, EW contains considerably lower levels of iron (~18 µM; USDA, 2010) than the yolk (~255

µM; USDA, 2010; Sauveur 1988). Thus, a focus on EW alone would not allow consideration of any potential (siderophore-dependent) utilisation of iron from the yolk. Therefore, to test the hypothesis that siderophore synthesis could better promote growth in eggs when a source of iron is present, further experiments were performed where *S.* Enteritidis was exposed to the yolk (see next section).

5.3.3 Does the ability to synthesise siderophores support *Salmonella* Enteritidis growth in egg white when a natural source (egg yolk) of iron is provided?

In the yolk, iron is bound to a protein called phosvitine. Phosvitin is an abundant (11% of yolk protein content) yolk phosphoglycoprotein with a molecular weight of 35 kDa containing 10% phosphorus and 6.5% carbohydrate (Mecham & Olcott, 1949). This protein carries 95% of yolk Fe^{3+} and contains 2–3 atoms of iron per molecule when isolated from hen egg, but its potential binding capacity is much higher (up to 70 atoms per molecule; Taborsky, 1980). Phosvitin has an affinity for iron of 10^{18} M^{-1} (Hegenauer *et al.*, 1979), slightly lower than of the EW oTf (K_a 10^{32} M^{-1}; Chart & Rowe, 1993). Phosvitine and oTf remain in the yolk and white compartments (respectively) due to the presence of the vitelline membrane (Figure 5.16).

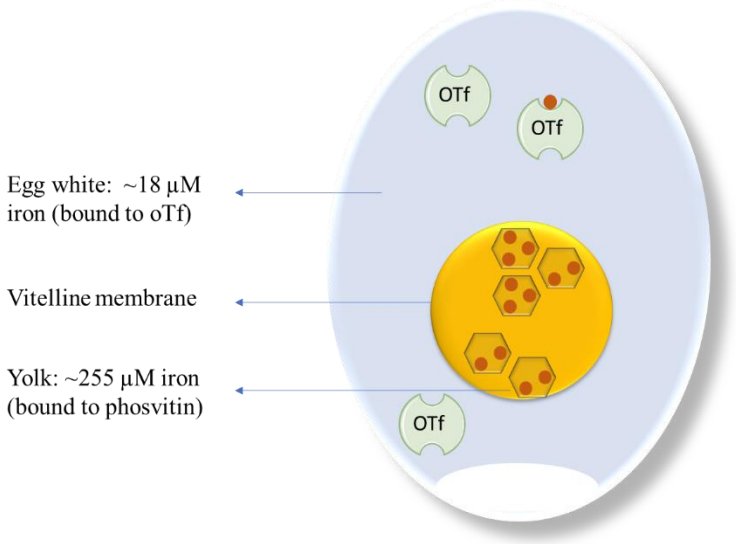

Figure 5.16. Iron distribution in eggs. EW has lower iron levels (~ 18 µM) than the yolk (~ 255 µM). Iron (drawn as brown circles) is bound to ovotransferrin (oTf indicated as green) in EW and to phosvitidin (drawn as hexagons) in the yolk. oTf has an iron binding capacity of 2 atoms and is saturated at ~5% (Sauveur, 1988) whereas phosvitin can bind up to 70 iron atoms and is saturated at ~3% (Taborsky, 1980).

The vitelline membrane is permeable to glucose (180 Da) and amino acids (~110 Da) (Garcia *et al.,* 1983; Pon *et al.,* 1985). Assuming that bacterial siderophores (~700 Da) can also cross the vitelline membrane, it can be hypothesised that *S*. Enteritidis could use its siderophores to acquire iron bound to phosvitin from the egg yolk. To test this, two models were designed, named "whole-egg model" and "dialysis model".

Whole-egg model. In this model, EW was inoculated with *S*. Enteritidis or its mutants *via* a needle through the eggshell. Precautions were taken to ensure that the vitelline membrane was not punctured, leaving the yolk *S*. Enteritidis free. After 24, 48 and 120 h incubation at 30 °C, the eggshell was broken and the EW collected before cell enumeration (section 2.9.2). *S*. Enteritidis and its mutants grew by more than 2 $\log_{10}$ CFU/mL by 120 h in this whole-egg model (Figure 5.17A), whereas only 1 $\log_{10}$ CFU/mL growth was observed in isolated EW (Figure 5.13). All strains displayed similar growth at 24 h, but at 48 h there was a growth difference with the WT exhibiting 0.9 $\log_{10}$ CFU/mL higher levels than the *entB* mutant suggesting a role for siderophores in egg colonisation. The growth difference was also maintained at 120 h, although it was reduced by 0.4 $\log_{10}$ CFU/mL (Figure 5.17A, 5.18A). There was also a modest growth difference (0.4 $\log_{10}$ CFU/mL) between the *iroBC* mutant with respect to the WT at 48 h, indicative of a role for salmochelin in egg colonisation (Figure 5.17A, 5.18A). This difference was not maintained at 120 h.

It should be noted that *S*. Enteritidis can penetrate the vitelline membrane when incubated at 30 °C for 72 h (Guan *et al.,* 2006). In our experiment, eggs were incubated at 30 °C for 120 h. Thus, *S*. Enteritidis could have colonised the yolk under these incubation conditions. Since the yolk is rich in nutrients, this medium could promote *S*. Enteritidis growth along with obscuring potential growth difference(s) between *S*. Enteritidis and its mutants. To ensure that *S*. Enteritidis remains in the EW compartment, a second model (dialysis-bag model) was used where the vitelline membrane separating the yolk and EW in the egg is substituted by an artificial dialysis membrane.

Dialysis-bag model. In the second model, EW was separated from the egg yolk by a dialysis membrane prior to EW inoculation with *S*. Enteritidis (section 2.9.2). The cut-off of the dialysis membrane was chosen at 12-14 kDa in order to retain bacterial cells in the EW and iron-bound phosvitine in the egg yolk, and to allow bacterial siderophores (below 1 kDa) to circulate between the two compartments. In a similar fashion to the "whole-egg

mode", the WT grew by more than 2 $\log_{10}$ CFU/mL by 120 h at 30 °C (Figure 5.17B). In this model, a mechanism for *S.* Enteritidis to acquire iron from egg yolk would be to synthesise siderophores that would cross the dialysis membrane and sequester iron from phosvitin before re-entering the EW compartment to deliver iron-charged siderophores to *S.* Enteritidis. A modest reduction in growth was observed for the *entB* and *iroDEN* mutants (0.4 and 0.2 $\log_{10}$ CFU/mL, respectively) with respect to the WT at 24 h. (Figure 5.17B, 5.18B). However, based on the basis of the error margin of the enumeration method (AFSSA, 2008), there was no reliablet difference in growth between strains at any time point. The higher overall growth in EW observed in the whole-egg and dialysis-bag models (with respect to isolated EW) might be due to diffusion of nutrients that can pass from the egg yolk to EW through the dialysis and vitelline membranes. Although experiments in whole egg model suggested a role for *S.* Enteritidis siderophores in egg colonisation, this could not be confirmed using the dialysis bag model. Addtional biological replicates are required to conclude on this matter.

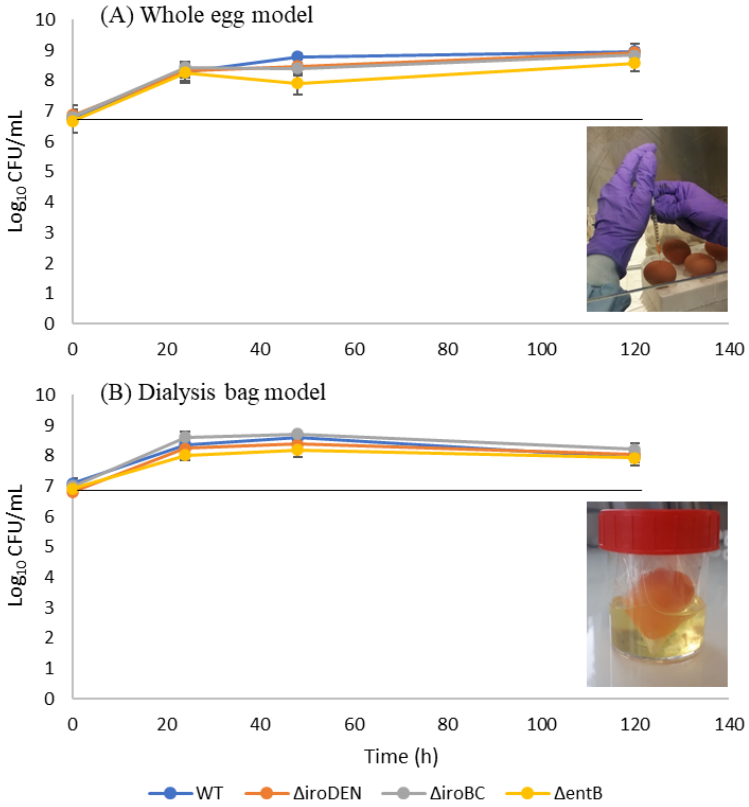

Figure 5.17. Growth of *S.* Enteritidis (and mutants deficient in siderophore production and/or utilisation) in when inoculated into EW within whole eggs (A) or using a "dialysis model" (B). Growth at 30 °C was monitored for 5 days. The straight line represents the inoculum: ~6.5 $\log_{10}$ CFU/mL. Error bars are the standard errors calculated from three technical replicates.

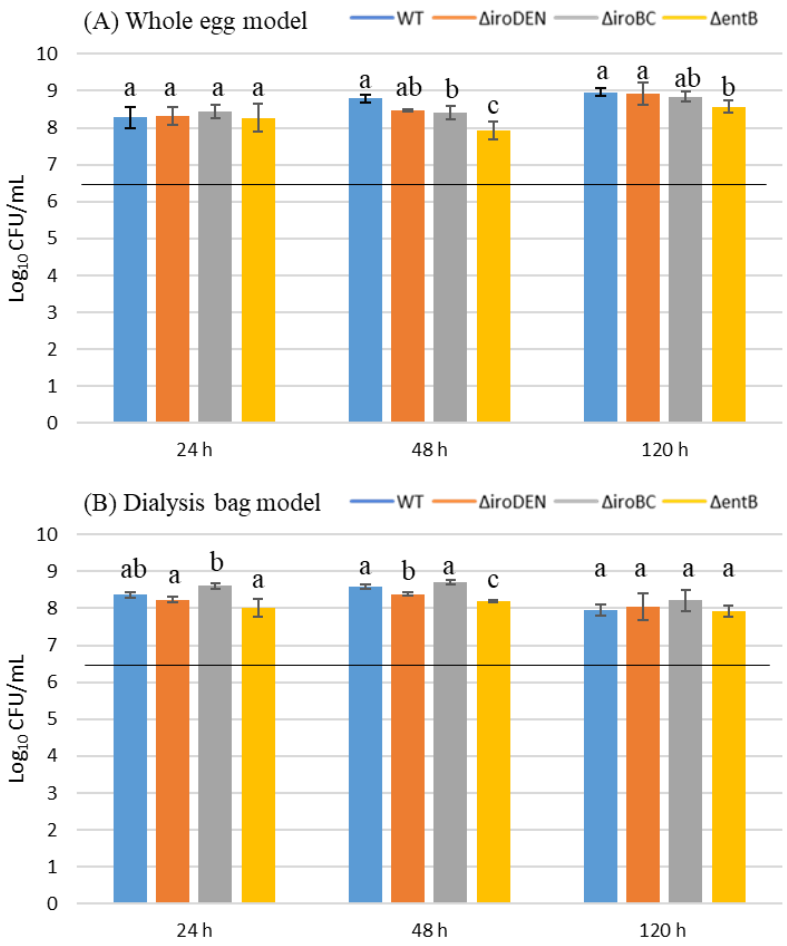

Figure 5.18. Growth of *S.* Enteritidis (and mutants deficient in siderophore production and/or utilisation) in when inoculated into EW within whole eggs (A) or using a "dialysis model" (B). These data are derived from those presented in Figure 5.17. The straight line represents the inoculum: ~6.5 $\log_{10}$ CFU/mL. Error bars are the standard errors calculated from three technical replicates. For each growth medium, one way-ANOVA followed by a multiple comparison of means (Tukey Contrasts) was achieved using R software (version 3.5.3). This allowed to identify groups significantly different (identified as "a", "b", and "c", p-value $\leqslant 0.05$).

5.4 Ex-FABP antibacterial activity (*via* its siderophore-binding capacity) observed in standard growth media is not observed in egg-white media

To further explore the potential role of siderophores in promoting *S.* Enteritidis growth and the antibacterial role of Ex-FABP, EW filtrate was used (EWF; section 2.1.1). *S.* Enteritidis and its mutants were inoculated into EWF at 6 $\log_{10}$ CFU/mL and incubated for 24 h at 30 °C (Figure 5.19).

Growth of S. *Enteritidis in EWF*. In EWF at 30 °C, growth of ~2 $\log_{10}$ CFU/mL was obtained for all strains after 24 h (Figure 5.19). This growth is enhanced compared to the bacteriostatic effect observed in EW (no growth after 24 h in EW; Figure 5.12F) using the same inoculum and incubation conditions. This was expected since macromolecules above 10 kDa, some of which that are potentially antimicrobial (e.g ovotransferrin, lysozyme, protease inhibitors, avidin, riboflavin-binding proteins and Ex-FABP) were removed from the medium. As suggested by Baron *et al.* (1997), EWF might contain sufficient nutrients for *Salmonella* growth. However, it is surprising to see such growth in a medium where iron is present at levels lower than in EW (< 0.02 µM *vs* 18 µM, respectively).

Growth of S. *Enteritidis in EWF supplemented with 5 µM Ex-FABP*. In EWF supplemented with 5 µM Ex-FABP, growth of the bacteria was of the same order of magnitude as obtained without Ex-FABP (Figure 5.19). However, there was a statistically significant, lower growth of the mutants compared to the WT. However, the difference was less than 0.5 $\log_{10}$ CFU/mL which is considered as not significant on the basis of the error margin of the enumeration method (AFSSA, 2008). Thus, the Ex-FABP antibacterial activity (*via* its siderophore-binding capacity), as observed in standard growth media, cannot be confirmed in EWF under the experimental conditions tested.

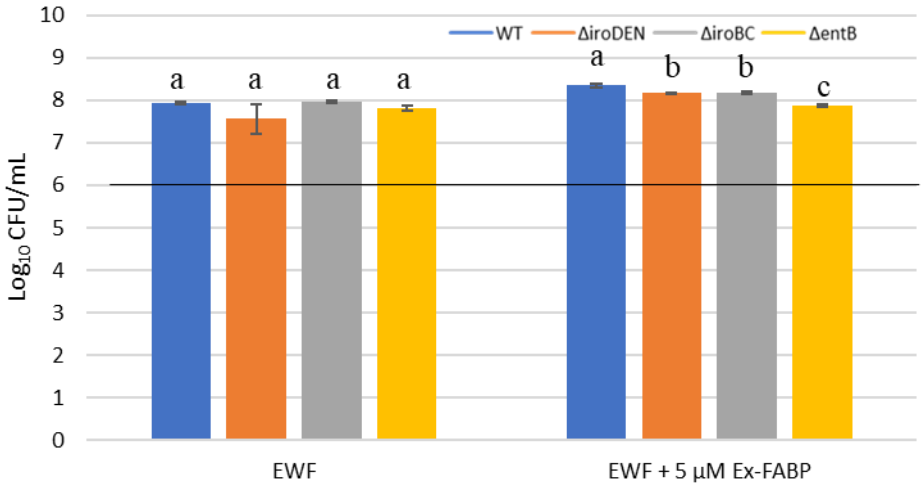

Figure 5.19. Growth of *S.* Enteritidis (and mutants deficient in siderophore production and/or utilisation) in EWF with and without 5 µM Ex-FABP (24 h incubation at 30 °C). The straight line represents the inoculum: ~6 $\log_{10}$ CFU/mL. Error bars are the standard errors calculated from three technical replicates. For each growth medium, one way-ANOVA followed by a multiple comparison of means (Tukey Contrasts) was achieved using R software (version 3.5.3). This allowed to identify groups significantly different (identified as "a", "b", and "c", p-value $\leqslant$ 0.05).

5.5 Conclusion and future work

S. Enteritidis growth dynamics in standard growth media (i.e. M9 or LB) and EW media (i.e. EW or EWF) are summarised in Table 5.2. It is important to note that different growth conditions were applied between these media. In standard growth medium, since the human lipocalin-2 was a positive control, physiological parameters were used (i.e. shaking, pH 7.4, 37 °C). In EW media, there was no shaking, the pH was elevated (9.3), and the temperature was of 30 °C (optimum for *S.* Enteritidis growth in EW).

S. *Enteritidis growth in iron-poor media*. EWF and M9 both have low iron contents: < 0.02 µM (section 2.1.1) and 0.1 µM (Outten & O'Halloran, 2001), respectively. However, unlike in M9 medium, addition of 5 µM Ex-FABP to EWF caused a minor growth reduction for the Δ*iroBC* mutant (Figure 5.19), which is considered as not significant on the basis of the error margin of the enumeration method (AFSSA, 2008). For future work, the experiment could be repeated with a range of Ex-FABP concentrations to determine if higher levels might be effective and to test whether there is a response of growth to concentration. However, the lack of any clear impact of Ex-FABP on growth in EWF might be related to the pH. Indeed, ITC showed that Ex-FABP affinity for enterobactin was lower in EWF (pH 9.3) than in TBS (pH 7.4). Furthermore, the incubation conditions differed between EWF and M9 medium (37 °C in M9 *vs* 30 °C in EWF; shaking at 200 rpm in M9 *vs* static in EWF). Shaking brings oxygen into the medium and could change the level of oxidation of iron, changing from a ferrous (Fe^{2+}) to a ferric (Fe^{3+}) state. To test the influence of pH, temperature and shaking on the activity of Ex-FABP, experiments in standard growth medium could be repeated with conditions used for growth in EWF (i.e. pH 9.3, 30 °C, and without shaking). These conditions could also be changed to reflect better the conditions of the egg when in the oviduct or just after laying (pH upon oviposition: ~7.6; hen body temperature: 42 °C).

S. *Enteritidis growth in iron-chelated media*. In EW, *S.* Enteritidis growth was weak, and no reliable difference was observed between the WT and its mutants (Figure 5.13). This might suggest that siderophore synthesis does not assist modest bacterial growth in the presence of 3.6 to 25.5 µM iron with excess oTf (Table 1.3). In standard growth medium, it was shown that siderophore synthesis better assists growth when chelated iron is present in the medium (LB with DIP) than in an iron-scarced medium (M9). As future work, oTf iron-saturation could be increased *via* iron addition to EW. This experiment could be achieved in a similar fashion to that reported by Kang *et al.* (2006), which

showed that *entF* and *entF*/*feoAB* mutations resulted in significant growth defects compared to the WT in EW supplemented with ammonium ferric citrate (incubated at 37 °C for 50 h). In addition, a competitive egg infection experiment, where *S*. Enteritidis and its mutants are supplied together in equal ratio could be used as a method to further test the impact of siderophores in promoting growth/survival in EW. It would also be interesting to test how other bacteria respond to Ex-FABP under EW conditions, particularly other Gram-negative genera able to colonise eggs (e.g *Escherichia, Alcaligenes, Proteus, Flavobacterium* and *Pseudomonas*; EFSA Panel on Biological Hazards, 2014).

Methodology limitations. Failure to identify any clear growth phenotype for the mutants in EW and EWF (Figure 5.13 and 5.19) indicates that the conditions employed were not suitable for detecting iron-dependent growth effects. The degree of growth observed in EW was weak and mutations had effects lower than the limitation of the detection method (need to achieve a 0.5 $\log_{10}$ difference; AFSSA, 2008). Hence, the experiments performed might have not been sufficiently sensitive to show the effects expected. Since fluorescence *in situ* hybridization (FISH) has been shown to be a suitable tool for the specific and reliable detection of *Salmonella* in eggs (Fang *et al.*, 2003; Almeida *et al.*, 2013), it could be used as a second method to monitor *S*. Enteritidis growth and survival.

A further issue is the lack of controls in section 5.3.2. Controls with preculture in EWF with added iron and preculture in LB without DIP should be included in future work. Total iron content could also have been tested (by ICP-OES) to assess intracellular iron storage. Also, additional biological replicates are needed to confirm trends observed in section 5.3.

Table 5.2. Summary of growth patterns observed for *S*. Enteritidis (and mutants deficient in siderophore production and/or utilisation) in standard growth media and in EW media after 24 h incubaction. For the WT, growth is arbitrary symbolised as a + in every medium. For *S*. Enteritidis mutants, a similar growth pattern to that of the WT grown in the same medium is represented by a "+", a lower growth as compared to the WT in the same medium is represented by a " – ".

Growth medium	**Iron status**	**WT**	**Δ*iroDEN***	**Δ*iroBC***	**Δ*entB***	**Interpretation**
Incubation at 37 °C, shaking, pH 7.4						
M9 (Figure 5.8)	Poor	+	+	+	+	All strains achieved the same growth, suggesting that *S*. Enteritidis is well suited to grow in iron-scarced environment, and this even without siderophore production.
M9 + Ex-FABP (Figure 5.8)	Poor	+	+	-	+	Growth of Δ*iroBC* was strongly inhibited, which demonstrates that *S*. Enteritidis capacity to convert enterobactin to salmochelin assists growth upon lipocalin exposure.
LB (Figure 5.9)	Rich	+	+	+	+	Growth of *S*. Enteritidis and its mutant was optimal.
LB + DIP (Figure 5.9)	Rich / chelated	+	+	+	-	Growth of Δ*entB* was strongly inhibited. This likely arises from its inability to effectively compete with DIP for iron due to its lack of enterobactin.
LB + DIP + Ex-FABP (Figure 5.9)	Rich / chelated	+	-	-	-	Provision of Ex-FABP had little impact on the weak growth of the Δ*entB* mutant seen in LB + DIP. However, growth Δ*iroBC*, and Δ*iroDEN* was strongly inhibited, which is consistent with the ability of Ex-FABP to sequester enterobactin.
Incubation at 30 °C, static, pH 9.3						
EWF (figure 5.19)	Poor	+	+	+	+	Like in M9, all strains exhibited the same growth behaviour, which confirms that *S*. Enteritidis can grow despite iron scarcity, and this even without the ability to synthesise siderophores.
EWF + Ex-FABP (figure 5.19)	Poor	+	+	+	+	Unlike in M9 medium, Ex-FABP supplementation did not lead to growth defect of the Δ*iroBC* mutant. This might be due to the EWF alkaline pH.
EW (Figure 5.13)	Poor / chelated	+	+	+	+	In EW, no reliable significant difference in growth was observed between the WT and its mutants. This might suggest that siderophore synthesis does not assist bacterial growth in EW but more it is more likely that the experiment was not sufficiently discerning to enable any relible difference to be identified.

Conclusion. In standard growth medium, Cal-γ and α1-ovoglycoprotein had no apparent effect on the growth of *S.* Enteritidis or its mutants in M9 medium, suggesting they do not act as siderocalins. In both M9 and LB with DIP, production of salmochelin allowed *S.* Enteritidis to escape Ex-FABP-mediated growth inhibition under iron restriction.

The remarkable resistance of *S.* Enteritidis to EW might not be strongly assisted by the ability to produce siderophores. The metal-acquisition pathways of *S.* Enteritidis in this medium will be further discussed in the next chapter. Furthermore, the antibacterial activity of Ex-FABP (*via* its siderophore-binding capacity) observed in standard growth media was not seen in EW media, under the conditions tested in the present study. Yet, this does not prevent Ex-FABP from playing a role upstream of laying in preventing systemic infection (*via* enhanced iron restriction) and subsequent hen oviduct contamination. This will also be further discussed in the next chapter.

Chapter 6. General discussion

6.1 *Salmonella* Enteritidis metal acquisition in egg white

This study confirmed that Ex-FABP binds enterobactin with high affinity, but not salmochelin. However, the other two EW lipocalins do not apparently bind enterobactin or salmochelin. Furthermore, this study showed that egg white contains micro-Molar levels of all three lipocalins, and Ex-FABP is present at concentrations that are sufficient to inhibit enterobactin-producing *Salmonella* when applied to iron-restricted media. Under low iron conditions, Ex-FABP inhibits enterobactin-dependent iron sequestration by *S.* Enteritidis. In EW, no evidence for a role for siderophores (or Ex-FABP) in *Salmonella* growth/survival has been found as yet. This surprising observation might be correlated with the weak growth of *S.* Enteritidis in EW and a lack of requirement for siderophores in persistence. This might also suggest that: (i) *S.* Enteritidis siderophore mediated iron-acquisition pathways is impaired in EW; or (ii) *S.* Enteritidis uses iron-acquisition pathways other than siderophore mediated iron-acquisition; or (iii) *S.* Enteritidis uses alternative metal-utilisation pathways.

6.1.1 *Salmonella* Enteritidis siderophore mediated iron-acquisition pathway

Previous studies reported that *S.* Enteritidis resistance in EW might be attributed to siderophore synthesis (Chart & Rowe, 1993; Kang *et al.,* 2006). However, the use of a siderophore non-producing strain (Δ*entB*) in this study showed that *S.* Enteritidis survival in EW might not require the ability to produce siderophores. It can be hypothesised that siderophore iron-acquisition pathways might be ineffective in EW.

Siderophore synthesis in EW conditions. Baron *et al.* (2017) explored *S.* Enteritidis global gene-expression after 45 min exposure to EW model medium (EWMM; 10% EW added to EWF) under bactericidal conditions (45 °C). They found an increase in expression of both *ent* and *iro* genes (coding for enterobactin and salmochelin iron-acquisition pathways, respectively) by *S.* Enteritidis. In another study conducted in our laboratory (Julien *et al.,* 2018), overexpression of these genes were confirmed by qRT-PCR after 45 min exposure to EWMM at 37, 40 and 42 °C. These findings correlated with the release of siderophores by *S.* Enteritidis in EWMM (Sankaranarayanan *et al.,* 2015). Using Calcein Blue, the concentration of siderophores released was estimated to be 1 to 2 µM equivalents of desferal at 37, 40 and 42 °C after 4 h incubation in EWMM. This suggest that *S.* Enteritidis can effecitvely synthesise siderophores in EW conditions.

Nevertheless, siderophore production and utilisation in EW remains to be further understood as Huang *et al.* (2019) observed an up-regualtion of the *iro* genes (~2-fold) but also a down-regulation of *ent* genes (~2-fold) after 24 h exposure to 80% EW at 37 °C. Besides, even if *S*. Enteritidis produces enterobactin and its derivatives, their import and utilisation might be impaired under EW conditions (i.e. high viscosity, alkaline pH, antimicrobial proteins and peptides, competition with oTf and Ex-FABP).

Siderophore export/import under EW conditions. S. Enteritidis exposure to EW can lead to bacterial membrane damage and dissipation of the pmf due to the presence of antimicrobial proteins (e.g. oTf; Aguillera *et al.*, 2003). Hence, the activity of proteins involved in siderophore import/export could be impaired in EW as follows:

- IroC (inner-membrane protein responsible for salmochelin export) and the FepBCDG system are considered to be ATP dependent (Figure 6.1). The strong induction of glycolysis by *S*. Enteritidis after 45 min EWMM exposure at 45 °C (Baron *et al.*, 2017) suggests that *S*. Enteritidis can produce ATP in EW by substrate-level phosphoryation, allowing IroC and FepBCDG to function despite any low pmf caused by membrane damage in EW. However, membrane damage could impair the function of transporters.
- EntS, shown to secrete enterobactin, is an efflux pump belonging to the Major Facilitator Superfamily (MFS). Hence its activity could be impaired by a low pmf.
- CirA, FepA and IroN (outer-membrane proteins responsible for enterobactin and salmochelin import) are both pmf and TonB-ExbBD (located in the inner membrane) dependent and thus their activity could also be impaired by membrane damage.

6.1.2 *Salmonella* Enteritidis iron-acquisition systems and internal storage

If siderophore mediated iron-acquisition is impaired under EW conditions, *S*. Enteritidis could cope with iron-restriction using other iron-acquisition pathways and/or its intracellular reserves (Figure 6.1).

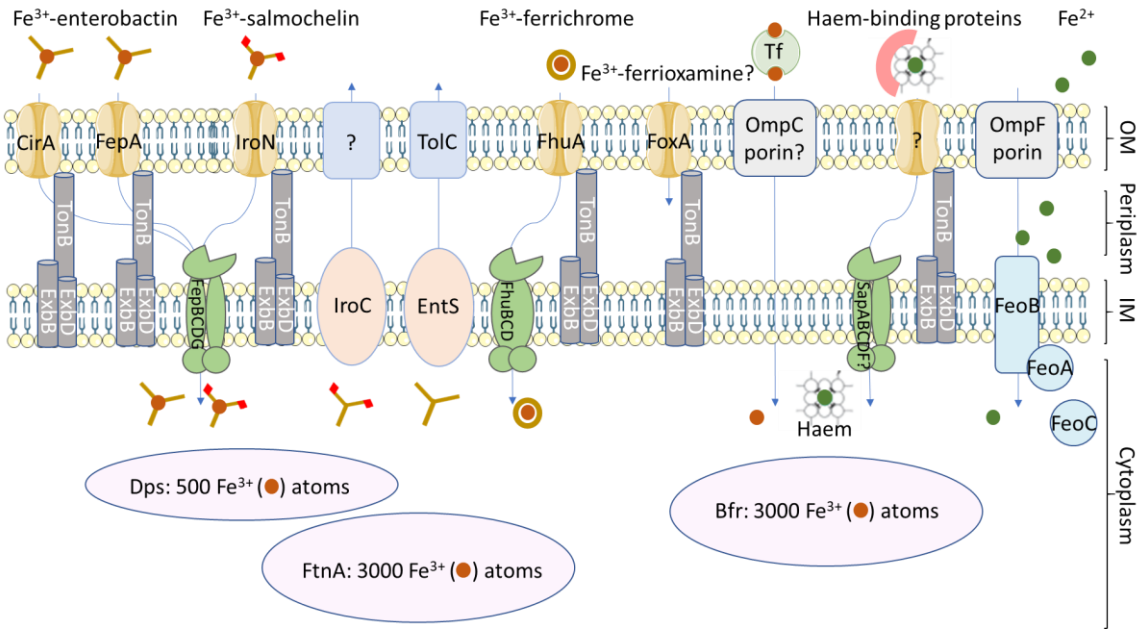

Figure 6.1. Potential iron acquisition pathways and iron storage in Salmonellae (partially adapted from *Page et al.*, 2019). Secreted enterobactin and salmochelin (*via* EntS, TolC and IroC) remove iron (Fe^{3+}, brown circles) from transferrins (Tf), and the siderophore-iron complexes are bound by specific receptors at the bacterial surface (IroN, FepA, and CirA). The iron-ferrichrome complex can be imported through the FhuABCD uptake system. A gene homologous to *foxA*, the gene encoding the outer membrane ferrioxamine receptor of *Yersinia enterocolitica* (Báumler & Hantke K, 1992), is also present in *S.* Enteritidis genome. Involvement of porin OmpC in Tf-binding has been suggested for *Salmonella* Typhimurium (Sandrini *et al.*, 2013). No outer membrane receptors for haem-binding proteins are described, however, the genes encoding for Sap transporter system (involved in haem-uptake in other Gram-negative bacteria: *Haemophilus influenzae*; Mason *et al.*, 2011), are present in *S.* Enteritidis genome. Free Fe^{2+} uptake is mediated by the FeoABC system. Alternative routes for driving Fe^{2+} uptake are the Mn^{2+} pathways: MntH and SitABCD. Salmonellae possesses three iron-storage proteins: Dps, ferritin A (FtnA) and bacterioferritin (Bfr; Osman & Cavet, 2011 for a review). OM and IM stand for outer- and inner-membrane, respectively.

Transferrin-recepetors. It has been shown that *S.* Typhimurium can utilise iron when exposed to human transferrin independently of extracellularly carriers such as siderophores (Choe *et al.*, 2017). This is in accordance with the finding that *S.* Typhimurium OmpC could be involved in Tf-binding (Sandrini *et al.*, 2013). However, utilisation of oTf as a source of iron is not the most likely hypothesis to explain growth in EW since *S.* Enteritidis grew better when oTf was removed from the medium (see *egg white filtrate experiments*, section 5.4).

Ferrichrome uptake. Ferrichrome is a cyclic hexapeptide belonging to the group of hydroxamate siderophores. Although the genes required for ferrichrome synthesis are present in some fungi, this is not the case in *S.* Enteritidis and *S.* Typhimurium genomes.

Furthermore, the inability for *S.* Enteritidis to produce siderophores other than enterobactin and salmochelin has been confirmed with the CAS plate assay carried out in the present work (section 5.1.3). Yet, it has been shown that a Δ*entB* mutant of *S.* Typhimurium can utilise the iron-ferrichrome complex as an effective growth factor (Pollack *et al.,* 1970). This is ascribed to the fact that *S.* Typhimurium genome contains the *fhuABCD* ferric hydroxamate uptake genes. Upon exposure of *S.* Enteritidis to EWMM, genes involved in ferric-hydroxamate uptake and ferric-hydroxamate utilisation were slightly up-regulated (~4.5-fold after 24 h incubation in EWMM; Baron *et al.,* 2017). However, this mechanism is unlikely to support iron acquisition since ferrichrome is unlikely to be present within EW, and the same issues raised above relating to impaired siderophore uptake due to membrane perturbation in EW would apply to the FhuABCD system.

Ferrous iron uptake. The Fe^{3+}-oTf complex should be the predominant source of iron in EW. However, if there were any free Fe^{2+}, *S.* Enteritidis could import it through its FeoABC high-affinity ferrous-iron transporter (for a review, see Carpenter & Payne, 2014). Both ferric and ferrous iron are important for *S.* Enteritidis survival in EW (Kang *et al.,* 2006), since both Δ*entF* and Δ*feoAB* mutants exhibited a lower survival rate than the WT after 70 h incubation at 37 °C. Furthermore, Liu *et al.* (2015) highlighted that the *S.* Typhimurium Feo system alone might be sufficient to provide iron for growth in epithelial cells (HeLa cells). However, Huang *et al.* (2019) observed a slight down-regulation of the *S.* Enteritidis *feoABC* operon (~0.5-fold) after 24 h exposure to 80% EW at 37 °C, which may reflect the requirement for anoxic conditions for strong Feo induction (Kammler *et al.,* 1993). Hence, the role of Feo system in *S.* Enteritidis iron acquisition in EW remains unclear and might vary depending on experimental conditions. Alternative routes to Feo system for driving Fe^{2+} uptake are the Mn^{2+} (MntH & SitABCD) and the Zn^{2+} uptake pathways (ZupT & YiiP) (Osman & Cavet, 2011). Interestingly, SitABCD was up-regulated when *S.* Enteritidis was exposed to EWMM for 45 min at 45 °C (Baron *et al.,* 2017). However, this uptake system has a higher affinity for manganese than for iron and its involvement in *S.* Enteritidis iron acquisition in EW remains to be defined.

Haem protein receptors. Hen hemoglobin and hemopexin proteins (binding free haem) could be used as a source of Fe^{2+}. Baron *et al.* (2017) have shown that the gene *ydiE* (coding a protein of unclear function related to the haem-utilization component, HemP of *Yersinia enterolitica*) is up-regulated at 45 min exposure to EWMM at 45 °C.

However, as for the other acquisition mechanisms described above, this mechanism is unlikely to enhance bacterial cell iron acquisition in EW, since iron-bound haem should be absent in the medium. The fact that haem and ferrichrome uptake systems are up-regulated in EW does not necessarily mean that they support *S*. Enteritidis growth in EW. Indeed, in iron deprived environments, Fur is de-repressed and activates all iron acquisition systems, effective or not.

Internal storage. S. Enteritidis possesses three iron storage proteins, Dps (500 atoms), ferritin A (3000 atoms), and heam-containg bacterioferritin (3000 atoms). Ferritin A and bacterioferritin might be involved in iron storage/detoxification whereas DPS is involved in protection from oxidative stress (Osman & Cavet, 2011). Baron *et al.* (2017) observed a down-regulation of *S*. Enteritidis iron-storage capacity, which provides additional evidence for the iron-restricted nature of EW. In the present study, the mobilisation of internal reserves was initially suggested as an explanation for *S*. Enteritidis growth in EW. However, even when deprived of iron prior to growth in EW, *S*. Enteritidis was still able to grow/survive in EW (section 5.3.2). This indicates that *S*. Enteritidis does not rely strongly on iron-internal iron stores to support its growth/survival in EW.

6.1.3 *Salmonella* Enteritidis alternative metal-utilisation pathways

In *E. coli*, intracellular iron concentration should be maintained at ~0.1 mM (Finney & O'Halloran, 2003). However, as described above, iron acquisition by *S*. Enteritidis in EW seems somewhat limited for non-producing-siderophore strains. In the present study, since *S*. Enteritidis is unable to grow when incubated in EW (at 30°C), but can persist, they would not be expected to require significant amounts of iron (section 5.3.1). However, during growth (growth of ~1 $\log_{10}$ CFU/mL in EW, section 5.3.2), access to a source of iron would be expected. As already described, *S*. Enteritidis might then be able to reprogram gene expression to use alternative iron utilisation pathways (Baron *et al.*, 2017; Huang *et al.*, 2019). This hypothesis is supported by the study of Baron *et al.* (2017) which showed that exposure of *S*. Enteritidis to EWMM for 45 min at 45 °C leads to de-repression of Fur, which in turn leads to the activation of: (i) alternative Fe-S cluster manufacturing pathway; (ii) iron rationing with replacement of iron-dependent proteins by manganese-dependent alternatives; (iii) manganese uptake pathways. This aspect is further elaborated below.

Induction of the alternative Fe-S cluster manufacturing pathway. Iron–sulphur (Fe–S) cluster proteins conduct essential functions in nearly all contemporary forms of life. In the *S*. Enteritidis genome, two operons implicated in Fe-S cluster assembly (*suf* and *isc*) have been shown to be up-regulated under EW exposure (Baron *et al.,* 2017; Huang e*t al.,* 2019). The main pathway leading to Fe-S cluster is driven by the the *isc*-encoded proteins. Nevertheless, Outten *et al.* (2004) have shown that the *isc*-encoded proteins cannot function effectively to synthesise Fe-S clusters when iron is limiting. The use of the *suf* alternative pathway might allow *S*. Enteritidis to adapt to the iron-restricted EW environment.

Iron rationing with replacement of iron-dependent proteins by manganese-dependent alternatives. When iron levels are reduced, *S*. Enteritidis cells can replace some proteins requiring Fe^{2+} as co-factor by proteins using Mn^{2+}. Under exposure to EWMM for 45 min at 45 °C, the gene coding for the iron-superoxide dismutase (*sodB*) was down-regulated. Reciprocally, the gene coding for manganese-superoxide (*sodA*) was up-regulated (Baron *et al.,* 2017. Likewise, in the same study, the *nrdHIEF* genes coding an alternative Mn-dependent ribonucleotide reductase (Martin & Imlay, 2011) were induced by 5.18- to 15.4-fold after 45 min incubation in EWMM (Baron *et al.,* 2017).

Induction of manganese uptake pathway. For manganese, both MntH and SitABCD transport systems are involved in its uptake. Baron *et al.* (2017) observed a greater induction response of the latter when *S*. Enteritidis was incubated in EWMM for 45 min at 45 °C. This might be explained by the fact that MntH exhibits optimal Mn^{2+} transport under acidic conditions whereas SitABCD has preference for alkaline pH (Kehres *et al.,* 2002). Although Salmonellae have zinc sensing systems (Zur and ZntR) (Osman & Cavet, 2011), as for manganese, this is only a trace element in EW (Table 1.3, section 1.2.1).

6.2 Could Ex-FABP be a component of the hen immune defence?

6.2.1 The role of the human lipocalin-2 in defence against pathogens

In the present study, experiments in M9 and LB with DIP have shown that Ex-FABP exerts antimicrobial activity on a salmochelin deficient *S*. Enteritidis *via* its siderophore-binding activity. However, the Ex-FABP antibacterial activity observed in standard growth media could not be observed in EW media.

Since Ex-FABP has been shown to be expressed in chicken lungs, liver and spleen following *E. coli* infection, its role in preventing bacterial infection prior to laying also needs to be considered (Garénaux *et al.,* 2013). Little in known about the antibacterial functions of Ex-FABP in hens; however, extensive data is available on its human homologue, LCN2. Elevated levels of LCN2 are found in plasma after bacterial infection (Lu *et al.,* 2019). In response to infection, both hepatocytes and hematopoietic cells (e.g neutrophils and macrophages) produce LCN2. Extracellular LCN2 secreted by hepatocytes limits systemic bacterial infection, whereas immune cells recruit LCN2 to the local site and against local bacterial infection (Li *et al.,* 2018). Inside the gut, LCN2 is suggested to maintain intestinal diversity and to regulate pathogenic bacterial survival through its interplay with siderophores (Guo *et al.,* 2017). Note that apart from siderophore production, LCN2 is also suspected to enhance the proinflammatory response by up-regulation of cytokines (Nelson *et al.,* 2007; Holden *et al.,* 2014; Wang *et al.,* 2019). Yet, the main function of LCN2 in the antibacterial innate immune response is to limit iron (Ellermann & Arthur, 2017). Since LCN2 and Ex-FABP have similar siderophore binding activities, it is reasonable to suggest that Ex-FABP could also play an important role in the hen's immunity against bacterial infection.

6.2.1 Ex-FABP might protect the hen oviduct from infection

In the case of vertical contamination of the egg (section 1.1.2), Salmonellae might have previously been orally taken up by the hen and entered the intestinal tract. Then, bacteria can colonise the intestinal lumen and invade the intestinal epithelial cells (Gantois *et al.,* 2009). In those cells, Salmonellae reside in vacuoles where they encounter severe metal starvation. To adapt to this environment, they have been shown to divide by up-regulating iron, manganese and zinc-uptake systems (Liu *et al.,* 2015; Steele-Mortimer, 2008). Salmonellae can also persist in macrophages (specialised in bacterial clearance) subsequently recruited to the site of infection. Successful infection of macrophages can then lead to the contamination of other organs (systemic contamination), including the reproductive tract (Gantois *et al.,* 2009). Thus, survival within macrophages is crucial for vertical contamination of eggs. In those cells, *Salmonella* is also facing iron restriction. Indeed, upon LPS exposure, the human lipocalin-2 is induced (Meheus *et al.,* 1993). Additionally, the level of haem oxygenase (a haem-degrading enzyme) is enhanced, further decreasing the intracellular iron pool in

macrophages (Gogoi *et al.,* 2019 for a review). It has also been shown that macrophages can limit the bioavailability of iron to the pathogen by up-regulating the iron-export protein ferroportin-1 (Collins, 2008; Brown *et al.,* 2015) and by lowering expression of ferritin (Nairz *et al.,* 2015).

Thus, prior to hen oviduct colonisation, *S*E encounters multiple environments scarce in iron (epithelial cells, M cells, activated macrophages and dendritic cells) where Ex-FABP could play a role in preventing systemic infection.

6.3 Conclusion and future work

Enumeration experiments suggested that the remarkable resistance of *S*. Enteritidis to EW is not strongly assisted by the ability to produce siderophores. To assess whether *S*. Enteritidis siderophore iron acquisition pathways are impaired in EW, EW could be supplemented with ferric-enterobactin and/or ferric salmochelin to determine if they can support growth. Ex-FABP antibacterial activity (*via* its siderophore-binding capacity) observed in standard growth media was not seen in EW. To determine whether Ex-FABP plays a role in preventing systemic infection (*via* enhanced iron restriction) leading to subsequent oviduct and egg contamination, further experiments could be conducted. Hens could be orally infected with *Salmonella* deficient in iron acquisition. Subsequently, orally infected hens would be sacrificed before bacterial counting in various tissues, including the oviduct. In these same tissues, quantitative RT-PCR (or immuno-detection) could be used to determine if Ex-FABP is induced upon infection (as described by Garénaux *et al.,* 2013 with *E. coli*). Indeed, the anti-Ex-FABP anibodies generated here could be used to screen hen tissues before and after infection to determine sites of Ex-FABP synthesis and its response to infection. Since mice knocked-out for lipocalin-2 synthesis were shown to be more susceptible to bacterial infection (Berger *et al.,* 2006), a transgenic hen deficient in Ex-FABP production could also be considered. This model could be used to determine if hens deficient in Ex-FABP are more likely to develop systemic infection and to lay contaminated eggs.

Conclusion

Recombinant EW lipocalins were successfully purified. The three lipocalins of EW, Ex-FABP, Cal-γ and α-1-ovoglycoprotein, were over-expressed and purified in order to investigate their EW concentrations and their ability to interact with the siderophores of *S.* Enteritidis.

Ex-FABP binds enterobactin with high affinity. The 16-fold preference of Ex-FABP for the ferrated form (K_d of 5.3 nM) of enterobactin over the iron-free form (K_d of 86.2 nM), and its lack of affinity for salmochelin were confirmed. However, Ex-FABP affinity for enterobactin might be lower in EW due to the specific pH. Neither Cal-γ or α1-ovoglycoprotein bind enterobactin or salmochelin.

EW contains micro-Molar levels of all three lipocalins. The semi-quantitative WB analysis indicated EW concentrations of 232.9, 5.6, and 5.1 µM for α1-ovoglycoprotein, Cal-γ, and Ex-FABP, respectively. These proteins are therefore the 4th, 11th and 12th most abundant proteins in EW, respectively.

Only Ex-FABP inhibits siderophore-dependent iron sequestration by Salmonella *Enteritidis.* In standard growth media, it was shown that salmochelin production allowed *S*E to escape Ex-FABP-mediated growth inhibition under iron restriction. Cal-γ and α1-ovoglycoprotein had no apparent effect on the growth of *S.* Enteritidis or its mutants under low- or sufficient-iron conditions, which is consistent with the observation that these lipocalins do not bind enterobactin or salmochelin.

Ex-FABP antibacterial activity in egg white. Ex-FABP antibacterial activity (*via* its siderophore-binding capacity) observed in standard growth media is not seen in egg white media. This surprising observation might be correlated with the weak growth of *S.* Enteritidis in EW and a lack of requirement for siderophores in persistence. Yet, further experiments are required to determine under which conditions siderophores may be needed to support EW colonisation by *S.* Enteritidis.

Overall, this study confirms that *S.* Enteritidis is very well suited to infection of, and survival within, eggs. Further, it provides significant insights to further understand how *S.* Enteritidis infects iron-scarced egg white to promote foodborne infection.

References

Abergel RJ, Moore EG, Strong RK & Raymond KN (2006) Microbial evasion of the immune system: structural modifications of enterobactin impair siderocalin recognition. *J. Am. Chem. Soc.* **128**: 10998–10999

AFSSA (2008) Avis de l'agence française de sécurité sanitaire des aliments concernant les références applicables aux denrées alimentaires en tant que critères indicateurs d'hygiène des procédés. Saisine n° 2007-SA-0174, Maisons-Alfort.

Aguilera O, Quiros LM & Fierro JF (2003) Transferrins selectively cause ion efflux through bacterial and artificial membranes. *FEBS Lett.* **548:** 5–10

Alabdeh M, Lechevalier V, Nau F, Gautier M, Cochet MF, Gonnet F, Jan S & Baron F (2011) Role of incubation conditions and protein fraction on the antimicrobial activity of egg white against *Salmonella* Enteritidis and *Escherichia coli*. *J. Food Prot.* **74:** 24–31

Alderton G, Ward WH & Fevold HL (1946) Identification of the bacteria-inhibiting iron-binding protein of egg white as conalbumin. *Arch. Biochem Biophys.* **11**: 9–13

Almeida C, Cerqueira L, Azevedo NF & Vieira MJ (2013) Detection of *Salmonella enterica* serovar Enteritidis using real time PCR, immunocapture assay, PNA FISH and standard culture methods in different types of food samples. *Int. J. Food Microbiol.* **161:** 16–22

Andersen KR, Leksa NC & Schwartz TU (2013) Optimized *E. coli* expression strain LOBSTR eliminates common contaminants from His-tag purification. *Proteins Struct. Funct. Bioinforma*. **81:** 1857-1861

Andrews SC, Norton I, Salunkhe AS, Goodluck H, Aly WSM, Mourad-Agha H & Cornelis P (2013) Control of iron metabolism in bacteria. *Met. Ions Life Sci.* **12**: 203-239

Andrews SC, Robinson AK & Rodríguez-Quiñones F (2003) Bacterial iron homeostasis. *FEMS Microbiol. Rev.* **27:** 215–237

ANSES (2017) Table de composition nutritionnelle des aliments. **https://ciqual.anses.fr/** Accessed 28 Jan 2020

Arrêté du 26 octobre 1998 relatif à la lutte contre les infections à *Salmonella* Enteritidis ou *Salmonella* Typhimurium dans les troupeaux de l'espèce *Gallus gallus* en filière ponte d'oeufs de consommation - NOR : AGRG9802175A

Bachman MA, Lenio S, Schmidt L, Oyler JE & Weiser JN (2012) Interaction of lipocalin 2, transferrin, and siderophores determines the replicative niche of *Klebsiella pneumoniae* during pneumonia. *MBio.* **3:** 1–8

Bags A & Neilands JB (1987) Ferric uptake regulation protein acts as a repressor, employing iron(II) as a cofactor to bind the operator of an iron transport operon in *Escherichia coli*. *Biochemistry* **26:** 5471–5477

Balbontín R, Villagra N, Pardos de la Gándara M, Mora G, Figueroa-Bossi N & Bossi L (2016) Expression of IroN, the salmochelin siderophore receptor, requires mRNA activation by RyhB small RNA homologues. *Mol. Microbiol.* **100:** 139–155

Banks JG, Board RG & Sparks NH (1986) Natural antimicrobial systems and their potential in food preservation of the future. *Biotechnol. Appl. Biochem.* **8:** 103-147

Bao GH, Clifton M, Hoette TM, Mori K, Deng S, Qiu A, Viltard M, Williams D, Paragas N, Leete T, Li X, Lee B, Kalandadze A, Ratner AJ, Carlos J, Schmidt-ott KM, Landry DW, Raymond KN & Roland K (2010) Iron traffics in circulation bound to a siderocalin (Ngal)-catechol complex. *Nat. Chem. Biol.* **6:** 602–609

Bao GH, Ho CT & Barasch J (2015) The ligands of neutrophil gelatinase-associated lipocalin. *RSC Adv.* **5:** 104363–104374

Baron F, Bonnassie S, Alabdeh A, Cochet MF, Nau F, Guérin-Dubiard C, Gautier M, Andrews SC & Jan S (2017) Global gene-expression analysis of the response of *Salmonella* Enteritidis to egg white exposure reveals multiple egg white-imposed stress responses. *Front. Microbiol.* **8:** 1–26

Baron F, Cochet MF, Ablain W, Grosset N, Madec MN, Gonnet F, Jan S & Gautier M (2006) Rapid and cost-effective method for micro-organism enumeration based on miniaturization of the conventional plate-counting technique. *Le Lait, INRA Editions.* **3:** 251-257

Baron F, Fauvel S & Gautier G (2000) Behaviour of *Salmonella* Enteritidis in industrial egg white: egg naturally contains factors inhibitory to *Salmonella* growth (ed

Sim J, Nakai N, Guenter W). *Egg nutrition and biotechnology.* Oxon: CAB International, pp 417–430

Baron F, Gautier M & Brulé G (1997) Factors involved in the inhibition of growth of *Salmonella* Enteritidis in liquid egg white. *J. Food Prot.* **60:** 1318–1323

Baron F, Gautier M & Brulé G (1999) Rapid growth of *Salmonella* Enteritidis in egg white reconstituted from industrial egg white powder. *J. Food Prot.* **62**: 585–591

Baron F, Jan S, Gonnet F, Pasco M, Jardin J, Giudici B, Gautier M, Guérin-Dubiard C & Nau F (2014) Ovotransferrin plays a major role in the strong bactericidal effect of egg white against the *Bacillus cereus* group. *J. Food Prot.* **77:** 955–962

Baron F, Nau F, Guérin-Dubiard C, Bonnassie S, Gautier M, Andrews SC & Jan S (2016) Egg white versus *Salmonella* Enteritidis! A harsh medium meets a resilient pathogen. *Food Microbiol.* **53:** 82–93

Barrow PA, Huggins MB, Lovell MA & Simpson JM (1987) Observations on the pathogenesis of experimental *Salmonella enterica* serovar Typhimurium infection in chickens. *Res. Vet. Sci.* **42:** 194–199

Bäumler AJ, Norris TL, Lasco T, Voigt W, Reissbrodt R, Rabsch W & Heffron F (1998) IroN, a novel outer membrane siderophore receptor characteristic of *Salmonella enterica*. *J. Bacteriol.* **180:** 1446–1453

Báumler AJ & Hantke K (1992) Ferrioxamine uptake in *Yersinia enterocolitica*: characterization of the receptor protein FoxA. *Mol. Microbiol.* **6:** 1309–1321

Benjamin WH, Turnbough CL, Posey BS & Briles DE (1985) The ability of *Salmonella* Typhimurium to produce the siderophore enterobactin is not a virulence factor in mouse typhoid. *Infect. Immun.* **50:** 392–397

Berger T, Togawa A, Duncan GS, Elia AJ, You-Ten A, Wakeham A, Fong HEH, Cheung CC & Mak TW (2006) Lipocalin 2-deficient mice exhibit increased sensitivity to *Escherichia coli* infection but not to ischemia-reperfusion injury. *Proc. Natl. Acad. Sci. U. S. A.* **103:** 1834–1839

Bister B, Bischoff D, Nicholson GJ, Valdebenito M, Schneider K, Winkelmann G, Hantke K & Süssmuth RD (2004) The structure of salmochelins: C-glucosylated enterobactins of *Salmonella enterica*. *BioMetals.* **17:** 471–481

Bjarnason J, Southward CM & Surette MG (2003) Genomic profiling of iron-responsive genes in *Salmonella enterica* serovar Typhimurium by high-throughput screening of a random promoter library. *J. Bacteriol.* **185:** 4973–4982

Bleuel C, Grosse C, Taudte N, Scherer J, Wesenberg D, Krauss GJ, Nies DH & Grass G (2005). TolC is involved in enterobactin efflux across the outer membrane of *Escherichia coli*. *J. Bacteriol.* **187:** 6701–6707

Boutten A, Dehoux M, Deschenes M, Rouzeau JD, Bories PN & Durand G (1992) α-1-acid glycoprotein potentiates lipopolysaccharide-induced secretion of interleukin-1β, interleukin-6 and tumor necrosis factor-α by human monocytes and alveolar and peritoneal macrophages. *Eur. J. Immunol.* **22:** 2687–2695

Braden CR (2006) *Salmonella enterica* serotype Enteritidis and eggs: a national epidemic in the United States. *Clin. Infect. Dis.* **43:** 512–517

Bradshaw JG, Shah DB, Forney E & Madden JM (1990) Growth of *Salmonella* Enteritidis in yolk of shell eggs from normal and seropositive hens. *J. Food Prot.* **53:** 1033–1036

Brown DE, Nick HJ, McCoy MW, Moreland SM, Stepanek AM, Benik R, O'Connell KE, Pilonieta MC, Nagy TA, Detweiler CS (2015) Increased ferroportin-1 expression and rapid splenic iron loss occur with anemia caused by *Salmonella enterica* serovar Typhimurium infection in mice. *Infect Immun.* **83:** 2290– 2299

Bullen JJ, Rogers HJ & Griffiths E (1978) Role of iron in bacterial infection. *Curr. Top. Microbiol. Immunol.* **80:** 1–35

Bullen JJ, Rogers HJ, Spalding PB & Ward CG (2005). Iron and infection, the heart of the matter. *FEMS Immunol. Med. Microbiol.* **43:** 325–330

Bullis KL (1977) The history of avian medicine in the U.S. II. Pullorum disease and fowl typhoid. *Avian Dis.* **21:** 422-9

Callewaert L, Aertsen A, Deckers D, Vanoirbeek KGA, Vanderkelen L, Van Herreweghe JM, Masschalck B, Nakimbugwe D, Robben J & Michiels CW (2008) A new family of lysozyme inhibitors contributing to lysozyme tolerance in gram-negative bacteria. *PLoS Pathog.* **4:** 1–9

Cancedda FD, Dozin B, Rossi F, Molina F, Cancedda R, Negri A & Ronchi S (1990) The Ch21 protein, developmentally regulated in chick embryo, belongs to the superfamily of lipophilic molecule carrier proteins. *J. Biol. Chem.* **265:** 19060–19064

Cancedda FD, Malpeli M, Gentili C, Marzo V Di, Bet P, Carlevaro M, Cermelli S & Cancedda R (1996) The developmentally regulated avian Ch21 lipocalin is an extracellular fatty acid-binding protein. *J. Biol. Chem.* **271:** 20163–20169

Cancedda FD, Manduca P, Tacchetti C, Fossa P, Quarto R & Cancedda R (1988) Developmentally regulated synthesis of a low molecular weight protein (Ch21) by differentiating chondrocytes. *J. Cell. Biol.* **107:** 2455–2463

Carpenter C & Payne SM (2014) Response to oxygen and iron availability. *J. Inorg. Biochem.* **133:** 110–117

Caza M, Lépine F & Dozois CM (2011) Secretion, but not overall synthesis, of catecholate siderophores contributes to virulence of extraintestinal pathogenic *Escherichia coli*. *Mol. Microbiol.* **80:** 266–282

Caza M, Lépine F, Milot S & Dozois CM (2008) Specific roles of the *iroBCDEN* genes in virulence of an avian pathogenic *Escherichia coli* O78 strain and in production of salmochelins. *Infect. Immun.* **76:** 3539–3549

Cermelli S, Zerega B, Carlevaro M, Gentili C, Thorp B, Farquharson C, Cancedda R & Cancedda FD (2000) Extracellular fatty acid binding protein (Ex-FABP) modulation by inflammatory agents: 'physiological' acute phase response in endochondrol bone formation. *Eur. J. Cell. Biol.* **79:** 155–164

Chart H & Rowe B (1993) Iron restriction and the growth of *Salmonella* Enteritidis. *Epidemiol. Infect.* **110:** 41–47

Chen W, Zhao X, Zhang M, Yuan Y, Ge L, Tang B, Xu X, Cao L & Guo H (2016) Protein expression and purification high-efficiency secretory expression of human neutrophil gelatinase- associated lipocalin from mammalian cell lines with human serum albumin signal peptide. *Protein Expr. Purif.* **118:** 105–112

Chenault SS & Earhart CF (1992) Identification of hydrophobic proteins FepD and FepG of the *Escherichia coli* ferrienterobactin permease. *J. Gen. Microbiol.* **138:** 2167–2171

Cherepanov PP & and Wackernagel W (1995) Gene disruption in *Escherichia coli*: Tc^R and Km^R cassettes with the option of Flp-catalyzed excision of the antibiotic-resistance determinant. *Gene.* **158:** 9–14

Choe Y, Yoo AY, Kim SW, Hwang J & Kang HY (2017) *Salmonella* Typhimurium SL1344 utilizing human transferrin-bound iron as an iron source regardless of siderophore-mediated uptake. *J. Life Sci.* **27:** 72–77

Claude M, Lupi R, Bouchaud G, Bodinier M, Brossard C & Denery-Papini S (2016) The thermal aggregation of ovalbumin as large particles decreases its allergenicity for egg allergic patients and in a murine model. *Food Chem.* **203:** 136–144

Clavijo RI, Loui C, Andersen GL, Riley LW & Lu S (2006) Identification of genes associated with survival of *Salmonella enterica* serovar Enteritidis in chicken egg albumen. *Appl. Environ. Microbiol.* **72:** 1055–1064

Clifton-Hadley FA, Breslin M, Venables LM, Sprigings KA, Cooles SW, Houghton S & Woodward MJ (2002) A laboratory study of an inactivated bivalent iron restricted *Salmonella enterica* serovars Enteritidis and Typhimurium dual vaccine against Typhimurium challenge in chickens. *Vet. Microbiol.* **89:** 167–179

Collins HL (2008) Withholding iron as a cellular defence mechanism–friend or foe? *Eur. J. Immunol.* **38:** 1803–1806

Commission Regulation 2006/1177/EC implementing Regulation (EC) No 2160/2003 of the European Parliament and of the Council as regards requirements for the use of specific control methods in the framework of the national programmes for the control of *Salmonella* in poultry

Correnti C, Clifton MC, Abergel RJ, Allred B, Hoette TM, Ruiz M, Cancedda R, Raymond KN, Cancedda FD & Strong RK (2011) Galline Ex-FABP is an antibacterial siderocalin and a lysophosphatidic acid sensor functioning through dual ligand specificities. *Structure.* **19:** 1796–1806

Coudevylle N, Geist L, Hötzinger M, Hartl M, Kontaxis G, Bister K & Konrat R (2010) The v-myc-induced Q83 lipocalin is a siderocalin. *J. Biol. Chem.* **285:** 41646–41652

Council Directive 92/117/EEC concerning measures for protection against specified zoonoses and specified zoonotic agents in animals and products of animal origin in order to prevent outbreaks of food-borne infections and intoxications (1992)

Council Directive 2003/99/EC of the European Parliament and of the Council on the monitoring of zoonoses and zoonotic agents, amending Council Decision 90/424/EEC and repealing Council Directive 92/117/EEC (2003)

Coy M & Neilands JB (1991) Structural dynamics and functional domains of the fur protein. *Biochemistry.* **30:** 8201–8210

Crouch ML, Castor M, Karlinsey JE, Kalhorn T & Fang FC (2008) Biosynthesis and IroC-dependent export of the siderophore salmochelin are essential for virulence of *Salmonella enterica* serovar Typhimurium. *Mol. Microbiol.* **67:** 971–983.

D'Ambrosio C, Arena S, Scaloni A, Guerrier L, Boschetti E, Mendieta ME, Citterio A & Righetti PG (2008) Exploring the chicken egg white proteome with combinatorial peptide ligand libraries. *J. Proteome Res.* **7:** 3461–3474

D'Aoust J & Maurer J (2007). *Salmonella* Species (ed Doyle M, Beuchat L). *Food Microbiology: Fundamentals and Frontiers.* Washington DC: ASM Press, pp 187-236

Darwin AJ (2005) The phage-shock-protein response. *Mol. Microbiol.* **57:** 621–628

Da Silva M, Beauclercq S, Harichaux G, Labas V, Guyot N, Gautron J, Nys Y & Rehault-Godbert S (2015) The family decrets of avian egg-specific ovalbumin and its related proteins Y and X. *Biol. Reprod.* **93:** 1–7

Datsenko KA & Wanner BL (2000) One-step inactivation of chromosomal genes in *Escherichia coli* K-12 using PCR products. *Proc. Natl. Acad. Sci. U. S. A.* **97:** 6640–6645

Davies RC, Neuberger A & Wilson BM (1969) The dependence of lysozyme activity on pH and ionic strength. *Biochim. Biophys. Acta.* **178**: 294-305

Demir M & Kaleli I (2004) Production by *Escherichia coli* isolates of siderophore and other virulence factors and their pathogenic role in a cutaneous infection model. *Clin. Microbiol. Infect.* **10:** 1011–1014

Dente L, Ciliberto G & Cortese R (1985) Structure of the human alpha 1-acid glycoprotein gene: sequence homology with other human acute phase protein genes. *Nucleic Acids Res.* **13:** 3941–3952

Derde M, Lechevalier V, Guerin-Dubiard C, Cochet MF, Jan S, BaronF, Gautier M, Vié V & Nau F (2013) Hen egg white lysozyme permeabilizes the *Escherichia coli* outer and inner membranes. *J. Agric. Food Chem.* **61:** 9922– 9929

Desert C, Guerin-Dubiard C, Nau F, Jan G, Val F & Mallard J (2001) Comparison of different electrophoretic separations of hen egg white proteins. *J. Agric. Food. Chem.* **49:** 4553–4561

Devireddy LR, Gazin C, Zhu X & Green MR (2005) A cell-surface receptor for lipocalin 24p3 selectively mediates apoptosis and iron uptake. *Cell.* **123:** 1293–1305

Devireddy LR, Hart DO, Goetz DH & Green MR (2010) A mammalian siderophore synthesized by an enzyme with a bacterial homolog involved in enterobactin production. *Cell.* **141:** 1006–1017

Di Marco E, Sessarego N, Zerega B, Cancedda R & Cancedda FD (2003) Inhibition of cell proliferation and induction of apoptosis by Ex-FABP gene targeting. *J. Cell. Physiol.* **196:** 464–473

Dozin B, Cancedda FD, Briata L, Hayashi M, Gentili C, Hayashi K, Quarto R & Cancedda R (1992) Expression, regulation, and tissue distribution of the Ch21 protein during chicken embryogenesis. *J. Biol. Chem.* **267:** 2979–2985

Du ZP, Wu BL, Wu X, Lin XH, Qiu XY, Zhan XF, Wang SH, Shen JH, Zheng CP, Wu ZY, Xu LY, Wang D & Li EM (2015) A systematic analysis of human lipocalin family and its expression in esophageal carcinoma. *Sci. Rep.* **5:** 1–14

Dunkley KD, Callaway TR, Chalova VI, McReynolds JL, Hume ME, Dunkley CS, Kubena LF, Nisbet DJ & Ricke SC (2009) Foodborne *Salmonella* ecology in the avian gastrointestinal tract. *Anaerobe.* **15:** 26–35

ECDC, EFSA (2017) Multicountry outbreak of *Salmonella* Enteritidis phage type 8, MLVA type 2-9-7-3-2 and 2-9-6-3-2 infections. Stockholm and Parma: ECDC and EFSA, pp 1–22

EFSA Panel on Biological Hazards (2014) Scientific opinion on the public health risks of table eggs due to deterioration and development of pathogens. *EFSA J.* **12:** 1–147

EFSA Panel on Biological Hazards (2019) Scientific Opinion on the *Salmonella* control in poultry flocks and its public health impact. *EFSA J.* **17**, 1–155

El-Gebali S, Mistry J, Bateman A, Eddy SR, Luciani A, Potter SC, Qureshi M, Richardson LJ, Salazar GA, Smart A, Sonnhammer ELL, Hirsh L, Paladin L, Piovesan D, Tosatto SCE & Finn RD (2019) The Pfam protein families database. *Nucleic. Acids. Res.* **47:** 427–432

Ellermann M & Arthur JC (2017) Siderophore-mediated iron acquisition and modulation of host-bacterial interactions. *Free Radic. Biol. Med.* **105:** 68–78

Ellison RT, Giehl TJ & LaForce FM (1988) Damage of the outer membrane of enteric gram-negative bacteria by lactoferrin and transferrin. *Infect. Immun.* **56:** 2774–2781

Fang Q, Brockmann S, Botzenhart K & Wiedenmann A (2003) Improved detection of *Salmonella* spp. in foods by fluorescent in situ hybridization with 23S rRNA probes: a comparison with conventional culture methods. *J. Food Prot.* **66:** 723–731

Finney LA & O'Halloran TV (2003) Transition metal speciation in the cell: insights from the chemistry of metal ion receptors. *Science.* **300:** 931–936

Fischbach MA, Lin H, Zhou L, Yu Y, Abergel RJ, Liu DR, Raymond KN, Wanner BL, Strong RK, Walsh CT, Aderem A & Smith KD (2006) The pathogen-associated *iroA* gene cluster mediates bacterial evasion of lipocalin 2. *Proc. Natl. Acad. Sci. U. S. A.* **103:** 16502–16507

Flo TH, Smith KD, Sato S, Rodriguez DJ, Holmes MA, Strong RK, Akira S & Aderem A (2004) Lipocalin 2 mediates an innate immune response to bacterial infection by sequestrating iron. *Nature.* **432:** 917–921

Flower DR (1996) The lipocalin protein family: structure and function. *Biochem. J.* **318:** 1–14

Flower DR, North ACT & Sansom CE (2000) The lipocalin protein family: structural and sequence overview. *Biochim. Biophys. Acta - Protein Struct. Mol. Enzymol.* **1482:** 9–24

Furrer JL, Sanders DN, Hook-Barnard IG & McIn- tosh MA (2002) Export of the siderophore enterobactin in *Escherichia coli*: involvement of a 43 kDa membrane exporter. *Mol. Microbiol.* **44:** 1225–1234

Gaber BP, Miskowski V & Spiro TG (1974) Resonance Raman Scattering from iron(III)- and copper(II)-transferrin and an iron(III) model compound. A spectroscopic interpretation of the transferrin binding site. *J. Am. Chem. Soc.* **96:** 6868–6873

Gachon AMF (1994) Lipocalines et transport de ligands hydrophobes. *Med. Sci.* **10:** 22–29

Gantois I, Ducatelle R, Pasmans F, Haesebrouck F, Gast R, Humphrey TJ & Van Immerseel F (2009) Mechanisms of egg contamination by *Salmonella Enteritidis*: review article. *FEMS Microbiol. Rev.* **33:** 718–738

Gantois I, Eeckhaut V, Pasmans F, Haesebrouck F, Ducatelle R & Van Immerseel F (2008) A comparative study on the pathogenesis of egg contamination by different serotypes of *Salmonella. Avian. Pathol.* **37:** 399–406

Gao Q, Wang X, Xu H, Xu Y, Ling J, Zhang D, Gao S & Liu X (2012) Roles of iron acquisition systems in virulence of extraintestinal pathogenic *Escherichia coli*: salmochelin and aerobactin contribute more to virulence than heme in a chicken infection model. *BMC Microbiol.* **12:** 1–12

Garénaux A, Houle S, Folch B, Dallaire G, Truesdell M, Lépine F, Doucet N & Dozois CM (2013) Avian lipocalin expression in chickens following *Escherichia coli* infection and inhibition of avian pathogenic *Escherichia coli* growth by Ex-FABP. *Vet. Immunol. Immunopathol.* **152:** 156–167

Garcia FJ, Pons A, Alemany M & Palou A (1983) Permeability of chicken egg vitelline membrane to glucose, gradients between albumen and yolk. *Comp. Biothem. Physiol.* **75:** 137–140

Garibaldi JA (1970) Role of microbial iron transport compounds in bacterial spoilage of eggs. *Appl. Microbiol.* **20:** 558–60

Gast RK & Holt PS (2000) Influence of the level and location of contamination on the multiplication of *Salmonella* Enteritidis at different storage temperatures in experimentally inoculated eggs. *Poult. Sci.* **79:** 559–563

Gehring AM, Mori I & Walsh CT (1998) Reconstitution and characterization of the *Escherichia coli* enterobactin synthetase from EntB, EntE, and EntF. *Biochemistry.* **37:** 2648–26594

Gentili C, Cermelli S, Tacchetti C, Cossu G, Cancedda R & Cancedda FD (1998) Expression of the extracellular fatty acid binding protein (Ex-FABP) during muscle fiber formation *in vivo* and *in vitro*. *Exp. Cell. Res.* **242:** 410–418

Gentili C, Tutolo G, Zerega B, Di Marco E, Cancedda R & Cancedda FD (2005) Acute phase lipocalin Ex-FABP is involved in heart development and cell survival. *J. Cell. Physiol.* **202:** 683–689

Goetz DH, Holmes MA, Borregaard N, Bluhm ME, Raymond KN & Strong RK (2002) The neutrophil lipocalin NGAL is a bacteriostatic agent that interferes with siderophore-mediated iron acquisition. *Mol. Cell* **10:** 1033–1043

Goetz DH, Willie ST, Armen RS, Bratt T, Borregaard N & Strong RK (2000) Ligand preference inferred from the structure of neutrophil gelatinase associated lipocalin. *Biochemistry.* **39:** 1935–1941

Gogoi M, Shreenivas MM & Chakravortty D (2019) Hoodwinking the big-eater to prosper: the *Salmonella* -macrophage paradigm. *J. Innate Immun.* **11:** 289–299

Gong DQ, Wilson PW, Bain MM, McDade K, Kalina J, Hervé-Grepinet, V, Nys Y, & Dunn IC (2010) Gallin; an antimicrobial peptide member of a new avian defensin family, the ovodefensins, has been subject to recent gene duplication. *BMC Immunol.* **11:** 1–15

Greene LH, Hamada D, Eyles SJ & Brew K (2003) Conserved signature proposed for folding in the lipocalin superfamily. *FEBS Lett.* **553:** 39–44

Grimont PAD & Weill FX (2007). Antigenic formulae of the *Salmonella* serovars, 9th ed. WHO Collaborating Centre for Reference and Research on *Salmonella*. Paris: Institut Pasteur

Guan J, Grenier C & Brooks BW (2006) *In vitro* study of *Salmonella* Enteritidis and *Salmonella* Typhimurium definitive type 104: survival in egg albumen and penetration through the vitelline membrane. *Poult. Sci.* **85:** 1678–1681

Guérin-Dubiard C, Pasco M, Mollé D, Désert C, Croguennec T & Nau F (2006) Proteomic analysis of hen egg white. *J. Agric. Food Chem.* **54:** 3901–3910

Guha-Thakurta P, Choudhury D, Dasgupta R & Dattagupta JK (2003) Structure of diferric hen serum transferrin at 2.8 A resolution. *Acta. Crystallogr. D. Biol. Crystallogr.* **59:** 1773–1781

Guo BX, Wang QQ, Li JH, Gan ZS, Zhang XF, Wang YZ & Du HH (2017) Lipocalin 2 regulates intestine bacterial survival by interplaying with siderophore in a weaned piglet model of *Escherichia coli* infection. *Oncotarget.* **8:** 65386–65396

Haginaka J, Seyama C & Kanasugi N (1995) Ovoglycoprotein-bonded HPLC stationary phases for chiral recognition. *Anal. Chem.* **67:** 2539–2547

Haginaka J & Takehira H (1997) Separation of enantiomers on a chiral stationary phase based on ovoglycoprotein. *J. Chromatogr. A.* **777:** 241–247

Hantke K, Nicholson G, Rabsch W & Winkelmann G (2003) Salmochelins, siderophores of *Salmonella enterica* and uropathogenic *Escherichia coli* strains, are recognized by the outer membrane receptor IroN. *Proc. Natl. Acad. Sci. U. S. A.* **100:** 3677–3682

Hegenauer J, Saltman P & Nace G (1979) Iron(III)-phosphoprotein chelates: stoichiometric equilibrium constant for interation of iron(III) and phosphorylserine residues of phosvitin and casein. *Biochemistry*. **18:** 3865–3879

Hervé-Grépinet V, Réhault-Godbert S, Labas V, Magallon T, Derache C, Lavergne M, Gautron J, Lalmanach AC & Nys Y (2010) Purification and characterization of avian β-defensin 11, an antimicrobial peptide of the hen egg. *Antimicrob. Agents Chemother.* **54:** 4401–4408

Hervé-Grépinet V, Meudal H, Labas V, Réhault-Godbert S, Gautron J, Berges M, Guyot N, Delmas AF, Nys Y & Landon C (2014) Three-dimensional NMR structure of hen egg gallin (chicken ovodefensin) reveals a new variation of the β-defensin fold. *J. Biol. Chem.* **289:** 7211–7220

Holden VI & Bachman MA (2015) Diverging roles of bacterial siderophores during infection. *Metallomics.* **7:** 986–995

Holden VI, Lenio S, Kuick R, Ramakrishnan SK, Shah YM & Bachman MA (2014) Bacterial siderophores that evade or overwhelm lipocalin 2 induce hypoxia inducible factor 1α and proinflammatory cytokine secretion in cultured respiratory epithelial cells. *Infect. Immun.* **82:** 3826–3836

Holmes MA, Paulsene W, Jide X, Ratledge C & Strong RK (2005) Siderocalin (Lcn 2) also binds carboxymycobactins, potentially defending against mycobacterial infections through iron sequestration. *Structure.* **13:** 29–41

Huang Z & Ung T (2013) Effect of alpha-1-acid glycoprotein binding on pharmacokinetics and pharmacodynamics. *Curr. Drug Metab.* **14:** 226–238

Huang X, Zhou X, Jia B, Li N, Jia J, He M, He Y, Qin X, Cui Y, Shi C, Liu Y & Shi X (2019) Transcriptional sequencing uncovers survival mechanisms of *Salmonella enterica* serovar Enteritidis in antibacterial egg. *mSphere.* **4:** 1–19

Humphrey TJ (1994) Contamination of egg shell and contents with *Salmonella* Enteritidis: a review. *Int. J. Food. Microbiol.* **21:** 31-40

Humphrey TJ & Whitehead A (1993) Egg age and the growth of *Salmonella* Enteritidis PT4 in egg contents. *Epidemiol. Infect.* **111:** 209–220

Huntington JA & Stein PE (2001) Structure and properties of ovalbumin. *J. Chromatogr. B Biomed. Sci. Appl.* **756:** 189–198

Ibrahim HR (1997) Insights into the structure-function relationships of ovalbumin, ovotransferrin, and lysozyme (ed Yamamoto T, Juneja LR, Hatta H, Kim M). *Hen eggs their basic and applied science.* New York: CRC Press, pp 37–56

Ibrahim HR, Iwamori E, Sugimoto Y & Aoki T (1998) Identification of a distinct antibacterial domain within the N-lobe of ovotransferrin. *Biochim. Biophys. Acta. – Mol. Cell. Res.* **1401:** 289–303

Ibrahim HR, Sugimoto Y & Aoki T (2000) Ovotransferrin antimicrobial peptide (OTAP-92) kills bacteria through a membrane damage mechanism. *Biochim. Biophys. Acta. – Gen. Subj*. **1523:** 196–205

Jackson BR, Griffin PM, Cole D, Walsh KA & Chai SJ (2013) *Salmonella enterica* serotypes and food commodities, *Emerg. Infect. Dis.* **19:** 1239–1244

Jovanovic G, Engl C, Mayhew AJ, Burrows PC & Buck M (2010) Properties of the phage-shock-protein (Psp) regulatory complex that govern signal transduction and induction of the Psp response in *Escherichia coli*. *Microbiology.* **156:** 2920–2932

Julien LA, Baron F, Bonnassie S, Nau F, Guérin C, Jan S & Andrews SC (2019) The anti-bacterial iron-restriction defence mechanisms of egg white; the potential role of three lipocalins in resistance against *Salmonella*. *BioMetals*. **32**, 453–467

Julien LA, Cochet MF, Bonnassie S, Nau F, Jan S & Baron F (2018) Iron-acquisition genes and siderophores production are induced by *Salmonella* Enteritidis in egg white at temperatures around the natural body temperature of hens. Oral communication at the International Symposium *Salmonella* and Salmonellosis (I3S). Saint Malo, France

Julien LA, Fau C, Baron F, Bonnassie S, Guérin C, Nau F, Gautier M, Karatzas KA, Jan S & Andrews SC (2020) The three lipocalins of egg-white: only Ex-FABP inhibits siderophore-dependent iron sequestration by *Salmonella* Enteritidis. *Front. Microbiol.* DOI: 10.3389/fmicb.2020.00913

Kammler M, Schon C & Hantke K (1993) Characterization of the ferrous iron uptake system of *Escherichia coli. J Bacteriol.* **175:** 6212–6219

Kang H, Loui C, Clavijo RI, Riley LW & Lu S (2006) Survival characteristics of *Salmonella enterica* serovar Enteritidis in chicken egg albumen. *Epidemiol. Infect.* **134:** 967–976

Kehres DG, Janakiraman A, Slauch JM & Maguire ME (2002) Regulation of *Salmonella enterica* serovar Typhimurium mntH transcription by H_2O_2, Fe^{2+}, and Mn^{2+}. *J. Bacteriol.* **184:** 3151–3158

Keller LH, Benson CE, Krotec K & Eckroade RJ (1995) *Salmonella* Enteritidis colonization of the reproductive tract and forming and freshly laid eggs of chickens. *Infect. Immun.* **63:** 2443–2449

Keller LH, Schifferli DM, Benson CE, Aslam S, Eckroade J & Eckroadea RJ (1997) invasion of chicken reproductive tissues and forming eggs is not unique to *Salmonella* Enteritidis. *Avian. Dis.* **41:** 535-539

Ketterer BB (1965) Protein of Hen's-egg white. *Biochem. J.* **96:** 372–376

Kinde H, Shivaprasad HL, Daft BM, Read DH, Ardans A, Breitmeyer R, Rajashera G, Nagaraja KV & Gardner IA (2000) Pathologic and bacteriologic findings in 27-week-old commercial laying hens experimentally infected with *Salmonella* Enteritidis phage type 4. *Avian Dis.* **44:** 239–248

Kjeldsen L, Johnsen AH, Sengeløv H & Borregaard N (1993) Isolation and primary structure of NGAL, a novel protein associated with human neutrophil gelatinase. *J. Biol. Chem.* **268:** 10425–10432

Konopka K, Bindereif A & Neilands JB (1982) Aerobactin mediated utilization of transferrin iron. *Biochemistry.* **24:** 6503–6508

Konopka K & Neilands JB (1984) Effect of serum albumin on siderophore-mediated utilization of transferrin iron. *Biochemistry.* **23:** 2122–2127

Kopeć W, Skiba T, Korzeniowska M, Bobak Ł & Trziszka T (2005) Activity of protease inhibitors and lysozyme of hen's egg white. *Polish J. Food Nutr. Sci.* **14:** 79–83

Kovacs-Nolan J, Phillips M & Mine Y (2005) Advances in the value of eggs and egg components for human health. *J. Agric. Food. Chem.* **53:** 8421–8431

Kremer JM, Wilting J & Janssen LH (1988) Drug binding to human alpha-1-acid glycoprotein in health and disease. *Pharmacol. Rev.* **40:**1-47

Lang ER & Rha C (1982) Apparent shear viscosity of native egg white. *J. Fd. Technol.* **17:** 595–606

Langman L, Young IG, Frost GE, Rosenberg H & Gibson F (1972) Enterochelin system of iron transport in *Escherichia coli:* mutations affecting ferric-enterochelin esterase. *J. Bacteriol.* **112:** 1142–1149

Li H, Feng D, Cai Y, Liu Y, Xu M & Xiang X (2018) Hepatocytes and neutrophils cooperatively suppress bacterial infection by differentially regulating lipocalin-2 and NETs. *Hepatology.* **68:** 1604–1620

Li W, Cui T, Hu L, Wang Z, Li Z & He ZG (2015) Cyclic diguanylate monophosphate directly binds to human siderocalin and inhibits its antibacterial activity. *Nat. Commun.* **6:** 1–9

Lin H, Fischbach MA, Liu DR & Walsh CT (2005) *In vitro* characterization of salmochelin and enterobactin trilactone hydrolases IroD, IroE, and Fes. *J Am. Chem. Soc.* **127:** 11075–11084

Lin LN, Mason AB, Woodworth RC & Brandts JF (1994) Calorimetric studies of serum transferrin and ovotransferrin. Estimates of domain interactions, and study of the kinetic complexities of ferric ion binding. *Biochemistry.* **33:** 1881–1888

Lin Y Te, Wu C Te, Huang JL, Cheng JH & Yeh KW (2016) Correlation of ovalbumin of egg white components with allergic diseases in children. *J. Microbiol. Immunol. Infect.* **49:** 112–118

Liu Y, Zhang Q, Hu M, Yu K, Fu J, Zhou F & Liu X (2015) Proteomic analyses of intracellular *Salmonella enterica* serovar Typhimurium reveal extensive bacterial adaptations to infected host epithelial cells. *Infect. Immun.* **83:** 2897–2906

Lock JL & Board RG (1992) Persistence of contamination of hens' egg albumen *in vitro* with *Salmonella* serotypes. *Epidemiol. Infect.* **108:** 389–396

Lomholt JP (1976) The development of the oxygen permeability of the avian egg shell and its membranes during incubation. *J. Exp. Zool*. **198:** 177–184

Louden BC, Haarmann D & Lynne AM (2011) Use of blue agar CAS assay for siderophore detection. *J. Microbiol. Biol. Educ.* **12:** 51-53

Lu F, Inoue K, Kato J, Minamishima S & Morisaki H (2019) Functions and regulation of lipocalin-2 in gut-origin sepsis : a narrative review. *Crit. Care.* **23:** 1–8

Luo M, Lin H, Fischbach MA, Liu DR, Walsh CT & Groves JT (2006) Enzymatic tailoring of enterobactin alters membrane partitioning and iron acquisition. *ACS Chem. Biol.* **1:** 29–32

Ma L & Payne SM (2012) AhpC is required for optimal production of enterobactin by *Escherichia coli*. *J. Bacteriol.* **194:** 6748–6757

Majowicz SE, Musto J, Scallan E, Angulo FJ, Kirk M, O'Brien SJ, Jones TF, Fazil A & Hoekstra RM (2010) The global burden of nontyphoidal *Salmonella* Gastroenteritis. *Clin. Infect. Dis.* **50:** 882–889

Mann K (2007) The chicken egg white proteome. *Proteomics.* **7:** 3558–3568

Mann K & Mann M (2011) In-depth analysis of the chicken egg white proteome using an LTQ Orbitrap Velos. *Proteome Sci.* **9:** 1–6

Martin JE & Imlay JA (2011) The alternative aerobic ribonucleotide reductase of *Escherichia coli*, NrdEF, is a manganese-dependent enzyme that enables cell replication during periods of iron starvation. *Mol. Microbiol.* **80:** 319–334

Mason KM, Raffel FK, Ray WC & Bakaletz LO (2011) Heme utilization by nontypeable *Haemophilus influenzae* is essential and dependent on sap transporter function. *J. Bacteriol.* **193:** 2527–2535

Matsunaga H, Sadakane Y & Haginaka J (2004) Identification of disulfide bonds and site-specific glycosylation in chicken alpha1-acid glycoprotein by matrix-assisted laser desorption ionization time-of-flight mass spectrometry. *Anal. Biochem.* **331:** 358–363

McPhie P (1971) Dialysis (ed Jakoby A). *Methods of Enzymology*. New York: Academic Press, pp 23–32

McQuiston JR, Herrera-Leon S, Wertheim BC, Doyle J, Fields PI, Tauxe R V & Logsdon JM (2008) Molecular phylogeny of the salmonellae: relationships among *Salmonella* species and subspecies determined from four housekeeping genes and evidence of lateral gene transfer events. *J. Bacteriol.* **190:** 7060–7067

Mecham DK & Olcott HS (1949) Phosvitin, the principal phosphoprotein of egg yolk. *J. Am. Chem. Soc.* **71:** 3670–3679

Meheus LA, Fransen LM, Raymackers JG, Blockx HA, Van Beeumen JJ, Van Bun SM & Van de Voorde A (1993) Identification by microsequencing of lipopolysaccharide-induced proteins secreted by mouse macrophages. *J. Immunol.* **151:** 1535–1547

Methner U (2018) Immunisation of chickens with live *Salmonella* vaccines – Role of booster vaccination. *Vaccine.* **36:** 2973–2977

Miroux B & Walker JE (1996) Overproduction of proteins in *Escherichia coli*: mutant hosts that allow synthesis of some membrane proteins and globular proteins at high levels. *J. Mol. Biol.* **260:** 289–298

Miyamoto T, Takahashi N, Sekine M, Ogawa T, Hidaka M, Homma H & Masaki H (2015) Transition of serine residues to the D-form during the conversion of ovalbumin into heat stable S-ovalbumin. *J. Pharm. Biomed. Anal.* **116:** 145–149

Montgomerie JZ, Bindereif A, Neilands JB, Kalmanson GM & Guze LB (1984) Association of hydroxamate siderophore (aerobactin) with *Escherichia coli* isolated from patients with bacteremia. *Infect. Immun.* **46:** 835–838

Moore DF, Rosenfeld MR, Gribbon PM, Winlove CP & Tsai CM (1997) Alpha-1 acid glycoprotein (orosomucoid) : interaction with bacterial lipopolysaccharide and protection from sepsis. *Inflammation.* **21:** 69–82.

Müller SI, Valdebenito M & Hantke K (2009) Salmochelin, the long-overlooked catecholate siderophore of *Salmonella. BioMetals.* **22:** 691–695

Nagase H, Harris ED, Woessner JF & Brew K (1983) Ovostatin : a novel proteinase inhibitor from chicken egg white. *J. Biol. Chem.* **258:** 7481–7489

Nairz M, Ferring-appel D, Casarrubea D, Matthias W, Weiss G, Galy B, Nairz M, Ferring-appel D, Casarrubea D, Sonnweber T, Viatte L & Schroll A (2015). Iron regulatory proteins mediate host resistance to *Salmonella* infection. *Cell. Host. Microbe.* **18:** 254–261

NCBI (National Center for Biotechnology Information) (2019). National Library of Medicine (US), National Center for Biotechnology Information. https://www.ncbi.nlm.nih.gov Accessed 14 Jan 2019

Neilands JB (1981) Microbial iron compounds. *Annu. Rev. Biochem.* **50:** 715–731

Nelson AL, Ratner AJ, Barasch J & Weiser JN (2007) Interleukin-8 secretion in response to aferric enterobactin is potentiated by siderocalin. *Infect. Immun.* **75:** 3160–3168

Nielsen BS, Borregaard N, Bundgaard JR, Timshel S, Sehested M & Kjeldsen L (1996) Induction of NGAL synthesis in epithelial cells of human colorectal neoplasia and inflammatory bowel diseases. *Gut.* **38:** 414–420

Nossal NG & Heppel LA (1966) The release of enzymes by osmotic shock from *Escherichia coli* in exponential phase. *J. Biol. Chem.* **241:** 3055–3062

Nys Y & Sauveur B (2004) Valeur nutritionnelle des oeufs. *INRA. Prod. Anim.* 385–393

O'Brien IG, Cox GB & Gibson F (1971) Enterochelin hydrolysis and iron metabolism in *Escherichia coli*. *Biochim. Biophys. Acta.* **237:** 537–549

O'Brien IG & Gibson F (1970) The structure of enterochelin and related 2,3-dihydroxy-N-benzoylserine conjugates from *Escherichia coli*. *Biochim. Biophys. Acta* **215:** 393–402

Omana DA & Wu J (2009) A new method of separating ovomucin from egg white. *J. Agric. Food Chem.* **57:** 3596–3603

Osman D & Cavet JS (2011) Metal sensing in *Salmonella*: implications for pathogenesis. *Adv. Microb. Physiol.* **58:**175-232

Outten FW, Djaman O & Storz G (2004) A *suf* operon requirement for Fe–S cluster assembly during iron starvation in *Escherichia coli*. *Mol. Microbiol.* **2004:** 861–872

Outten CE & O'Halloran TV (2001) Femtomolar sensitivity of metalloregulatory proteins controlling zinc homeostasis. *Science.* **80:** 292: 2488–2492

Pagano A, Crooijmans R, Groenen M, Randazzo N, Zerega B, Cancedda R & Dozin B (2003) A chondrogenesis-related lipocalin cluster includes a third new gene, CALγ. *Gene.* **305:** 185–194

Page MGP (2019) The role of iron and siderophores in infection, and the development of siderophore antibiotics. *Clin. Infect. Dis.* **69:** 529–S537

Pan Z, Carter B, Núñez-García J, AbuOun M, Fookes M, Ivens A, Woodward MJ & Anjum MF (2009) Identification of genetic and phenotypic differences associated with prevalent and non-prevalent *Salmonella* Enteritidis phage types: analysis of variation in amino acid transport. *Microbiology.* **155:** 3200–3213

Pollack JR, Ames BN & Neilands JB (1970) Iron transport in *Salmonella* Typhimurium: mutants blocked in the biosynthesis of enterobactin. *J. Bacteriol.* **104:** 635–639

Pollack JR & Neilands JB (1970) Enterobactin, an iron transport compound from *Salmonella* Typhimurium. *Biochem. Biophys. Res. Commun*. **38:** 989–992

Pons A, García FJ, Palou A & Alemany M (1985) Permeability of chicken egg vitelline membrane to amino acids-binding of amino acids to egg proteins. *Comp. Biochem. Physiol.* **82:** 289–292

Qin X, He S, Zhou X, Cheng X, Huang X, Wang Y, Wang S, Cui Y, Shi C & Shi X (2019) Quantitative proteomics reveals the crucial role of YbgC for *Salmonella enterica* serovar Enteritidis survival in egg white. *Int. J. Food. Microbiol.* **289:** 15–126

Rabsch W, Hargis BM, Tsolis RM, Kingsley RA, Hinz KH, Tschape H, Baumler AJ (2000) Competitive exclusion of *Salmonella* Enteritidis by *Salmonella* Gallinarum in poultry. *Emerg. Infect. Dis.* **6:** 443-8

Rabsch W, Methner U, Voigt W, Tscha H, Reissbrodt R & Williams PH (2003) Role of receptor proteins for enterobactin and 2 , 3-dihydroxybenzoylserine in virulence of *Salmonella enterica. Infect. Immun.* **71:** 6953–6961

Rabsch W, Voigt W, Reissbrodt R, Tsolis RM & Bäumler AJ (1999) *Salmonella* Typhimurium IroN and FepA proteins mediate uptake of enterobactin but differ in their specificity for other siderophores. *J. Bacteriol.* **181:** 3610–3612

Raffatellu M, George MD, Akiyama Y, Hornsby MJ, Nuccio SP, Paixao TA, Butler BP, Chu H, Santos RL, Berger T, Mak TW, Tsolis RM, Bevins CL, Solnick J V, Dandekar S & Bäumler AJ (2009) Lipocalin-2 resistance confers an advantage to *Salmonella enterica* serotype Typhimurium for growth and survival in the inflamed intestine. *Cell. Host. Microbe.* **5:** 476–486

Raivio TL (2014) Everything old is new again: an update on current research on the Cpx envelope stress response. *Biochim. Biophys. Acta*. **1843:** 1529–1541

Réhault-Godbert S, Labas V, Helloin E, Hervé-Grépinet V, Slugocki C, Berges M, Bourin MC, Brionne A, Poirier JC, Gautron J, Coste F & Nys Y (2013) Ovalbumin-related protein X is a heparin-binding ov-serpin exhibiting antimicrobial activities. *J. Biol. Chem.* **288:** 17285–17295

Růzicková V (1994) Growth and survival of *Salmonella* Enteritidis in selected egg foods. *Vet. Med.* **39:** 187–195

Sadakane Y, Matsunaga H, Nakagomi K, Hatanaka Y & Haginaka J (2002) Protein domain of chicken alpha(1)-acid glycoprotein is responsible for chiral recognition. *Biochem. Biophys. Res. Commun.* **295:** 587–590

Saito S, Tsuda H & Michimata T (2002) Prostaglandin D2 and Reproduction. *Am. J. Reprod. Immunol.* **47:** 295–302

Sambrook J & Russell DW (2001) A Laboratory Manual. *Molecular Cloning.* Cold Spring Harbor Laboratory Press

Sandrini S, Masania R, Zia F, Haigh R & Freestone P (2013) Role of porin proteins in acquisition of transferrin iron by enteropathogens. *Microbiol.* **159:** 2639–2650

Sankaranarayanan R, Alagumaruthanayagam A & Sankaran K (2015) A new fluorimetric method for the detection and quantification of siderophores using Calcein Blue, with potential as a bacterial detection tool. *Appl. Microbiol. Biotechnol.* **99**, 2339–2349

Santos AC, Roberts JA, Cook AJC, Simons R, Sheehan R, Lane C, Adak GK, Clifton-Hadley FA & Rodrigues LC (2011) *Salmonella* Typhimurium and *Salmonella* Enteritidis in England: Costs to patients, their families, and primary and community health services of the NHS. *Epidemiol. Infect.* **139:** 742–753

Sauveur B (1988) Structure, composition et valeur nutritionnelle de l'œuf. *Reproduction des volailles et production d'œufs.* Paris: INRA, pp 347-374

Schade A & Caroline L (1944) Raw hen egg white and the role of iron in growth inhibition of *Shigella dysenteriae, Staphylococcus aureus, Escherichia coli* and *Saccharomyces cerevisiae*. *Science*. **100**: 14–15

Schmid K (1975) Acute-phase proteins: alpha-1-acid glycoprotein (ed Putman FW). *The plasma proteins: structure, function and genetic control.* New York: Academic Press, pp 183–192

Schneider DJ, Roe AL, Mayer RJ & Que L (1984) Evidence for synergistic anion binding to iron in ovotransferrin complexes from resonance raman and extended X-ray absorption fine structure analysis. *J. Biol. Chem.* **259:** 9699–9703

Schneider WR & Doetsch RN (1974) Effect of viscosity on bacterial motility. *J. Bacteriol.* **117:** 696–701

Sharp PF & Powell CK (1931) Increase in the pH of the white and yolk of hens' eggs. *Ind. Eng. Chem.* **23:** 196–199

Sharp PF & Whitaker R (1927) The relation of the hydrogen ion concentration of egg white to its germicidal action. *J. Bacteriol.* **14:** 17–46

Shivaprasad HL (2000) Fowl typhoid and pullorum disease. *Rev. Sci. Tech. Off. int. Epiz.* **19:** 405–424

Sia AK, Allred BE & Raymond KN (2013) Siderocalins: siderophore binding proteins evolved for primary pathogen host defense. *Curr. Opin. Chem. Biol.* **17:** 150–157

Skare JT, Ahmer BMM, Seachord CL, Darveau RP & Postle K (1993) Energy transduction between membranes: TonB, a cytoplasmic membrane protein, can be chemically cross-linked *in vivo* to the outer membrane receptor FepA. *J. Biol. Chem.* **268:** 16302–16308

Sørensen HP & Mortensen KK (2005) Soluble expression of recombinant proteins in the cytoplasm of *Escherichia coli. Microb. Cell Fact.* **4:** 1–8

Steele-Mortimer O (2008) The *Salmonella*-containing Vacuole – Moving with the *Times Curr. Opin. Microbiol.* **11:** 38–45

Studier FW, Rosenberg AH, Dunn JJ & Dubendorff JW (1990) Use of T7 RNA polymerase to direct expression of cloned genes. *Methods Enzymol.* **185**: 60–89

Taborsky G (1980) Iron binding by phosvitin and its conformational consequences. *J. Biol. Chem.* **255:** 2976–2985

Thomas S, Maynard ND & Gill J (2015) DNA library construction using Gibson Assembly. *Nat. Methods.* **12:** 1–2

Tindall BJ, Grimont PAD, Garrity GM & Euzéby JP (2005) Nomenclature and taxonomy of the genus *Salmonella*. *Int. J. Syst. Evol. Microbiol.* **55:** 521–524

Trüper HG (2005) The type species of the genus *Salmonella* Lignieres 1900 is *Salmonella enterica* (*ex* Kauffmann and Edwards 1952) Le Minor and Popoff 1987, with the type strain LT2^{T}, and conservation of the epithet enterica in *Salmonella enterica* over

all earlier epithets that may be applied to this species. Opinion 80. *Int. J. Syst. Evol. Microbiol.* **55:** 519–520

Tullett SG & Board RG (1976) Oxygen flux across the integument of the avian egg during incubation. *Br. Poult. Sci.* **17:** 441–450

Urade Y & Hayaishi O (2000) Biochemical, structural, genetic, physiological, and pathophysiological features of lipocalin-like prostaglandin D synthase. *Biochim. Biophys. Acta - Protein Struct. Mol. Enzymol.* **1482:** 259–271

USDA National Nutrient Database for Standard Reference (2010) Release 23. http://www.ars.usda.gov/ba/bhnrc/ndl Accessed 15 Dec 2018

Valdebenito M, Crumbliss AL, Winkelmann G & Hantke K (2006) Environmental factors influence the production of enterobactin, salmochelin, aerobactin, and yersiniabactin in *Escherichia coli* strain Nissle 1917. *Int. J. Med. Microbiol.* **296:** 513–520

Valenti P, Antonini GRH, Visca P, Orsi N & Antonini E (1983) Studies of the antimicrobial activity of ovotransferrin. *Int. J. Tissue. React.* **5:** 97–105

Valenti P, Stasio A De, Mastromarino P, Seganti L, Sinibaldi L & Orsi N (1981) Influence of bicarbonate and citrate on the bacteriostatic action of ovotransferrin towards staphylococci. *FEMS Microbiol. Lett.* **10:** 77–79

Valenti P, Visca P, Antonini G & Orsi N (1985) Antifungal activity of ovotransferrin towards genus *Candida*. *Mycopathologia* **89:** 169–175

Vignaud ML, Cherchame E, Marault M, Chaing E, Le Hello S, Michel V, Jourdan-Da Silva N, Lailler R, Brisabois A & Cadel-Six S (2017) MLVA for *Salmonella enterica* subsp. *enterica* serovar Dublin: Development of a method suitable for inter-laboratory surveillance and application in the context of a raw milk cheese outbreak in France in 2012. *Front. Microbiol.* **8:** 1–10

Vylder JDE, Raspoet R, Dewulf J, Haesebrouck F, Ducatelle R, Immerseel & F Van (2013) *Salmonella* Enteritidis is superior in egg white survival compared with other *Salmonella* serotypes. *Poult. Sci. Assoc. Inc.* **92:** 842–845

Wang Q, Li S, Tang X, Liang L, Wang F & Du H (2019) Lipocalin 2 protects against *Escherichia coli* infection by modulating neutrophil and macrophage function. *Front. Immunol.* **10:** 1–13

Wang Y, Li Y, Xu T, Shi Z & Wu Q (2015) Experimental evidence for growth advantage and metabolic shift stimulated by photophosphorylation of proteorhodopsin expressed in *Escherichia coli* at anaerobic condition. **112:** 947–956

Ward LR, de Sa JDH & Rowe B (1987) A phage-typing scheme for *Salmonella* Enteritidis. *Epidemiol. Infect.* **99:** 291–294

Warszawska JM, Weiss G, Knapp S, Warszawska JM, Gawish R, Sharif O, Sigel S, Doninger B, Lakovits K, Mesteri I, Nairz M, Boon L, Spiel A, Fuhrmann V, Strobl B, Müller M & Schenk P (2013) Lipocalin 2 deactivates macrophages and worsens pneumococcal pneumonia outcomes. *J. Clin. Invest.* **123:** 3363–3372

Watts RE, Totsika M, Challinor VL, Mabbett AN, Ulett GC, Voss JJ De & Schembri MA (2012) Contribution of siderophore systems to growth and urinary tract colonization of asymptomatic bacteriuria *Escherichia coli*. *Infect. Immun.* **80:** 333–344

Wesierska E, Saleh Y, Trzizka T, Kopec W, Siewinski M & Korzekwa L (2005) Antimicrobial activity of chicken egg white cystatin. *World. J. Microbiol. Biotechnol.* **21:** 59-64

White HB, Dennison BA, Della Fera MA, Whitney CJ, McGuire JC, Meslar HW & Sammelwitz PH (1976) Biotin-binding protein from chicken egg yolk. Assay and relationship to egg white avidin. *Biochem. J.* **157:** 395–400

Williams PH & Carbonetti NH (1986) Iron, siderophores, and the pursuit of virulence: Independence of the aerobactin and enterochelin iron uptake systems in *Escherichia coli*. *Infect. Immun.* **51:** 942–947

Winter WP, Buss EG, Clagett CO & Boucher RV (1967) The nature of the biochemical lesion in avian renal riboflavinuria-II. The inherited change of a riboflavin-binding protein from blood and eggs. *Comp. biochem. Phys.* **22:** 897-906

Yadav NK & Vadehra DV (1977) Mechanism of egg white resistance to bacterial growth. *J. Food Sci.* **42:** 4–6

Zaheer K (2015) An updated review on chicken eggs: production, consumption, management aspects and nutritional benefits to human health. *Food Nutr. Sci.* **6:** 1208–1220

Zhao Y & Natarajan V (2014) Lysophophatidic acid (LPA) and its recepotrs: role in airway inflammation and remodeling. *Biochim. Biophys. Acta* **1831:** 86–92

Zhu M, Valdebenito M, Winkelmann G & Hantke K (2005) Functions of the siderophore esterases IroD and IroE in iron-salmochelin utilization. *Microbiol.* **151:** 2363–2372

Appendices

Appendix 1. Map of the *iroD*, *iroE* and *iroN* genes knocked-out using the λRed disruption system, with the corresponding nucleotide sequence below it. Target genes are coloured in green: *iroD*, blue: *iroE*, purple: *iroN*. Deletion primers used are bold and underlined. Confirmation primers are highlighted in yellow. The sequence removed has a length of 4428 bp.

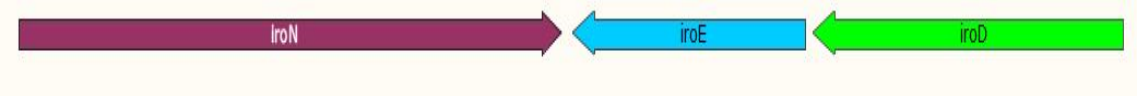

ACCCTTCCCGGATTTATTGGCAAAGCGGAGCCCGGACAGAGAGTCATATTGCAAAATCCCGTTTCTGTTTTCTT
ATGACCAGATTTTTGCGGTCGAAAGATTGCCTTTTTCTTAATTGAATGATAATTATTATCATTAGCATATGATAA
TAATTACTATATAGCCGTAACCTGGCAAGGATGTGAGC**TTGAGGGCAACAGCGCTACTTTAGACATTATTTAG**
GGAATGGGTATGAAAGTTAATAAGTTCCTCTGGTTAATAACCGTGGTTTCTACAGGGGTTAATAGTCCATTAT
CAGCAGCAGAATCTACAGACGACAACGGCGAAACGATGGTGGTTGAATCCACTGCCGAGCAAGTATTAAAGC
AACAGCCGGGCGTTTCGATTATTACTCGTGACGATATTCAGAAGAATCCTCCCGTTAACGATCTTGCCGATATT
ATTCGTAAGATGCCTGGGGTTAATCTTACCGGCAATAGCGCCTCGGGGACGCGCGGAAATAACCGACAAATTG
ATATTCGTGGTATGGGGCCGGAAAATACCTT .....CTTTATCGGTGACACGGTTCAGGC
GAACATAAACCCCCCGCAGAGGAGAGGCGGCACGCCACAGGAAGGTGACTTCCCGTTCATCGTCTGCGCCGT
TAATGGCTGTCACCAGCGGCAGTGCGAGCGAGTTTGCTTCTCGCCAGAAGTGAGAAGCGTCAACCTGGCTTCC
GGCGGCGAGTTGGCGGCGAAGGCGCGTAGCGGTCTGTATAGCGACAGGAGCGACGGGCGG**GCTCAGTCTCA**
TTCTTTGTATTCCATCTCATTTATATTTCGGTTAGTACTAATAGCTAAAGCGGCTGTTACAGGAACAGCCGCTT
GCGGGCTTTCTTTTGCGTAAATCGTGGCGATAA

Appendix 2. Map of the *iroB*, *iroC* genes knocked-out using the λRed disruption system, with the corresponding nucleotide sequence below it. Target genes are coloured in red: *iroB*, yellow: *iroC*. Deletion primers used are bold and underlined. Confirmation primers are highlighted in yellow. The sequence removed has a length of 4853 bp.

AAATCATCACATGATCAAGGGTCGTATTTGTTATTGCATTTTTCAAATGATATTGGTAATTATTATCATTCTCATT
AATG**ACTTGTTCGATTTATGACGTGGAGAGAGAGGATTTCTCATGCGTATTCTG**TTTGTCGGTCCACCACTGT
ATGGACTGCTATACCCTGTGCTGTCCCTGGCGCAAGCGTTTCGTGTTAATGGCCATGAAGTGCTGATTGCAAGC
GGTGGAAAATTTGCACAGAAAGCAGCCGAAGCTGGGTTGGTGGTATTTGACGCTGCGCCTGGTTTCGATTCG
GAAGCGGGTTATCGCCGTCAGGAGGCATTACGAAAAGAAAATAACATTGGAACAAAAATGGGGAACTTCTCA
TTCTTCAGCGAAGAGATGACTG ……TTCGCTGCCAGACA
GCAGCGACACGGAGGTGGAGATCGCGGCGCGACAGGCGGGACTCTTTGAAACTGTGCAACATCTGCCGCTGG
GGTTCCGTACTCCGGTCAATAACGGCGGCACGGATCTGTCCGCGGGCCAGCGTCAGTTGATTGCCCTCGCCCG
CGCCCACCTGGCGCAGGCGCATATTCTGCTGCTCGACGAGGCGACAGCGCGTATCGACCGTAGCGCCGAGGA
GCGCTTAATGACCTCGCTTACCAGGGTGACGCATACCGAGAAACGCATCGCGCTTATCGTCGCGCACCGGCTG
ACCACCGCTCGCCGTTGCGATGTTATTGTCGTAATCGATAAAGGATGTATCGCTGAATATGGCAGCCATGAGC
AGTTGATAGCGACTCATGGCCTGTATGCTCGTCTGTGGCGGGACAGCATCGGCCAGACACGCGATACGCAAG
GAGAGGTCATAGGATAGTTTTTATCGCCACGATTTACGCAAAAGAAAGCCCGCAAGCGGCTGTTCCTGTAACA
GCCGCTTTAGCTATTAGTACTAACG

Appendix 3. Map of the *entB* gene knocked-out using the λRed disruption system, with the corresponding nucleotide sequence below it. Target genes are coloured in dark blue: *entB*. Deletion primers used are bold and underlined. Confirmation primers are highlighted in yellow. The sequence removed has a length of 968 bp.

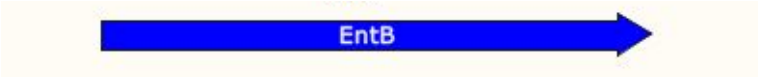

AGCATGGAAGATGAACTGCTGGGAGAAAAAAGTTGCGCATATCTGGTGGTAAAAGAGCCGCTGCGAGCGGT
ACAGGTACGCCGTTTCCTGCGAGAGCAGGGCGTGGCGGAATTTAAATTACCGGATCGCGTAGAGTGCGTTGC
GTCACTGCCGCTGACGCCGGTTGGTAAAGTCGATAAAAAACAATTACGCCAGCG**GTTGGCGTCACGTTCACCG**
CTCTGAAGGAGAAAGAGAGATGGCAATCCCGAAACTACAGTCTTACGCGCTGCCCACCGCACTGGATATCCC
GACCAACAAAGTGAACTGGGCATTTGAGCCGGAGCGCGCTGCGCTGCTCATCCACGATATGCAGGATTACTTT
GTCAGCTTTTGGGG……TGAAAACCTGATTGATTATGGCCTGGATTCAGTAC
GCATGATGGGGCTGGCAGCGCGCTGGCGTAAAGTACACGGCGATATCGACTTCGTGATGCTGGCGAAAAACC
CGACCATTGACGCCTGGTGGGCGCTGCTTTCTCGCGGGGTAGAG**TAA**TGGCCTGTATTGATTTTTCAGACAAA
ACGGTATGGGTGACCGGGGCGGGGAAAGGGATCGGTTACGCGACGGCGCTGGCGTTTGTCGACGCCGGGG
CGCGGGTGATCGGCTTCGATCGCGAATTTACGCAAGAGAATTATCCCTTTGCTACCGAAGTCATGGATGTGGC
GGATGCCGCACAGGTTGCGCAGGTGTGCCAGCGTGTGTTGCAAAAAACGCCGCGGCTGGATGTGCTGGTCAA
CGCCGCCGGTATTTTGCGTATGGGAGCGACCGACGCGCTTAGCGTCGACGACTGGCAGCAGACATTTGCGGTC
AATGTGGGCG

Appendix 4. Codon optimised nucleotide sequences and corresponding translation sequences of lipocalin genes in overexpression plasmids: pET-lcn2 (A); pET-Ex-FABP (B); pET-Cal-γ (C); and pET-α1-glyc (D). The plasmid sequences are underscored; NdeI and XhoI sites are in yellow highlight; pelB sequence is in green highlight. The translation product amino acid sequence shows the 'additional' residues (not present in the native protein) highlighted: blue, Leu-Glu peptide introduced by inclusion of the XhoI restriction site; and purple, hexa-His tag. Nucleotide sequences were determined by Sanger sequencing (Eurofins) and are shown in the 5′ to 3′ direction.

A. LCN2 sequence once cloned into pET21a:

5'AGGAGATATACATATGCAGGATAGCACCAGCGATCTGATTCCGGCACCGCCTCTGAGCAA
AGTTCCGCTGCAGCAGAATTTTCAGGATAATCAGTTTCAAGGCAAGTGGTATGTTGTTGGTC
TGGCAGGTAATGCAATTCTGCGTGAAGATAAAGATCCGCAGAAAATGTATGCCACCATCTAT
GAACTGAAAGAGGACAAAAGCTATAACGTTACCAGCGTTCTGTTTCGCAAAAAAAAGTGCG
ATTATTGGATCCGTACCTTTGTTCCGGGTTGTCAGCCTGGTGAATTTACCCTGGGTAACATTA
AAAGCTATCCGGGTCTGACCAGCTATCTGGTTCGTGTTGTTAGCACCAATTATAACCAGCAT
GCCATGGTGTTCTTCAAAAAAGTTAGCCAGAATCGCGAGTACTTCAAAATTACCCTGTATGG
TCGTACCAAAGAACTGACCAGCGAGCTGAAAGAAAACTTTATTCGTTTTAGCAAAAGCCTGG
GTCTGCCGGAAAATCATATTGTGTTTCCGGTTCCGATTGATCAGTGTATTGATGGCCTCGAGC
ACCACCACCACCACCACTGA**3'**

Translated sequence:

MQDSTSDLIPAPPLSKVPLQQNFQDNQFQGKWYVVGLAGNAILREDKDPQKMYATIYELKEDKS
YNVTSVLFRKKKCDYWIRTFVPGCQPGEFTLGNIKSYPGLTSYLVRVVSTNYNQHAMVFFKKVS
QNREYFKITLYGRTKELTSELKENFIRFSKSLGLPENHIVFPVPIDQCIDGLEHHHHHH*

B. Ex-FABP sequence once cloned into pET21a:

5'AGGAGATATACATATGAAATACCTGCTGCCGACCGCTGCTGCTGGTCTGCTGCTCCTCGCT
GCCCAGCCGGCGATGGCCGCAGCAACAGTTCCGGATCGTAGCGAAGTTGCAGGTAAATGGT
ATATTGTTGCACTGGCAAGCAACACCGATTTTTTTCTGCGTGAAAAAGGCAAGATGAAGATG
GTTATGGCACGTATTAGCTTTCTGGGTGAAGATGAACTGGAAGTTAGCTATGCAGCACCGAG
TCCGAAAGGTTGTCGTAAATGGGAAACCACCTTCAAAAAAACCAGTGATGATGGCGAACTG
TATTATAGCGAAGAAGCCGAAAAAACCGTTGAAGTTCTGGATACCGACTATAAAAGCTATG
CCGTTATTTTTGCGACCCGTGTTAAAGATGGTCGTACCCTGCACATGATGCGTCTGTATAGCC
GTAGCCGTGAAGTTAGCCCGACCGCAATGGCAATTTTTCGTAAACTGGCACGTGAACGCAAT
TATACCGATGAAATGGTTGCAGTTCTGCCGAGCCAAGAGGAATGTAGCGTTGATGAAGTTCT
CGAG CACCACCACCACCACCACTGA**3'**

Translated sequence:

MKYLLPTAAAGLLLLAAQPAMAAATVPDRSEVAGKWYIVALASNTDFFLREKGKMKMVMAR
ISFLGEDELEVSYAAPSPKGCRKWETTFKKTSDDGELYYSEEAEKTVEVLDTDYKSYAVIFATRV
KDGRTLHMMRLYSRSREVSPTAMAIFRKLARERNYTDEMVAVLPSQEECSVDEVLEHHHHHH*

C. α1-ovoglycoprotein sequence once cloned into pET21a:

5’AGGAGATATACATATGAAATACCTGCTGCCGACCGCTGCTGCTGGTCTGCTGCTCCTCGCT
GCCCAGCCGGCGATGGCCACCGAAAGTCCGACATGTGCACCGCTGGTTCCGGCAGATATGG
ATAATGCAACCGTTGATCGTCTGTTAGGTCATTGGGTGTATATTATGGGTGCAAGCCAGTAT
CCGCCTCACATGGCAGAAATGCGTGAACTGAAATATGCAACCTTTACACTGTTTCCGGGTAG
CCATGAAGATGAATTTAATGTGACCGAAATTATGCGCCTGAATGAAACCTGTGTTGTGAAAA
ACAGCAGCAAAATTCATGTGTTTCGCCATAATAGCACCCTGACACACGAAGATGGTCAGGTT
GTTAGCATGGCCGAACTGATTCATAGCGATAAAGACCTGTTTATCCTGAAGCACTTCAAAGA
TAATCATGTTGGTCTGAGCCTGAGCGCACGTACCGCAGAAGTTACCAAAGAACAGCTGGAA
GAATTTGAAGCACAGCTGCGTTGTCATGGTTTTAAACTGGAAGAAGCCTTTATTACGAGCCC
GAAAGATGCATGTCCGGCAGCCGGTGAAGAAACCGGTGAAGGTAGCGCAGCAACAGCAGA
ACCGCAGCTGGGCCTCGAGCACCACCACCACCACCACTGA3’

Translated sequence:

MKYLLPTAAAGLLLLAAQPAMATESPTCAPLVPADMDNATVDRLLGHWVYIMGASQYPPHMA
EMRELKYATFTLFPGSHEDEFNVTEIMRLNETCVVKNSSKIHVFRHNSTLTHEDGQVVSMAELIH
SDKDLFILKHFKDNHVGLSLSARTAEVTKEQLEEFEAQLRCHGFKLEEAFITSPKDACPAAGEET
GEGSAATAEPQLGLEHHHHHH*

D. Cal-γ sequence once cloned into pET21a:

5’AGGAGATATACATATGAAATACCTGCTGCCGACCGCTGCTGCTGGTCTGCTGCTCCTCGCT
GCCCAGCCGGCGATGGCCAATAGCATTCCGGTTCAGGCAGATTTTCAGCAGGATAAACTGGC
AGGTCGTTGGTATAGCATTGGTCTGGCAAGCAATAGCAACTGGTTCAAAGATAAAAAGCAT
CTGCTGAAGATGTGCACCACCGATATTGCAGTTACCGCAGATGGTAATATGGAAGTTACCAG
CACCTATCCGAAAGGTGAACAGTGTGAAAAACGTAACAGCCTGTATATTCGTACCGAACAG
CCTGGTCGTTTTAGTTATACCAATCCGCGTTGGGGTAGCAATCATGATATTCGTGTTGTGGAA
ACCAACTATGATGAATATGCACTGGTTGCGACCCAGATTAGCAAAAGCACCGGTAGCAGCA
ATATGGTTCTGCTGTATAGCCGTACCAAAGAAGTTGCACCGCAGCGTCTGGAACGTTTTATG
CAGTTTAGCCAAGAACAGGGTCTGAAAGATGAAGAAATTCTGATTCTGCCGCAGACCGATA
AATGTATGGCAGATGCAGCACTCGAGCACCACCACCACCACCACTGA**3’**

Translated sequence:

MKYLLPTAAAGLLLLAAQPAMANSIPVQADFQQDKLAGRWYSIGLASNSNWFKDKKHLLKMC
TTDIAVTADGNMEVTSTYPKGEQCEKRNSLYIRTEQPGRFSYTNPRWGSNHDIRVVETNYDEYA
LVATQISKSTGSSNMVLLYSRTKEVAPQRLERFMQFSQEQGLKDEEILILPQTDKCMADAALEHH
HHHH*

Appendix 5. Protein overproduction over time post IPTG induction (0.5 mM). Maximum production occurred at 4 h post induction.

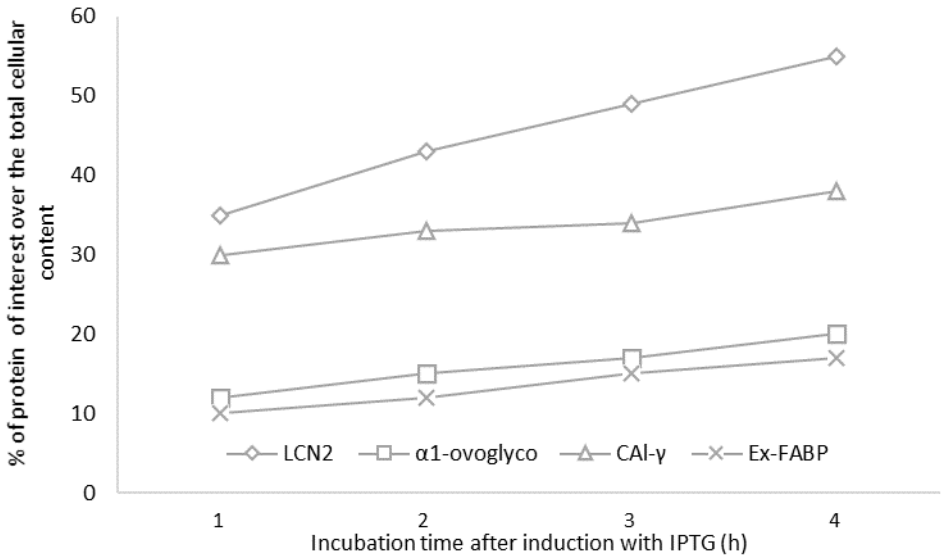

Appendix 6. Isothermal Titration Calorimetry blank for (A) Ex-FABP in TBS pH 7.4 at 30 °C (B) Ex-FABP in EWF pH 9.2 at 30 °C (C) LCN2 in TBS pH 7.4 at 30 °C. ITC was achieved by doing 29 injections (10 µL) of buffer in an adiabatic well containing 5 µM of lipocalins.

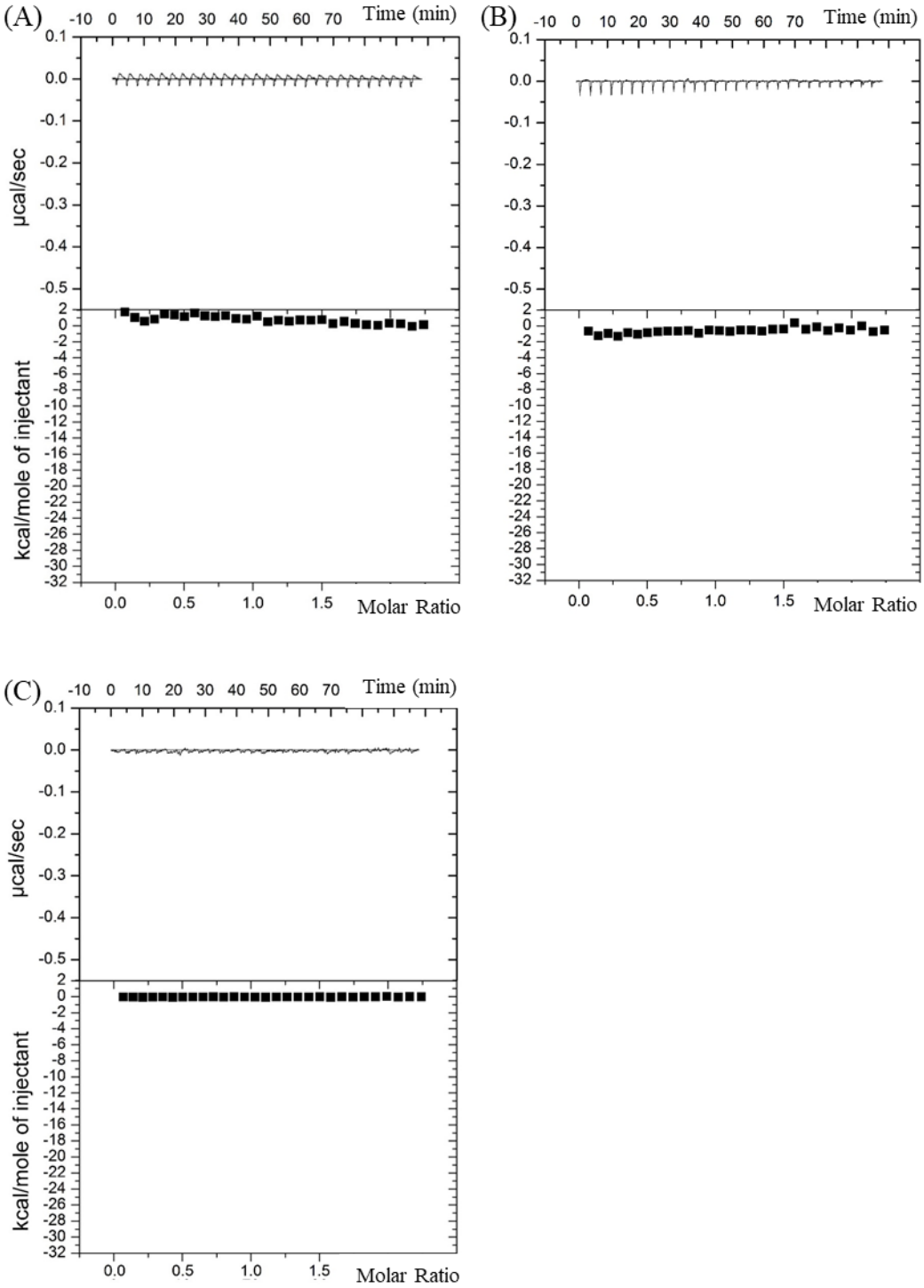

Appendix 7. Measurement of affinity of (A) Ex-FABP for Fe-Ent (A) LCN2 for Fe-Ent (B). Isothermal Titration Calorimetry was achieved with 29 injections (10 µL) of 50 µM ligand (Fe-Ent) in an adiabatic well containing 5 µM of lipocalin. Experiments were achieved in TBS (20 mM Tris, 500 mM NaCl, 1.3% DMSO, pH 7.4) at 30 °C.

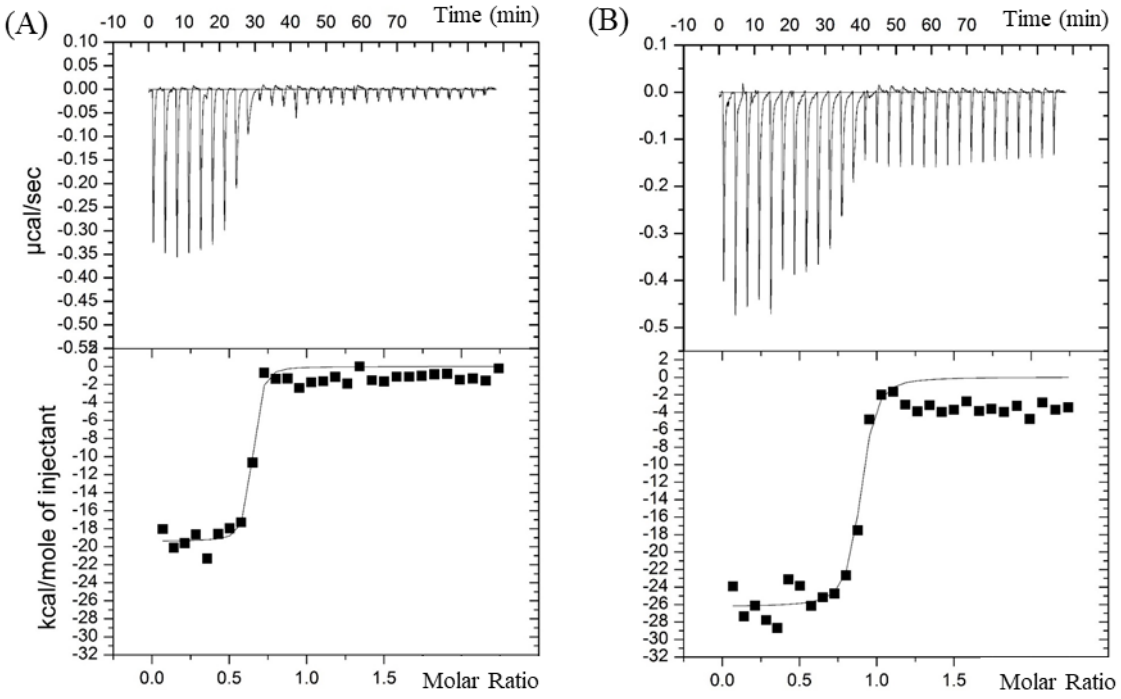

Appendix 8. Electrophoretic analysis of DNA fragments resulting from PCR of genomic DNA isolated from Cam^S and Amp^S mutant candidates (primers Table 2.5, section 2.1.5). PCR products were subjected to electrophoresis in a 0.7% agarose, 0.5X TBE gel (section 2.2.2). Products match the size (100 bp) of clean deletion after removal of the Cat cassette.

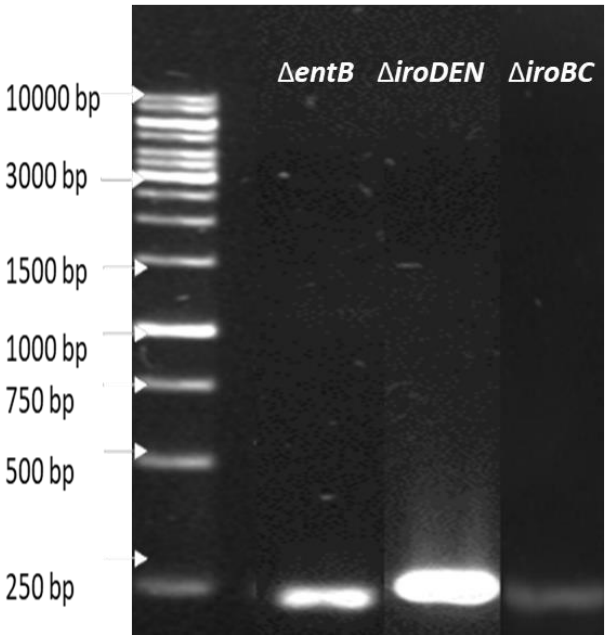

DOCTORAT ECOLOGIE
BRETAGNE GEOSCIENCES
LOIRE AGRONOMIE ALIMENTATION

University of Reading

Titre : Influence du blanc d'œuf sur les mécanismes d'acquisition du fer chez *Salmonella* Enteritidis

Salmochéline, entérobactine, Ex-FABP, Cal-γ, α1-ovoglycoprotéine, blanc d'œuf, *Salmonella* Enteritidis

Résumé: *Salmonella* Enteritidis est le pathogène le plus fréquemment identifié dans les œufs et ovoproduits au sein de l'Union Européene. Pour coloniser les œufs, *S.* Enteritidis doit surmonter de nombreux obstacles liés à l'activité antibactérienne du blanc d'œuf (BO). Un des mécanismes antibactériens majeurs du BO est la restriction en fer imposée par l'ovotransferrine (protéine liant le fer ferrique, Fe^{3+}). Pour pallier cette carence, *S.* Enteritidis est capable de synthétiser deux types de sidérophores, l'entérobactine et la salmochéline, capables d'acquérir le fer des protéines de l'hôte. Cependant, le BO contient également une protéine de type lipocaline (Ex-FABP) connue pour séquestrer l'entérobactine. Deux autres lipocalines, Cal-γ et l'α1-ovoglycoprotéine ont été identifiées dans le BO, mais leur capacité à séquestrer des sidérophores restait à explorer. L'objectif de ce projet était d'étudier l'activité antimicrobienne de trois lipocalines du BO par leur capacité à séquestrer les deux sidérophores de *S.* Enteritidis. Les résultats montrent que Cal-γ et l'α1-ovoglycoprotéine ne sequestrent ni l'entérobactine ni la salmochéline. Nos observations confirment qu'Ex-FABP lie uniquement l'entérobactine et non la salmochéline. En milieux de culture, *S.* Enteritidis échappe à l'inhibition de croissance induite par Ex-FABP grâce à la synthèse de salmochéline. Néanmoins, le rôle antimicrobien d'Ex-FABP *via* la séquestration de sidérophores n'a pas été observé dans le BO. Ceci pourrait être lié à la faible croissance de *S.* Enteritidis dans le BO et au fait que les sidérophores ne semblent pas être nécessaires à sa survie dans ce milieu.

Understanding the relationship between antibacterial activity and iron-restriction mechanisms in egg-white

Salmochelin, enterobactin, Ex-FABP, Cal-γ, α1-ovoglycoprotein, egg white, *Salmonella Enteritidis*

Summary: *Salmonella* Enteritidis is the most prevalent food-borne pathogen associated with egg-related outbreaks in the European Union. In order to colonise eggs, *S.* Enteritidis must resist the powerful anti-bacterial activities of egg white (EW). Possibly, the major EW antibacterial property is iron restriction, which results from the presence of the Fe^{3+}-binding protein, ovotransferrin. To circumvent iron restriction, *S.* Enteritidis synthesise two types of catecholate siderophores, enterobactin and salmochelin, that can chelate iron from host iron-binding proteins. However, EW contains a lipocalin (Ex-FABP) that is known to bind enterobactin. Two other lipocalins, Cal-γ and α1-ovoglycoprotein, are found in EW but their siderophore-binding potential was yet to be explored The aim of this project was to study the antimicrobial activity of three EW lipocalins through sequestration of bacterial siderophores synthesised by *S.* Enteritidis. Among those lipocalins, Cal-γ and α1-ovoglycoprotein were shown to bind neither enterobactin nor salmochelin. Further, it was confirmed that Ex-FABP binds only enterobactin and not salmochelin. In standard growth media, *S.* Enteritidis escaped Ex-FABP-mediated growth inhibition thanks to salmochelin synthesis. However, no clear antibacterial activity was observed for Ex-FABP in EW. This surprising observation might be correlated with the weak growth of *S.* Enteritidis in EW and a lack of requirement for siderophores in persistence.